CENTRE FOR ECONOMIC POLICY RESEARCH

CEPR PRESS

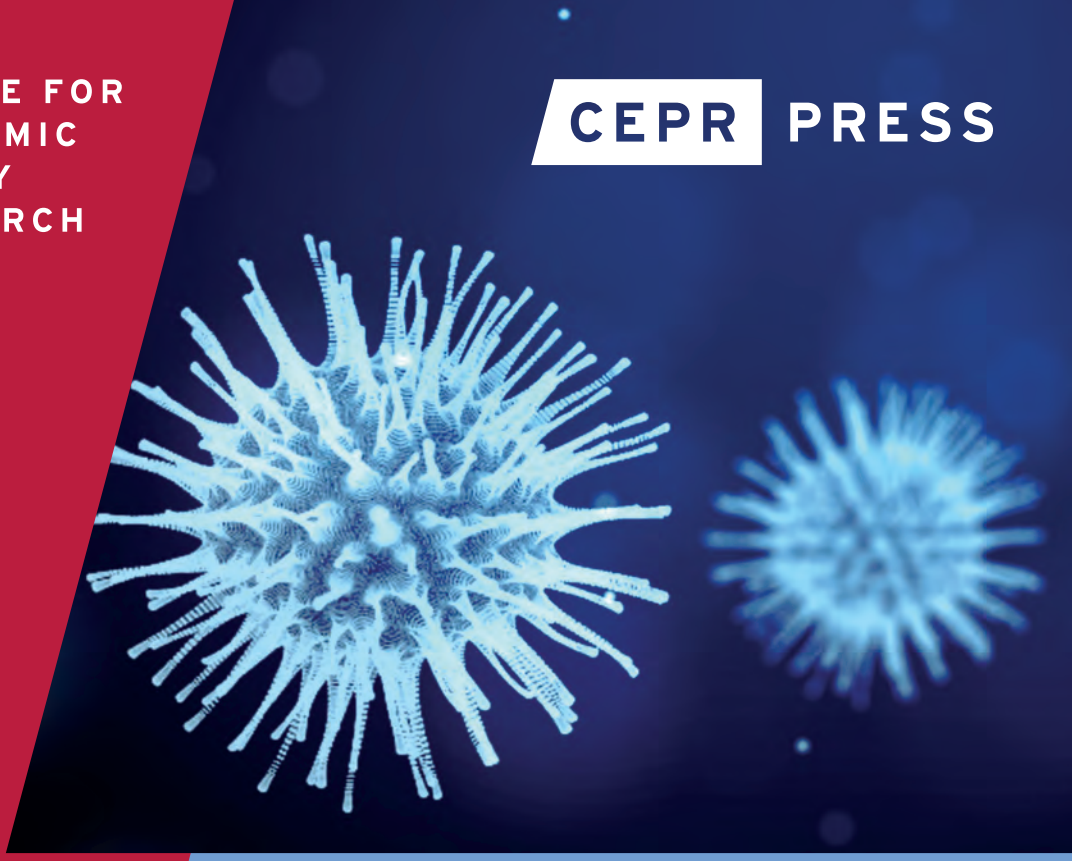

COVID ECONOMICS

VETTED AND REAL-TIME PAPERS

ISSUE 13
4 MAY 2020

TESTING VS. QUARANTINE
David Berger, Kyle Herkenhoff and Simon Mongey

WHO GETS SICK IN NYC?
Milena Almagro and Angelo Orane-Hutchinsonn

CULTURAL AND ECONOMIC DISCRIMINATION
Annie Tubadji, Don J Webber and Fred Boy

TARGETING WHO STAYS AT HOME
Neha Bairoliya and Ayse Imrohoroglu

DARK TRADING
Gbenga Ibikunle and Khaladdin Rzayev

LOCKDOWN AND TESTING EFFECTS
Akbar Ullah and Olubunmi Agift Ajala

VOLUNTARY DISTANCING
William Maloney and Temel Taskin

STARTUPS: ACHILLE'S HEEL?
Petr Sedláček and Vincent Sterk

Covid Economics
Vetted and Real-Time Papers

Covid Economics, Vetted and Real-Time Papers, from CEPR, brings together formal investigations on the economic issues emanating from the Covid outbreak, based on explicit theory and/or empirical evidence, to improve the knowledge base.

Contact: Submissions should be made at https://portal.cepr.org/call-papers-covid-economics-real-time-journal-cej. Other queries should be sent to covidecon@cepr.org.

The Centre for Economic Policy Research (CEPR)

The Centre for Economic Policy Research (CEPR) is a network of over 1,500 research economists based mostly in European universities. The Centre's goal is twofold: to promote world-class research, and to get the policy-relevant results into the hands of key decision-makers. CEPR's guiding principle is 'Research excellence with policy relevance'. A registered charity since it was founded in 1983, CEPR is independent of all public and private interest groups. It takes no institutional stand on economic policy matters and its core funding comes from its Institutional Members and sales of publications. Because it draws on such a large network of researchers, its output reflects a broad spectrum of individual viewpoints as well as perspectives drawn from civil society. CEPR research may include views on policy, but the Trustees of the Centre do not give prior review to its publications. The opinions expressed in this report are those of the authors and not those of CEPR.

Editorial Board

Ethics

Covid Economics will publish high quality analyses of economic aspects of the health crisis. However, the pandemic also raises a number of complex ethical issues. Economists tend to think about trade-offs, in this case lives vs. costs, patient selection at a time of scarcity, and more. In the spirit of academic freedom, neither the Editors of *Covid Economics* nor CEPR take a stand on these issues and therefore do not bear any responsibility for views expressed in the journal's articles.

Covid Economics
Vetted and Real-Time Papers

Issue 13, 4 May 2020

Contents

An SEIR infectious disease model with testing and conditional quarantine 1
David Berger, Kyle Herkenhoff and Simon Mongey

The determinants of the differential exposure to COVID-19 in New York City and their evolution over time 31
Milena Almagro and Angelo Orane-Hutchinson

Cultural and economic discrimination by the Great Leveller: The COVID-19 pandemic in the UK 51
Annie Tubadji, Don J Webber and Fred Boy

Macroeconomic consequences of stay-at-home policies during the COVID-19 pandemic 71
Neha Bairoliya and Ayse Imrohoroglu

Volatility, dark trading and market quality: Evidence from the 2020 COVID-19 pandemic-driven market volatility 91
Gbenga Ibikunle and Khaladdin Rzayev

Do lockdown and testing help in curbing Covid-19 transmission? 138
Akbar Ullah and Olubunmi Agift Ajala

Determinants of social distancing and economic activity during COVID-19: A global view 157
William Maloney and Temel Taskin

Startups and employment following the COVID-19 pandemic: A calculator 178
Petr Sedláček and Vincent Sterk

CEPR PRESS

Covid Economics **Issue 13, 4 May 2020**

An SEIR infectious disease model with testing and conditional quarantine[1]

David Berger,[2] Kyle Herkenhoff[3] and Simon Mongey[4]

Date submitted: 28 April 2020; **Date accepted:** 29 April 2020

We extend the baseline Susceptible-Exposed-Infectious-Recovered (SEIR) infectious disease epidemiology model to understand the role of testing and case-dependent quarantine. During a period of asymptomatic infection, testing can reveal infection that otherwise would only be revealed later when symptoms develop. Along with those displaying symptoms, such individuals are deemed known positive cases. Quarantine policy is case-dependent in that it can depend on whether a case is unknown, known positive, known negative, or recovered. Testing therefore makes possible the identification and quarantine of infected individuals and release of non-infected individuals. We fix a quarantine technology—a parameter determining the differential rate of transmission in quarantine—and compare simple testing and quarantine policies. We start with a baseline quarantine-only policy that replicates the rate at which individuals are entering quarantine in the US in March, 2020. We show that the total deaths that occur under this policy can occur under looser quarantine measures and a substantial increase in random testing of asymptomatic individuals. Testing at a higher rate in conjunction with targeted quarantine policies can (i) dampen the economic impact of the coronavirus and (ii) reduce peak

1 We thank David Dam, Meghana Gaur and Chengdai Huang for excellent research assistance. The views expressed in this study are those of the author and do not necessarily reflect the position of the Federal Reserve Bank of New York or the Federal Reserve System.
2 Associate Professor of Economics at Duke, University.
3 Senior Economist, Federal Reserve Bank of New York; Assistant Professor, University of Minnesota.
4 Assistant Professor, Kenneth C. Griffin Department of Economics, University of Chicago.

Covid Economics 13, 4 May 2020: 1-30

symptomatic infections—relevant for hospital capacity constraints. Our model can be plugged into richer quantitative extensions of the SEIR model of the kind currently being used to forecast the effects of public health and economic policies.

Covid Economics 13, 4 May 2020: 1-30

"Once again, our key message is: test, test, test."
— @WHO, March 16, 2020

"We suggest a strategy of massive testing that goes far beyond the group currently being tested — those most likely infected. Instead, we need to test as many people as possible. If we know who is infected, who is not and who has recovered, we could greatly relax social isolation requirements and send both the uninfected and the recovered back to work."
— Searchinger (Princeton), LaManita (Virginia Tech.), Douglas (Cornell Med.), March 23, 2020, Washington Post

Introduction

The goal of this paper is to better understand the role of testing asymptomatic cases and targeted quarantine in the trajectory of the coronavirus pandemic. To do so, we incorporate incomplete information in the textbook SEIR model (Susceptible-Exposed-Infectious-Recovered) (Kermack and McKendrick, 1927)[1], which allows researchers to study potential policies that vary depending on whether an individual case is an unknown, known positive, known negative, or recovered (see Figure 1). This extension allows unknown, asymptomatic cases to be resolved by testing and allows researchers to understand the trade-off between *quarantining everyone* at large social cost versus *testing everyone* and applying quarantine in a more directed fashion.

We include the minimal necessary modifications of the SEIR model in order to be able to address the public health effects of testing asymptomatic cases while stilling nesting the SEIR model. In the SEIR model an individual may be characterized as being in one of four health states: susceptible (S), exposed (E), infected (I) and recovered (R). Since our aim is to try to understand the role of asymptomatic transmission and how testing and / or quarantine of asymptomatic cases can effect the prorogation of infection and mortality, our key modifications therefore make policies contingent on what is known about an individual. With incomplete information, an individual that has contracted the corona virus, but is yet to present symptoms, will be infectious and subject to the quarantine rule for unknown cases. If tested, however, the true health state of the individual is revealed and they are subject to the same quarantine rules as known positive cases. Similarly such an individual, if untested, cannot be subject to quarantine policies that apply to known positive cases.

We calibrate the model to data on the spread of the coronavirus and medical outcomes. As a baseline we simulate the model without policy interventions, which delivers the same trajectory for the pandemic as the SEIR model. We then consider a benchmark counterfactual with common quarantine measures and no testing. We then ask the question, *If we increase testing, how much can we relax quarantine measures while making sure that deaths do not increase?* We show that increasing testing can accommodate extensive relaxation of quarantine measures. If we assume that economic output, and social well-being are inversely proportional to the number of individuals quarantined, this implies that testing asymptomatic individuals can result in a pandemic with smaller economic losses and social costs while keeping the human cost constant.

[1]Recent empirical evidence from random samples drawn in an Italian town suggest that around 50 to 75 percent of infected cases are asymptomatic: Link to La Repubblica article, March 16, 2020.

Covid Economics 13, 4 May 2020: 1-30

CEPR PRESS

A. Information – No testing

	Asymptomatic	Symptomatic
Not infected	Unknown	-
Infected		Positive

B. Information - Testing

	Asymptomatic	Symptomatic
Not infected	Negative	-
Infected	Positive	Positive

C. Example of targeted policies – No testing

	Asymptomatic	Symptomatic
Not infected	Partial	-
Infected	quarantine	Full quarantine

D. Example of targeted policies – Testing

	Asymptomatic	Symptomatic
Not infected	Release	-
Infected	Full quarantine	

Figure 1: Incomplete information, testing, and an example of targeted quarantine policies

Covid Economics 13, 4 May 2020: 1-30

Our analysis comes with a number of important caveats. First and more importantly, we are not epidemiologists. After consulting with epidemiologists and doing a thorough literature review, however, we concluded there was not a framework for discussing some of the pressing public health policy questions of the early quarantine period: in particular the potential role of broad testing in ameliorating quarantine measures.[2] Some models feature testing conditional on developing symptoms which allows for better care and reduced mortality, but to the best of our knowledge no models considered testing asymptomatic individuals so that positive cases can be recognized and isolated.

Second, our model does not feature the full set of features that one would desire in order to make quantitative statements and predictions. These would include transmission across geography, an age distribution of individuals with systematically different probabilities of infection conditional on contact with a positive case, or non-perfect testing (false negatives). We also do not model the *medical care* block in detail and abstract from issues such as congestion of medical services as in the standard SEIR model. Our hope for this paper is that it demonstrates that incomplete information, testing and conditional policies can be simply and intuitively integrated into richer models. We view the technical and computational costs low relative to the payoffs.[3]

Third, for most of this paper we fix an *effectiveness* of quarantine in reducing meeting rates of individuals. We assume that complete isolation is off the table, however note here that improving quarantine would have large effects. Therefore our exercise should be interpreted as follows: given access to a quarantine technology of some fixed effectiveness, how does testing allow that technology be applied differently across individuals, potentially mitigating costs of the pandemic. A different paper could be written on the quantitative effects of increasing the effectiveness of quarantine. In Section 7 we repeat our main counterfactual under a more effective quarantine and show how testing allows quarantine measures to be relaxed even further.

Finally, our model is *not* a behavioural economic model that integrates an epidemiological model as in Kremer (1996) or the equilibrium model of Greenwood, Kircher, Santos, and Tertilt (2019). We think understanding the role

[2]We could of course be wrong. Moreover, we do not wish to implicate any of the epidemiologists who graciously answered our questions and read this draft if we indeed are. We would be very happy to learn from medical professionals and epidemiologists that we have misread the literature and that this has been studied before.

[3]Specifically, while the SIER model augmented for quarantine would have 8 states—the 4 S-E-I-R states each augmented for quarantine and non-quarantine—our model requires 12 states, with the additional 4 states reflecting the information structure of the model.

Covid Economics 13, 4 May 2020: 1-30

of testing in information acquisition should be key to any such integration. A simple S(E)IR model integrated into an economic model with only common (non-targeted) quarantine / lock-down policies available will *unavoidably* lead to a trade-off between mortality and economic activity. More quarantine, less mortality, and vice versa. By increasing testing of asymptomatic cases and conditional quarantine, we show that the model can deliver constant mortality rates and higher economic activity, as measured by the fraction of individuals who are healthy and out of quarantine. Theories of economic-activity vs. mortality trade-offs with only a lock-down policy available to the policy-maker are therefore discussions of second best policies, while testing presents a potentially better option.

This paper has seven sections. Section 1 reviews the related SEIR literature and recent papers using this model to quantify the effects of the corona virus pandemic. Section 2 reviews some of the data regarding infection and mortality, as well as policy responses in the form of testing and quarantine measures. Section 3 describes the model. Section 4 provides details of how we calibrate the model and provides baseline simulations of the pandemic under no policy response. This replicates the familiar trajectories of infection and mortality of SEIR models that have been used to model the evolution of the pandemic. Section 5 provides our main counterfactuals, where we compare the consequences of *common quarantine and no testing* with *targeted quarantine and testing* policies. Section 7 repeats these counterfactuals under a more effective quarantine technology. Section 8 concludes.

1 Literature review

Brauer and Castillo-Chavez (2012) provide a summary of recent SEIR models. SEIR stands for Susceptible, Exposed (people not yet infectious), Infectious, and Removed (quarantined or immune). In particular, they discuss frameworks of quarantine (setting aside individuals who are exposed) and isolation (setting aside individuals who are infected, often called hospitalization).

A recent policy paper by Imperial College COVID-19 Response Team (2020) incorporates several policy parameters into an SEIR model that is enriched to accommodate geographical transmission and age dependency of transmission and mortality rates.[4] In particular, they consider a model with quarantine, asymptomatic patients, and testing of *hospitalized* patients, with policy thresholds that depend on positive test rates. Their predictions have been reported widely in the press. Our contribution is to model (i) the matching process between different subgroups, thus endogenizing R_0, and (ii) highlighting the importance of *testing asymptomatic patients* and, (iii) quarantine policies that are contingent on the testing outcomes. Lastly, we use our measure of the fraction of individuals quarantined as a measure of loss of economic activity. This allows us to evaluate the role of widespread testing which, as a policy, may have a similar mortality rates but lower quarantine rates.

Recent examples of testing and diagnosis in an SEIR model include Chowell, Fenimore, Castillo-Garsow, and Castillo-Chavez (2003) who model the Severe acute respiratory syndrome (SARS) epidemic in 2002. The purpose of testing and diagnosis in Chowell, Fenimore, Castillo-Garsow, and Castillo-Chavez (2003) is an improvement in healthcare, which reduces the rate of recovery from nearly one half.[5] In our model, the role for testing and

[4] At the time of writing the codes for Imperial College COVID-19 Response Team (2020) were not publicly available, and the paper does not feature any equations that would allow a researcher to replicate their model.

[5] They report a SARs incubation period of 2 to 7 days, with most infected individuals either recovering after 7 to 10 days, or dying. The

Covid Economics 13, 4 May 2020: 1-30

diagnosis is being able to efficiently target quarantine measures. Contemporaneous work by Hornstein (2020) and Piguillem and Shi (2020) also consider various testing policies in an SEIR model.

Recent examples of quarantine in an SEIR model include Feng (2007) who derive closed form expressions for the maximum and final rates of infection. Feng (2007) has two notions of quarantine: one in which exposed individuals (who may not be infectious) are set aside, and another in which infectious individuals are set aside (often discussed as hospitalization). In our model, quarantine is similarly case dependent, but can only depend on observed health status. Exposed individuals that do not display symptoms cannot be quarantined without being identified in a random testing of asymptomatic individuals.

Empirically, the literature has begun to document the rate of transmission and incubation periods. Wu, Leung, and Leung (2020) compile a summary of $\mathcal{R}_0$ across various viruses (SARS-CoV, MERS-CoV, Commonly circulating human CoVs (229E, NL63, OC43, HKU1)), and estimate an SEIR model with international outflows. Using data from Wuhan, they report an $\mathcal{R}_0$ of 2.68, and an incubation period of 6.1 days. The World Health Organization (2020) report that the time from symptom recovery to detection fell from 12 days in early January to 3 days in early February 2020. After symptom onset, it typically takes 2 weeks for a mild case to recover, or 3 to 6 weeks for severe cases.

The applied literature has also begun to document the role of quarantine in reducing transmission, and the rate of asymptomatic transmission. Kucharski, Russell, Diamond, Liu, Edmunds, Funk, Eggo, Sun, Jit, Munday, et al. (2020) estimate that in China, the basic reproductive rate $\mathcal{R}_0$ fell from 2.35 one week before travel restrictions on Jan 23, 2020, to 1.05 one week after travel restrictions. They use an SEIR model and estimated on this data to forecast the epidemic in China, extending the model to explicitly account for infections arriving and departing via flights. Using data from Wuhan, Wang et al (2020) report a baseline reproductive rate of 3.86, that fell to 0.32 after the vast lock-down intervention. They also find a high rate of asymptomatic transmission, leading us to consider the asymptomatic state to be infectious as opposed to the baseline SEIR model which assumes that the 'exposed' state is non-infectious.[6] A high rate of asymptomatic carry of the virus has been identified in Iceland, one of the few countries to adopt random testing of asymptomatic individuals.[7]

In the recent economics literature Atkeson (2020b) provides a review of the SIR model. Fenichel (2013) compares social planner and decentralized solutions for lock-down in an SIR model where all individuals recover. Alvarez, Argente, and Lippi (2020), and Farboodi, Jarosch, and Shimer (2020) study optimal lock-down policy in an SIR model with the possibility of death. The latter compares the solution of the planner's problem to a decentralized equilibrium in which individuals choose their level of engagement with the economy understanding the health risks they face. Eichenbaum, Rebelo, and Trabandt (2020) and Glover, Heathcote, Krueger, and Ríos-Rull (2020) nest a similar SIR model in quantitative general equilibrium macroeconomic models of consumption, savings and labor supply. The latter includes heterogeneity by age, income and assets with age-varying transmission and mortality risk. These papers consider lock-down as the only available tool to the policy-marker. Our contri-

SARS mortality rate is 4 percent or more. They estimate a basic reproductive number $R_0 = 1.2$. They model a diagnosis rate and diagnosed state. Individuals recover at a fast rate if diagnosed (8 days without diagnosis, 5 days with diagnosis).

[6] https://www.medrxiv.org/content/10.1101/2020.03.03.20030593v1

[7] https://www.buzzfeed.com/albertonardelli/coronavirus-testing-iceland. "Early results from deCode Genetics indicate that a low proportion of the general population has contracted the virus and that about half of those who tested positive are non-symptomatic".

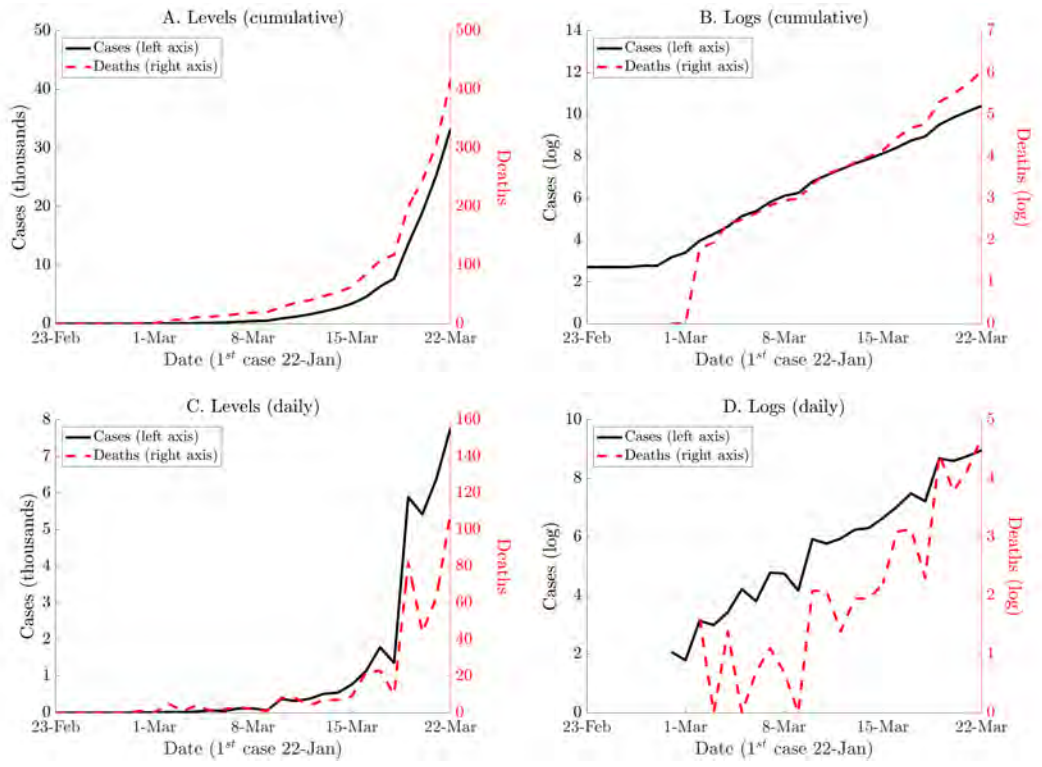

Figure 2: US cumulative cases and deaths - 4 weeks up to March 22

Notes: Source: John Hopkins CSSE, https://github.com/CSSEGISandData/COVID-19. Data reflect non-repatriated cases, and so exclude the cases from the Diamond Princess and Grand Princess cruise ships.

bution is to enrich the underlying SEIR by introducing scope for testing policies which may mitigate the output costs of quarantine policies while not exacerbating the decline in output. It would be relatively straight-forward to integrate the information structure of our model into these models in order to evaluate the economic benefits of broad based testing.

2 Data on cases, deaths, quarantine and testing

This section provides a short overview of the evolution of the coronavirus pandemic in the United States.

Cases. The first case was reported in the U.S. on January 22, 2020. Figure 2 plots the evolution of confirmed cases and deaths resulting from COVID-19.[8] Table 1 reports the growth rate of cases (new cases divided by cumulative

[8]We include our tabulations of the source data on our websites. At the moment data on recoveries is not particularly accurate, however we can add this later.

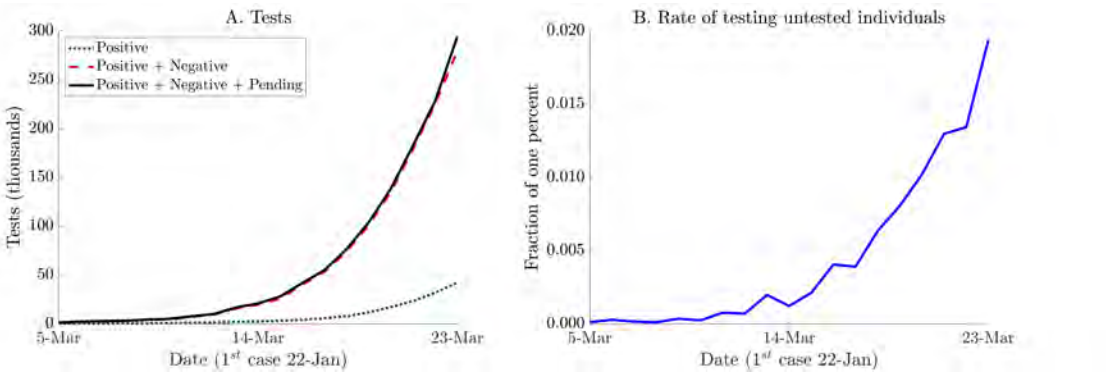

Figure 3: US testing

Notes: Source: John Hopkins CSSE, https://github.com/CSSEGISandData/COVID-19. Panel B plots the fraction of the untested population that is tested each day. Let T_t be total cumulative tests—the black line in Panel A—, then Panel B plots $(T_t - T_{t-1})/(340m - T_t)$. The y-axis of Panel B is in fractions of one percent, i.e. 0.01 on the y-axis corresponds to a daily testing rate of 0.01 percent.

cases) using different measurements. There are several dates with outlier growth rates due to testing rollouts. The growth rate of cases is roughly 40 percent with these outliers included, and closer to 30 percent when we exclude the outliers. Due to the lack of testing, the growth rate of cases in January and February is zero, thus lowering the overall growth rate of cases significantly.

Deaths. Figure 2 also plots the number of deaths and the cumulative number of deaths. Similar to the number of cases, the number of deaths is stagnant prior to March. It then grows at a high rate with pronounced spikes. The average growth rate in deaths is 48 percent per day, but also includes significant outliers due to sudden changes in reporting.

Testing. Figure 3 reports cumulative tests and the testing rate per day. At its peak to date, the US tested just short of 0.02 percent of its untested population in a single day. We will use this rate to benchmark the rates of testing considered in counterfactuals. In particular we will consider testing rates that are significantly higher than what we currently observe in the United States.

Quarantine. Table 2 reports the fraction of individuals who are quarantined in the United States. There are large discrete jumps in the quarantine rate when California, New York, and Illinois announced state-wide shelter in place orders.[9] This is another important policy parameter. We must convert this series into a daily quarantine rate. Roughly 24% of the population was quarantined over the course of 19 days since March 4, 2020. We approximate this with a quarantine rate of roughly 1% per day. More quarantines have followed rapidly *during* the writing of this article.

[9]We will refer to New York's policy as shelter-in-place, despite alternative language used by the government of New York.

Covid Economics 13, 4 May 2020: 1-30

Table 1: US average daily growth rate of cases

Since first case on 1/22	21.2%
March - From 1st to 19th	40.8%
March - From 1st to 19th - Exclusing outliers with rates $\geq$ 50%	31.1%

Source: Derived from data available from John Hopkins CSSE, https://github.com/CSSEGISandData/COVID-19.

Table 2: US quarantine

Date	Event	Quarantined	Frac. of US Pop.
3/4/2020		0	0.00%
3/10/2020	New Rochelle	79,946	0.02%
3/16/2020	Bay Area	6,747,000	1.98%
3/19/2020	California	39,639,946	11.66%
3/21/2020	Illinois, New Jersey	61,193,957	17.99%
3/22/2020	New York	80,647,518	23.72%

Source: Dates of enactment taken from various news outlets

3 Model

Throughout this section Figure 4 and Figure 5 may be useful to the reader. Figure 4 maps our model of *transmission* into the SEIR model. Figure 5 overlays this with our model of *information* and testing.

3.1 Overview

We make five modifications to the standard SEIR model.

1. **Health states.** As shown in Figure 4 we relabel these states in order to make a later distinction in terms of testing and quarantine. These we call *health states*. We allow for the possibility that the *exposed* state is infectious in order to introduce asymptomatic transmission into the model.

   i. Non-infected, Asymptomatic (NA) - Individuals that have not been exposed to the virus, and are by definition asymptomatic. This corresponds to **S** in the SEIR model: *Susceptible.*

   ii. Infected, Asymptomatic (IA) - Individuals that have met an infected individual but are as yet asymptomatic. This corresponds to **E** in the SEIR model: *Exposed.* Relative to the SEIR model we allow that these individuals may also transmit the virus albeit at a lower frequency.

   iii. Infected, Symptomatic (IS) - Individuals that have met an infected individual and are now showing symptoms. This corresponds to **I** in the SEIR model: *Infectious.*

   iv. Recovered, Asymptomatic (RA) - Infected individuals that have entered the recovery phase and are no longer infected. As in the textbook SEIR model we assume these individuals are immune.[10] This corresponds to **R** in the SEIR model: *Recovered.*

[10]To the best of our knowledge there is no empirical evidence regarding immunity following COVID-19. A quantitative version of this model would want to take this into account. This is not the point of departure studied in this paper.

Covid Economics 13, 4 May 2020: 1-30

CEPR PRESS

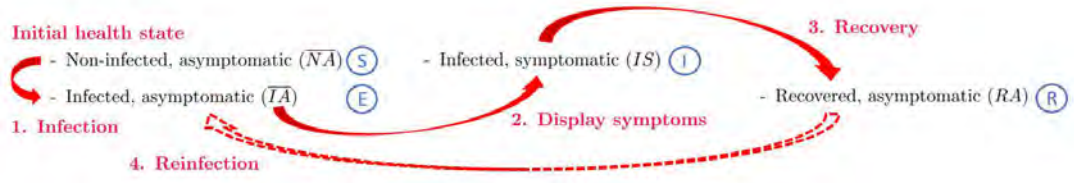

Figure 4: Transmission and the relationship between our model and the SEIR model

Notes: This figure shows how our states map into the SEIR model. To understand the role of testing we group the *asymptomatic* states S, E and label these *Non-infected,Asymptomatic* (NA) and *Infected, Asymptomatic* (IA). Without testing, authorities nor individuals are able to differentiate between these states. To denote this lack of information, we put a bar over them: $\overline{NA}, \overline{IA}$. Exposed individuals show symptoms, which is the I state of the SEIR model. We label this *Infected, Symptomatic* (IS). Individuals may then recover, which is the R state of the SEIR model. We label this *Recovered, Asymptomatic* (IA).

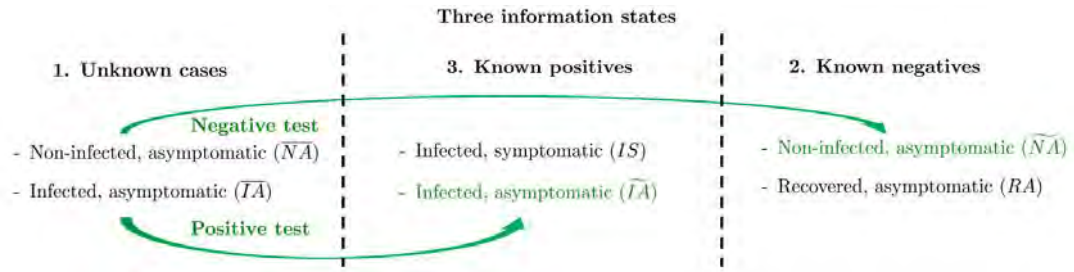

Figure 5: SEIR model with incomplete information and testing of asymptomatic individuals

Notes: This figure augments Figure 4 to show how we extend the SEIR model to accommodate testing and incomplete information. We add two additional states that can be revealed by testing, which differentiate asymptomatic individuals $\{\overline{NA}, \overline{IA}\}$. We denote these with a tilde: $\widetilde{IA}$ for identified infected, asymptomatic cases, and $\widetilde{NA}$ for identified non-infected, asymptomatic cases. We assume that symptomatic cases IS are instantly identifiable so are *known positives*, and that recovered cases have been tracked such that RA cases are *known negatives*.

Figure 4 tracks an individual case through these states. In terms of *medical transmission*, we assume that *infected* individuals are contagious, although with different rates of transmission. The different rates of transmission nest the case that only IS individuals can transmit the disease, which is the case in the SEIR model. *Non-infected* individuals cannot transmit the disease $\{NA, RA\}$.

The medical block of the model is very simple and could be enriched in many ways.[11] Following the standard SEIR model: (i) infected asymptomatic individuals show symptoms at rate δ, (ii) infected, symptomatic individuals recover at rate ω^R and die at rate ω^D. Note that all individuals that become infected show symptoms at some point, this could be relaxed.

2. **Incomplete information.** We allow for incomplete information, as described in Figure 5. In terms of policy,

[11] See http://gabgoh.github.io/COVID/index.html by Gabriel Goh for an example of an SEIR model of *Transmission Dynamics* that appends a rich model of *Clinical Dynamics* which models hospitalization, length of hospital stay, and more. These states would intercede between IS, RA and D, which is not the focus of this paper.

Covid Economics 13, 4 May 2020: 1-30

Covid Economics 13, 4 May 2020: 1-30

we assume that unless tested, individuals without symptoms are indistinguishable and so must be treated in the same way by quarantine policy. To achieve this we distinguish between two types of NA and IA individuals. Adding these new cases in green to Figure 4 gives Figure 5. In the first case the diagnosis regarding infection is unknown. These are *unknown cases* which we denote $\overline{NA}$ and $\overline{IA}$. In the second case the diagnosis regarding infection is known, which we denote $\widetilde{NA}$ and $\widetilde{IA}$. This information structure implies that testing and quarantine policies can not distinguish between the following pairs of cases: unknown cases $\{\overline{NA}, \overline{IA}\}$, known positives $\{\widetilde{IA}, IS\}$, and known negatives $\{\widetilde{NA}, RA\}$. Our assumption that $\{\widetilde{NA}, RA\}$ are not distinguishable is a simplifying assumption in order to maintain a finite set of states, which we discuss below.

3. **Meeting and transmission rates.** We assume that the underlying parameters consist of an explicit interaction of *social meeting rates*, which are mutable to quarantine / social distancing policies, and *medical transmission rates*, which are the medical rates of transmission between two individuals that meet.

   We denote quarantine and non-quarantine states by Q and NQ, respectively. Interacted with our 4 health states, plus two additional information states, this gives 12 total states that individuals can be in. The *meeting rates* of non-quarantined individuals is given by λ, and for quarantined individuals by λ^Q. We interpret the ratio factor by which quarantine reduces the rate of social interaction (λ/λ^Q) as the *quarantine technology* and treat it as a parameter.

   We denote the *transmission rates* by $\rho^A(\rho^S)$ for asymptomatic (symptomatic) cases to accommodate evidence that transmission rates are higher in symptomatic cases. These give the probability that, conditional on meeting an infected case $(\overline{IA}, \widetilde{IA}, IS)$, a non-infected individual $(\overline{NA}, \widetilde{NA})$ becomes infected. Crucially, individuals do not know who is infected, and do not know that they have met an infected person.[12]

4. **Testing.** We introduce a role for testing. Our information structure has assumed that when symptoms present, the individual and society know that the individual is infected. In this paper we do not cover testing of symptomatic individuals, although this is obviously a hugely important area.[13] We assume that testing of asymptomatic individuals takes place at a rate τ. Testing fully reveals an individual's health state. Tests do not produce false negatives or false positives.

   An issue arises in that individuals who have previously tested negative can become infected. This would require them to transition to either $\widetilde{IA}$ or $\overline{IA}$. If we assume either, then they move into a different group for the purpose of policy. However the transition would not be observed since the individual remains asymptomatic. Addressing this completely would require significantly enriching the model.[14] To avoid this, and

[12] This seems like a reasonable assumption to us despite one of the requisites for testing in many countries being that individuals can identify an infected individual that they interacted with.

[13] Note that in our model if we were to test symptomatic individuals then all tests would yield positives. In the data a small fraction of tests yield positives. In the US our interpretation of this is not that the US is testing asymptomatic people, but rather that individuals with similar symptoms due to common colds and the flu are being tested. To introduce testing of symptomatic individuals one would really want to extend the model to introduce an additional disease that presents observationally identical symptoms that can then be separated by testing.

[14] A richer model would include something like the following. Individuals tests are viewed as 'good' for some number of days. Policies may therefore apply to individuals who were tested in, say, the 'last 60 days'. It is understood that some of these individuals would become infected and this would not be observed unless re-tested or symptoms develop. Given the law of large numbers, one could write down the

in the spirit of this paper being a first step, we assume that testing has a 'tagging' property, such that the transition from $\widetilde{NA}$ to $\widetilde{IA}$ is observed. We highlight this in the notes to Table 3.

5. **Conditional quarantine.** We allow for quarantine policy and restrict this to depend on the *observable* health state of the individual. To keep the Markovian structure of the SEIR model, we quarantine individuals at constant rates. When there is no testing, individuals are moved from non-quarantine (NQ) to quarantine (Q) at rates ξ^u, ξ^+, ξ^r, for unknown, known positive and recovered cases. When there is testing, individuals are moved from non-quarantine (NQ) to quarantine (Q) at rates ξ^u, ξ^-, ξ^+, ξ^r, for unknown, known negative, known positive, and recovered cases, where now the known positive cases include $\widetilde{IA}$ individuals. We assume a set of corresponding rates at which individuals are *released* from quarantine: r^u, r^-, r^+, r^r.

3.2 Transmission

Given the above description of the model, we now describe transition rates of individuals between states. We work in continuous time and when simulating the model we consider a discrete time approximation in which a period is one hour and days are 14 hours long.

States. Individuals in the model are in one of 13 states:

- {Non-infected & Asymptomatic}×{Quarantine, Non-quarantine}×{Unknown, Known negative} → 4 states
- {Infected & Asymptomatic}×{Quarantine, Non-quarantine}×{Unknown, Known positive} → 4 states
- {Infected & Symptomatic} ×{Quarantine, Non-quarantine} → 2 states
- {Recovered & Aymptomatic} ×{Quarantine, Non-quarantine} → 2 states
- Deceased → 1 state

There is initially a distribution of a unit mass of individuals. When we simulate the model, we will assume that these individuals are non-quarantined, asymptomatic and unknown cases, with a small number being infected: $\overline{NA}, NQ$ and $\overline{IA}, NQ$. We denote the mass of individuals in a state X in period t by M_t^X.

Social interaction. In order to transmit the disease, individuals must first meet. We assume random matching. Non-quarantined individuals meet other individuals at rate λ, while quarantined individuals meet others at rate λ^Q. To save on notation we use, for example, NA to denote both $\overline{NA}$ and $\widetilde{NA}$ when distinguishing between the two is not relevant.

The conditional probabilities of meetings are as follows. The mass of individuals that are out in the world to bump into is given by M_t, and depends on the mass of individuals that are quarantined and non-quarantined:

$$M_t = \lambda M_t^{NQ} + \lambda^Q M_t^Q.$$

law of motion for the fraction of 'tested negatives' that have since become positive. In this model individuals would require re-testing to keep track of the pandemic, a clear necessary extension of this model in order to use it quantitatively.

Covid Economics 13, 4 May 2020: 1-30

The masses of non-quarantined and quarantined individuals are given by:

$$M_t^{NQ} = M_t^{NA,NQ} + M_t^{IA,NQ} + M_t^{IS,NQ} + M_t^{RA,NQ} \quad ,$$
$$M_t^{Q} = M_t^{NA,Q} + M_t^{IA,Q} + M_t^{IS,Q} + M_t^{RA,Q}.$$

Conditional on meeting an individual, the probability that the individual is infected (non-infected) is given by π_t^I (π_t^N):

$$\pi_t^I = \frac{M_t^I}{M_t} = \frac{\lambda M_t^{I,NQ} + \lambda^Q M_t^{I,Q}}{M_t} = \frac{\lambda\left[M_t^{IA,NQ} + M_t^{IS,NQ}\right] + \lambda^Q\left[M_t^{IA,Q} + M_t^{IS,Q}\right]}{M_t} \quad ,$$
$$\pi_t^N = \frac{M_t^N}{M_t} = \frac{\lambda M_t^{A,NQ} + \lambda^Q M_t^{A,Q}}{M_t} = \frac{\lambda\left[M_t^{NA,NQ} + M_t^{RA,NQ}\right] + \lambda^Q\left[M_t^{NA,Q} + M_t^{RA,Q}\right]}{M_t}.$$

Conditional on meeting an infected individual, the probability that the infected individual is symptomatic (asymptomatic) is given by π_t^{IA} (π_t^{IS}):

$$\pi_t^{IA} = \frac{\lambda M_t^{IA,NQ} + \lambda^Q M_t^{IA,Q}}{M_t^I} \quad , \quad \pi_t^{IS} = \frac{\lambda M_t^{IS,NQ} + \lambda^Q M_t^{IS,Q}}{M_t^I}.$$

Infection. When individuals meet an infected individual, they become infected with probability ρ^A (ρ^S) if the individual they meet is asymptomatic (symptomatic). Once infected, an individual does not know that they are infected as they are initially asymptomatic. A test, which occurs at rate τ, would reveal that they are infected, and the subject to quarantine policies of infected individuals. We assume that infected individuals all show symptoms and do not transition straight to a recovery.[15] Infected, asymptomatic, individuals show symptoms at a rate δ. Infected symptomatic individuals then recover at rate ω^R and die at rate ω^D. Recovered individuals gain complete immunity in our experiments.

Transmission rate. Combining the above, the rate of infection of a quarantined (non-quarantined) person is given by $\lambda^Q\alpha_t$, $(\lambda\alpha_t)$, where α_t is the probability of infection conditional on a random meeting:

$$\alpha_t = \pi_t^I\left[\pi_t^{IS}\rho^S + \pi_t^{IA}\rho^A\right].$$

Note that the infection rate can be written

$$\lambda\alpha_t = \left(\rho^S\lambda\right) \times \pi_t^I\left[\pi_t^{IS} + \pi_t^{IA}\left(\frac{\rho^A}{\rho^S}\right)\right].$$

[15] This is to avoid the issue of having *recovered* individuals that do not know that they were ever infected. We plan to extend this later on. The issue with this possibility is that we proliferate the state-space, adding a new state of Recovered, Uninformed, Asymptomatic. This will be *different* to Non-infected, Uninformed, Aysmptomatic, due to the different immunity properties of the Recovered individual. Such a recovered individual can then become infected, and so on and so forth, creating infinitely many states. Our assumption that all infected individuals eventually know that they are infected by showing symptoms, and then know that they have recovered keeps the state-space finite while still allowing for the key addition of asymptomatic transmission and incomplete information.

Covid Economics 13, 4 May 2020: 1-30

Data on the rate of transmission alone will be insufficient to separately identify ρ^S and λ, although below we discuss how variation in quarantine policy may be able to estimate these separately in future research.

3.3 Transition rates

As an example of the mechanics of the model, we describe the full set of transition rates for non-infected asymptomatic individuals, and infected asymptomatic individuals. These are the two cases that can be distinguished by testing asymptomatic individuals. Table 3 provides transition rates between all 13 states. Along with initial conditions for the distribution of individuals across health and information states is sufficient to simulate the model.

3.3.1 Non-infected, asymptomatic individuals

We consider this state as all non-infected individuals in the model are assumed to begin in one of these states. There are four possible states for non-infected, asymptomatic individuals. They can be an *unknown* or *known negative* case, and they can be *non-quarantined* or *quarantined*.

1. Consider an individual that is an unknown case and non-quarantined: $\overline{NA}, NQ$.
   - **Quarantine -** At rate ξ^u they take up quarantine and transition to $\overline{NA}, Q$
   - **Infection -** At rate λ they meet a random individual. With probability $\pi_t^I \pi_t^{IS}$ $\left(\pi_t^I \pi_t^{IA}\right)$ that individual is infected and symptomatic (asymptomatic). The individual then becomes $\overline{IA}, NQ$ with probability $\rho^S\left(\rho^A\right)$ depending on who the meeting is with. The total transition rate to $\overline{IA}, NQ$ is therefore $\lambda\alpha_t$.
   - **Testing -** At rate τ, they are tested and since tests are perfect, learn they are not infected, so transition to being a known negative case: $\widetilde{NA}, NQ$.
2. Consider an individual that is an unknown case and quarantined: $\overline{NA}, Q$.
   - **Quarantine -** At rate r^u they are released from quarantine and transition to $\overline{NA}, NQ$.
   - **Infection -** The rate of infection is lower in quarantine: $\lambda^Q\alpha_t \leq \lambda\alpha_t$.
   - **Testing -** At rate τ, they are tested, learn they are not infected, and transition to being a known negative case: $\widetilde{NA}, Q$.
3. Consider an individual that is a known negative case and non-quarantined: $\widetilde{NA}, NQ$
   - **Quarantine -** Since they are recognized as a negative case they may be quarantined at a lower rate $\xi^- \leq \xi^u$. A policy of indiscriminate quarantine would have $\xi^- = \xi^u$. A policy that allows negative cases to circulate would have $\xi^- = 0$.
   - **Infection -** The individual still becomes infected at rate $\lambda\alpha_t$ and in this case becomes an known infected, asymptomatic case: $\widetilde{IA}, NQ$.
4. Consider an individual that is a known negative case and quarantined: $\widetilde{NA}, Q$

Covid Economics 13, 4 May 2020: 1-30

- **Quarantine -** Since they are recognized as a negative case they may be released from quarantined at a higher rate $r^- \geq r^u$. A policy of indiscriminate quarantine would have $r^- = r^u$. A policy that allows negative cases to circulate would have $r^- = 1$.
- **Infection -** The rate of infection is now reduced to $\lambda^Q \alpha_t$

3.3.2 Infected, asymptomatic individuals

For brevity we consider the case only for non-quarantined individuals.

1. Consider an individual that is a unknown case: $\overline{IA}, NQ$
   - **Quarantine -** Since they are also unknown cases, the rate of quarantine is the same that which must face $\overline{NA}, NQ$ individuals. At rate ξ^u they transition to quarantine: $\overline{IA}, Q$.
   - **Infection -** Since they are already infected there is no transition to infection.
   - **Testing -** At rate τ, they are tested and since tests are perfect, learn they are not infected, so transition to being a known positive case: $\overline{IA}, NQ$.
2. Consider an individual that is a known positive case: $\widetilde{IA}, NQ$
   - **Quarantine -** Since this is a known case then it can be subjected to the same rate of quarantine as infected, symptomatic cases. At rate ξ^+ they transition to quarantine: $\widetilde{IA}, Q$.
   - **Infection -** Since they are already infected there is no transition to infection.
   - **Testing -** Since they are already tested there is no further testing.

3.3.3 Transition rates between all states

Using the above logic and the structure of the model we can construct the matrix of flows between all 12 active states and into the deceased state. Table 3 describes all such transition rates.

3.3.4 Nesting the SEIR and SIR models

The SEIR model is nested in our model under the following parameter restrictions.

- No quarantine: $\lambda / \lambda^Q = 1$
- No asymptomatic transmission: $\rho_A / \rho_S = 0$
- No testing: $\tau = 0$

In this case individuals move from $\overline{NA} \to \overline{IA} \to IS \to RA$, which correspond to the $SEIR$ states. To obtain the SIR model, additionally set $\delta = 1$, such that infectiousness is immediate.

Covid Economics 13, 4 May 2020: 1-30

Covid Economics 13, 4 May 2020: 1-30

A. Initial state		B. Next instant states												
		Non-infected, Asymptomatic				Infected, Asymptomatic				Infected, Symptomatic		Recovered		Dead
		$\overline{NA}, NQ$	$\overline{NA}, Q$	$\widetilde{NA}, NQ$	$\widetilde{NA}, Q$	$\overline{IA}, NQ$	$\overline{IA}, Q$	$\widetilde{IA}, NQ$	$\widetilde{IA}, Q$	IS, NQ	IS, Q	RA, NQ	RA, Q	D
NA	$\overline{NA}, NQ$		ξ^u	τ		$\lambda\alpha_t$								
	$\overline{NA}, Q$	r^u			τ		$\lambda^Q\alpha_t$							
	$\widetilde{NA}, NQ$				ξ^-			$\lambda\alpha_t$						
	$\widetilde{NA}, Q$			r^-					$\lambda^Q\alpha_t$					
IA	$\overline{IA}, NQ$						ξ^u	τ		δ				
	$\overline{IA}, Q$					r^u			τ		δ			
	$\widetilde{IA}, NQ$								ξ^+	δ				
	$\widetilde{IA}, Q$							r^+			δ			
IS	IS, NQ										ξ^+	ω^R		ω^D
	IS, Q									r^+			ω^R	ω^D
R	RA, NQ												ξ^r	
	RA, Q											r^r		

Table 3: Transition rates between health and information states

Notes: This table gives the transition rates between states. Note that in any instant only one transition can occur. For example, an individual that is infected and asymptomatic and not quarantined may transition to symptomatic and quarantined, but *not* to symptomatic and not-quarantined. The individual then may transition from symptomatic and non-quarantined into quarantine. **Blue** terms refer to policies applied to *unknown cases*. **Red** terms refer to policies applied to *known positive cases*. **Green** terms refer to policies applied to *known negative cases*. The **Pink** terms are the result of the testing-as-tagging assumption: once tested and *known negative*, the transition to infection is observed so the individual becomes a *known positive*.

Covid Economics 13, 4 May 2020: 1-30

3.4 Measurement

3.4.1 Basic reproduction number

Consider a hypothetical 'date-zero' case. An individual is in the state $\overline{IA}, NQ$, while the rest of the population is in $\overline{NA}, NQ$ and there are no quarantine procedures in place. A summary statistic of the transmission rate is the expected number of infections caused by this single infected person: $\mathcal{R}_0^{IA,NQ}$. We can state this recursively as follows. At rate δ the individual becomes symptomatic, which will change their medical transmission rate to $\rho^S \geq \rho^A$:[16]

$$\mathcal{R}_0^{IA,NQ} = \lambda\rho^A + (1-\delta)\,\mathcal{R}_0^{IA,NQ} + \delta\mathcal{R}_0^{IS,NQ}$$
$$\mathcal{R}_0^{IS,NQ} = \lambda\rho^S + \left(1-\omega^R-\omega^D\right)\mathcal{R}_0^{IS,NQ}.$$

This implies that

$$\mathcal{R}_0^{IS,NQ} = \lambda\frac{\rho^S}{\omega^R+\omega^D} \quad , \quad \mathcal{R}_0^{IA,NQ} = \frac{\rho^S\lambda}{\delta}\left[\frac{\rho^A}{\rho^S} + \frac{\delta}{\omega^R+\omega^D}\right] \tag{1}$$

The nested case of the *SIR* model, which removes the *exposed* state, is obtained by setting $\delta = 1$ and has a *transmission rate* $\mathcal{R}_0 = \rho\lambda/\left(\omega^D+\omega^R\right)$.

We can try to use data on transmission rates from Wuhan to bound the effectiveness of quarantine. We view the Wuhan response as a *quarantine everyone* policy. If everyone is quarantined then

$$\mathcal{R}_0^{IA,Q} = \frac{\rho^S\lambda^Q}{\delta}\left[\frac{\rho^A}{\rho^S} + \frac{\delta}{\omega^R+\omega^D}\right]$$

therefore the relative rates of transmission pre- and post-quarantine policy are informative of λ/λ^Q which is our measure of the *quarantine technology*: $\lambda^Q/\lambda = \mathcal{R}_0^{IA,Q}/\mathcal{R}_0^{IA,NQ}$. In Wuhan, $\mathcal{R}_0^{IA,NQ} = 3.86$, while post qurantine measures leads to$\mathcal{R}_0^{IA,Q} = 0.32$. The Wuhan *quarantine technology* delivers $\lambda^Q/\lambda \approx 0.10$. We therefore view this as an *upper bound* on the quarantine technology in the United States: $(\lambda^Q/\lambda)_{US} \in [0.10, 1.00]$.

3.4.2 Measures of activity

To summarize some of our results we construct five metrics: Output, symptomatic infection, reported cases, mortality and social well-being.

Output. A reasonable approximation of economic activity is that it scales with the number of non-quarantined workers. We further assume that quarantined workers are $A_{rel} \in [0,1)$ less productive than non-quarantined workers, and that symptomatic workers do not produce. We therefore define output Y_t as

$$Y_t = M_t^{NA,NQ} + M_t^{IA,NQ} + M_t^{RA,NQ} + A_{rel}\left(M_t^{NA,Q} + M_t^{IA,Q} + M_t^{RA,Q}\right).$$

[16] In the case where $\rho^I = \rho^A$ and the transition from asymptomatic to symptomatic is instantaneous—i.e. as in the SIR model—then we have the recursion $\mathcal{R}_0 = \lambda\rho + (1-\omega^D-\omega^R)\,\mathcal{R}_0$ which gives $\mathcal{R}_0 = \lambda\rho/\left(\omega^D+\omega^R\right)$.

Parameter		Source / Target	Value
A. Known medical			
Rate at which infected become symptomatic	δ	6 days incubation period	$1/6$
Relative rate of asymptomatic transmission	ρ^A/ρ^S	No current evidence	1
Recovery	ω^R	14 day recovery period	$1/14$
Mortality	ω^D	Mortality rate of 1 percent	$\left(0.01/0.99\right) \times \omega^R$
B. Calibrated			
Rate of meeting	λ	Normalized contact rate	1
Rate of transmission	ρ^S	Given λ, gives $\mathcal{R}_0^{IA,NQ} = 2.5$	0.0091
C. Policy parameters			
Effectiveness of quarantine technology	λ^Q/λ	Half of that implied by Wuhan $\Delta\mathcal{R}_0$	0.5
Testing of unidentified and asymptomatic cases	τ	25 to 50 times peak US testing rate	0.5% per day
Quarantine rates for observable cases	$\left\{\xi^u, \xi^-, \xi^+, \xi^r\right\}$	See Section 5	
Release rates from quarantine for observable cases	$\left\{r^u, r^-, r^+, r^r\right\}$	See Section 5	

Table 4: Model parameters and values

In the initial period all individuals are non-quarantined, so $Y_0 = 1$. Therefore Y_t is in units of the percent change in output from the initial period.

Symptomatic infection. A reasonable approximation of the load on the hospital system is that it scales with the number of infected, symptomatic individuals. We therefore simply report symptomatic infection: M_t^{IS}.

Testing and reported cases. Cases are reported when an asymptomatic infection case is tested, which occurs at rate τ, or the instant an asymptomatic infection becomes symptomatic, which occurs at rate δ. Give $R_t = 0$, then

$$\Delta R_t = (\tau + \delta)\, M_t^{\overline{IA}}.$$

Mortality. Since the death state is absorbing total mortality is simply $X_t = M_t^D$. In our counterfactuals we consider combinations of testing and quarantine policies that keep this number at the end of the pandemic constant, and compare the implications for symptomatic infections and output.

4 Calibration

4.1 Parameters

Parameter values are given in Table 4. The parameters of the model can be classified intro three groups. The first relate to *'known' medical* parameters, which would be the equivalent of technological parameters in an economic

Covid Economics 13, 4 May 2020: 1-30

Covid Economics 13, 4 May 2020: 1-30

model, and that we can take from the literature that has formed so far.[17] Obviously the extent to which these parameters are well understood will evolve over time and we may use this information later on. The second relate to parameters that are similarly technological in that we think that they represent immutable features of the model, but that we do not have values for and require calibration. The third are policy parameters and relate to (i) testing rates, (ii) effectiveness of quarantine, (iii) rules for quarantine. We describe these in the next section when describing our counterfactuals.

Known medical. We assume that the rate at which infected individuals transition from asymptomatic to symptomatic cases, δ, is such that the average incubation period is 6 days (Wu, Leung, and Leung, 2020). World Health Organization (2020) report that the average recovery period is 14 days for mild infections, we therefore set $\omega^R = 1/14$. There is little data on the relative rates of infection of symptomatic and asymptomatic individuals.[18] We assume a common infection rate: $\rho^A \Big/ \rho^S = 1$.

From surveying estimates we target a mortality rate of 1 percent. In the model we denote this by π^D, which is the fraction of individuals experiencing symptoms (IS) that die. Then

$$\pi^D = \frac{\omega^D}{\omega^R + \omega^D}.$$

We use this to determine ω^D given ω^R and $\pi^D = 0.01$.

Unknown and calibrated. We use empirical estimates of the *rate of basic transmission* and equation (1) to calibrate λ and ρ^S. We treat $\mathcal{R}_0^{IA,NQ}$ as data, taking the value of 2.5, which is in the middle of the range of empirical estimates. Using equation (1) provides an equation in two unknowns $\{\lambda, \rho^S\}$.

Without further data these parameters cannot be separately identified. We therefore set $\lambda = 1$ and back out the implied ρ^S that is consistent with (1). To match the same basic rate of transmission requires

$$\rho^S = \frac{\mathcal{R}_0^{IA,NQ}}{\frac{\lambda}{\delta}\left[\left(\frac{\rho^A}{\rho^S}\right) + \frac{\delta}{\omega^R + \omega^D}\right]}.$$

In the future, within-region across-time variation in quarantine measures may allow us to separately identify $\{\lambda, \rho^S\}$. We set the quarantine technology $\lambda^Q/\lambda = 0.50$.

5 Counterfactuals

Our aim is to provide a small handful of counterfactuals with a minimal set of parameters. The configuration of these parameters is given in Table 5, and their values are given in Table 6. Section 5 and Section 6 refer to Case 1 in

[17] A number of recent papers have also discussed significant measurement challenges, e.g. Atkeson (2020a), Stock (2020) and Hortaçsu, Liu, and Schwieg (2020). For these reasons we interpret our calibration as a proof of concept.

[18] https://www.buzzfeed.com/albertonardelli/coronavirus-testing-iceland. "Early results from deCode Genetics indicate that a low proportion of the general population has contracted the virus and that about half of those who tested positive are non-symptomatic".

these tables, we consider Case 2—in which we repeat the exercise under more effective quarantine—in Section 7

Initial conditions. We seed the economy by choosing initial conditions that replicate the U.S. COVID-19 experience. We assume an initial infected population of 300 individuals and 1 detected case. We measure all model and data counterparts as of the 100th detected case.

Vaccine. We abstract from the long-run, and instead focus on testing and quarantine in the current phase of the pandemic. Consistent with this, we assume that in each case a vaccine is introduced to the economy after 500 days. The vaccine moves individuals in any of the NA states through to RA, NQ state, which makes them immune. The vaccine rolls out slowly, at a rate of 0.10 percent per day.

Counterfactuals. We then consider three different cases for the policy parameters: $\left\{\xi^u, \xi^-, \xi^+, \xi^r\right\}$, $\left\{r^u, r^-, r^+, r^r\right\}$, τ. We express these parameters as daily rates, despite the model being hourly. With so many parameters we have many degrees of freedom. We constrain these parameters in a simple way across counterfactuals so that we can be precise, but others may wish to consider many alternatives. We consider one at the end. Given that we have assumed immunity, in all cases we set the quarantine rate of recovered individuals ξ^r to zero and their release rate r^r to 1.

Baseline. Our baseline model features no quarantine and no testing. With no testing ξ^- and r^- are off the table, since no unknown cases are tested and identified as negative. We then set $\xi^+ = \xi^u = 0$ and $r^+ = r^u = 1$.[19] This is the worst-case scenario in which the government does nothing to stop the spread of the virus.

Policy interventions. We consider two policy interventions that capture broad quarantine and targeted quarantine with testing. These policies begin on March 18th, which is two weeks after the first 100 cases are reported in the data and in the model. Aiming to cut down on parameters, we assume that in both cases known positive cases are quarantined and not released: $\xi^+ = 1$, $r^+ = 0$. We therefore have 6 parameters remaining: ξ^u and r^u in the quarantine case, and ξ^u, ξ^-, r^u and r^- in the testing case.

1. No testing - Common Quarantine. Our first policy is an approximation of what we have observed in the United States in March, 2020. In this counterfactual there is no testing of asymptomatic individuals and so no *known negative* cases. There is therefore a common quarantine rate for all asymptomatic individuals. We set this rate in counterfactual number 2 to $\xi_2^u = 0.010$, implying a 1 percent per day quarantine rate. This is in line with the data in Table 2, in which roughly 24 percent of the US population was quarantined within 19 days. We assume that the rate of release from quarantine is zero.

[19] For technical reasons, when we set a parameter to 1 we set it to a number $> .98$ percent per day (effectively 1).

Covid Economics 13, 4 May 2020: 1-30

2. Testing - Targeted quarantine. Our second policy assumes that the government tests asymptomatic individuals at a rate τ. While the US is testing at a rate of roughly 0.01 percent of the population per day.[20] We assume that the US increases its testing capacity by roughly 50 fold to $\tau = 0.5\%$ per day. In levels, this would require testing 1,700,000 *asymptomatic* people per day, while the US is currently testing around 50,000 *symptomatic* people per day.

In the spirit of our paper being a proof of concept, we choose for comparison a very simple policy. We maintain the rate of quarantine of unknown cases and assume that known negatives are not released ($r_3^- - = 0$). These stack the decks *against* the testing policy having large effects. The only targeted quarantine measure that we take is to assume that non-quarantined known negative cases are quarantined at rate $\xi_3^- = \Delta \times \xi_2^-$, with $\Delta < 1$. We then choose a value for Δ such that the policy delivers the same number of total deaths as the common quarantine policy. This procedure delivers a value of $\Delta = 0.20$. When testing asymptomatic cases, the rate of quarantine of known negative cases can be cut by a factor of five without increasing the total number of deaths caused by the pandemic.

6 Results

Figure 6 plots our main results where we compare counterfactuals one and two. Statistics for these are given in Tables 7, 8, 9, which include the Baseline simulation. Panel A plots the cumulative number of reported cases. Panel B plots the number of infected, symptomatic cases. Given a constant rate of symptoms requiring medical attention, we can think of Panel B as capturing the number of individuals entering the hospital system. Panel C plots the cumulative fraction of the population that dies. Panel D plots measured output under the assumption that non-quarantined individuals produce 50 percent as much as quarantined individuals ($A_{rel} = .5$).[21]

Cases. Common quarantine is effective at slowing the cumulative number of reported cases. Testing and targeted quarantine are slightly more effective.

Case load. Panel B plots the fraction of infected symptomatic individuals in the economy. Both counterfactual policies 'flatten the curve' relative to the baseline. The reduction in peak infection load is lower under the testing policy. If we interpret case load as the stress put on hospital capacity, targeted quarantine with testing generates the smallest peak load of cases. Common quarantine pushes the peak infection back by about 170 days, whereas the targeted quarantine with testing tends to put the peak case load back by 250 days, buying an additional quarter to prepare the medical system. Table 9 reports these statistics.

Deaths. Quarantine is an effective tool at reducing the number of deaths. The current US common quarantine policy, if continued to be enacted at the same rate (1% of the U.S. population entering quarantine per day), would more than halve the fraction of the population that dies from the disease. Table 7 reports the deaths in levels in

[20] Countries like South Korea are testing at a rate of approximately 0.05 percent per day. This comes from reports of South Korean testing capacity of 20,000 per day (https://www.wired.co.uk/article/south-korea-coronavirus) and a population in South Korea of 51.47 million.

[21] While this number is very low, Dingel and Neiman (2020) estimate that only 40% of jobs can be plausibly done from home.

Covid Economics 13, 4 May 2020: 1-30

CEPR PRESS

A. Counterfactuals	B. Parameters								
	Quarantine rates				Release rates				Testing
	ξ^+	ξ^u	ξ^-	ξ^r	r^+	r^u	r^-	r^r	τ
Baseline - Do nothing	0	0	—	0	1	1	—	1	0
Case 1 - Quarantine technology - $\lambda^Q/\lambda = 0.50$ - Section 5 & 6									
1. No testing - Common quarantine	1	ξ^u	—	0	0	0	—	1	0
2. Testing - Targeted quarantine	1	ξ^u	$\left(\Delta \times \xi^u\right)$	0	0	0	0	1	τ
Case 2 - Strong quarantine technology - $\lambda^Q/\lambda = 0.30$ - Section 7									
1. No testing - Common quarantine	1	ξ^u	—	0	0	0	—	1	0
2. Testing - Targeted quarantine	1	$\left(\psi \times \xi^u\right)$	0	0	0	0	0	1	τ

Table 5: Configuration of policy parameters for each counterfactual

Notes: This table gives the configurations of the policy parameters of the model under our three counterfactuals. Recovered individuals are immune and so never quarantined and always released. In the **Baseline case** there is no quarantine and no testing. Under the **1. No testing - Common quarantine** policy there is no testing, so uninfected and infected asymptomatic cases cannot be distinguished. Symptomatic cases are the only known positives, and these are completely quarantined and not released. Unknown cases are quarantined at rate ξ_2^u and not released. Under the **2. Testing - Targeted quarantine** policy there is testing of asymptomatic individuals at rate $\tau > 0$. Negative, asymptomatic cases are distinguished, quarantined at a lower rate, but released at the same rate as unknown cases. Given a value of τ we choose Δ such that overall deaths from Cases 1 and 2 are equivalent.

Description	Policy parameter	Daily rate
1. No testing - Common quarantine		
Common quarantine rate	ξ^u	1.0 %
2. Testing - Targeted quarantine		
Testing rate	τ	0.50 %
Case 1 - Quarantine technology $\lambda^Q/\lambda = 0.50$		
Differential quarantine rate: Known negatives	Δ	0.20
Case 2 - Strong quarantine technology $\lambda^Q/\lambda = 0.30$		
Differential quarantine rate: Unknown cases	ψ	0.30

Table 6: Counterfactual parameters

Notes: The parameter Δ is chosen so that both counterfactuals incur the same total deaths.

each of the scenarios. We deliberately set the parameters of the targeted quarantine policy to deliver the same cumulative deaths as the common quarantine policy, as can be seen clearly in Figure 6C. The testing policy backloads these deaths. In the short run, there are fewer deaths, but in the long run, as known negative cases are quarantined at a lower rate, total deaths converge.

Covid Economics 13, 4 May 2020: 1-30

CEPR PRESS

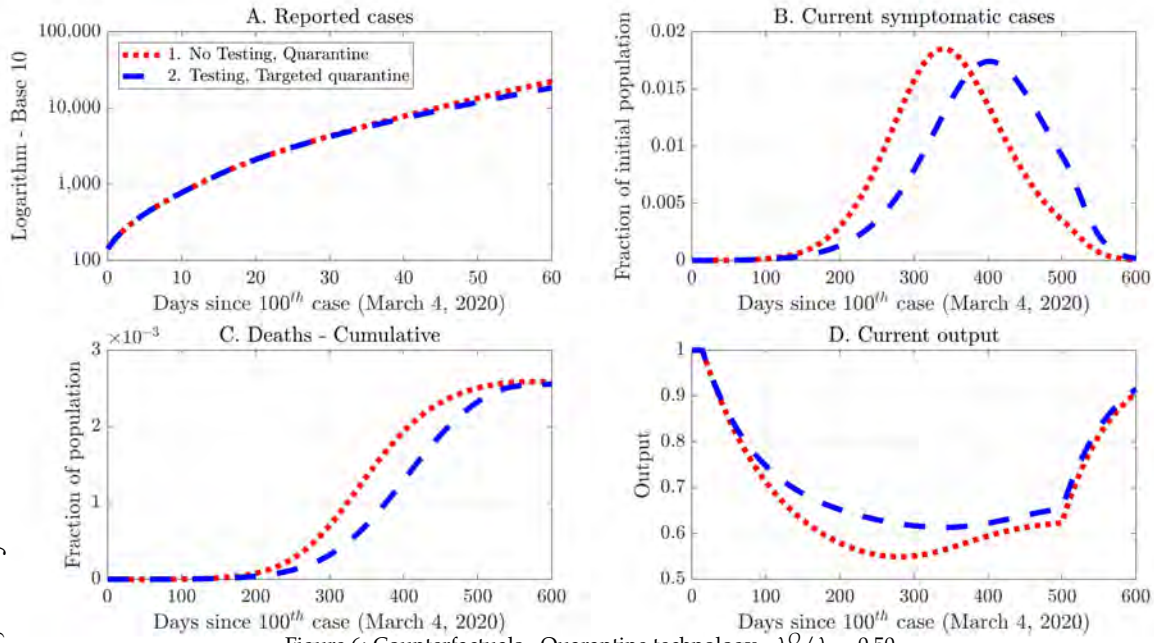

Figure 6: Counterfactuals - Quarantine technology - $\lambda^Q/\lambda = 0.50$

Notes: The red dotted line corresponds to the counterfactual **1. No testing - Common quarantine**. The blue dashed line corresponds to the counterfactual **2. Testing - Targeted quarantine**. Output is total non-quarantined, asymptomatic workers. Output in period zeros is equal to one since all workers are non-quarantined and asymptomatic.

Output. Table 7 shows that the baseline economy features very little output loss, driven entirely by the massive loss of life. This is the only tradeoff of quarantine in the textbook SEIR model: if a government quarantines individuals to reduce deaths, the lower output. The testing model and policy provide a third way, where output losses are less, due to relaxed quarantine but the *same* number of deaths is achieved.

In other words, targeted quarantine and testing alters the output-death tradeoff. With extra degrees of freedom in terms of policy, the government can do better than common quarantine both in terms of *deaths and output*. Figure 6D shows this clearly. Under targeted quarantine and testing, fewer individuals needs to be quarantined, output is significantly higher in the first 100 days of the pandemic and recovers more quickly. Accumulating output produced each period over the first year of the pandemic, output is 10 percent higher under the testing policy. in the long run the change in output only reflects the loss of life over the pandemic, and both policies deliver the same loss of life, long run output is the same.

We also report these results relative to pre-COVID-19 levels in Table 8. With targeted quarantine, the level of output is 10 percent higher in the first 200 days than with common quarantine, and then the two economies recover at a similar rate.

Covid Economics 13, 4 May 2020: 1-30

Experiment	Deaths			
	After 100 days	After 200 days	After 300 days	After 600 days
A. Deaths in Levels				
Baseline - Do nothing	10,013	2,572,026	3,037,155	3,040,479
1. No testing - Common quarantine	731	23,989	228,605	879,634
2. Testing - Targeted quarantine	603	12,306	102,605	868,471
B. Deaths Relative to Baseline				
1. No testing - Common quarantine	-9,282	-2,548,036	-2,808,550	-2,160,845
2. Testing - Targeted quarantine	-9,410	-2,559,719	-2,934,550	-2,172,008

Table 7: Counterfactual Deaths

Caution. While we do not want readers to interpret our numbers literally since we are not epidemiologists and this is a not a rich quantitative SEIR model, we view Figure 6, panels C and D as illustrating our main point: targeted quarantine allows governments that can implement significant testing to produce more output than under the common quarantine policy. If the medical system produces fewer deaths under a more distant and lower peak case load, then the testing policy would also deliver fewer deaths. The policy can produce fewer deaths and higher output.

6.1 Robustness

For brevity we make one note regarding the robustness of our results to enriching the *medical block* of the model. We use this to highlight the usefulness of benchmarking counterfactuals.

Quantitative models being used to forecast the trajectory of the pandemic have richer medical blocks that incorporate congestion and capacity constraints in the health care system. From our understanding of these models we think that the following is true. Take an SEIR model and append an arbitrarily rich medical block. Now consider two policies A and B that deliver the same *total number of infections* over the pandemic—that is, the area underneath the curve in Figure 6B. If policy A has a lower peak than policy B then policy A will result in fewer deaths than policy B.

We have constructed our counterfactuals such that the area under the epidemiology curves are the same. To see this recall that there is a constant rate of transition from symptomatic states to death. Therefore, under the law of large numbers, fixing the total number of deaths across counterfactuals by construction fixes the total number of infections across counterfactuals as well. That is, we know that by construction we have *flattened the curve* in moving from the common quarantine to the test and targeted quarantine policy. Under a richer medical block, the testing and quarantine policy will result in fewer deaths.

7 More effective quarantine

Before concluding we consider how our counterfactual and available policies change under a more effective quarantine, that is a lower λ^Q/λ. Recall that we considered a value of 0.10 for this statistic for Wuhan, and in out main

Covid Economics 13, 4 May 2020: 1-30

Experiment	Output			
	After 100 days	After 200 days	After 300 days	After 600 days
1. Baseline - Do nothing	1.00	0.91	0.99	0.99
2. No testing - Common quarantine	0.72	0.58	0.55	0.90
3. Testing - Targeted quarantine	0.75	0.65	0.62	0.91

Table 8: Counterfactual Output: $\left(Output_t = M_t^{A,NQ} + 0.50 \times M_t^{A,Q}\right)$

Experiment	Peak infection	Days to peak
A. Levels		
Baseline - Do nothing	68,368,137	166
1. No testing - Common quarantine	6,288,619	341
2. Testing - Targeted quarantine	5,921,942	403
B. Percent relative to Baseline		
1. No testing - Common quarantine	-90.80 %	105.42 %
2. Testing - Targeted quarantine	-91.34 %	143.77 %

Table 9: Counterfactual Peak Infections

counterfactual exercise considered a half as effective quarantine technology in the US, such that $\lambda^Q/\lambda = 0.50$. We now consider a more effective quarantine, halfway between these with $\lambda^Q/\lambda = 0.30$. Now with a more effective quarantine, even if we set $\Delta = 0$ and quarantine no individuals that have tested negative, then the policy generates fewer deaths than the no testing, common quarantine policy. This gives extra space for policy to reduce quarantining other individuals. We again model this simply, reducing the rate of quarantine of *unknown cases* to $\psi \times \xi^u$, with $\psi \leq 1$. Table 5 and Table 6 describe this additional counterfactual, and show that we can set $\psi = 0.30$ and still incur the casualties from the epidemic as the baseline quarantine policy. Figure 7 shows that this substantially reduces the decline in our measure of output, and again 'flattens the curve' in terms of projected symptomatic infections.

8 Conclusion

This short paper conceptualizes a minor and easily implemented change to the standard SEIR model of infectious disease transmission. We assume that quarantine policies can only depend on observed health states, which creates a role for testing in distinguishing between infected and non-infected asymptomatic individuals. We demonstrate via a simple calibration of the model, that testing asymptomatic individuals can stand-in for costly quarantine measures. We make this notion precise by simultaneously reducing quarantine measures and increasing testing such that the overall mortality rate of the pandemic remains constant at '*Quarantine Everyone*' levels. With fewer individuals quarantined, we infer that output of the economy would decline substantially less. Thus, targeted quarantine and testing alters the output-death tradeoff. The government can do better than common quarantine both in terms of *deaths and output*.

Covid Economics 13, 4 May 2020: 1-30

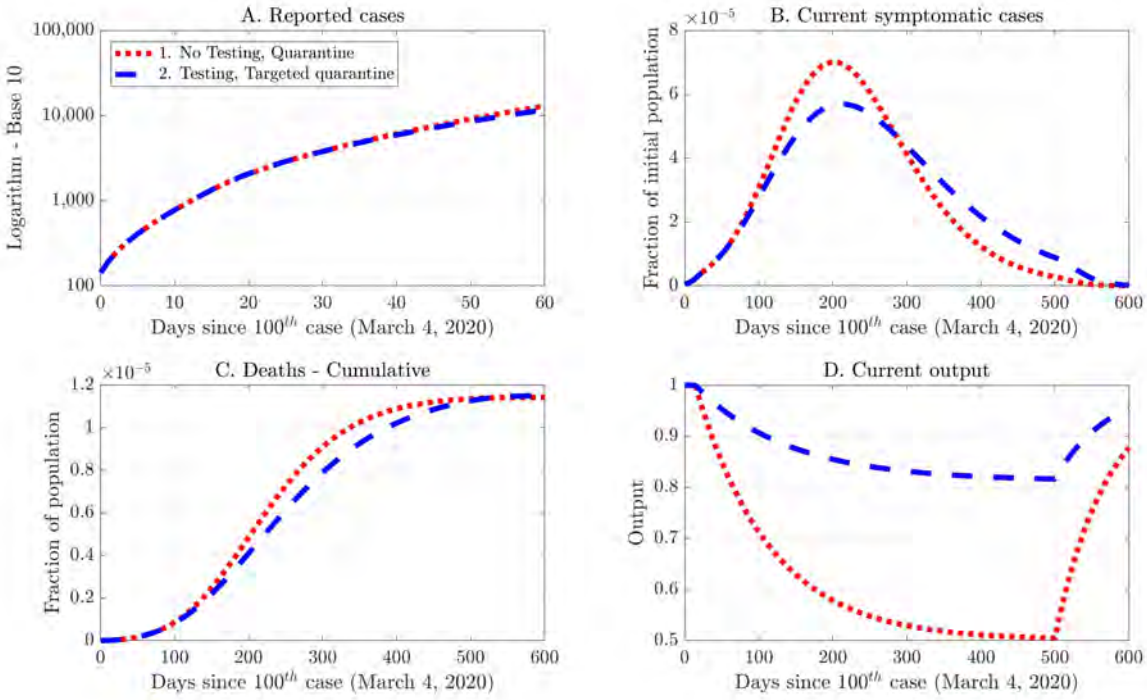

Figure 7: Counterfactuals - More effective quarantine technology - $\lambda^Q/\lambda = 0.30$

Notes: The red dotted line corresponds to the counterfactual **1. No testing - Common quarantine**. The blue dashed line corresponds to the counterfactual **2. Testing - Targeted quarantine**. Output is total non-quarantined, asymptomatic workers. Output in period zeros is equal to one since all workers are non-quarantined and asymptomatic.

The model here is not immediately applicable for serious quantitative work. However, we think that our exercises show that adding incomplete information and a role for testing through targeted quarantine does not overly complicate the baseline model and allows discussion of testing policies that cannot be discussed in the baseline complete information model. These additional features could be integrated into more quantitative epidemiology models that append to the SEIR model demographics, geography, imperfect immunity, and so on.

Covid Economics 13, 4 May 2020: 1-30

References

ALVAREZ, F. E., D. ARGENTE, AND F. LIPPI (2020): "A Simple Planning Problem for Covid-19 Lockdown," NBER Working Paper 26981, National Bureau of Economic Research.

ATKESON, A. (2020a): "How Deadly Is COVID-19? Understanding The Difficulties With Estimation Of Its Fatality Rate," NBER Working Paper 26965, National Bureau of Economic Research.

——— (2020b): "What Will Be the Economic Impact of COVID-19 in the US? Rough Estimates of Disease Scenarios," Working Paper 26867, National Bureau of Economic Research.

BRAUER, F., AND C. CASTILLO-CHAVEZ (2012): *Mathematical Models in Population Biology and Epidemiology*, vol. 2 of *Texts in Applied Mathematics*. Springer.

CHOWELL, G., P. FENIMORE, M. CASTILLO-GARSOW, AND C. CASTILLO-CHAVEZ (2003): "SARS outbreaks in Ontario, Hong Kong and Singapore: The role of diagnosis and isolation as a control mechanism," *Journal of Theoretical Biology*, 224(1), 1–8.

DINGEL, J., AND B. NEIMAN (2020): "How Many Jobs Can be Done at Home?," NBER Working Paper 26948, National Bureau of Economic Research.

EICHENBAUM, M. S., S. REBELO, AND M. TRABANDT (2020): "The Macroeconomics of Epidemics," Working Paper 26882, National Bureau of Economic Research.

FARBOODI, M., G. JAROSCH, AND R. SHIMER (2020): "Internal and External Effects of Social Distancing in a Pandemic," NBER Working Paper 27059, National Bureau of Economic Research.

FENG, Z. (2007): "Final and peak epidemic sizes for SEIR models with quarantine and isolation," *Mathematical Biosciences & Engineering*, 4(4), 675–686.

FENICHEL, E. P. (2013): "Economic considerations for social distancing and behavioral based policies during an epidemic," *Journal of Health Economics*, 32(2).

GLOVER, A., J. HEATHCOTE, D. KRUEGER, AND J.-V. RÍOS-RULL (2020): "Health versus Wealth: On the Distributional Effects of Controlling a Pandemic," NBER Working Paper 27046, National Bureau of Economic Research.

GREENWOOD, J., P. KIRCHER, C. SANTOS, AND M. TERTILT (2019): "An Equilibrium Model of the African HIV/AIDS Epidemic," *Econometrica*, 87(4), 1081–1113.

HORNSTEIN, A. (2020): "Social Distancing, Quarantine, Contact Tracing, and Testing: Implications of an Augmented SEIR-Model," Discussion paper, Federal Reserve Bank of Richmond.

HORTAÇSU, A., J. LIU, AND T. SCHWIEG (2020): "Estimating the Fraction of Unreported Infections in Epidemics with a Known Epicenter: an Application to COVID-19," NBER Working Paper 27028, National Bureau of Economic Research.

IMPERIAL COLLEGE COVID-19 RESPONSE TEAM, T. (2020): "Impact of non-pharmaceutical interventions (NPIs) to reduce COVID19 mortality and healthcare demand," *Mimeo*.

KERMACK, W. O., AND A. G. MCKENDRICK (1927): "A Contribution to the Mathematical Theory of Epidemics," *Proceedings of the Royal Society of London. Series A, Containing Papers of a Mathematical and Physical Character*, 115(772), 700–721.

Covid Economics 13, 4 May 2020: 1-30

KREMER, M. (1996): "Integrating Behavioral Choice into Epidemiological Models of AIDS*," *The Quarterly Journal of Economics*, 111(2), 549–573.

KUCHARSKI, A. J., T. W. RUSSELL, C. DIAMOND, Y. LIU, J. EDMUNDS, S. FUNK, R. M. EGGO, F. SUN, M. JIT, J. D. MUNDAY, ET AL. (2020): "Early dynamics of transmission and control of COVID-19: a mathematical modelling study," *The Lancet Infectious Diseases*.

PIGUILLEM, F., AND L. SHI (2020): "The Optimal Covid-19 Quarantine and Testing Policies," Discussion paper, Einaudi Institute for Economics and Finance (EIEF).

STOCK, J. H. (2020): "Data gaps and the policy response to the novel coronavirus," NBER Working Paper 26902, National Bureau of Economic Research.

WORLD HEALTH ORGANIZATION, T. (2020): "Report of the WHO-China Joint Mission on Coronavirus Disease 2019," *Mimeo*.

WU, J. T., K. LEUNG, AND G. M. LEUNG (2020): "Nowcasting and forecasting the potential domestic and international spread of the 2019-nCoV outbreak originating in Wuhan, China: a modelling study," *The Lancet*, 395(10225), 689–697.

Covid Economics 13, 4 May 2020: 1-30

Covid Economics 13, 4 May 2020: 1-30

APPENDIX

A Additional tables and figures

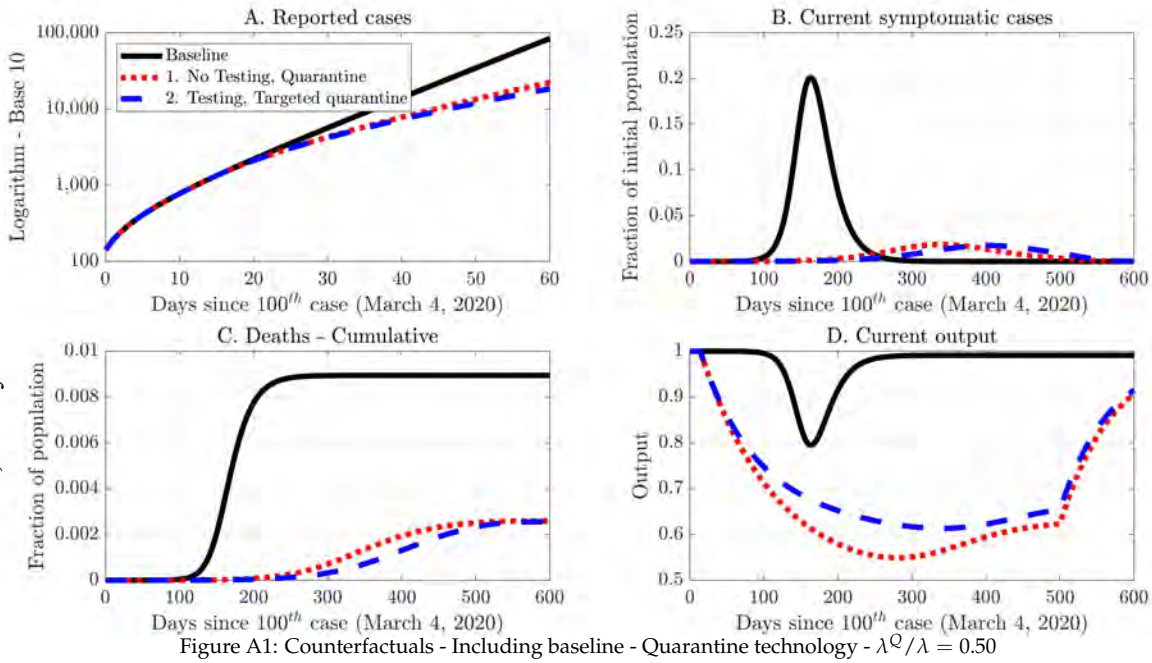

Figure A1: Counterfactuals - Including baseline - Quarantine technology - $\lambda^Q/\lambda = 0.50$

Notes: In each panel the black solid line corresponds to counterfactual **Baseline - Do nothing**. The red dotted line corresponds to the counterfactual **1. No testing - Common quarantine**. The blue dashed line corresponds to the counterfactual **2. Testing - Targeted quarantine**. Output is total non-quarantined, asymptomatic workers. Output in period zero is equal to one since all workers are non-quarantined and asymptomatic.

Covid Economics 13, 4 May 2020: 1-30

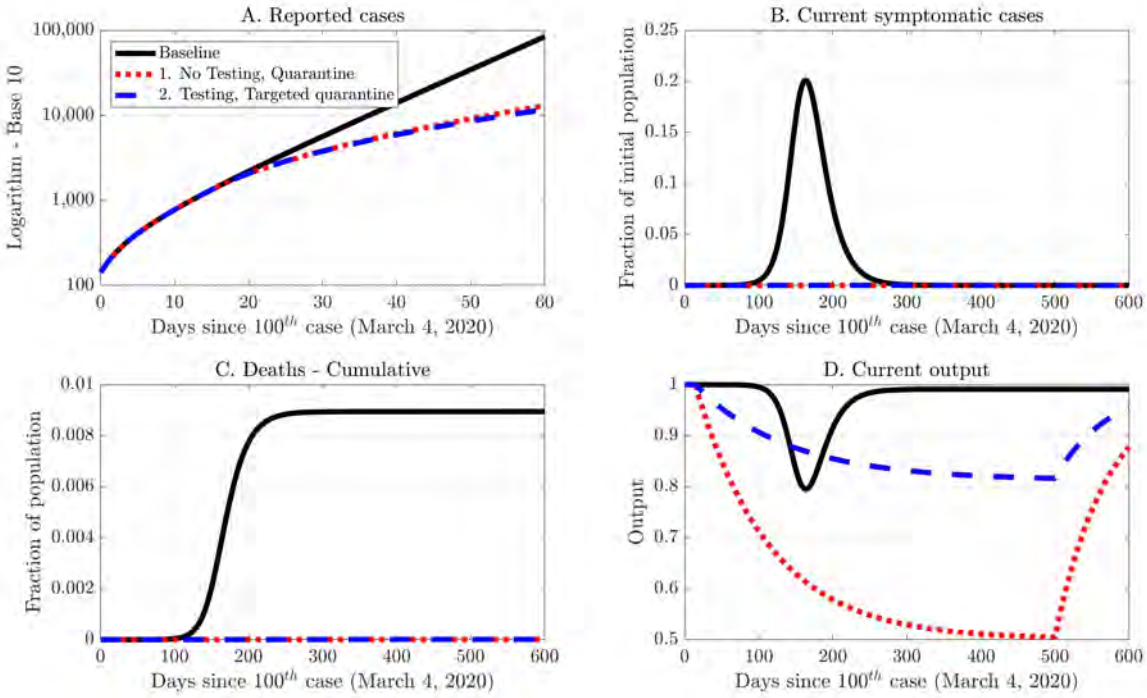

Figure A2: Counterfactuals - Including baseline - More effective quarantine technology - $\lambda^Q/\lambda = 0.30$

Notes: In each panel the black solid line corresponds to counterfactual **Baseline - Do nothing**. The red dotted line corresponds to the counterfactual **1. No testing - Common quarantine**. The blue dashed line corresponds to the counterfactual **2. Testing - Targeted quarantine**. Output is total non-quarantined, asymptomatic workers. Output in period zero is equal to one since all workers are non-quarantined and asymptomatic.

The determinants of the differential exposure to COVID-19 in New York City and their evolution over time[1]

Milena Almagro[2] and Angelo Orane-Hutchinson[3]

Date submitted: 28 April 2020; **Date accepted:** 29 April 2020

In this paper, we explore different channels to explain the disparities in COVID-19 incidence across New York City neighborhoods. To do so, we estimate several regression models to assess the statistical relevance of different variables such as neighborhood characteristics and occupations. Our results suggest occupations are crucial for explaining the observed patterns, with those with a high degree of human interaction being more likely to be exposed to the virus. Moreover, after controlling for occupations, commuting patterns no longer play a significant role. The relevance of occupations is robust to the inclusion of demographics, with some of them, such as income or the share of Asians, having no statistical significance. On the other hand, racial disparities still persist for Blacks and Hispanics compared to Whites, although their magnitudes are economically small. Additionally, we perform the same analysis over a time window to evaluate how different channels interact with the progression of the pandemic, as well as with the health policies that have been set in place. While the coefficient magnitudes of many occupations and demographics decrease over time, we find evidence consistent with higher intra-household contagion as days go by. Moreover, our

1 We thank Michael Dickstein, Jonathan T. Elliott, and Daniel Waldinger for their useful comments. Any errors or omissions are our own.
2 PhD Candidate, Department of Economics, New York University.
3 PhD Candidate, Department of Economics, New York University.

findings also suggest a selection on testing, whereby those residents in worse conditions are more likely to get tested, with such selection decreasing over time as tests become more widely available.

Covid Economics 13, 4 May 2020: 31-50

CEPR PRESS

Covid Economics 13, 4 May 2020: 31-50

1 Introduction

The impact of COVID-19 has affected different locations to very different extents, with some areas being hit harder than others all over the world. Much of this variation is explained by characteristics such as the number of international travellers, weather conditions, local policies to control the pandemic, and when those policies were implemented. Surprisingly, large differences exist even across smaller geographical units such as neighborhoods *within* a city. For example, Figure 1 shows the differences in the rates of positive tests by zip code of residence in New York City (NYC).

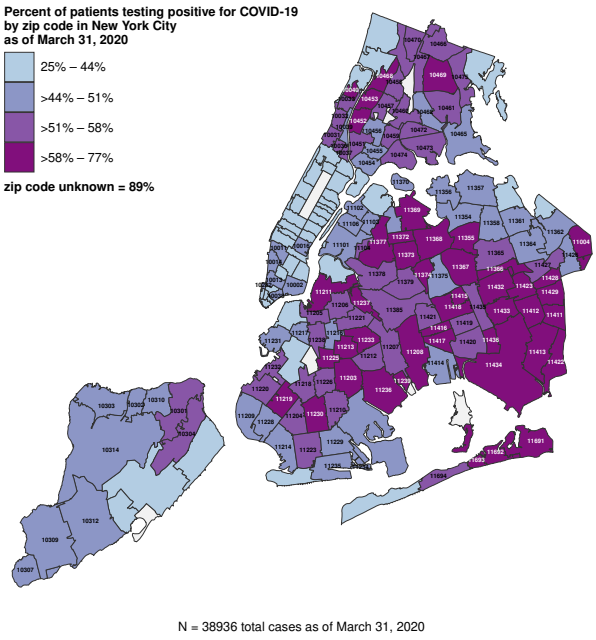

Figure 1: Map of the rate of positives by zip code as of March 31, 2020.

From simple inspection, zip codes with the highest rates are found in the boroughs of Bronx, Brooklyn, and Queens. These boroughs are also home to the majority of Blacks and Hispanics living in NYC.[1]

These spatial correlations between the incidence of the pandemic and demographics have garnered the attention of many economists and policy makers. For example,

[1]These groups compose 29% and 56%, respectively, of all Bronx residents, 31% and 19% for Brooklyn, and 17% and 28% in the case of Queens.

Covid Economics 13, 4 May 2020: 31-50

Borjas (2020) and Schmitt-Grohé et al. (2020) show that the much of the spatial disparities of testing and positive rates across NYC neighborhoods is explained by demographics. Given that COVID-19 does not intrinsically discriminate across demographic groups, the reason for such disparities still remains an open question. Hence, our goal is to assess the importance of a set of observable channels, such as population density, commuting patterns, and occupations, that explain the existing spatial differences in NYC.

To understand the relevance of different mechanisms, we use data on the number of tests and positives across NYC zip codes provided by DOH.[2] Because these data have been released (almost) on a daily basis, we are able to keep track of the number of tests and the fraction of those that are positive since April 1. We combine the data on testing with neighborhood and demographic indicators, which are provided by the American Community Survey (ACS). Namely, we use zip code level data on population density, commuting patterns, income, as well as race and age composition. We also include employment data; the ACS provides the number of workers employed at different occupations, all at the zip code level. We compute the share of workers across different occupations relative to the working-age population to understand how differences in labor composition can affect the incidence of COVID-19.

Because we focus on highlighting observable channels that are likely to explain the spatial differences to COVID-19 exposure, we estimate several specifications highlighting the importance of new variables at each step. Throughout the analysis, our dependent variable is the fraction of tests showing a positive result across NYC zip codes.[3] We start by including a small set of neighborhood controls, such as commuting patterns, population density, and health controls. In all of our specifications, we also include the share of the population being tested, which we call "tests-per-capita." The limited availability of tests in NYC has forced health authorities to constrain testing to people showing sufficiently acute symptoms or determined to be at high risk of infection. Hence, we expect the number of tests administered to be very close to the population in that segment.[4] Therefore, we use the number of tests per capita as a proxy for the overall level of the spread of the pandemic *within* a neighborhood. We find that when the number of tests per capita increases, the share of positive tests also increases. This result stems from both variables co-moving with the true

[2]Unfortunately, at the time of this analysis, there is no data available with the number of deaths by zip code.

[3]We could also focus on the number of positive tests per capita. We refrain from doing so for two reasons. First, random testing has not been possible in NYC, as only those with certain conditions are tested because of limited capacity. Second, Borjas (2020) points out that the incidence of different variables on positive results per capita is composed of two things: A differential incidence on those who are tested, but also a differential incidence on those with a positive result conditional on being tested. Therefore, we believe that the fraction of positive tests is the variable that correlates the most with the actual spread of the disease within a neighborhood throughout our sample.

[4]As a matter of fact, at earlier dates, tests were performed only on those who required hospitalization.

Covid Economics 13, 4 May 2020: 31-50

number of infected people within a neighborhood. However, we also find that, as testing becomes more widely available and more tests are performed on the asymptomatic population, the magnitude of tests-per-capita decreases over our analyzed time period.

We then analyze the role of occupations, motivated by the fact that they vary in their degree of human interaction. Those with high levels of human contact are more likely to be exposed to the virus.[5] We do so by including the share of workers for 13 categories in each zip code constructed from the ACS according to their degree of human interaction. The results show that, indeed, occupations are a key component in explaining the observed differences across NYC areas. For example, in our preferred specification including demographics and borough fixed effects, we find that a one-percentage-point increase in the number of workers employed in transportation, an occupation that has been declared essential and has a high degree of exposure to human interaction, increases the share of positive tests by 2% for April 1, one month into the pandemic. Moreover, we show that after controlling for occupations, length of commute and the use of public transport are not significant.[6]

Additionally, these results are robust to the inclusion of demographics, as well as borough fixed effects.[7] Including demographics leads to several striking patterns. Whereas simple correlations show that wealthier neighborhoods have a lower rate of positives, we show that income is not significant when occupations are included. However, we still see significant and positive effects on positive rates for minorities. These results could be because minorities are less likely to get tested, or have to be in worse conditions than whites in order to get tested.[8] However, whether these racial disparities are economically relevant can be questioned. Moreover, their magnitudes decrease over time as more testing becomes available – with Asians showing no statistical significance at the end of our sample. For example, on April 1, one month after the pandemic started in NYC, we find that a one-percentage point increase in the share of Blacks correlates with an increase of 0.34% in the share of positive tests, for an average number of 51% of positive cases. By April 20th, these numbers are 0.15% and 54%, respectively. For Hispanics, the disparity is larger, where a one-percentage-point increase in their population corresponds to an increase of 0.38% and 0.23% in the rate of positives, for the same two dates.

Our daily analysis also reveals that, as the stay-at-home orders starts to be effective, the magnitude of many occupations decreases as days go by. For example, a one-percentage-point increase in the number of workers employed in transportation

[5]Michaels et al. (2019) show that interactive occupations have become more important in larger metros over time. A recent paper by Barbieri et al. (2020) shows evidence of this mechanism for workers in Italy.

[6]Harries (2020) argues that the NYC subway was crucial for spreading the pandemic in NYC. More recently, Furth (2020) shows that "local infections are negatively correlated with subway use."

[7]We use similar controls to those in Borjas (2020) for comparability purposes.

[8]Some evidence that this is plausible mechanism can be found in `www.modernhealthcare.com/safety-quality/long-standing-racial-and-income-disparities-seen-creeping-covid-19-care`

Covid Economics 13, 4 May 2020: 31-50

decreases its size to 1% as of April 20, almost two months into the pandemic and one month after the stay-at-home order went into effect. On the other hand, we still find a rather stable coefficient of household size over time, which is consistent with the stay-at-home order being more helpful at mitigating contagion at work or in public spaces than within the household.

We conclude that much of the disparity in the rates of positives can be explained by different demographic groups being more or less representative across different occupations. In particular, a key channel appears to be the differences in exposure to human contact across jobs. However, our results also suggest that the relevance of these variables decreases over time, and that this change occurs in tandem with an increase in intra-household contagion as days go by. These trends are consistent with the progression of the pandemic and its interaction with the policies set in place. Two immediate policy implications arise from our analysis. First, it would be desirable to target these more sensitive groups of occupations with the distribution of protective gear, testing, and vaccination. This policy should not only be considered for their own risk of exposure, but also for the risk to others due to potential spillovers on the rest of the population. Second, local governments could give access to temporary shelter to those households that are forced to live in a reduced shared space.

2 Data description and patterns

Our source of incidence rates of COVID-19 and the number of tests performed is the NYC DOH data release. The DOH releases (almost) daily data on the cumulative count of COVID-19 cases and the total number of residents that have been tested, divided by the zip code of residence. We have collected data from April 1 to April 26, with only April 2 and April 6 missing from our sample.[9]

We obtain demographic and occupation data at the zip code level from the ACS. The demographic characteristics we include are zip code median income, average age, racial breakdown, and health insurance status. We also include commuting-related variables: average commute time to work as well as means of transportation. We plot a simple correlation between the share of positive tests and demographics. We see that shares of Blacks and Hispanics are positively correlated with rate of positive tests, a flat relationship for the share of Asians, and a negative relationship for income, as shown in Figure 2.

[9]Unfortunately these days have never been made publicly available.

Covid Economics 13, 4 May 2020: 31-50

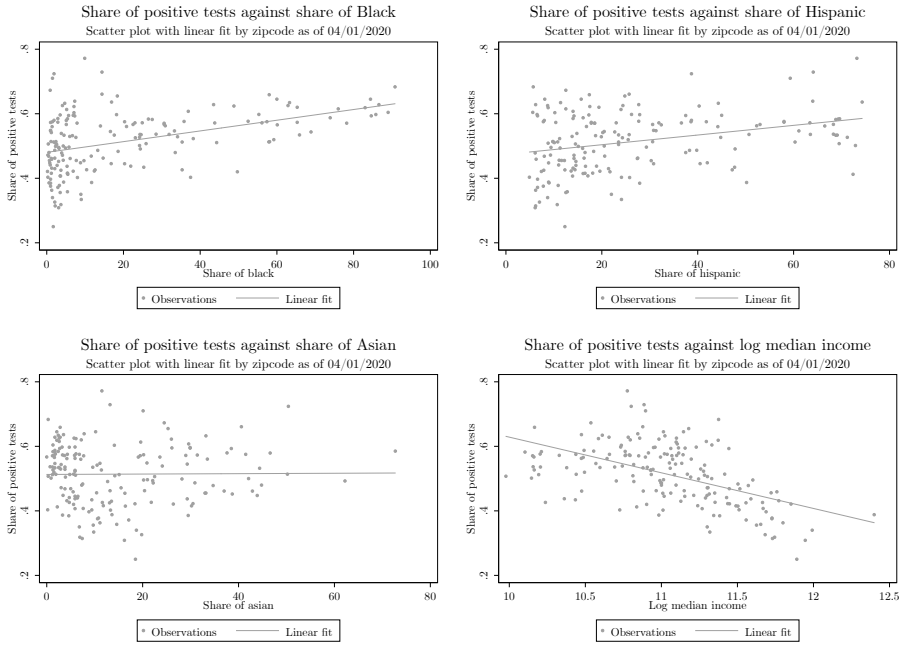

Figure 2: Share of positive tests against demographics by zip code

We also construct the shares of the working-age population employed at different occupation categories. The ACS provides the number of workers employed in each of the occupations listed in column 2 of Table 1 by zip code of residence. We then categorize them according to the groups listed in column 1 of Table 1. We do so by taking into account their essential definition, spatial correlations between them, and similarity in work environments and social exposure.[10] Table 1 shows the occupation groups that we use in our regressions. Summary statistics for all variables included

[10]Leibovici et al. (2020) rank occupations according to an index of occupational contact-intensity, defined from a survey by O*NET. They use ACS individual-level data at the four digit Standard Occupation Classification (SOC) level and match it to 107 ACS-defined occupations. Unfortunately, we only observe occupations at the SOC first level of aggregation for zip code data and cannot match their classification to our spatial distribution. Nonetheless, our categorization closely follows the intensity index grouping for the more specific group of occupations when aggregated to the first SOC level. More importantly, when defining our 13 categories, we avoid mixing occupations with large differences in their contact-intensity values. For robustness we have also performed our analysis with two alternative classifications for occupations. First, we divided occupations between essential and non-essential as declared by the US government. Second, we used the four categories defined in Kaplan et al. (2020). In both cases, the high level of aggregation lead to non-significant estimates or results that were hard to reconcile with observational evidence.

CEPR PRESS

in our empirical analysis can be found in Table 2.

Table 1: Occupation categories

Category	ACS Occupations
(1) Essential - Professional	Management, Business, Finance
(2) Non essential - Professional	Computer and Mathematical, Architecture and Engineering, Sales and Related, Community and Social Services, Education, Training, and Library, Arts, Design, Entertainment, Sports, and Media Administrative and Office Support
(3) Science fields	Life, Physical, and Social Science
(4) Law and related	Legal
(5) Health practitioners	Health practitioners
(6) Other health	Health technologists, technicians, and Healthcare Support
(7) Firefighting	Firefighting and prevention
(8) Law enforcement	Law enforcement
(9) Essential - Service	Food Preparation and Serving, Building and Grounds Cleaning and Maintenance
(10) Non essential - Service	Personal Care and Service
(11) Industrial, Natural resources and Construction	Construction and Extraction, Material Moving, Farming, Fishing, and Forestry, Production
(12) Essential - Technical	Installation, Maintenance, and Repair
(13) Transportation	Transportation

Finally, Table 2 presents the summary statistics of all the variables that are used in our analysis.

Table 2: Summary statistics

Variable	Mean	Std. Dev.	p10	Median	p90
Share of positive tests	0.563	0.085	0.438	0.583	0.645
Tests per Capita	0.018	0.006	0.012	0.017	0.026
Median Income (in 000's)	68.604	31.878	34.122	62.202	115.084
Share $\geq 20, \leq 40$	0.323	0.084	0.246	0.308	0.433
Share $\geq 40, \leq 60$	0.258	0.033	0.220	0.261	0.296
Share ≥ 60	0.200	0.079	0.132	0.190	0.276
Share Male	0.477	0.029	0.446	0.479	0.508
Household Size	2.683	0.537	1.930	2.750	3.300
% Black	0.200	0.240	0.010	0.076	0.600
% Hispanic	0.263	0.195	0.078	0.189	0.634
% Asian	0.144	0.139	0.017	0.094	0.335
Density (in 000's)	43.380	31.045	10.784	36.639	90.075
% Public Transport	0.532	0.150	0.312	0.543	0.712
Commuting Time (in mins)	40.647	7.054	27.200	42.100	48.100
% Uninsured	0.089	0.043	0.042	0.084	0.143
% Essential - Professional	0.126	0.089	0.046	0.092	0.285
% Essential - Service	0.065	0.033	0.035	0.060	0.107
% Essential - Technical	0.014	0.009	0.004	0.013	0.022
% Health practitioners	0.029	0.018	0.009	0.026	0.050
% Other health	0.038	0.024	0.010	0.035	0.073
% Firefighting	0.012	0.009	0.003	0.012	0.023
% Law enforcement	0.007	0.007	0.001	0.006	0.014
% Ind. and Construction	0.054	0.027	0.014	0.056	0.090
% Transportation	0.029	0.016	0.004	0.032	0.048
% Non ess. - Professional	0.279	0.075	0.195	0.271	0.359
% Science fields	0.006	0.007	0.001	0.004	0.015
% Law and related	0.018	0.026	0.003	0.008	0.049
% Non ess. - Service	0.032	0.013	0.016	0.032	0.047

Covid Economics 13, 4 May 2020: 31-50

Covid Economics 13, 4 May 2020: 31-50

3 Results

3.1 General Results

In this section, we present the main empirical results for our four different specifications. Our unit of analysis is the zip code, and all models include the share of positive tests as the dependent variable. Additionally, we include tests-per-capita as a proxy for the overall spread of infection within the neighborhoods. The first model includes some widely discussed potential factors of the spread of COVID-19 in NYC: density and commuting patterns, specifically, log of population density, percentage of workers using public transport, average commute time, and the percentage of the population who is uninsured. Our second model expands by including our proposed mechanism, namely, the percentage of the working-age population employed in each of the 13 occupation categories defined in Table 1. The third specification adds demographic controls related to income, age, gender, household size, and race. Finally, we include borough fixed effects in our last model. Exploiting the fact that we have daily data over multiple days, we estimate a separate regression for each of them, allowing us to detect any time patterns in the correlations. Therefore, in all of our specifications we run the following regression equation

$$\text{share of positive tests}_{it} = \alpha_t + \beta_t \text{tests per capita}_{it} + \gamma_t X_i + \epsilon_{it},$$

where the set of controls X_i vary according to the description above.

The first model shows the effect of the variables commonly used to explain the incidence of COVID-19 in NYC. Whereas Harries (2020) finds subway use was a major factor of the virus spread, we find it does not have a significant effect. This result could be due to the lack of cross-neighborhood variation to identify this effect, because most New Yorkers use public transportation in their daily commute. Nonetheless, commute time is a significant factor. For example, for April 20 a four-minute increase in commute time, a 10% increase on average, correlates with a 0.02-point increase in the share of positive tests, equivalently to approximately a 4-percentage-point increase in the share of positive tests.[11] We also find a positive and significant effect of the share of the uninsured population on the rate of positives for most of our sample. This result may be explained by uninsured patients only being willing to be tested under very acute symptoms in the fear of medical charges. For April 20, we find that a one-percentage-point increase in the share of uninsured population being correlated with a 1.7-percentage-point increase. Although the magnitude of this variable decreases as we include other covariates, its estimated coefficient remains positive and significant.

In specification (2) we test the importance of different occupations. We include the variables defined as the shares of the working-age population employed in these occupations, so the coefficients are relative to the working-age but not employed population. The coefficients can be read as the effect of a one-percentage-point increase

[11] The average rate of positive tests on April 20 was 54%.

Covid Economics 13, 4 May 2020: 31-50

in the population employed in the particular category on the share of positive tests. We find some occupations explain a significant part of the variation in COVID-19 incidence. On the one hand, an increase in the share of workers employed in non-essential - professional, other health (not health practitioners), and transportation occupations are all associated with a higher percentage of positive tests. On the other hand, higher shares of workers in the science fields category, legal occupations, and law enforcement have a negative correlation with the share of positive tests. These results are discussed further in the time-trends section.

Perhaps surprisingly, under this specification, commute time no longer has a significant effect. This result suggests commuting patterns are closely related to occupations, and most of the explanatory variation for commuting patterns may come through this channel. This result also implies the existence of within-city location and mobility patterns that are occupation specific.

We include demographic variables in the third model. Despite the strong correlation between the share of positive tests and demographic characteristics, the results for specification (3) show that some of them can be explained through the occupation mechanism. Notably, the income effect disappears when we control for occupations, suggesting the previous correlation is due to income differences across jobs. Still, some demographic effects remain significant, even after including borough fixed effects. For example, on April 20, a one-percentage-point increase in the share of Blacks and Hispanics leads to a 0.15% and 0.23% increase respectively in the rate of positives, an effect that is economically small. A plausible explanation for these patterns could be driven by a racial bias on the incidence of testing, as pointed out by Borjas (2020). Another explanation is differences in adherence to the shelter-in-place policy, as explored by Coven and Gupta (2020). We also find that household size has positive correlation with test outcomes. On April 20, Adding one extra person to the average household, a 37% increase, corresponds with a 7% increase in the percentage of positive tests. Although neighborhood density does not explain variation in the share of positive tests, density in households appears to do so, with increasing magnitude over time.

The tests-per-capita coefficient is positive and highly significant across all days for specification (4). Because of the scarcity of tests, testing was only performed on those showing sufficiently severe symptoms or who had a high risk of infection. As argued above, we interpret this variable as a proxy for the rate of infections within the neighborhood.[12] Its magnitude decreases over time as testing becomes more available and accessible to the rest of the population.

[12]A potential concern is large differences in the age distribution across NYC zip codes. In the data, we find that the average age in NYC ranges from 27.5 to 45.5 across neighborhoods in NYC, with the exception of zip code 11005. It is a fairly small zip code with 1700 residents, an average age of 76, and mainly composed of retired immigrant women. Given such differences, we have excluded it from our analysis.

Covid Economics 13, 4 May 2020: 31-50

Table 3: Dependent variable - share of positive tests as of April 1, 2020

	(1) Nbhd Controls		(2) + Occupations		(3) + Demographics		(4) + Borough FE	
Tests per Capita	9.017***	(2.879)	11.186***	(2.447)	10.773***	(2.249)	12.050***	(2.386)
Log Density	0.015	(0.014)	0.022*	(0.012)	0.015	(0.012)	0.032***	(0.011)
% Public Transport	-0.015	(0.072)	0.013	(0.068)	0.053	(0.070)	-0.059	(0.062)
Log Commuting Time	0.237***	(0.046)	-0.016	(0.083)	0.009	(0.075)	-0.054	(0.062)
% Uninsured	1.002***	(0.141)	0.662***	(0.246)	0.336	(0.215)	0.150	(0.180)
% Essential - Professional			0.156	(0.271)	0.695***	(0.238)	0.766***	(0.236)
% Non ess. - Professional			0.669***	(0.189)	0.615***	(0.181)	0.544**	(0.216)
% Science fields			-4.703***	(1.294)	-3.745***	(1.064)	-2.965***	(1.118)
% Law and related			-0.410	(0.801)	-0.875	(0.754)	-1.427**	(0.697)
% Health practitioners			-0.432	(0.421)	-0.167	(0.431)	-0.167	(0.386)
% Other health			0.947***	(0.321)	0.027	(0.412)	0.346	(0.402)
% Firefighting			2.743**	(1.072)	1.624	(1.109)	1.629*	(0.965)
% Law enforcement			-0.301	(1.215)	0.815	(1.089)	-0.223	(1.016)
% Essential - Service			-0.100	(0.354)	0.258	(0.347)	0.245	(0.300)
% Non ess. - Service			0.769	(0.561)	1.166**	(0.509)	1.154**	(0.483)
% Ind. and Construction			1.091**	(0.437)	1.208***	(0.402)	0.839**	(0.401)
% Essential - Technical			-2.025*	(1.133)	-0.457	(0.979)	-0.319	(0.881)
% Transportation			1.752***	(0.588)	1.718***	(0.527)	1.102**	(0.469)
Log Income					-0.008	(0.034)	-0.010	(0.033)
Share ≥ 20, ≤ 40					-0.346*	(0.176)	-0.357**	(0.173)
Share ≥ 40, ≤ 60					-0.855***	(0.222)	-0.611**	(0.237)
Share ≥ 60					-0.380**	(0.175)	-0.347*	(0.197)
Share Male					-0.050	(0.267)	-0.146	(0.264)
Log Household Size					0.076	(0.073)	0.037	(0.061)
% Black					0.149***	(0.039)	0.175***	(0.040)
% Hispanic					0.003	(0.050)	0.194***	(0.050)
% Asian					0.136**	(0.053)	0.141***	(0.050)
Bronx							-0.014	(0.023)
Brooklyn							0.086***	(0.022)
Queens							0.084***	(0.024)
Staten Island							0.083***	(0.027)
Constant	-0.671**	(0.264)	-0.149	(0.342)	0.110	(0.372)	0.196	(0.334)
Observations	174		174		174		174	
R^2	0.514		0.694		0.785		0.839	

Weighted OLS by population size. Robust standard errors in parentheses

* $p < 0.10$, ** $p < 0.05$, *** $p < 0.01$, *** $p < 0.01$

Covid Economics 13, 4 May 2020: 31-50

Table 4: Dependent variable - share of positive tests as of April 10, 2020

	(1) Nbhd Controls		(2) + Occupations		(3) + Demographics		(4) + Borough FE	
Tests per Capita	1.913**	(0.832)	1.713*	(0.921)	1.795**	(0.763)	3.904***	(0.675)
Log Density	0.022*	(0.013)	0.018*	(0.010)	0.013	(0.008)	0.022***	(0.007)
% Public Transport	-0.001	(0.060)	0.012	(0.056)	0.095*	(0.056)	-0.004	(0.041)
Log Commuting Time	0.262***	(0.040)	0.019	(0.069)	0.022	(0.060)	-0.023	(0.045)
% Uninsured	1.038***	(0.104)	0.521***	(0.187)	0.316**	(0.136)	0.290***	(0.103)
% Essential - Professional			-0.003	(0.203)	0.579***	(0.177)	0.484***	(0.179)
% Non ess. - Professional			0.419**	(0.173)	0.354**	(0.166)	0.257*	(0.138)
% Science fields			-3.021***	(1.082)	-3.094***	(0.905)	-2.334***	(0.812)
% Law and related			-0.604	(0.525)	-1.050**	(0.480)	-1.293***	(0.422)
% Health practitioners			-0.248	(0.372)	-0.061	(0.379)	-0.124	(0.281)
% Other health			0.753***	(0.258)	-0.275	(0.302)	0.238	(0.231)
% Firefighting			1.282	(0.880)	-0.042	(0.869)	0.456	(0.570)
% Law enforcement			-1.859	(1.149)	-1.217	(0.892)	-1.323*	(0.751)
% Essential - Service			0.159	(0.262)	0.198	(0.280)	0.127	(0.199)
% Non ess. - Service			0.359	(0.471)	0.844**	(0.417)	0.781**	(0.350)
% Ind. and Construction			0.472	(0.332)	0.497*	(0.279)	0.101	(0.225)
% Essential - Technical			-0.729	(0.854)	-0.150	(0.718)	-0.474	(0.531)
% Transportation			1.824***	(0.419)	1.639***	(0.377)	0.831***	(0.299)
Log Income					-0.024	(0.023)	-0.027	(0.021)
Share ≥ 20, ≤ 40					-0.243**	(0.122)	-0.246**	(0.097)
Share ≥ 40, ≤ 60					-0.510***	(0.181)	-0.228	(0.149)
Share ≥ 60					0.127	(0.114)	-0.017	(0.115)
Share Male					0.453**	(0.180)	0.249	(0.171)
Log Household Size					0.167***	(0.054)	0.111***	(0.042)
% Black					0.165***	(0.030)	0.114***	(0.026)
% Hispanic					0.018	(0.041)	0.130***	(0.034)
% Asian					0.047	(0.043)	0.018	(0.030)
Bronx							-0.040***	(0.014)
Brooklyn							0.053***	(0.015)
Queens							0.058***	(0.016)
Staten Island							-0.022	(0.023)
Constant	-0.765***	(0.228)	0.010	(0.269)	-0.137	(0.258)	0.107	(0.213)
Observations	174		174		174		174	
R^2	0.674		0.801		0.871		0.921	

Weighted OLS by population size. Robust standard errors in parentheses

* $p < 0.10$, ** $p < 0.05$, *** $p < 0.01$, *** $p < 0.01$

Covid Economics 13, 4 May 2020: 31-50

Table 5: Dependent variable - share of positive tests as of April 20, 2020

	(1) Nbhd Controls		(2) + Occupations		(3) + Demographics		(4) + Borough FE	
Tests per Capita	0.667	(0.485)	0.262	(0.560)	0.381	(0.497)	2.553***	(0.476)
Log Density	0.024**	(0.011)	0.015*	(0.009)	0.011	(0.008)	0.016***	(0.006)
% Public Transport	0.010	(0.055)	-0.001	(0.050)	0.080	(0.053)	-0.017	(0.040)
Log Commuting Time	0.232***	(0.034)	0.001	(0.060)	0.004	(0.055)	-0.008	(0.042)
% Uninsured	0.924***	(0.099)	0.417**	(0.171)	0.296**	(0.129)	0.351***	(0.098)
% Essential - Professional			-0.210	(0.168)	0.294*	(0.165)	0.235	(0.160)
% Non ess. - Professional			0.329**	(0.147)	0.274*	(0.152)	0.224*	(0.122)
% Science fields			-1.931*	(1.016)	-2.318***	(0.861)	-1.609**	(0.784)
% Law and related			-0.492	(0.456)	-0.851*	(0.460)	-0.898**	(0.397)
% Health practitioners			-0.155	(0.357)	0.010	(0.387)	-0.206	(0.278)
% Other health			0.815***	(0.232)	-0.053	(0.272)	0.365	(0.221)
% Firefighting			0.379	(0.829)	-0.765	(0.876)	-0.156	(0.556)
% Law enforcement			-1.970*	(1.049)	-1.472*	(0.820)	-1.344**	(0.655)
% Essential - Service			0.312	(0.229)	0.205	(0.242)	0.082	(0.171)
% Non ess. - Service			-0.046	(0.437)	0.455	(0.378)	0.578*	(0.296)
% Ind. and Construction			0.271	(0.317)	0.246	(0.271)	-0.079	(0.209)
% Essential - Technical			-0.785	(0.724)	-0.603	(0.617)	-0.908*	(0.487)
% Transportation			1.253***	(0.364)	1.083***	(0.327)	0.541*	(0.293)
Log Income					-0.021	(0.022)	-0.022	(0.019)
Share ≥ 20, ≤ 40					-0.169	(0.115)	-0.208**	(0.090)
Share ≥ 40, ≤ 60					-0.389**	(0.161)	-0.198	(0.126)
Share ≥ 60					0.248**	(0.108)	0.002	(0.104)
Share Male					0.540***	(0.166)	0.318**	(0.150)
Log Household Size					0.167***	(0.047)	0.099***	(0.036)
% Black					0.140***	(0.030)	0.081***	(0.026)
% Hispanic					0.027	(0.036)	0.125***	(0.033)
% Asian					0.015	(0.043)	0.012	(0.031)
Bronx							-0.062***	(0.014)
Brooklyn							0.034**	(0.014)
Queens							0.023	(0.015)
Staten Island							-0.064***	(0.022)
Constant	-0.682***	(0.195)	0.201	(0.232)	-0.076	(0.236)	0.111	(0.196)
Observations	174		174		174		174	
R^2	0.673		0.800		0.866		0.920	

Weighted OLS by population size. Robust standard errors in parentheses

* $p < 0.10$, ** $p < 0.05$, *** $p < 0.01$, *** $p < 0.01$

Covid Economics 13, 4 May 2020: 31-50

3.2 Daily comparison and time trends

In this section we present a time-variant analysis that could provide insights on both the evolution of the pandemic effects as well as the health policies in place. Figures 3 to 5 show the time evolution of the coefficients for specification (4). The result for the tests-per-capita variable is particularly salient; we observe a strong correlation on the share of positive tests that becomes progressively smaller over time. This result could be reconciled with the fact that in the earlier days of the crisis, testing was severely limited. Zip codes with more tests implied a higher share of people at high risk of having the disease. So, a key takeaway from the results of our daily comparison is the importance of widespread testing, because it allows us to identify the mechanisms that explain demographic and occupational differences in COVID-19 exposure.

Notable time trends exist in the correlations associated with occupations. Higher shares of essential - professional and non-essential - service categories were associated with higher percentage-point increases in the rate of positive tests at earlier dates. On April 1, a one-percentage-point increase implied a 1.5- and a 2.2-percentage point increase in the positive rate of tests. However, they eventually decrease, averaging closer to a 0.3- and a one-percentage-point increase respectively on April 20, with essential - professional not being statistically significant. A plausible explanation is that these professions are either non-essential, or have the highest shares of remote workers. Although they were highly exposed to the virus in the beginning, once the workers shelter in place, their correlation with positive tests subsides. The opposite happens in science fields and law occupations — they are negatively correlated with COVID-19 incidence in the beginning, but the effect trends towards zero.

We find interesting patterns for the essential occupations as well. An additional percentage point in the share of transportation workers is associated with between a 0.5- and a one-percentage-point increase in the rate of positive tests. The effect seems to decay over time, but at a slower rate than other occupations. This result could be due to its essential designation, but also due to its relatively high-exposure nature. The share of industrial, natural-resources, and construction occupations starts off with a positive correlation with COVID-19 incidence. However, a week after the general stay-at-home order, the governor determined construction was not essential, and this order could explain the eventual attenuation of the correlation. Law-enforcement-occupation shares have a consistently negative correlation on the share of positive, whereas firefighter shares have a declining trajectory toward zero. A plausible explanation for this difference could be the partnership between the NYPD and health care groups to provide free testing to its members.[13] Furthermore, the NYPD provided additional work flexibility for members with pre-existing conditions and extensive sick leave. It's possible that early adoption of these measures protected the most vulnerable workers from infection right from the onset. [14]

[13] www.nypost.com/2020/04/03/nypd-partners-with-health-care-groups-to-test-cops-for-covid-19/
[14] More information on this can be read in www.policemag.com/548778/

Covid Economics 13, 4 May 2020: 31-50

The share of the uninsured population increasingly predicts the variation in positive test results. We find that an additional percentage point in the share of uninsured predicts an almost 0.3-percentage-point increase in the share of positive tests. Although many health care providers are waiving COVID-19-related out-of-pocket costs, these fees remain very high for the uninsured, and so a higher incidence of COVID-19 in this group could imply a severe financial burden. Although still significant, the effect of neighborhood density declines over time, and the opposite occurs for household size. The stay-at-home order could mitigate part of the risk of high neighborhood density, while increasing the probability of within-household infections.

Finally, another outstanding time pattern is that the coefficients on racial composition decrease in magnitude as the selection of testing decreases. This result may suggest a stronger racial-selection component is at play among those in worse conditions at earlier dates. For example, an explanation for this pattern could be that black citizens were less likely to be tested or had to be in worse conditions to access testing compared to white citizens.[15]

4 Conclusions and policy implications

In this paper, we present evidence showing that occupations are an important channel for explaining differences in the rates of COVID-19 across neighborhoods. Using data from NYC at the zip code level, we study the relationship between the share of positive tests and the share of workers in different occupations. The DOH provides daily updates of COVID-19 test data, allowing us to study the aforementioned relationships over multiple days and to detect time patterns in their magnitudes.

We begin by showing descriptive evidence of the heterogeneous incidence of positive cases across neighborhoods, income, race, gender, and household size. A zip code's median income is negatively correlated with its share of positive tests. Conversely, we find that the shares of Black and Hispanic residents, and average household size positively correlate with the share of positive tests. Highlighting these differences is important because these observations confirm that the disease has had more harmful effects on vulnerable communities. Finding an occupation mechanism that explains it could guide policy measures intended to alleviate its impact.

We estimate several models to explore the effect of occupations. Our first specification only includes neighborhood characteristics, such as the use of public transportation and the average length of daily commutes. Although commuting patterns have been put forth as a major factor in the spread of the disease in NYC, we show that, after including occupation controls, they fail to significantly explain variation in share of positive tests at the zip code level.

nypd-implements-policy-to-protect-most-vulnerable-officers-from-covid-19

[15] Some evidence that this is plausible mechanism can be found in www.modernhealthcare.com/safety-quality/long-standing-racial-and-income-disparities-seen-creeping-covid-19-care

Covid Economics 13, 4 May 2020: 31-50

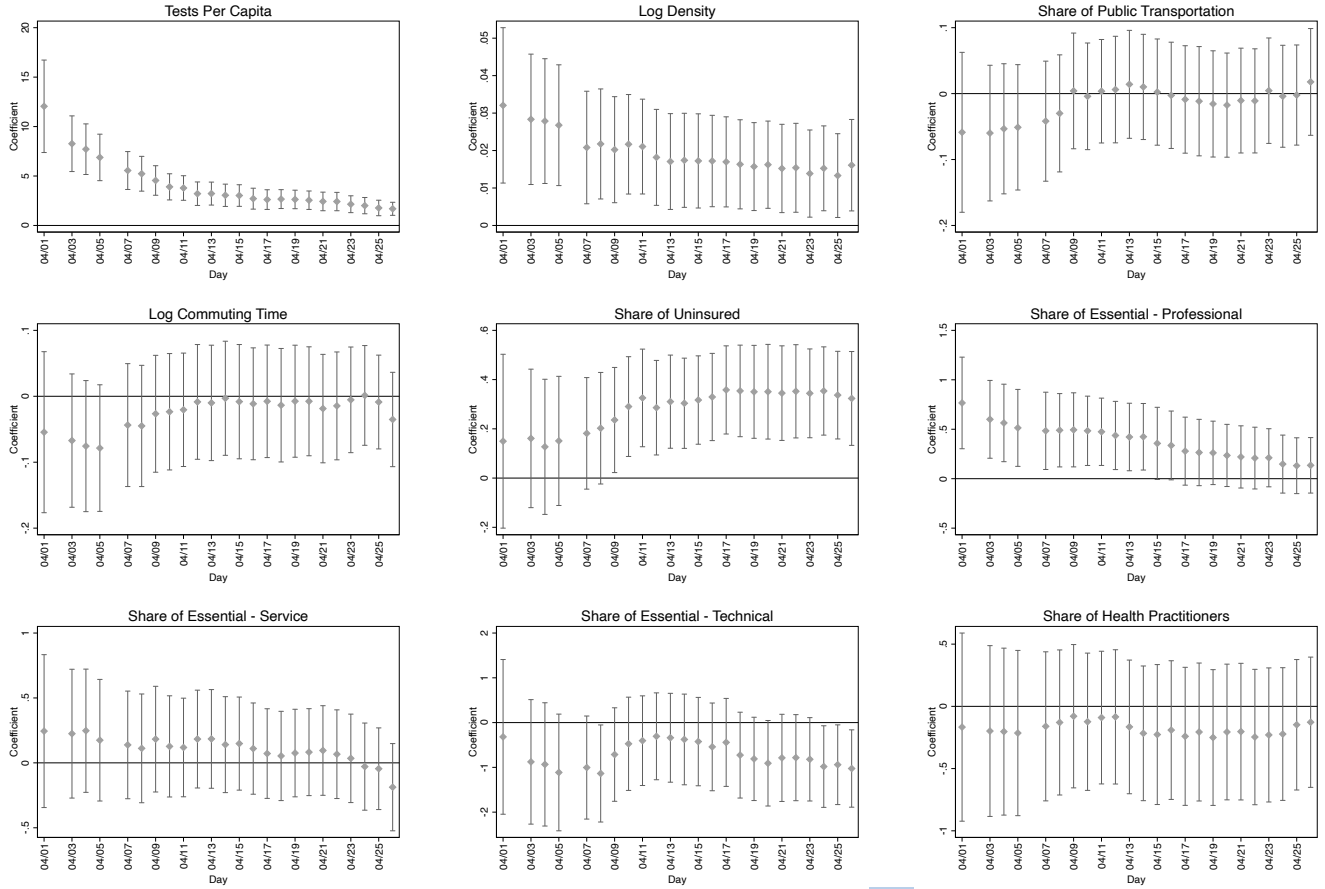

Figure 3: Regression coefficients of specification (4) over time

Covid Economics 13, 4 May 2020: 31-50

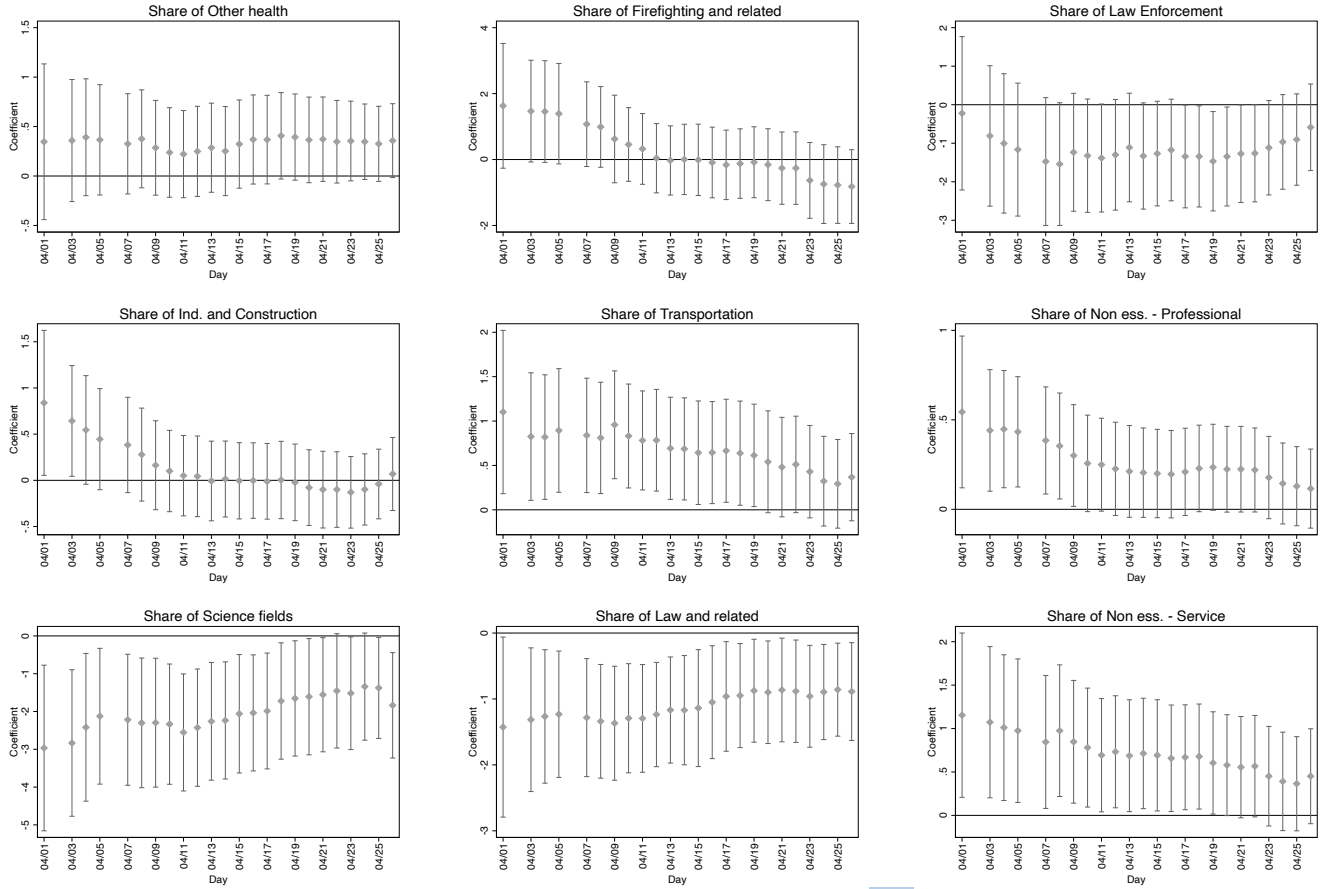

Figure 4: Regression coefficients of specification (4) over time

Covid Economics 13, 4 May 2020: 31-50

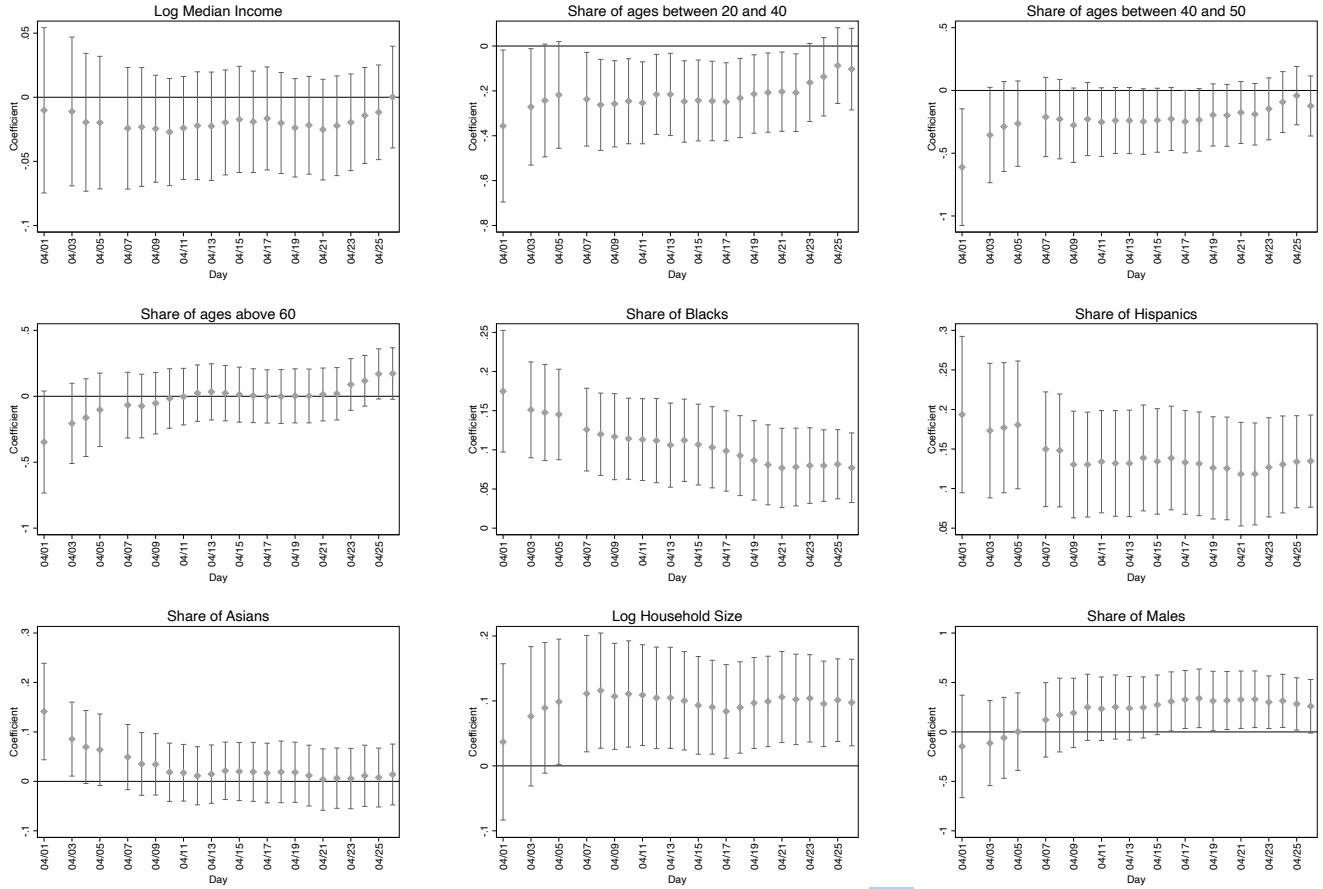

Figure 5: Regression coefficients of specification (4) over time

Covid Economics 13, 4 May 2020: 31-50

We find the strongest positive correlation on the share of positive tests with the share of workers in Transportation, Industrial, Natural-resources, Construction, and Non essential - Professional, with clear time trends in their estimated coefficients. For example, in the case of Transportation, a one-percentage-point increase in the share of workers in these occupations leads to a one- to two-percentage-point increase in the rates of positive results. Although the other two have a significant effect in positive shares at earlier dates, their magnitude becomes insignificant by the end of our sample period. This trend could be a result of the stay-at-home order. Conversely, higher shares of workers in Science Fields and Law Enforcement reduce the number of positive rates, with Science Fields decreasing in magnitude over time.

When adding demographic controls, we observe that racial patterns do persist, suggesting that the occupation mechanism does not fully explain all of the racial differences. However, their magnitude is small and arguably not economically relevant. Income and most age groups do not contribute to explaining the variation in positive tests, suggesting the occupation mechanism can explain to a greater extent the disparities along those demographics observed in the data.

In all of our regression models we include the number of tests per capita, and find that it is a strong predictor of the share of positive tests. However, its relative importance declines over time, as tests become more widely available. Moreover, as this variable loses relevancy, more of the variation in COVID-19 incidence is explained through the occupation channel.

Our results suggest clear implications for policy. First, they highlight the importance of mass testing in enabling clean identification of the relevant channels that increase the risk of infection. Second, once these channels are identified, policy-makers can target specific groups in the provision of protective gear, tests, and vaccinations. The purpose of this policy is twofold: while it provides extra protection against the disease for those who are more vulnerable, it also has positive spillovers on the rest of the population. For example, a policy that starts vaccinating and/or testing those workers with higher rates of human interaction affects not only those directly targeted by the policy, but also those who are likely to be in contact with them. Moreover, our results also suggest that health insurance condition, namely lack of insurance, plays a significant role, and its importance increases over time. Hence, local governments could incentivize the population without medical insurance to get tested, implementing policies such as full coverage of out-of-pocket costs in relation to COVID-19. Finally, we provide suggestive evidence that the stay-at-home order has mitigated contagion rates at work or in public spaces, while it has increased the probability of intra-household infections. This last result suggests the importance of policy or guidance measures to decrease spread within households.

CEPR PRESS

References

Barbieri, T., Basso, G., and Scicchitano, S. (2020). Italian workers at risk during the covid-19 epidemic. *Unpublished Manuscript*.

Borjas, G. J. (2020). Demographic determinants of testing incidence and covid-19 infections in new york city neighbourhoods. *Covid Economics, Vetted and Real-Time Papers*.

Coven, J. and Gupta, A. (2020). Disparities in mobility responses to covid-19. *Working Paper*.

Furth, S. (2020). Automobiles seeded the massive coronavirus epidemic in new york city. Available at `https://marketurbanism.com/2020/04/19/automobiles-seeded-the-massive-coronavirus-epidemic-in-new-york-city/`.

Harries, J. E. (2020). The subways seeded the massive coronavirus epidemic in new york city. *NBER Working Papers*.

Kaplan, G., Moll, B., and G., V. (2020). Pandemics according to hank. Available at `https://benjaminmoll.com/wp-content/uploads/2020/03/HANK_pandemic.pdf`.

Leibovici, F., Santacreu, A. M., and Famiglietti, M. (2020). Social distancing and contact-intensive occupations. Available at `https://www.stlouisfed.org/on-the-economy/2020/march/social-distancing-contact-intensive-occupations`.

Michaels, G., Rauch, F., and Redding, S. J. (2019). Task specialization in us cities from 1880 to 2000. *Journal of the European Economic Association*, 17(3):754–798.

Schmitt-Grohé, S., Teoh, K., and Uribe, M. (2020). Covid-19: Testing inequality in new york city. *NBER Working Papers*.

Covid Economics 13, 4 May 2020: 31-50

Covid Economics **Issue 13, 4 May 2020**

Cultural and economic discrimination by the Great Leveller: The COVID-19 pandemic in the UK

Annie Tubadji,[1] Don J Webber[2] and Fred Boy[3]

Date submitted: 24 April 2020; **Date accepted:** 28 April 2020

This article presents a spatial analysis of COVID-19 mortality rates across England and Wales in the early part of the pandemic (3/January/2020 to 27/March/2020). It assesses whether cultural and/or economic discrimination enhanced the vulnerability of groups of people and places. We used data on lung cancer deaths in non-pandemic times as an instrument for mortality rates during the pandemic and explored the relationship between COVID-19 mortality rates and the Brexit vote. Results suggest that the effects of cultural discrimination on COVID-19-related mortality is five times greater than the economic effect, and deaths were 19 percent higher in pro-Brexit areas.

Covid Economics 13, 4 May 2020: 51-70

1 Senior Lecturer in Economics, Swansea University.
2 Professor of Managerial Economics, Sheffield University Management School.
3 Associate Professor in Business, Swansea University.

Covid Economics 13, 4 May 2020: 51-70

1. Introduction

Early UK mortality statistics relating to the COVID-19 pandemic[1] reveal that the number of deaths were consistently larger in London, but it is widely known that cities are the most economically unequal places (Mingione, 1996; Glaeser *et al.*, 2009). A closer examination of the data may reveal a more nuanced pattern about the propensity of different groups of people to die from the COVID-19 virus and their spatial patterns within and between conurbations; for instance, is the probability of dying from COVID-19 higher in specific socioeconomic or deprived groups who co-locate spatially? Although fine-grain individual-level statistical analyses of the COVID-19 pandemic are currently not feasible due to data availability, it is possible to gain insights into these issues by exploring available spatial data and by contrasting their socioeconomic characteristics.

Geographies of deprivation have been cautiously analysed in attempts to understand the reasons for the Brexit vote (Rodríguez-Pose, 2018; McCann, 2019). Deprived areas experience more precarious socioeconomic conditions and higher levels of uncertainty, poorer diets and greater stress, and therefore their citizens have lower immune systems (Zaman *et al.*, 1997; Bray *et al.*, 2008; Berry *et al.*, 2012; Kim *et al.*, 2013; Matzner, 2013). Moreover, the onset of multimorbidity occurs 10-15 years earlier for people living in the most deprived areas compared with people living in the most affluent areas, with socioeconomic deprivation strongly associated with multimorbidity including poor mental health (Barnett *et al.*, 2012). Meanwhile, the country is already expected to experience a negative economic shock at the end of the Brexit implementation period (Los *et al.*, 2017). The current study alerts that the current pandemic is likely to exacerbate and deepen existing inequalities on the brink of a post-Brexit economic shock.

This study investigates how regional inequalities, in terms of deprivation and cultural discrimination, are reflected in the current and future consequences of the COVID-19 pandemic. Our paper has three aims: (i) to map the geography of the COVID-19 pandemic across England and Wales; (ii) to examine the relationship between the geography of the pandemic and the geography of deprivation and cultural diversity; and (iii) to identify the places that are becoming more economically vulnerable and more at risk of the consequences of economic shocks that are expected due to the lock-down and to follow the end of the Brexit implementation period.

Using historic and current data for England and Wales on regional development, cultural and economic disparities, and COVID-19 mortality, this study applied data decomposition and 2SLS IV methods of analysis to improve understanding of the spatial disparities in the COVID-19 death toll. We explain disparities in the COVID-19 death toll in terms of the overall socioeconomic milieu of deprivation and the interaction of deprivation with cultural and economic belonging. We also add to the literature by identifying places that are experiencing faster rates of increase in economic instability in terms of unemployment and small business failure in order to identify the probable locations of future extreme deprivation. Thus, we highlight areas in which COVID-19 exacerbates inequalities leading to possible consequent social unrest.

[1] We are aware that improvements to COVID-19 mortality data are required and that constant updates and corections are being made. However, these updates regard the methods of data collection for the entire sample and therefore they do not concern the inequalities that are between groups within the sample. One and the same measurement error is most likely to be incurred across the groups, and therefore the between group effects should remain unaffected.

We reveal that the effect of cultural discrimination on COVID-19-related mortality was five times greater than the economic effect, and that deaths were 19 percent higher in pro-Brexit areas. Our study brings closer attention to places that are likely to experience increases in grievances from being left behind. New grievances, which may coincide with economic change in the post-Brexit transition period and the morbidity and mortality consequences of the COVID-19 virus, will deepen existing inequalities. As growing economic inequality is known to be associated with social unrest (Hirschman and Rothschild, 1973; Benabou and Tirole, 2006, 2009, 2011, 2016), urgent measures are needed to support and alleviate both economic losses, ongoing health issues and psychological traumas; this is especially the case in places where COVID-19 aggravates inequality and is associated with past tendencies towards social unrest due to deprivation and existing feelings of being left behind.

The structure of this paper is as follows. Section 2 briefly summarises the voluminous literature on economic inequality in the UK. This section also reviews what we know about the geographies of deprivation and the Brexit vote, and how these link to what we know about inequality and the unrest-generating tunnel effect. Section 3 elucidates the suitability of the Culture-Based Development (CBD) methodology for the analysis of economic and cultural discrimination that may lead to disparities in the death toll and social unrest. Section 4 outlines our analytical framework, hypotheses and data, with the empirical results presented in Section 5. Section 6 concludes and highlights some of our most important policy implications.

2. Historical Roots of Inequality in the UK

The UK is traditionally and historically a society of deep economic and social class division. Stobart (2011) outlines the quality of life of affluent people over the 1710-1790 period and describes the contemporaneous lavish Veblenian consumption of goods that signalled social status. Meanwhile, Perry (2005) and Gazeley and Verdon (2014) depict the dire conditions of households living in poverty in 18th Century England. An overarching dynamic of poverty in the UK also pervades the present, as is clear from the work of Smith and Middleton (2007). The historic roots of economic inequality in the UK were never successfully expunged, and they developed nuances that reflect new discriminatory trends and socioeconomic marginalization across gender, geography, ethnic and age groups that permeate into the 21th century (Lindert, 2000; Niemietz, 2009; Davies and Joshie, 2018; Cribb *et al*., 2018).

The geography of inequality in the UK exposes one of the most severe signs of this deep-seated problem and its historical roots. Some studies reveal persistent inequalities in endowments and investments, as illustrated through the history of construction of the motorway network (Merriman, 2009). Spatial inequalities in the UK have many aspects, but one that has gained particular attention and traction in the literature is the cultural dimension (Massey, 1979; Lindert, 1996, 2000; Hall, 1997; Martin, 2004; Wei, 2015), which has been shown to have a trace of spatial persistence into the modern day (Hills, 2010).

Documents reporting the economic history of pandemics, and specifically in the UK, are full of examples of connecting economic deprivation and inequality with mortality. Examples include the plague in London and its grave-digging practices (Howson, 1961; Hardling, 1989; Mack, 1991) and the foot-and-mouth disease (Woods, 2013). The effects of a health crisis are not irreversible and proper policymaking interventions could abate their ramifications for economic development. For example, explorations into the effects of malaria on the development of Southern European countries demonstrate that the health parameter did not determine the developmental path of these countries thanks to economic

Covid Economics 13, 4 May 2020: 51-70

policy (Bowden *et al*., 2008), suggesting that beneficial economic interventions can put economies on to a preferable developmental path.

The issues of inequality and vulnerability that we are raising here are, of course, not unique for Britain. From a global perspective, inequality and pandemics have always been related, and the fall of empires are often accompanied by pandemics, such as plagues. Some researchers argue that the fall of empires have been due to growing inequality, leading to a deterioration in the health condition of the poor and greater exposure to foreign germs by the increasingly mobile rich (Kohn, 2007; Turchin, 2007). The relevance of these historical studies has been raised recently elsewhere in the context of the COVID-19 case (Turchin, 2020; Spinney, 2020), as have the contributory effects of social factors in other global diseases such as Ebola (Grépin *et al*., 2020). Thus, historic or path dependent inequality is likely to be linked to the current spread of COVID-19 in a socioeconomically and spatially uneven manner, and timely policy interventions are essential to ameliorate the conditions and avoid destabilizing the socioeconomic development in the country.

There is also historical evidence about how the deprived were often exploited in times of pandemics, such as the increased use of the Black labour force during pandemic times in South Africa (Packard, 1989). Similar sector-specific tendencies seem not far from modern reality in the UK when we see construction workers continuing to work during COVID-19 social distancing and lockdown periods. Health care workers in elderly care homes also must put themselves in the front line to fight against this pandemic, and these jobs tend to be low-paid and undertaken by women. There is an endogenous relationship here, as individuals' decisions to comply or otherwise with social-distancing regulations depend at least in part on economic incentives, which themselves responded to current economic policy and expectations of future policies (Chang and Velasco, 2020). However, although individuals across the income divide may time-discount at different rates and therefore respond to economic incentives in different ways, it is good to know that inequalities in testing for the COVID-19 virus appears to be almost non-existent (Schmitt-Grohé *et al*., 2020). Poverty and inequality do need political will during a crisis in order to be ameliorated, as the market tends to widen existing inequalities.

Thus, historic lessons seem to teach us that pandemic diseases can exacerbate existing inequalities, and these growing inequalities often lead to the fall of the unjust and unequal empires that created them. Although we are not necessarily expounding the fall in political regimes due to the COVID-19, our analysis elucidates that the spatial disparities in the COVID-19 death toll are related to the overall socioeconomic milieu of deprivation and the interaction of deprivation with cultural and economic belonging. Below we identify places that are experiencing faster rates of increase in economic instability in terms of unemployment and small business failure and therefore identify locations that are at greater likelihood of future extreme deprivation and consequent social unrest within England and Wales.

Modern Deprivation and Brexit

The geographies of deprivation in the UK have been one of the most widely debated explanations for the Brexit vote. Applications of different quantitative indicators and methodologies show that regions that are socioeconomically backward are also the ones that voted for Brexit. While the Brexit vote had other additional complex triggering mechanisms, protest voting as a form of mutiny by those left behind has been documented in the economic literature. Hirschman and Rothschild (1973) coined the term "the tunnel effect" to refer to the the fact that perceived economic unevenness and increasing inequality are bound to create feelings of being 'left behind' (p. 551) once a threshold level of inequality is surpassed and

Covid Economics 13, 4 May 2020: 51-70

this can lead to social unrest. Further theoretical work and empirical evidence for the tunnel effect is provided in the work of some leading cultural economists (Benabou and Tirole, 2006, 2009, 2011; Alesina and Fuchs-Schündeln, 2007; Acemoglu and Robinson, 2010, 2012; Passarelli and Tabellini, 2013), political economists (Scheve and Stasavage, 2006) and other recent high-profile contributions (Kerr, 2014).

Existing links between the sentiment of being left behind and other socioeconomic factors in the context of radical voting, such as migration and human capital concentration across space, have been documented for the UK (Tubadji, Colwell and Webber, 2020), and the Netherlands (Tubadji, Burger and Webber, 2020).[2] Those papers build on Hirschman and Rothschild's (1973) and Tiebout's (1956) models and show that existing deprivation and a lack of outmigration among the autochthonous population signals a perception of increasing deprivation and a cultural milieu of relatively poor opportunities for both outward and upward mobility. Such feelings of being 'stuck behind' exacerbate the feeling of being left behind; the strength of this psychological state was, in turn, expressed in a generalized political protest vote. We highlight an alert that these feelings of being stuck behind are likely to result in greater protests nationally and perhaps worldwide, as these are known consequences of fiscal policy interventions (Ponticelli and Voth, 2020).

3. Hypothesis about the UK Geographies of COVID-19

If there are spatially distinct cultural and economic discriminatory factors that enhance the vulnerability of groups of people and places, then it is opportune to employ a method that takes account of such cultural and economic factors. One novel paradigm that is growing in importance and use is the Culture Based Development (CBD) approach (Tubadji and Nijkamp, 2015, 2016, 2018; Tubadji, Angelis and Nijkamp, 2015, 2016; Tubadji *et al.* 2019). This paradigm is grounded on the premise that there is a cultural bias underpinning economic choices that predetermines the operation and outcome of any socioeconomic system in a path dependent manner (Tubadji, 2012, 2013, 2020a,b,c). The importance of cultural driven path dependence in the UK[3] has been highlighted by Huggins and Izushi (2007) and McCann (2016).

This study adopts the CBD paradigm in order to delve deeper into the cultural and economic disparities across the UK and to identify the reasons for inequalities in the COVID-19 death toll. The highly plausible short-run socioeconomic consequences of this experienced inequality include the aggravated economic situation of individuals and businesses in deprived areas, expressed in disproportionally greater and increasing rates of unemployment and business failure (for evidence on Norway, see Mamelund *et al*., 2020[4]). Moreover, the CBD approach emphasises that existing cultural and economic inequalities create and strengthen both a path dependency towards the exacerbation of economic deprivation of those already left behind and the potential for more significant pockets of future social unrest.

The CBD approach postulates that: (i) cultural (ethnic) and economic discrimination and deprivation create feelings of being left behind among people and regions; (ii) these feelings have a cumulative nature and (iii) these feelings create path dependencies, as the experience of discrimination cannot be immediately removed through a policy intervention. The approach also suggests that policy intervention to abate discrimination can create a new

[2] Similar links between socioeconomic development and ultra-right voting exist for Greece (Tubadji and Nijkamp, 2019).

[3] For an overview of the importance of cultural path dependency for economic development in other countries, see Audretsch and Fritsch (2002), Fritsch and Mueller (2007), Fritsch *et al.* (2019) and Fritsch *et al.* (2020).

[4] See Alnes Haslie and Nøra (2020) for an English translation.

Covid Economics 13, 4 May 2020: 51-70

path dependent chain reaction. Abating the present discrimination is argued to be essential for the prevention of the escalation of social unrest that is driven by being left behind. Thus, the CBD approach to understanding the current geographies of the COVID-19 pandemic, its causes and aftermaths, can be summarized in three testable null hypotheses:

H01: Geographies of cultural discrimination ***within*** regions do not predict regional disparities in mortality from COVID-19.

H02: Past geographies of deprivation in the UK do not predict the mortality from COVID-19.

H03: Mortality from COVID-19 does not predict the growth of deprivation (and therefore instability and radicalization) in a region.

These null hypotheses are already testable given the available regional data. As the current health crisis unfolds, peaks and finally resolves, more detailed data will permit the generation of deeper insight and forecasting. Meanwhile, if the validity of these hypotheses is confirmed, then they can become instrumental in forming the basis of an effective warning system for policymakers in Britain who are interested in abating the movement towards greater instability and radicalisation.

4. Modelling the effects of the COVID-19 pandemic

Regional analyses that provide evidence of the causes and consequences of the COVID-19 pandemic are dependent on the availability of data, which are still in their infancy and ever evolving. The immediacy of the crisis to the time of writing limits the size of the available dataset, but the health reporting systems already in place in the UK make such datasets valuable in terms of regional indicators. Currently available data for England and Wales for the number of deaths from COVID-19 are only available at the regional level (10 NUTS1 regions) and from the 3rd of January to the 27th of March 2020 (13 weeks). See Appendix 1 for information on the sources and descriptive statistics for each variable.

Data corresponding to the number of COVID-19 deaths originates from the ONS and are tallies of COVID-19-related weekly deaths in hospitals. We use this data in levels and as a percentage of the population in a region in January 2020. As the percentage is very small, we multiply it by 1000 to enhance visualization and to enable more explicit interpretation of the magnitudes of the effects. Our instrumental variable for the number of deaths from COVID-19 is the number of lung cancer deaths from the previous year. We obtain the percentage of patients per population in the region and use this as an instrumental variable in our regressions.

We have data on the share of Black, Asian, other-non-White, other and Whites per region. To quantify cultural discrimination, we first sum the percentages of Black and Asian and other non-White, and we use the mean value of this sum to identify the state of a region as culturally and ethnically more diverse than the rest of the country. We generate a dummy variable equal to 1 when the sum of Black, Asian and other non-White population in the region is above the average for the country. We used this variable to calculate the cultural and ethnic decomposition and the amount of cultural discrimination.

We use three approaches to quantify the relative economic deprivation of a region. First, we use the average value of the Multiple Deprivation Index (MDI) for each region. However, this variable is a better statistical indicator of deprivation at a lower administrative

Covid Economics 13, 4 May 2020: 51-70

division than the region. Therefore, as a second approach, and building on the knowledge that urban areas are wealthier than rural areas, we use the percentage of the region's population that resides in an urban area. Third, as the pro-Brexit vote in the 2016 elections was associated with greater relative deprivation and stronger feelings of being left behind, we use the percentage of the pro-Brexit vote of a region as an alternative measure for deprivation. This variable is also of interest in itself because COVID-19 may have implications for regional development and for the political development of the UK in the near future when Brexit is implemented fully.[5]

Method

We implement the Blinder-Oaxaca data panel decomposition analysis for testing H01 and H02. The test for each hypothesis is analogical, with variation only for the group for which the decomposition has been implemented. To test H01, our group for decomposition is the above average level of deprivation[6]. In the case of H02 being the above average non-White cultural and ethnic composition of a region. The decomposition procedure serving to identify the degree of discrimination between two groups can be stated as in model (1):

$$Death\_Toll_A = \alpha_A + \beta_A X_A \quad (1.1)$$
$$Death\_Toll_B = \alpha_B + \beta_B X_B \quad (1.2)$$
$$hat\_Death\_Toll_A = \alpha_A + \beta_A\, hat\_X_A \quad (1.3)$$
$$hat\_Death\_Toll_B = \alpha_B + \beta_B\, hat\_X_B \quad (1.4)$$
$$Discrimination = (\alpha_A - \alpha_B) + (\beta_A - \beta_B) * hat\_Death\_Toll \quad (1.5)$$

where the *hat* values are predicted values, based on the regressions of (1.1) and (1.2), groups *A* and *B* are the discriminated group and the rest of the population respectively, and *X* is the set of independent variables that explain the outcome variable of interest. As we have data for 10 regions over 13 time periods, *X* also contains controls for this panel structure.

To test H01, we define group *A* as equal to 1 when the cultural-ethnic geographical pattern across regions contain an above average concentration of the Black, Asian and non-White population. To test H02, we define group *A* using the economic deprivation measured as an above average level of deprivation.

To test H03, we use an instrumental variable along a 2SLS approach and estimate model (2):

$$Econ\_Dev = \alpha + \beta_1\, hat'\_Death\_Toll + \beta_2 X + e_1 \quad (2)$$

where the local economic development (*Econ_Dev*) is a dependent variable, which we quantify using alternative measures of the claimant count per head of population, the number of SMEs in the region, or the percentage of pro-Brexit vote. Local economic development is explained by the death toll in the region and a collection of control variables, *X*, which includes population density. We use the percentage of lung cancer deaths to purge the

[5] Although we have numerous potential control variables (see Appendix 1) we cannot use all of them as controls because of the emergence of collinearities and the limited number of observations. Hence, instead we present results based on the most parsimonious economic modelling approach with the aim of achieving stable, reliable, plausible and feasible econometric estimates.

[6] This is identified as a below average value of the MDI index, as the MDI increases from 1 to infinity and higher value indicate lower deprivation.

Covid Economics 13, 4 May 2020: 51-70

economic endogeneity of the death toll, and then denote the respective purged variable[7] as *hat'_Death_Toll*. The predicted value of the death toll (*hat'_Death_Toll*) is then used to estimate at a second stage the *Econ_Dev* outcome, as shown in equation (2).

5. Results

We first present some descriptive statistics by looking at the distribution of deaths per region. We divide the regions into two groups: those above and below the mean of the UK's MDI, after which we label regions as 'less deprived' and 'more deprived' relative to the MDI average.[8] Mortality histograms for absolute and population-adjusted ratios are presented in Figure 1. This figure reveals that when we consider the absolute number of deaths, it seems that regions with less deprivation (implying more urbanization and higher incomes and productivity) are the places with a slightly higher number of deaths. However, when we consider the population-adjusted mortality indicator, the pattern now reveals that places with greater deprivation ('more deprived regions') are experiencing a greater death toll.

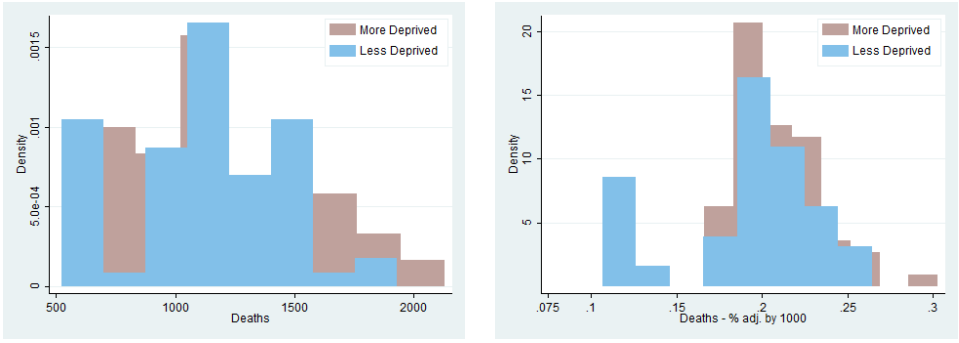

Figure 1: Deaths in more and less deprived regions, numbers and percentages
Notes: The figure the weekly number of deaths per less deprived and more deprived regions. The figure to the left presents raw numbers and the figure to the right presents the percentage of deaths by number of people living in the region (the percentage is multiplied by 1000 for easier visualization purposes).

Inspection of the top panels in Figure 2 reveals that there appears to be an historic distribution of greater lung cancer deaths that is related to the COVID-19 regional death toll. This suggests that deprivation-related health status could be a predisposition to COVID-19 mortality. It also indicates that economic and health deprivations are often co-located throughout the country and jointly create pockets of intensified vulnerability.

[7] The procedure of the IV 2SLS is fully followed so the economic purging of the *Death_Toll* variable includes all regressors and the instrumental variable.

[8] As the measurement of the MDI represents a score which increases with the decrease of deprivation, 1 stands for the most deprived region and every other positive score is considered a value of lesser level of deprivation. We have considered this in the definition of more and less deprived regions with regard to the mean value of the MDI.

Covid Economics 13, 4 May 2020: 51-70

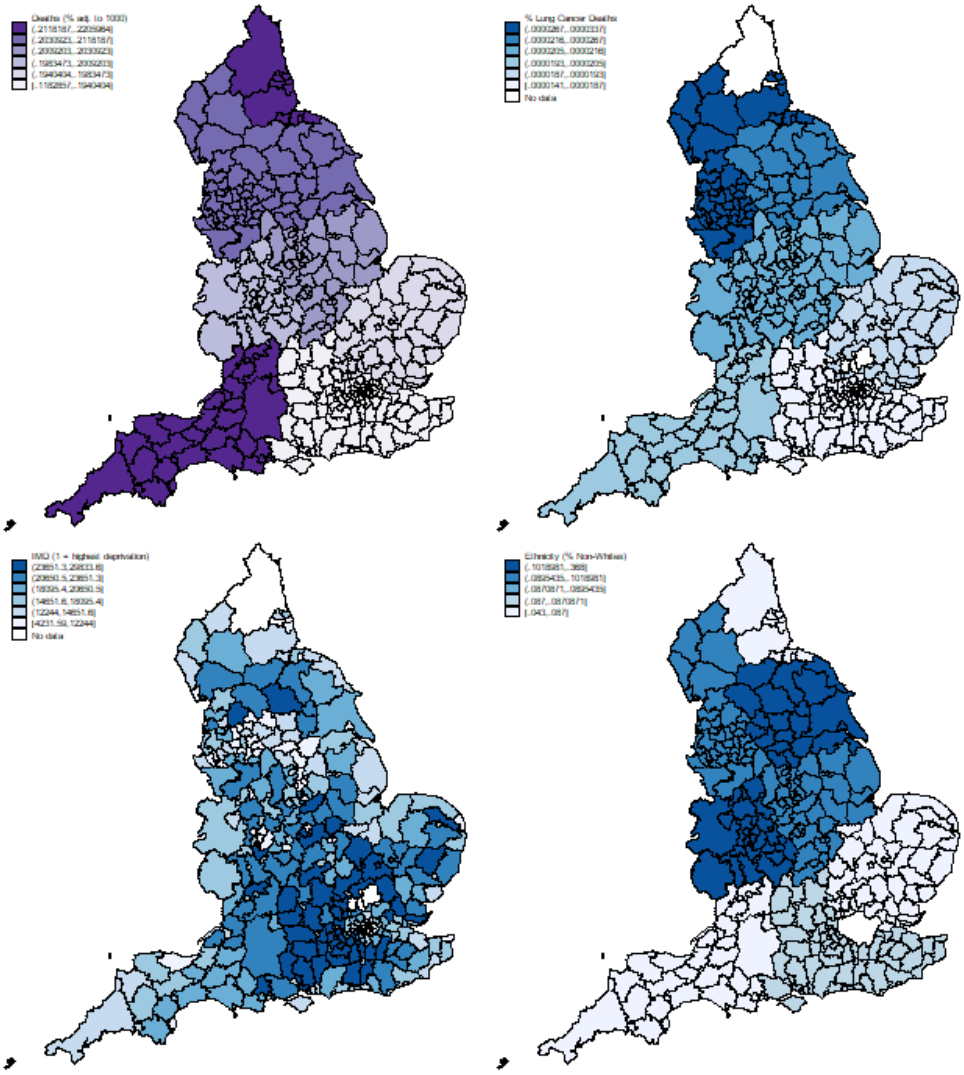

Figure 2: COVID-19 deaths (%), lung cancer, cultural (Non-white), deprivation (IMD)
Notes: The figure maps clockwise from top-left: COVID-19 deaths (%), lung cancer deaths (%), non-white population (%) and index of multiple deprivation (where 1 is the highest value).

Furthermore, as can be seen in Figure 2, the purple-coloured geographical distribution of COVID-19 mortality rates seems to be consistent both with the geography of deprivation (where lighter shading is associated with more deprivation; see footnote 9) and with the geography of ethnic diversity (where darker shading is associated with greater proportion of ethnic minorities). While ethnic diversity predicts COVID-19 death rates in the middle and eastern parts of the UK, the north and south-west regions seem to have a coincidence of deprivation and greater death toll. Cultural diversity seems to have some association with the

death toll of a more complex nature, with potentially economically endogenous character. Yet, both drivers of deprivation (economic disparity and ethnic diversity) seem to be associated with a higher COVID-19 death toll.

Cultural and Economic Discrimination in Mortality

To delve deeper into the realities of the COVID-19 death toll, we employ a detailed data decomposition analysis. Table 1 presents the aggregate part of the decomposition for two specifications. Specification (1) shows the decomposition by prevalence of the non-White population, while specification (2) shows the decomposition by level of economic deprivation, reflecting H01 and H02 respectively.

Table 1: Decomposition for Cultural and Economic Discrimination

dep. var.	Spec. 1 Cultural Discrimination Death Toll (% adj.) coef.	z-value		Spec. 2 Economic Discrimination coef.	z-value	
Differential						
Prediction_A	0.206	89.09	***	0.202	67.39	***
Prediction_B	0.160	17.81	***	0.191	36.66	***
Discrimination	0.047	5.06	***	0.011	1.86	*
N	117			117		
R-sq	0.17			0.13		

Notes: Blinder-Oaxaca.

Traditionally, we think first of economic deprivation. As can be seen from Table 1, a more fine-grain examination of economic deprivation in specification (2) reveals that the death toll is concentrated in more deprived areas, but there is only a 1-percentage point difference. However, when the cultural discrimination is analyzed in specification (1), it becomes clearer that the areas with greater than average concentrations of non-White populations experience a 5-percentage point higher death toll. The latter finding is also in line with reports from the USA and elsewhere, where Black and other non-White populations are experiencing greater exposure, contagion and death rates than their White counterparts (Arnold *et al*., 2020). This highlights the importance of the cultural element and corroborates the need to test H01.

To crosscheck the validity of these results, we make a within-method triangulation robustness check in the following manner. As the aggregation of the MDI is not an ideal measure and as it is an index available only for England (thereby stopping us from implementing the analysis for Wales), we use alternative measures of deprivation: first, above average percentages of population in urban areas, and second, above average percentages of people in rural areas. We implement the same data decomposition analysis as before but this time using the two above alternative variables to define group *A*. These results are presented in Table 2.

Covid Economics 13, 4 May 2020: 51-70

Table 2: Decomposition for Cultural and Economic Discrimination

	Spec. 1			Spec. 2		
	Economic Discrimination					
	Urban			Rural		
dep. var.	Death Toll (% adj.)					
	coef.	z-value		coef.	z-value	
Differential						
Prediction_A	0.191	36.66	***	0.202	67.39	***
Prediction_B	0.202	67.39	***	0.191	36.66	***
Difference	-0.011	-1.86	*	0.011	1.86	*
N	117			117		
R-sq	0.13			0.79		

Notes: Blinder-Oaxaca.

Table 2 shows an indifference to the alternative variable for quantifying deprivation as the sizes of the coefficients remain the same across different specifications, thereby suggesting that the aggregate IMD measure is sufficiently good to distinguish between the regions in terms of their level of deprivation. The above analysis shows that the null hypotheses of H01 and H02 can be easily rejected, as there exists both economic and cultural/ethnic discrimination in the death toll across England and Wales. Moreover, the effect of cultural/ethnic discrimination seems to be about five times the size of the effect of economic deprivation. This highlights again that our cultural hypothesis has greater significance for the socioeconomic process of discrimination in the UK during this pandemic.

Future Societal Vulnerability Due to the Path-Dependency in Discrimination

While it is important to secure economic and social resilience (Martin, 2012; Reggiani *et al*., 2015), it is even more important to prevent the development of vulnerabilities that blight the resilience of a place. Vulnerabilities affect a region's resilience to economic shocks, just as a weaker immune system predisposes a person to death during a flu contagion. Inspired by this reasoning, we want to disentangle historical vulnerability from the predisposition to death from COVID-19. In serious cases, the COVID-19 virus restricts a person's capacity to transport oxygen in their respiratory system by causing pneumonia, which is an inflation of the lungs. It is then logical to employ the incidence of lung cancer deaths in a region from a previous period as an instrumental variable to explain mortality in the current pandemic.

Set within a 2SLS approach, we used the economically purged instrument of the COVID-19 death toll to explain the regional unemployment claimant count (H03, Specification 1) and the regional concentration of small businesses (H03, Specification 2). In addition, we used the same estimation procedure but looked at the relationship between the percentage of the pro-Brexit vote share and the concentration of COVID-19-related deaths (H03, Specification 3).

Several observations can be identified in Table 3. First, the percentage of lung cancer deaths in a region predicts the COVID-19 mortality in a strongly significant positive manner, suggesting that health predisposition indeed affects the death toll. This is to be expected from a statistical perspective, because the correlation coefficient between the death toll and its instrumental variable – the percentage of lung cancer deaths – is already high (0.59).

Covid Economics 13, 4 May 2020: 51-70

Table 3: 2SLS-IV for COVID-19 deaths, unemployment claims and businesses

	Spec. 1 UNEMPLOYMENT						Spec. 2 SMEs						Spec. 3 BREXIT					
dep. var.	Death Toll (above avg)			Unemployment			Death Toll (above avg)			Small and Medium Businesses (Num.)			Death Toll (above avg)			Pro-Brexit Vote (%)		
lunc_cancer_deaths	0.004	3.59	***				0.004	3.59	***				0.004	3.59	***			
deaths_perc_adj. (above avg.)				0.020	2.61	**				-0.580	-3.58	***				19.335	2.97	**
ppl2020	-1.77E-07	-8.07	***	1.06E-09	1.02		-1.77E-07	-8.07	***	5.87E-08	2.71	**	-1.77E-07	-8.07	***	8.15E-07	0.94	
FE week	YES			YES			YES			YES			YES			YES		
_cons	1.175	7.17	***	0.011	0.89		1.175	7.17	***	0.597	2.42	*	1.175	7.17	***	35.768	3.61	***
N	130			130			130			130			130			130		
R-sq	0.52			0.99			0.52			0.41			0.52			0.99		

Notes: The table presents 3 specifications of IV 2SLS estimation, where percentage of lung cancer deaths is the IV for COVID-19 deaths. The dependent variable in Spec. (1) is unemployment (in terms of % claimant count per population); in Spec. (2) it is number of SMEs and in Spec. (3) it is pro-Brexit vote (in %).

Second, there is a strong positive relationship between being in a deprived area, as characterised by high levels of unemployment, and the COVID-19 deaths (Specification 1). There is a similar corroborating but stronger relationship between the pro-Brexit vote share and COVID-19 deaths (Specification 3). The number of SMEs in a region seems to be negatively associated with the COVID-19 death rate, suggesting that COVID-19 had a weaker effect on economically prosperous places[9].

Collating these results together suggests that if the UK economy suffers over the longer term, then it is primarily because the most severe economic impact of the COVID-19 pandemic has been on the most economically vulnerable and left behind parts of our population, thereby having an important negative effect on the demand side of the economy through lower consumption; after all, the poorer sections of the population have a higher marginal propensity to consume. Thus, the feeling of perceived deprivation will be even stronger than the actual level of aggravation of the socioeconomic inequality. Moreover, we know from the estimations in Table 1 that economic deprivation is associated with higher COVID-19 death rates by a relatively small 1 percentage point and the effect of the cultural/ethnic discrimination effect is five times greater with a 5 percentage points increase, suggesting that both cultural and economic discrimination enhance the COVID-19 death rate. From Specification 3 in Table 3 we learn further that for each 1 percent increase in the death toll, there is an increase of 19 percentage points in the probability that the area is pro-Brexit. We explore the reasons for this result in Figure 4 through the inspection of histograms for anti- and pro-Brexit areas.

As seen from Figure 4, the impact of COVID-19 mortality is higher and more concentrated around the mean in areas that voted more strongly for Brexit, indicating that areas that are already feeling left behind and voted more strongly for Brexit seem to have experienced a higher COVID-19 death toll in the early part of the pandemic in the UK. Part of the reason for this could be connected to higher local levels of stress, more depression and lower levels of life satisfaction, which could be the focus of future research. Importantly, the above results indicate that we reject null hypothesis H03. Moreover, if the consequences of COVID-19 mortality are increases in unemployment and greater business failure in areas that are hit harder from the COVID-19 outbreak, then this pandemic will be similar to previous pandemics in that the more deprived, more-culturally diverse places and especially the left behind places will suffer the greatest economic loss. They are also more likely not to recover from the lock-down as they are likely to have lower levels of savings to tide them over and therefore more businesses may fail locally too due to lower local purchasing power. This

[9] The standard postestimation tests suggest the adequacy of the method employed.

effect is likely to be exacerbated further if such areas have greater proportions of people in casual work and who are therefore not receiving any pay during the lock-down period. Such intensified economic deterioration of already deprived places is likely to affect their feelings of being left behind.

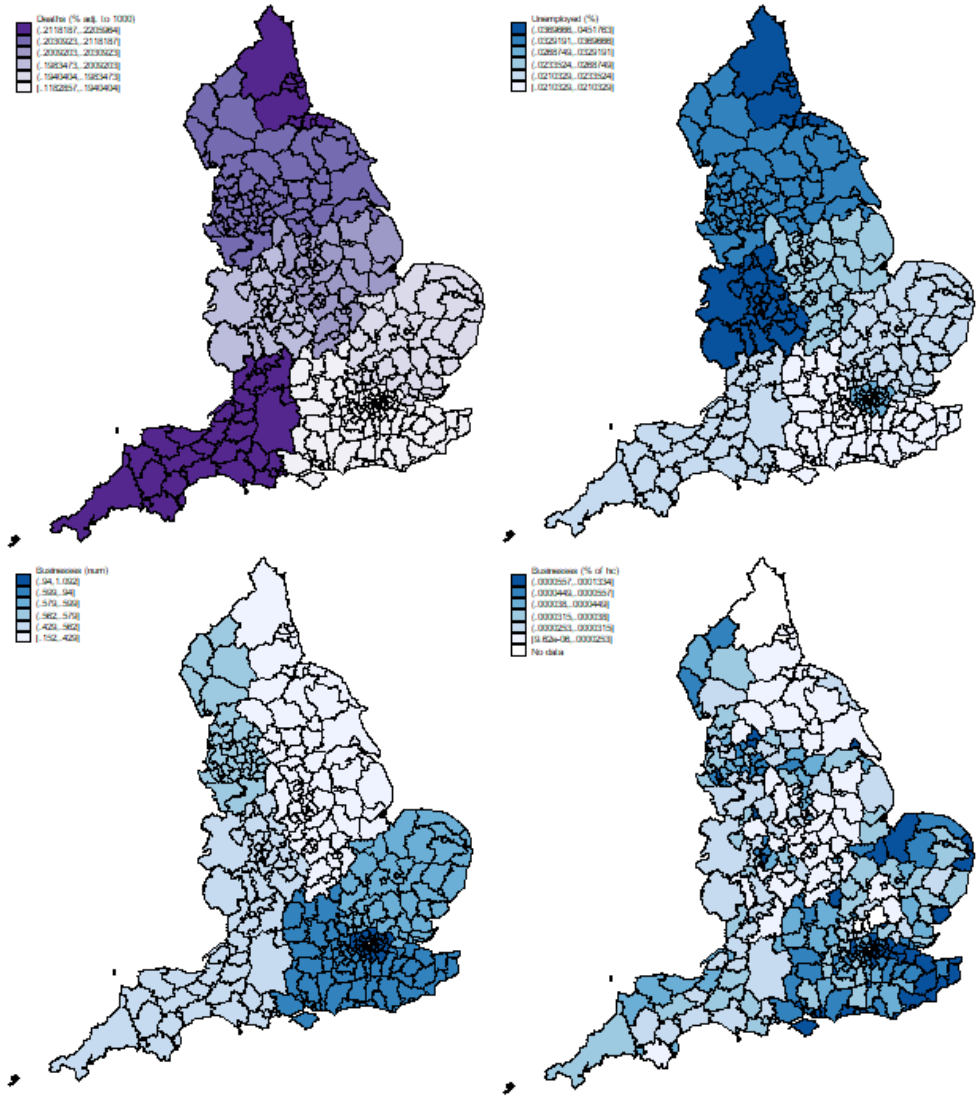

Figure 3: Deaths (%), Unemployment, Business (num and %)
Notes: The figure maps clockwise from top-left: COVID-19 deaths (%), unemployment (%), small and medium businesses (number) and small and medium businesses (% of highly educated).

Covid Economics 13, 4 May 2020: 51-70

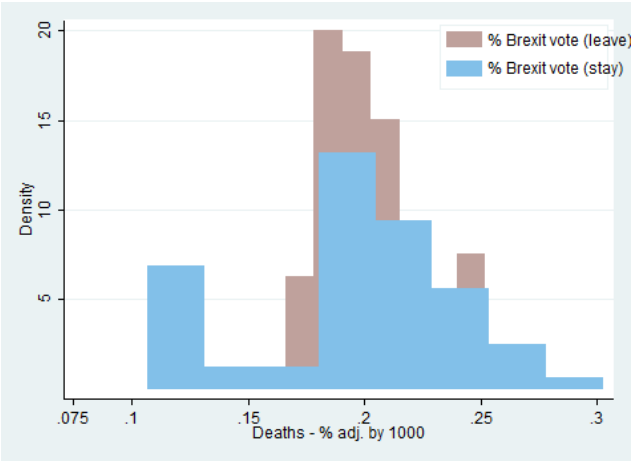

Figure 4: Deaths (%) and Brexit vote
Notes: The figure shows histograms of COVID-19 deaths for regions with below and above Brexit mean vote.

6. Conclusion

The unfolding COVID-19 pandemic is an extraordinary, unanticipated global phenomenon that gives scholars of all kinds the opportunity to understand how a sudden shock affects portions of the population differentially. In a seminal piece, Scheidel (2017) poses the argument that "catastrophic levellers" which wipe out tens of millions of lives globally, such as the Black Death, the Russian revolutions or the World Wars, no longer exist in industrial societies. The current study asked the question: what if such rare events had become only 'partial levellers' in poorly redistributive social democracies, where one part of the population is healthy, resilient, and benefits from excellent socioeconomic infrastructure, and another is plagued with the opposite?

Our study argues that unprecedented economic and cultural class cleansing is occurring throughout the world during the COVID-19 pandemic but at a low level of consciousness; we draw our evidence from the UK. The pandemic seems to affect disproportionately the economically and socially more vulnerable, but this vulnerability is defined even more broadly than before. Most vulnerable to COVID-19 are those groups of citizens who were previously subject to unconscious economic and cultural discrimination.

The current study amassed historical economic and social data at the regional level and extracted regional economic insights on the geographic spread, determinants and potential consequences of the COVID-19 pandemic. Using a relatively but necessarily small dataset at the NUTS1 level for England and Wales over the early part of the pandemic period, this study proposes a Culture-Based Development (CBD) methodology for the identification of the importance of economic and cultural discrimination, highlighting its implications for future social unrest. The CBD methodology for economic and cultural discrimination relies on a detailed data decomposition analysis, while the economic impact of the pandemics relies on an IV 2SLS estimation approach.

Our empirical approach provides evidence that poorer, more socioeconomically deprived and more rural areas experienced a disproportionately greater death toll. In this context, the cultural discrimination effect of the death toll seems to be five times stronger than the economic discrimination effect across the UK regions. The most dominant effect,

Covid Economics 13, 4 May 2020: 51-70

however, amounting to almost 19 percentage points of impact, is the association between COVID-19 mortality and social unrest tendencies (related to the 2016 Brexit vote). This suggests that those places that are feeling left behind and who voted for Brexit seem to be the places that are experiencing the strongest losses per head of the population from the current pandemic. If we roll the reel forward, the dismal implications of these findings are clear: further social radicalization due to economic and cultural discrimination is to be expected on the horizon and especially in pro-Brexit voting areas. A further negative economic shock is expected in the UK at the end of 2020 with the implementation of Brexit. Thus, areas with greater vulnerability created during the pandemic will are more likely to have their local economies stuck into development traps, which will prolong the stagnation and possibly will lead to greater radicalization of places that are pockets of deprivation and discrimination.

Plans to create greater socioeconomic resilience should be formulated in time to support the most vulnerable groups and localities, and specifically the places which experience greater cultural and economic discrimination and feel left behind. Use of the current findings and methodology can enable the identification of spatial pockets of vulnerability that need to receive socioeconomic interventions to improve regional economic resilience.

Cultural and economic discrimination and their socioeconomic consequences are most prominent areas for the application of the Culture-Based Development research paradigm. Nevertheless, there are many other aspects of the socioeconomic condition of the pandemic situation that should not be neglected. The CBD approach could be used to explore aspects of the latter since every economic question is sensitive to its cultural context, as the CBD approach is specialized in handling and understanding the impact of cultural contexts and the impact from the complex dynamic sociocultural system of formal and informal institutions more generally.

The cultural context is essential when analyzing regional development, and therefore makes context-related ceteris paribus assumptions unrealistic (Nijkamp, 2007). Such context-related effects in the case of the COVID-19 pandemic include: economic impoverishment and its effect on ordinary citizens mental health, the role and support of the cultural sector in repairing poor mental health conditions, and the difference that using fiscal rather than monetary policy can have on improving the mental health of an economy's citizens. These further aspects can also be handled by the CBD paradigm, which can offer analysis and policy recommendations along individual, regional and macro-level lines to ensure socioeconomic support is efficiently targeted at the region and groups hit hardest by the pandemic.

In summary, this paper has applied the CBD analytical approach to identify how the path dependent geography of cultural and economic discrimination predict the locations with high number of deaths in the UK during the early part of the COVID-19. This study also demonstrates how this information can be used to identify places that are endangered by falling into development traps with greater perceived deprivation in left behind regions. These regions are also the places where post-Brexit social unrest can be expected to emerge due to increased inequality throughout the current pandemic. Inequality creates vulnerability and is thus a source of destabilization of places under a variety of negative external shocks, such as the exogenous COVID-19 pandemic or the forthcoming endogenous economic shock of Brexit. Timely efforts for alleviating the inequality might be a way to prevent and build greater socioeconomic resilience across the UK.

Covid Economics 13, 4 May 2020: 51-70

Covid Economics 13, 4 May 2020: 51-70

Reference

Acemoglu, D. and Robinson, J. A. (2010). Why is Africa poor?. Economic history of developing regions, 25(1), 21-50.

Acemoglu, D. and Robinson, J. A. (2012). Why nations fail: The origins of power, prosperity, and poverty. Crown Books.

Alesina, A. and Fuchs-Schuendeln, N. (2007). Goodbye Lenin (or not?): The effect of communism on people's preferences. American Economic Review, 97(4), 1507-1528.

Alnes Haslie, N and S. Nøra (2020) Norwegian Study Looks at How the Coronavirus Pandemic is Affecting People's Health and Careers, Oslomet, available online at: https://www.oslomet.no/en/research/featured-research/how-the-coronavirus-pandemic-is-affecting-people-s-health-and-careers

Arnold, D., W. Dobbie, and P. Hull (2020) Measuring Racial Discrimination in Bail Decisions, Becker Friedman Institute, Working paper No. 2020-33,

Audretsch, D. B. and Fritsch, M. (2002). Growth regimes over time and space. Regional Studies, 36(2), 113-124

Barnett, K., Mercer, S. W., Norbury, M., Watt, G., Wyke, S., Guthrie, B. (2012) Epidemiology of multimorbidity and implications for health care, research, and medical education: a cross-sectional study. The Lancet, 380(9836), 37-43.

Benabou, R. and Tirole, J. (2011). Identity, morals, and taboos: Beliefs as assets. The Quarterly Journal of Economics, 126(2), 805-855.

Benabou, R. and Tirole, J. (2016). Mindful economics: The production, consumption, and value of beliefs. Journal of Economic Perspectives, 30(3), 141-64.

Benabou, R. and J. Tirole (2006), Belief in a Just World and Redistributive Politics, Quarterly Journal of Economics, 121(2), 699-746.

Benabou, R. and J. Tirole (2009), Over My Dead Body: Bargaining and the Price of Dignity, American Economic Review, 99(2), 459-465.

Berry, A., Bellisario, V., Capoccia, S., Tirassa, P., Calza, A., Alleva, E. and Cirulli, F. (2012). Social deprivation stress is a triggering factor for the emergence of anxiety-and depression-like behaviours and leads to reduced brain BDNF levels in C57BL/6J mice. Psychoneuroendocrinology, 37(6), 762-772.

Bowden, S., Michailidou, D. M., & Pereira, A. (2008). Chasing mosquitoes: An exploration of the relationship between economic growth, poverty and the elimination of malaria in Southern Europe in the 20th century. Journal of International Development: The Journal of the Development Studies Association, 20(8), 1080-1106.

Bray, C., Morrison, D. S. and McKay, P. (2008). Socioeconomic deprivation and survival of non-Hodgkin lymphoma in Scotland. Leukemia *and* lymphoma, 49(5), 917-923.

Chang, R. and A. Velasco (2020) 'Economic policy incentives to preserve lives and livelihoods,' *NBER working paper* #27020.

Cribb, J., Norris Keiller, A. and Waters, T. (2018). Living standards, poverty and inequality in the UK: 2018 (No. R145). IFS Report.

Davies, H., & Joshi, H. (1998). Gender and income inequality in the UK 1968–90: the feminization of earnings or of poverty?. *Journal of the Royal Statistical Society: Series A (Statistics in Society),* 161(1), 33-61.

Fritsch, M. and Mueller, P. (2007). The persistence of regional new business formation-activity over time–assessing the potential of policy promotion programs. Journal of Evolutionary Economics, 17(3), 299-315.

Fritsch, M., Obschonka, M., Wahl, F. and Wyrwich, M. (2020). The deep imprint of Roman sandals: evidence of long-lasting effects of Roman rule on personality, economic performance, and well-being in Germany.

Fritsch, M., Sorgner, A., Wyrwich, M. and Zazdravnykh, E. (2019). Historical shocks and persistence of economic activity: evidence on self-employment from a unique natural experiment. Regional Studies, 53(6), 790-802.

Gazeley, I. and Verdon, N. (2014). The first poverty line? Davies' and Eden's investigation of rural poverty in the late 18th-century England. Explorations in Economic History, 51, 94-108.

Glaeser, E. L., Resseger, M. and Tobio, K. (2009). Inequality in cities. Journal of Regional Science, 49(4), 617-646.

Grepin, K. A., Poirier, M. J. and Fox, A. M. (2020). The socioeconomic distribution of exposure to Ebola: Survey evidence from Liberia and Sierra Leone. SSM-Population Health, 10, 100472.

Hall, S. (1997). Culture and power. Radical Philosophy, 86, 24-41.

Harding, V. (1989). 'And one more may be laid there': the Location of Burials in Early Modern London. The London Journal, 14(2), 112-129.

Hills, J. (2010). An anatomy of economic inequality in the UK-report of the national equality panel. LSE STICERD Research Paper No. CASEREPORT60.

Hirschman, A. O. and M. Rothschild (1973) The changing tolerance for income inequality in the course of economic development, Quarterly Journal of Economics, 87(4): 544-566.

Howson, W. G. (1961). Plague, poverty and population in parts of north-west England, 1580-1720. Transactions of the Historic Society of Lancashire and Cheshire, 112, 29-55.
Huggins, R. A. and Izushi, H. (2007). Competing for knowledge: creating, connecting and growing. Routledge.
Kandul, S. and Ritov, I. (2017). Close your eyes and be nice: Deliberate ignorance behind pro-social choices. *Economics Letters*, 153, 54-56.
Kerr, W. R. (2014). Income inequality and social preferences for redistribution and compensation differentials. *Journal of Monetary Economics*, 66, 62-78.
Kim, Pilyoung, Gary W. Evans, Michael Angstadt, S. Shaun Ho, Chandra S. Sripada, James E. Swain, Israel Liberzon and K. Luan Phan. "Effects of childhood poverty and chronic stress on emotion regulatory brain function in adulthood." *Proceedings of the National Academy of Sciences* 110, no. 46 (2013): 18442-18447.
Kohn, G. C. (2007). Encyclopaedia of plague and pestilence: from ancient times to the present. Infobase Publishing.
Lindert, P. H. (1996) What Limits Social Spending?, Explorations Econ. Hist., 33:1, pp.1–34

Lindert, P. H. (2000). Three centuries of inequality in Britain and America. Handbook of income distribution, 1, 167-216.
Los, B., McCann, P., Springford, J. and M Thissen (2017) The mismatch between local voting and the local economic consequences of Brexit, Regional Studies, 51(5): 786-799.
Mack, A. (Ed.). (1991). In time of plague: the history and social consequences of lethal epidemic disease. NYU Press.
Mamelund, S. E., Ingelsrud, M. H. and Steen, A. H. (2020). Arbeidslivsbarometerets koronaundersøkelse-preliminære funn per 6. april 2020.
Martin, R. and B. Gardiner (2019) The resilience of cities to economic shocks: A tale of four recessions (and the challenge of Brexit), Papers in Regional Science, 98:1801-1832.
Martin, R. (2012) "Regional economic resilience, hysteresis and recessionary shocks." Journal of Economic Geography, 12(1), 1-32.
Martin, R. L. (2004). The contemporary debate over the North-South divide: images and realities of regional inequality in late-twentieth-century Britain. Cambridge Studies in Historical Geography, 37, 15-43.
Massey, D. (1979). In what sense a regional problem? Regional studies, 13(2), 233-243.
Matzner, Pini, Ofir Hazut, Reut Naim, Lee Shaashua, Liat Sorski, Ben Levi, Avi Sadeh, Ilan Wald, Yair Bar-Haim, and Shamgar Ben-Eliyahu. "Resilience of the immune system in healthy young students to 30-hour sleep deprivation with psychological stress." Neuroimmunomodulation 20, no. 4 (2013): 194-204.
McCann, P. (2016). The UK regional-national economic problem: Geography, globalisation and governance. Routledge.
McCann, P. (2019). Perceptions of regional inequality and the geography of discontent: Insights from the UK. Regional Studies, doi: 10.1080/00343404.2019.1619928.
Merriman, P. (2009). Driving spaces: a cultural-historical geography of England's M1 motorway (Vol. 17). John Wiley *and* Sons.
Mingione, E. (1996). Urban Poverty in the Advanced Industrial World: Concepts, Analysis and Debates Enzo Mingione, University of Padova. Urban poverty and the underclass, 3.
Niemietz, K. (2009). Poverty in Britain, past and present. *Economic Affairs*, 29(4), 48-54.
Nijkamp, P. (2007) Ceteris paribus, spatial complexity and spatial equilibrium: An interpretative perspective, Regional Science and Urban Economics, 37: 509-516.
Osberg, L. (2002). Trends in poverty: the UK in international perspective: how rates mislead and intensity matters (No. 2002-10). ISER Working Paper Series.
Packard, R. M. (1989). White plague, black labor: Tuberculosis and the political economy of health and disease in South Africa (Vol. 23). University of California Press.
Passarelli, F. and Tabellini, G. (2013). Emotions and political unrest. CESifo Working Paper Series No. 4165
Perry, R. (2005). Representations of Poverty in Eighteenth-Century Fiction (Vol. 95, p. 441). Wiley-Blackwell.
Piketty, T. and Saez, E. (2006). The evolution of top incomes: a historical and international perspective. American economic review, 96(2), 200-205.
Ponticelli, J. and Voth, H. J. (2020). Austerity and anarchy: Budget cuts and social unrest in Europe, 1919 - 2008. Journal of Comparative Economics, 48(1), 1-19.
Reggiani, A., Nijkamp, P. and Lanzi, D. (2015). Transport resilience and vulnerability: The role of connectivity. Transportation research part A: policy and practice, 81, 4-15.
Rodriguez-Pose, A. (2018) The revenge of the places that don't matter (and what to do about it). Cambridge Journal of Regions, Economy and Society, 11(1): 189-209.
Scheidel, W. (2017) *The great leveller. Violence and the history of inequality from the stone-age to the twenty-first century*, Princeton, Princeton University Press.

Covid Economics 13, 4 May 2020: 51-70

Scheve, K. and Stasavage, D. (2006). Religion and preferences for social insurance. Quarterly Journal of Political Science, 1(3), 255-286.
Schmitt-Grohé, S., Teoh, K. and Uribe, M. (2020) 'COVID-19: testing inequality in New York City,' *NBER working paper* #27019
Smith, N., and S. Middleton (2007) A review of poverty dynamics research in the UK. © Loughborough University.
Spinney, L. (2020) Coronavirus outbreak: Inequality doesn't just make pandemics worse, it could cause them, The Guardian, 13/04/2020
Stobart, J. (2011). Gentlemen and shopkeepers: supplying the country house in eighteenth-century England. *The Economic History Review*, 64(3), 885-904.
Tiebout, C. (1956) A pure theory of local expenditures. Journal of Political Economy, 64(5), 416-424.
Tubadji A and P Nijkamp (2015) Cultural Gravity Effects among Migrants: A Comparative Analysis of the EU15, Economic Geography, 91(3): 343-380.
Tubadji A and P Nijkamp (2018) Revisiting the Balassa-Samuelson effect: International tourism and cultural proximity, Tourism Economics 24(8): 915-944.
Tubadji, A. (2012) Culture-Based Development: Empirical Evidence for Germany. International Journal of Social Economics, 39(9):690-703.
Tubadji, A. (2013) Culture-Based Development: Culture and Institutions Economic Development in the Regions of Europe. International Journal of Society Systems Science, 5(4):355-391.
Tubadji, A. (2020a) Narrative Economics of Religion: The Witch Question, Manuscript.
Tubadji, A. (2020b) Ceteris Paribus and Fixed Effects in Regional and Cultural Economics, forthcoming.
Tubadji, A. (2020c) UK Witches: Social Signalling for People and Places Left Behind, Manuscript.
Tubadji, A. and P. Nijkamp (2016). Six degrees of cultural diversity and RandD output efficiency. Letters in Spatial and Resource Sciences, 9(3), 247-264.
Tubadji, A. and P. Nijkamp (2019) Cultural attitudes, economic shocks and political radicalization. Annals of Regional Science, 62(3): 529-562.
Tubadji, A., Dietrich, H., Angelis, V., Haas, A. and Schels, B. (2019). Fear-of-failure and cultural persistence in youth entrepreneurship: Comparative analysis: Greece versus Germany. Journal of Small Business *and* Entrepreneurship, 1-26.
Tubadji, A., M. Burger and D. J. Webber (2020) Geographies of Discontent and Cultural Fiscal Policy in the Netherlands, forthcoming.
Tubadji, A., R. Huggins and P. Nijkamp (2020) Firm Survival as a Function of Individual and Local Uncertainties: An Application of Shackle's Potential Surprise Function, Journal of Economic Issues, forthcoming.
Tubadji, A., T. Colwell and D. J. Webber (2020) Voting with Your Feet versus Brexiting: The Tale of Those Stuck Behind, forthcoming.
Tubadji, A., V. Angelis and P. Nijkamp (2015). Endogenous Intangible Resources and their Place in the Institutional Hierarchy, Review of Regional Research: Jahrbuch fur Regionalwissenschaft, 36(1): 1-28.
Tubadji, A., V. Angelis and P. Nijkamp (2016). Cultural Hysteresis, Entrepreneurship and Economic Crisis: An Analysis of Buffers to Unemployment after Economic Shocks, Cambridge Journal of Regions, Economy and Society, 9(1): 103-136.
Turchin, P. (2007) "Modelling periodic waves of integration in the Afro-Eurasian world-system." Globalization as Evolutionary Process. Routledge, 2007. 181-209.
Turchin, P.(2020) Coronavirus and Our Age of Discord, Cliodynamica - A Blog about the Evolution of Civilizations, 05/04/2020.
Wei, Y. D. (2015). Spatiality of regional inequality. Applied Geography, 61, 1-10.
Woods, A. (2013). A manufactured plague: the history of foot-and-mouth disease in Britain. Routledge.
Zaman, Mohammad Mostafa, Nobuo Yoshiike, Anisul Haque Chowdhury, Md Qumrul Jalil, Razia Sultana Mahmud, Gnulam Mohammed Faruque, Mian Abdur Rouf, KMHS Sirajul Haque, and Heizo Tanaka. "Socioeconomic deprivation associated with acute rheumatic fever. A hospital-based case-control study in Bangladesh." Paediatric and perinatal epidemiology 11, no. 3 (1997): 322-332.

Covid Economics 13, 4 May 2020: 51-70

Appendix: Descriptive Statistics – Data

Type	Variable	Definition	Source	Obs	Mean	Std. Dev.	Min	Max
time	*week*	Due to ONS death statistics being on weekly basis	ONS	130	7	3.756132	1	13
place	*region*	England and Wales (NUTS1)	ONS	13				
Main raw variable	*rankofimds~v*	Mudliple Deprivation Index (score 1 to infinite, where 1 is highest deprivation)	ONS	117	16023.85	2801.63	13037.88	20723.45
	rankofeduc~g	Mudliple Deprivation in educational aspects (score 1 to infinite, where 1 is highest deprivation)	ONS	117	15773.9	2188.45	13265.88	19617.95
	lunc_cance~s	patience with lung cancer in the region (number)	ONS	130	130.5217	36.68	83.45	211.05
	deaths	Covid-19 deaths	ONS	130	1151.877	355.41	522	2132
	total_deaths	total deaths in Covid-19 period	ONS	130	11542.85	979.64	10645	14058
	deaths_0114	Covid-19 deaths in age category	ONS	130	17.38462	4.08	12	26
	deaths_1544	Covid-19 deaths in age category	ONS	130	290	34.15	189	321
	deaths_4564	Covid-19 deaths in age category	ONS	130	1325.385	89.40	1202	1517
	deaths_6574	Covid-19 deaths in age category	ONS	130	1858.769	128.35	1744	2198
	deaths_7584	Covid-19 deaths in age category	ONS	130	3270	306.02	2967	4014
	deaths_85m~e	Covid-19 deaths in age category	ONS	130	4731.6	503.17	4205	5995
	m_deaths_~1y	Male number of Covid-19 deaths in age category	ONS	130	27.6	5.51	14	38
	m_death~0114	Male number of Covid-19 deaths in age category	ONS	130	10.3	2.90	5	15
	m_death~1544	Male number of Covid-19 deaths in age category	ONS	130	187.5	24.07	115	214
	m_death~4564	Male number of Covid-19 deaths in age category	ONS	130	789.1	71.61	666	938
	m_death~6574	Male number of Covid-19 deaths in age category	ONS	130	1091.2	68.92	999	1270
	m_death~7584	Male number of Covid-19 deaths in age category	ONS	130	1742.7	151.35	1579	2096
	m_deaths_8~e	Male number of Covid-19 deaths in age category	ONS	130	1904.5	170.74	1725	2359
	f_deaths_~1y	Female number of Covid-19 deaths in age category	ONS	130	22.1	4.96	14	31
	f_death~0114	Female number of Covid-19 deaths in age category	ONS	130	7.1	2.98	4	14
	f_death~1544	Female number of Covid-19 deaths in age category	ONS	130	102.5	11.51	74	119
	f_death~4564	Female number of Covid-19 deaths in age category	ONS	130	536.3	32.13	490	616
	f_death~6574	Female number of Covid-19 deaths in age category	ONS	130	767.5	63.79	694	928
	f_death~7584	Female number of Covid-19 deaths in age category	ONS	130	1527.3	159.56	1361	1918
	f_deaths_8~e	Female number of Covid-19 deaths in age category	ONS	130	2827.2	336.17	2480	3636
	asian	Percentage Asian population in the region	ONS	130	6.65	4.692	2	18.5
	black	Percentage Black population in the region	ONS	130	2.69	3.631	0.5	13.3
	mixed	Percentage population of mixed background in the region	ONS	130	1.96	1.103	0.9	5
	white_british	Percentage White-British in the region	ONS	130	83.15	13.469	44.9	93.6
	white_other	Percentage other white ethnic origin in the region	ONS	130	4.71	3.591	1.7	14.9
	other	Percentage other ethnic origin in the region	ONS	130	0.86	0.866	0.3	3.4
	rankofimds~v	Mudliple Deprivation Index (score 1 to infinite, where 1 is highest deprivation)	ONS	117	16023.85	2801.63	13037.88	20723.45
	rankofeduc~g	Mudliple Deprivation in educational aspects (score 1 to infinite, where 1 is highest deprivation)	ONS	117	15773.9	2188.45	13265.88	19617.95
Instrumental variable	*lunc_cance~s*	patience with lung cancer in the region (number)	ONS	130	130.5217	36.68	83.45	211.05

Covid Economics 13, 4 May 2020: 51-70

Covid Economics 13, 4 May 2020: 51-70

Type	Variable	Definition	Source	Obs	Mean	Std. Dev.	Min	Max
Available Controls	*all_ages*	Number of people in age group	NOMIS	130	5911581	2036054	2657909	9133625
	age_0_15	Number of people in age group	NOMIS	130	1131117	425660.9	474998	1834795
	age_16_24	Number of people in age group	NOMIS	130	635212	206578	298268	950440
	age_25_49	Number of people in age group	NOMIS	130	1946456	813038.8	821725	3659254
	age_50_64	Number of people in age group	NOMIS	130	1115672	350838.5	540546	1768493
	age_65over	Number of people in age group	NOMIS	130	1083125	333545.7	522372	1761765
	all_male	Male number of people in age group	NOMIS	130	2921525	1012630	1305486	4500331
	age_m_0_15	Male number of people in age group	NOMIS	130	579612.1	218171.2	244096	938617
	age_m_16_24	Male number of people in age group	NOMIS	130	326686.2	105107	154271	490684
	age_m_25_49	Male number of people in age group	NOMIS	130	971145.8	413191.1	404985	1862524
	age_m_50_64	Male number of people in age group	NOMIS	130	549185	173853.1	263667	874414
	age_m_65over	Male number of people in age group	NOMIS	130	494896	151407	238467	800343
	all_female	Female number of people in age group	NOMIS	130	2990056	1023660	1352423	4633294
	age_fe_0_15	Female number of people in age group	NOMIS	130	551504.6	207494.4	230902	896178
	age_fe_16_24	Female number of people in age group	NOMIS	130	308525.8	101504.8	143997	459756
	age_fe_25_49	Female number of people in age group	NOMIS	130	975309.7	400123.2	416740	1796730
	age_fe_50_64	Female number of people in age group	NOMIS	130	566487.1	177016.1	276879	894079
	age_fe_65o^r	Female number of people in age group	NOMIS	130	588228.6	182235.3	283905	961422
	locationqu.manufacture	location quotient for manufactyring	NOMIS	130	1.15	0.386	0.28	1.64
	locationqu.cars	location quotient for car production	NOMIS	130	1.28	1.051	0.16	3.89
	avg_house_price	Avwerage houseprice in the pregion	NOMIS	130	239846	101338	130977	483922
	monthly_ch_house_price	monthly change of average house price in the region	NOMIS	130	0.44	1.218	-2	2.1
	annual_ch_house_price	Annual change of average hous eprice in the region	NOMIS	130	2.22	0.719	1.2	3.9
	total2007	Total population in 2007	NOMIS	130	5507111	1840698	2550818	8446500
	urban2007	Urban population in 2007	NOMIS	130	4495461	1885534	2019379	8058311
	rural2007	Rural population in 2007	NOMIS	130	1011651	524824.1	15389	1711035
	job_density	Job density	ONS	130	0.842	0.08	0.73	1.02
	ppl2020	Total population in 2020	ONS	130	5977847	2073808.00	2674568	9235982
	numberofbuiness	number of small and medium businesses	NOMIS	130	0.5411	0.28	0.152	1.092
	claimant^n20	claimant count jan 2020	NOMIS	130	108562.9	39907.19	59280	181195
	claimant^b20	claimant count feb 2020	NOMIS	130	110298.3	40816.30	59402	186044
	empl_ra^2020	employment ratio	ONS	130	76.24	2.68	71.7	80
Derived variables used in estimations	*unempl*	number claimant counts per head of population	derived	130	0.031	0.008	0.021	0.045
	deaths_perc	number of Covid-19 deaths per head of population	derived	130	0.0002	0.0000355	0.0001	0.0003
	dumm_deaths	dummy equal to 1 if percentage of deaths in the region is above the average for the country	derived	130	0.53	0.50	0	1
	ppl_density	Job density as a proxy of population density	derived	130	0.84	0.08	0.73	1.02
	ethnic_cultural	sum of people with Asian, black and mixed origin per population	derived	130	0.11	0.09	0.04	0.37
	employed_perc	employment ratio	derived	130	76.24	2.68	71.70	80
	imd	IMD total	derived	117	16023.85	2801.632	13037.88	20723.45
	capital	based on average house price per region as a proxy	derived	130	239846	101338	130977	483922
	ln_capital	natural logarythm of the derived variable capital	derived	130	12.31	0.38	11.78	13.09
	urban	percentage of people in the region who live in urban areas	derived	130	0.798	0.097	0.671	0.998
	sectoral_spec	location quotient for cars	derived	130	1.279	1.05	0.16	3.89
	male	percentage of population who is male	derived	130	0.49	0.00	0.49	0.50
	age above 45	percentage of people above the age of 45	derived	130	0.19	0.03	0.12	0.22
	deaths_perc_adj	percentage of Covid-19 deaths per population (adjusted by 1000 for magnitude)	derived	130	0.20	0.04	0.11	0.30
	perc_lung	percentage of lung cancer patients per region	derived	130	2.32E-05	5.47E-06	1.41E-05	3.37E-05

Notes: The table presents the main descriptive statistics for the available variables in our dataset, their definition and their source.

CEPR PRESS

Covid Economics **Issue 13, 4 May 2020**

Macroeconomic consequences of stay-at-home policies during the COVID-19 pandemic

Neha Bairoliya[1] and Ayse Imrohoroglu[2]

Date submitted: 28 April 2020; **Date accepted:** 28 April 2020

Older adults and those with underlying medical conditions seem especially vulnerable to the COVID-19 pandemic. The U.S. government's efforts to contain the infection, on the other hand, have a disproportionate impact on the working age population. To be able to capture the impact of the pandemic and the resulting mitigation efforts on a population that is heterogeneous by age, income and health status, we use an overlapping generations model that mimics the U.S. economy along those dimensions in 2020. We introduce an unexpected COVID-19 shock in the economy and examine the resulting impact on aggregate output, labor supply, savings, and consumption behavior of the different agents. We find that mitigation efforts that target certain age and health groups result in significantly smaller disruptions in the economy. Going forward, introducing subsidies to those with underlying health conditions and/or the elderly to self isolate might prove to be a useful path in opening up the economy.

Covid Economics 13, 4 May 2020: 71-90

1 Assistant Professor of Finance and Business Economics, University of Southern California.
2 Professor of Finance and Business Economics, University of Southern California.

Covid Economics 13, 4 May 2020: 71-90

1 Introduction

There is ample evidence that older adults and those with underlying medical conditions seem especially vulnerable to the COVID-19 pandemic. Meanwhile, efforts to mitigate the spread of the infection in the U.S. have included closing all businesses that are deemed unessential. This has resulted in more than 26 million initial claims for unemployment insurance in five weeks. In order to examine the effects of COVID-19 and the resulting mitigation efforts on the economy, we use an overlapping generations model where agents are heterogeneous with respect to age, income, and health status. All individuals retire exogenously at age 65 and may live up to age 100. Survival probabilities at each age depend on the education level and the health status of an agent. We calibrate this economy based on historical data on demographics, survival probabilities, and health status. Distribution of income, age, and health status in the model matches the most recently available U.S data at which point we subject the economy to a large, unexpected health shock which infects a large fraction of the population and changes their survival probabilities. The government's response to the pandemic includes efforts to quarantine parts of the population. Consequently, a fraction of the population is forced to stay home. Government provides pandemic assistance to help those unemployed. We calibrate the impact of the disease in the population under different assumptions on the progression of the infection and trace the changes in the economy's labor, capital, saving, and output in the short-run and in the long-run for several different scenarios.

We calibrate our benchmark experiments with mitigation to a projected number of 60,000 deaths in the U.S. and a fatality rate of 0.3%. We assume the mitigation measures taken in the U.S. to result in 50% of the population to be unproductive for three months. Since the time period in the model is a year, this corresponds to 12.5% of the population to stay home for a year. While there are significant uncertainties regarding many of these measures, their precise level is less of a concern for the three main experiments we conduct. In these experiments, we keep the fatality rate, the infection rate, and the precent of the population under quarantine the same and just change the population sub-group that faces the stay-at-home orders. In the first case, we implement the lockdown by randomly quarantining 12.5% of the population. In the second case, we quarantine only the older population (73 and older) who make up 12.5% of the population. Finally, in the third case, we quarantine agents based on their health status. Specifically, we impose stay home restrictions on all individuals in the *bad* health state and those 80 and older and in *fair* health state.

Unsurprisingly, we find the largest economic declines to happen under the first scenario, i.e, the case where a random quarantine of 12.5% of the population is imposed. This is primarily due to the fact that an indiscriminate lockdown prevents the healthy and highly productive members of the economy from contributing to the economic activity. On the other hand, quarantining the unhealthy/older individuals with low/zero labor productivity, hurts economic output substantially less. For example, output declines by 13% under random lockdown as opposed to 1.8% where stay home restrictions are based on health status. We interpret the findings from these experiments useful for thinking about ways to opening up the economy. Allowing the workforce to return to work while asking the elderly or those in a bad health state to stay home

Covid Economics 13, 4 May 2020: 71-90

may have significant economic benefits. Of course, it is not obvious if, in reality, these three cases would lead to the same infection and fatality rates. On the one hand, the elderly and those in bad health states are the most vulnerable to this pandemic. Such a policy may help reduce the risks they face. On the other hand, some of the current mitigation measures are directed at reducing the interactions between people and may prove more effective in reducing the spread of the disease. There is not enough evidence to help pin down the effectiveness of different mitigation measures in reducing the spread of the disease at the moment, however. Some other possible ways to open up the economy that are discussed involve large scale testing, contact tracing, isolating those who test positive, and allowing individuals with antibodies to go back to work. Given the possible political challenges involved in these options, introducing subsidies to those with underlying health conditions and the elderly might prove to be a useful path in opening up the economy.

We also conduct experiments and document the macroeconomic consequences of COVID-19 assuming no mitigation efforts by the government based on implications of an SIR model.[3] Currently there is significant uncertainty regarding several key parameters governing the health impact of the pandemic. In order to understand the economic consequences of COVID-19, one needs to know the infection rate, the mortality rate, and of course how long the pandemic would last. One of the most important parameters, but also the most difficult to pin down, is the fatality rate — fraction of those infected dying from the disease. A major issue in getting reliable estimates of this parameter is due to the lack of knowledge of the true infection rate in the population. Individuals who are tested are usually those showing mild/severe symptoms. Given that a large fraction of the population may be asymptomatic, hence undiagnosed, makes any available estimate of the fatality rate biased upwards. To navigate this issue, we use data from Iceland which is known to have carried out significant random testing and use a fatality rate of 0.3%. Current experiments conducted in LA county and Santa Clara county point to similar fatality rates. We compare the economic consequences of the pandemic under different assumptions on the reproduction number, which defines the mean number of secondary cases generated by one primary case with no mitigation efforts, based on the SIR model. Using reproduction numbers commonly mentioned in the epidemiology literature we estimate that the pandemic could have infected 84% to 95% of the population in a year if unmitigated. With a fatality rate of 0.3% an unmitigated pandemic would have led to large number of deaths. Next, we compare the results in the unmitigated cases to our benchmark experiment where the government imposed stay-at-home restrictions leads to much lower infection rates. Since mitigation involves agents to be ordered to stay at home, the decline in output in this economy is about double the decline in the economies without mitigation. However, taking into account the value of statistical lives lost in the unmitigated cases easily erases the extra gains in output.

Overall, our main findings indicate significant differences in the economic consequences of who to quarantine during this pandemic. We find that stay home recommendations that are based on health and age reduce the economic severity of the pandemic by more than 10 percentage points of GDP under very conservative

[3]Standard Inflammatory Response (SIR) model describes the dynamics of the progression of an epidemic. See Kermack and McKendrick (1927), and Anderson and May (1991).

Covid Economics 13, 4 May 2020: 71-90

estimates. Going forward, it may be possible to introduce subsides to the elderly or those with underlying health conditions to self-isolate until a vaccine or a cure is available. Fiscal consequences of such a policy are likely to be much lower than what is currently spent on pandemic assistance which includes providing unemployment insurance to a large fraction of the working-age population.

2 The Model

We model the initial steady state of the economy based on the historical behavior of the U.S. economy along several dimensions such as the distribution of income, age and health status. We account for the aging population in the U.S. by changing the population growth rate along the transition path and follow the economy as it reaches a future steady state with a higher old-age dependency ratio as compared to the initial steady state. The transition from the initial steady state to the final one without the disruptions caused by the pandemic form our baseline U.S. economy. Next, we shock the first transition period (2020) by an unexpected health shock and examine the new transition to the same future steady state under several different assumptions on the transmission of the diseases and the containment efforts by the government. We assume that the time period is a year and the impact of the pandemic on infections lasts one year. Eventually the economy converges to the same final steady state as the impact of any pandemic-induced policy or health changes last as long as the youngest generation in the population that got exposed to the shock.

2.1 Initial Steady State

Consider an economy populated by J overlapping generations. In each period a new generation is born whose mass grows at rate n. Individuals are assumed to enter the economy with several exogenous characteristics that do not change over the life-cycle. Specifically, each individual is assumed to be of some education type $e \in \epsilon_d$ where $\Pi^{es}(\epsilon_d)$ denotes the invariant joint probability measure over education type of an incoming generation.

In each period, individuals are characterized by health status $h \in \mathcal{H}$. Agents are assumed to enter the economy in the highest health state $\overline{h}$. Health then evolves stochastically over the life-cycle. The stochastic process for health status follows a finite-state Markov chain with stationary transitions over time. The Markov process is assumed to differ by age, and level of education, but is otherwise identical and independent across agents:

$$Q^h_{je}(h, \mathcal{H}) = Prob(h' \in \mathcal{H} \,|h, j, e) = Q^h_{je}(h, \mathcal{H}),$$

Agents of age j, education e, and health status h survive to age $j+1$ with positive probability ψ_{jeh}. At age J, individuals die with probability one.

In each period, individuals are endowed with a unit of time that may be devoted to leisure or to earning wages in a competitive labor market. An individual's productivity in the labor market has an age-, education-specific (ϵ_{je}), and health specific component (ξ_h) estimated directly from the data and an idiosyncratic shock (η). The stochastic process for the labor productivity shock follows a finite-state Markov chain with stationary transitions over time and which is identical and independent across all agents:

$$Q_t^{\eta}(\eta, \mathcal{E}) = Prob(\eta' \in \mathcal{E} \mid \eta) = Q^{\eta}(\eta, \mathcal{E}).$$

Let $\Pi^{\eta}(\mathcal{E})$ denote the invariant probability measure associated with Q^{η}. All individuals retire exogenously at age j_r, at which point labor productivity is equal to zero ($\epsilon_{je} = 0 \; \forall j \geq j_r$) and they receive social security income SS_e which is a function of their education level.

An agent's preferences over consumption and leisure follow an additive time separable utility function given by:

$$E\left\{\sum_{j=1}^{J} \beta^{j-1} u(c_j, \ell_j)\right\}$$

where β is a per-period discount factor, c consumption, and ℓ hours worked. Expectations are taken with respect to stochastic processes for health status and labor productivity.

2.1.1 Market Structure and the Government

We assume individuals are unable to insure against idiosyncratic health and labor productivity risk by trading private insurance contracts. Furthermore, we assume there are no annuity markets to insure against mortality risk. Agents may self-insure by saving one-period risk-free bonds that earn interest rate r. However, agents are not permitted to maintain a negative asset position between periods (i.e. borrowing is not allowed). A non-negative asset limit ensures agents do not die in debt. Assets from the deceased are distributed evenly in a lump-sum fashion across all individuals entering the economy the following period. These unintended bequests are denoted by Tr.

The government uses labor income taxes, τ_l, to fund the Social Security system. In addition, there are lump-sum taxes Tx that are used to fund a minimum consumption level, $\underline{c}$ for the poorest in the society.

2.1.2 Technology

Aggregate output (Y) is produced by a representative firm using the technology:

$$Y = AK^{\alpha}N^{1-\alpha} \qquad \alpha \in (0,1), \tag{1}$$

where K and N are the aggregate capital stock and labor inputs (measured in efficiency units), A is total factor productivity, and α is the capital share. The representative firm maximizes profits such that the rental

Covid Economics 13, 4 May 2020: 71-90

rate of capital, r, and the wage rate w, are given by:

$$r = \alpha A(K/N)^{\alpha-1} - \delta \quad and \quad w = (1-\alpha)A(K/N)^{\alpha}. \tag{2}$$

2.1.3 Decision Problem

At the initial steady state, an individual can be characterized by a vector of state variables $z = (a, \eta, j, e, h)$, where a is current holdings of one-period, risk-free assets, η is a stochastic labor productivity shock, j is age, e is level of education, h is health status. Given this state vector, an agent chooses consumption c, labor supply ℓ, and next period assets a' to maximize expected lifetime utility. The decision problem facing an agent is given by:

$$\nu(z) = \max_{c,\ell,a'} \{u(c,\ell) + \beta\psi_{jeh} E_{\eta' h' x'}[\nu(z')]\}$$

subject to

$$c + a' = y_j + (1+r))(a + Tr(j=1)) - Tx,$$

where

$$y_j = \begin{cases} w\left(1-\tau^{\ell}\right)\epsilon_{je}\xi_h\eta\ell & \text{if} \quad j < j_r \\ SS_e & \text{if} \quad j \geq j_r, \end{cases} \tag{3}$$

and

$$a' \geq 0, \quad c \geq 0, \quad 0 \leq \ell \leq 1$$

where value function $\nu(.)$ is the expected discounted lifetime utility with a given state vector. Note that expectations are taken with respect to stochastic processes for health status and labor productivity. The first constraint is the budget constraint while the final line gives the borrowing constraint followed by feasibility constraints on consumption and labor. Emergency relief is exogenously given when consumption $\underline{c}$ is unattainable, in which case $a' = 0$, $c = \underline{c}$, and $\ell = \bar{\ell}$.

Covid Economics 13, 4 May 2020: 71-90

Covid Economics 13, 4 May 2020: 71-90

2.2 COVID-19

We model COVID-19 as a health shock totally unexpected in its scale. We calibrate the progression of the disease in the population under different assumptions on the mitigation process. Some individuals in the economy get hit with this unexpected health shock in 2020, become infected, and face a big change in their survival probabilities. Infection status x effects both the labor productivity, which now takes the form $\epsilon_{je}\xi_h\theta_x$ and the survival probability ψ_{jehx} of the agents. In addition, some fraction of the population is ordered to stay home and are not able to work. We assume that individuals who become unemployed due to the lockdown receive government provided temporary pandemic assistance (PA). The decision problem is given by:

$$V(z) = max_{c,l,a'}\left\{u(c,l) + \beta\psi_{jehx}EV(z')\right\}$$

subject to

$$c + a' = y_j + (1+r)\left(a + Tr\left(j=1\right)\right) - Tx,$$

$$y_j = \begin{cases} w\left(1-\tau^{\ell}\right)\epsilon_{je}\xi_h\eta\ell & \text{if} \quad j < j_r \quad and \quad q=0, x=0 \\ w\left(1-\tau^{\ell}\right)\epsilon_{je}\xi_h\theta_x\eta\ell & if \quad j < j_r \quad and \quad q=0, x=1 \\ PA & if \quad j < j_r \quad and \quad q=1, \forall x \\ SS_e & if \quad j \geq j_r \quad for \quad \forall q, \forall x \end{cases} \tag{4}$$

$$a' \geq 0, \quad c \geq 0, \; 0 \leq l \leq 1$$

3 Calibration

We calibrate the model in two steps. In the first step, we calibrate a set of parameters outside the model. In the second step, we assume that the initial balanced growth economy is 2019 and jointly calibrate the remaining parameters to match moments in the U.S. economy in that year. The following subsections describe our calibration exercise in detail.

3.1 Preferences and Demographics

Each model period is one year. Individuals enter the economy at age 20 (model period $j = 1$) and die with probability one at age 100 (model period $J = 80$). The growth rate of new 20 year old individuals in each cohort (n) for the initial steady state is set at 0.3% in order to match an old-age dependency ratio of 28% in 2020 (UN 2019).[4] We assume that retirement is exogenous for all agents at age 65 (model period $j_r = 45$),

[4]The old age dependency ratio is of people older than 64 to those aged 20-64.

which is the *Normal Retirement Age (NRA)* for claiming Social Security (SS) benefits in the U.S.[5]

Preferences over consumption and leisure are assumed to follow a standard Cobb-Douglas utility function:

$$u\left(c_j, \ell_j\right) = \frac{\left[c_j^{\gamma}\left(1-\ell_j\right)^{1-\gamma}\right]^{1-\sigma}}{1-\sigma},$$

where σ controls risk aversion and γ determines the relative weight of consumption. Note that utility exhibits decreasing absolute risk aversion, which is standard in most reasonable preference classes. We set the value of $\gamma = 0.39$ to match the average fraction of time working to a third of the time endowment. We assume $\sigma = 3.56$, which implies an inter-temporal elasticity of substitution, $\frac{-1}{\gamma(1-\sigma)-1}$, of 0.5. The time discount factor β is set to 0.96 match an annual capital-output ratio of 3.0.

3.2 Labor Productivity

The labor productivity in the model comprises of the stochastic component η, the health specific component ξ_h, and a deterministic age- and education-specific component ϵ_{je}. We estimate the Markov chain for the stochastic component of productivity by assuming an underlying AR(1) process in logs:

$$\ln\left(\eta'\right) = \rho \ln\left(\eta\right) + \epsilon_{\eta}, \quad \epsilon_{\eta} \sim N\left(0, \sigma_{\eta}^2\right).$$

Parameters governing the stochastic process for productivity shocks are taken from Fuster, A. İmrohoroğlu, and S. İmrohoroğlu 2007.[6] We then use the Tauchen method to approximate this process with a Markov chain over four discrete states.

We allow the fixed education state to take two possible values $\{college, non-college\}$. We use to data from the U.S. Census Bureau to fix the share of college graduates to 28.6% in the model.[7] We use the deterministic age- and education-specific labor productivity ϵ_{je} estimates from Conesa, Costa, et al. 2018. Finally, we set ξ_h to 1 for agents in best health state. For the bottom two health states, we set $\xi_h = 0.78$ and $\xi_h = 0.66$ to match the ratio of earnings for agents in fair and best health and poor and best health states respectively.

3.3 Health and Mortality

Health can take three possible values $\{good, fair, bad\}$ in the model. We identify these health states in the Health and Retirement Study (HRS) data from the self-reported health status variable.[8] Health transitions

[5]Social Security benefits can be claimed as early as age 62 and NRA is slightly different for different birth cohorts. SS benefit claim is also independent from labor supply decisions. However, we simplify these aspects of the program in the model to reduce computational burden.

[6]The authors use an income process which is education specific. We adjust their estimate for the average population.

[7]Current Population Survey, Annual Social and Economic Supplement, 2018.

[8]The Health and Retirement Survey asks respondents to self report their health on a scale of 1 to 5 where 1 is "Excellent", 2 is "Very Good", 3 is "Good", 4 is "Fair"and 5 is "Poor". For computational simplicity, the 5-point scale is converted into a 3

Covid Economics 13, 4 May 2020: 71-90

Covid Economics 13, 4 May 2020: 71-90

Figure 1: Survival Probability by Age, Health and Education R0=3.1

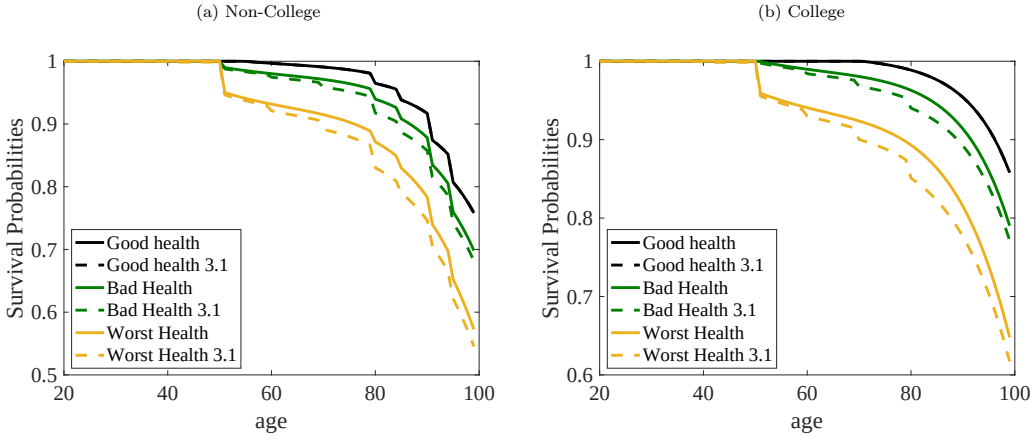

across these states are then estimated by running an ordered probit of self-reported health status on previous year health status, education, cohort, and a quadratic function of age. We assume that individuals are in the best health state until age 50. This is mainly due to the fact that we do not observe these transitions for younger individuals in our micro dataset.[9]

Survival probabilities in the model vary with age, education and health status ψ_{jeh}. These probabilities cannot be directly derived from HRS as it does not sample the institutionalized population. So we estimate these survival probabilities in two steps following Conesa, Kehoe, et al. 2020. First, we estimate the raw profiles from the HRS data. The HRS Tracker file has information on death dates of the respondents which are used to construct age and health specific survival probabilities by running an ordered probit model of death indicator on self-reported health status, age quadratic, education and cohort dummies as mentioned earlier. In a second step, we adjust these profiles to match both the age-specific survival probabilities in the National Vital Statistics System data and the education survival premium. Figure 1 summarizes the survival probabilities by age, health, and education status. In addition, the dashed lines show the changes that take place in the survival probabilities due to the COVID-19 shock under a non-mitigated case that is explained in more detail in Section 3.5.

point scale by grouping individuals of "Excellent" and "Very Good" health into the good health category and those in "Good" and "Fair" into the "fair" category

[9]The HRS is a longitudinal sample of non-institutionalized individuals in the U.S., over the age of 50.

Covid Economics 13, 4 May 2020: 71-90

3.4 Government Transfers

The Social Security replacement rate is set to 44% following Fuster, A. İmrohoroğlu, and S. İmrohoroğlu 2007. We set the consumption floor at 2.26% of income per capita in the baseline economy to match the average annual Supplemental Nutrition Assistance Program benefits reported by the United States Department of Agriculture. The government also funds a pandemic relief package – a lump sum transfer of 25% of income per capita — for those who experience a quarantine shock. Table 1 summarizes the calibration of the economic parameters.

Table 1: Economic Parameters

Parameter	Value	Source / Target
Cohort growth n	0.3%	Dependency ratio = 28%
Retirement age j_r	65	Age of SS eligibility
Share of college graduates	28.6%	U.S. Census Bureau
Discount factor β	0.96	K/Y = 3.0
Risk aversion σ	3.56	IES = 0.5
Consumption weight γ	0.39	Average hours = 0.33
Persistence ρ	0.83	[Fuster et al., 2007]
Variance σ_η^2	0.022	
Capital income share α	0.36	
Period depreciation δ	5.9%	[Castaneda et al., 2003]
Social Security replacement rate	0.44	[Fuster et al., 2007]
Pandemic Assistance	25%	
Consumption floor $\underline{c}$	0.026	SNAP
Labor on floor $\bar{\ell}$	0.33	Assumption

3.5 COVID-19 Shock

We calibrate the benchmark economy with mitigation to a projected number of 60,000 deaths in the U.S. One of the most important parameters but also the most difficult to pin down is the fatality rate — fraction of those infected dying from the disease. A major issue in getting reliable estimates of this parameter is due to the lack of knowledge of the true infection rate in the population. Individuals who are tested are usually those showing mild/severe symptoms. Given that a large fraction of the population maybe asymptomatic, hence undiagnosed, makes any available estimate of the fatality rate biased upwards. To navigate this issue, we use data from Iceland which is known to have carried out significant random testing to obtain a the fatality rate (0.3%).[10] However, the fatality rate by itself does not provide information on the age and health distribution of fatalities. It is important for the model to capture the fact that the fatalities from the disease are concentrated disproportionately among the elderly and the unhealthy individuals. We use age specific fatality rate estimates from Riou et al. 2020 and scale the survival probabilities for the bottom two health groups using the age and health specific scale. For the latter, we assume that those in the worst health

[10]Recent USC-LA County study also points to fatality rates of 0.1-03% (https://reason.com/2020/04/20/l-a-county-antibody-tests-suggest-the-fatality-rate-for-covid-19-is-much-lower-than-people-feared/).

states are affected twice as badly as those in the middle health state. We also do not scale the mortality for those below the age of 40 in the model as the fatality rates are very low for those below 40. Table 2 summarizes the age-specific fatality rates used in our experiments. The fatality rate of 0.3 along a death rate of 0.018 (60,000 deaths in the U.S. population) implies 6.1% of the population to be infected within a year.

Table 2: Fatality Rate = 0.3%

Age group	Fatality rate (%)*	Age-specific scale**
20-29	0.19	0
30-39	0.38	0
40-49	0.82	1x
50-59	2.7	3x
60-69	9.4	9x
70-79	20	20x
80+	36	37x

*Riou et al. 2020

**x differs by health state and infection scenario.

We assume that the mitigation measure involves 50% of the population to be quarantined for a quarter. Given that the model period is a year, this implies 12.5% of the population being quarantined for a year which results in an infection rate to 6.1%. Lastly, we calibrate the decline in the productivity of workers based on the number of days lost due to the illness. Given the average duration of the disease of 18 days, we assume that individuals experience zero productivity for those days, implying an annual productivity drop of 5% in the period of infection.

For the experiments where the pandemic is not mitigated, we calibrate the parameters needed to describe the COVID-19 infection shock using some of the predictions of an SIR model. This model tracks the progression of the disease in a country where the total population is divided into three categories: those who are susceptible to the disease (S), who are actively infected with the disease (I), and those who are no longer contagious (R). Progression of the disease in the population depends on the transition between these states where social distancing measures help reduce the spread. An important parameter in these calculations is the reproduction number which defines the mean number of secondary cases generated by one primary case with no mitigation efforts. There is significant uncertainty regarding this parameter. In our calibration, we consider R_0 equal to 3.1 based on H. Wang et al. 2020 and 2.2 based on Fauci, Lane, and Redfield 2020 which result in 94.7% and 84.4% of the population to be infected within a year respectively.[11] Dashed lines in Figure 1 display the changes in survival probabilities under the unmitigated case with R_0 equal 3.1 for different age, health status, and eduction groups. The implied transmission rate in the benchmark model with social distancing measures is 1.23 which results in 6.1% of the population to be infected within a year.

[11] Imai et. al (2020) estimate an R0 between 1.5 and 3.5 using data from Wuhan China. Wang et. al (2020) set R0=3.1 based on the Imai et. al data while Fauci et. al (2020) use an R0 of 2.2. See Atkeson 2020 for a summary.

Covid Economics 13, 4 May 2020: 71-90

Table 3 summarizes the calibration of the different cases describing the COVID-19 pandemic.

Table 3: COVID-19 Scenarios

	Mitigated ($R_t = 1.23$)			Unmitigated (R_t)	
	Case 1	Case 2	Case 3	3.1	2.2
Infection rate (%)	6.1	6.1	6.1	94.7	84.4
Fatality rate (%)	0.3	0.3	0.3	0.3	0.3
Deaths rate (%)	0.018	0.018	0.018	0.28	0.25
Quarantine rate (%)	12.5	12.5	12.5	-	-

4 Results

Initial steady state of this economy resembles the U.S. in terms of the age distribution, health distribution, and income distribution as well other macroeconomic targets such as the capital output ratio and hours worked. Tables 4 to 6 summarize some of these properties.

Table 4: Income Distribution

	Share of Income (%)				
	Income Quintiles				
	0-20%	20-40%	40-60%	60-80%	80-100%
Data	3	6.5	10.9	18.1	61.4
Model	0.45	3.53	11.17	30.96	53.89

Table 5: Age Distribution

	Age Share			
	20-40	40-60	60-80	80-100
Data	0.36	0.34	0.25	0.05
Model	0.36	0.34	0.23	0.07

Table 6: Health Status by Education

	Education			
	Data		Model	
	Non College	College	Non College	College
Good	0.32	0.53	0.21	0.28
Fair	0.55	0.42	0.55	0.55
Poor	0.13	0.05	0.24	0.17

Covid Economics 13, 4 May 2020: 71-90

As discussed earlier, we shock the U.S. economy with COVID-19 in the first transition period. In order to disentangle the behavioral response of the households to the shock from other general equilibrium effects, we keep wage, interest rate, taxes, Social Security benefit levels, need based government transfers and accidental bequests fixed at baseline transition levels. In the first set of experiments, we examine different mitigation measures in a calibration that is designed to mimic the current projections for the U.S. economy. In Section 4.3 we analyze the impact of the disease on population health and economic outcomes without any mitigation measures from the government to contain the virus. These cases correspond to an $R_0 = 3.1$ and 2.2 respectively.

4.1 Different Mitigation Measures

In this section, we analyze the economic impact of different mitigation measures, keeping infection rate the same. Specifically, we experiment with different ways of implementing the lockdown under the low infection scenario ($R_0 = 1.23$). In the first case, we implement the lockdown by randomly quarantining 12.5% of the population. In the second case, we quarantine only the older population (73 and older).[12] Finally, in the third case, we quarantine agents based on their health status. Specifically, we impose the lockdown on all individuals in the *bad* health state and those 80 and older and in *fair* health state. It is not surprising that we find the largest economic declines under the first scenario. This is primarily due to the fact that indiscriminate lockdown prevents the healthy and highly productive members of the economy from contributing to the economic activity. On the other hand, quarantining the unhealthy/older individuals with low/zero labor productivity, while maintaining the same infection rate, hurts economic output substantially less.[13] As can be seen from Figure 2, output declines by 13% under random lockdown as opposed to 1.8% where lockdown is based on health status. The decline in output when the elderly are quarantined (Case 2) is much smaller (0.6%) and is solely due to the decline in effective hours worked by the infected working age population. The decline in hours worked in Case 2 is primarily due to some of the working age agents deciding to lower their work hours while infected. In Case 3, there is an additional decline in hours due to some of the agents in *bad* health status to be ordered to stay home as a part of the mitigation measure. Naturally, in case 1, the additional decline in hours is due to a large fraction of the population being ordered to stay home. Both wealth and consumption declines, in the periods of and following the infection, are the highest is the first case as well due to reduced earnings of the productive working-age population.

[12]Note that quarantining any fraction of the retirees (those 65 and older) will result in the same economic outcome. However, we report the lockdown for 73 and older for the sake of keeping the quarantine rate fixed at 12.5% across all experiments. While our assumption of 65 and over being retired underestimates the contributions of that age group to economic output, the labor force participation rate of 73 and over is relatively small in the data.

[13]We assume that quarantining different sub-groups (while keeping the number the same) will result in the same infection rate. In practice, the rate of spread of infection can differ depending on who is quarantined under the lockdown.

Covid Economics 13, 4 May 2020: 71-90

Covid Economics 13, 4 May 2020: 71-90

Figure 2: Experiments – Different Mitigation Methods

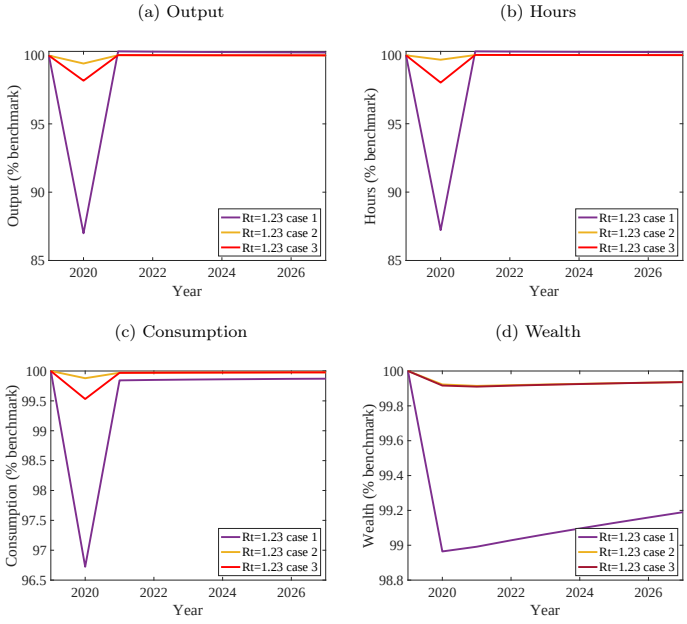

Note: All variables are normalized by their baseline levels to reflect the changes under each experiment relative to baseline transitions.

Figure 3 shows the changes in macroeconomic aggregates by different age and education groups of the productive workforce. The *young* refers to those 20 to 49 years and the *old* refers to those 50 to 64 years old. In these graphs, we first note that contrary to the *old*, the macroeconomic aggregates of the *young* under cases 2 and 3 are exactly identical. This is mainly due to the fact that health starts declining after age 50 in the model, as a result the quarantine based on health or age affect them in the same way — though decline in productivity due to infection. A second interesting observation is that while consumption declines between non-college and college graduates are somewhat similar (4.2 and 4.8% respectively for the young under case 1 for instance), declines in aggregate wealth are somewhat more disparate (1.6 and 2.4% respectively). This is due to the fact that the flat PA amount (25% of average national baseline earnings) corresponds to an income shock of varying magnitudes for different sub-groups in the model. For instance, among the lowest productivity workers, PA for those with a college degree is roughly 55% lower than their baseline earnings and only 32% lower for the non-college group. Finally, somewhat related to the previous point, we find that the aggregate wealth of the non-college old under the health experiment suffers the smallest decline (refer

to figure 3f) due to somewhat generous PA amounts for this group. We discuss the heterogenous response of individuals towards these different mitigation measures and pandemic assistance in more detail in the next section.

Figure 3: Experiments – Different Mitigation Methods (Age and Human Capital)

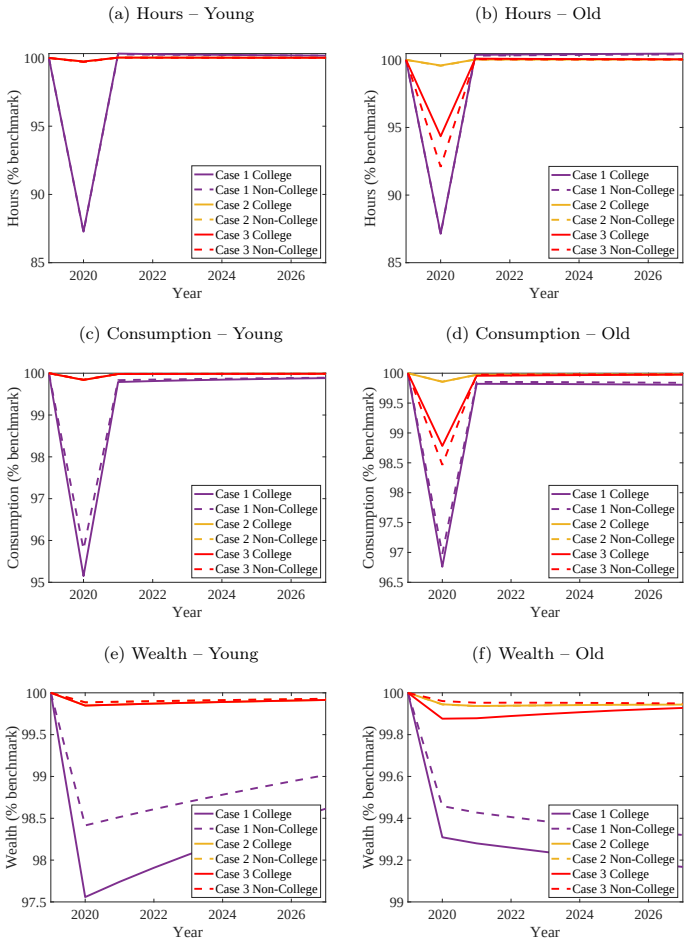

Note: All variables are normalized by their baseline levels to reflect the changes under each experiment relative to baseline transitions.

Covid Economics 13, 4 May 2020: 71-90

Note that we have assumed that under all these experiments, infection rates would stay the same (6.1%). Of course, it is not obvious if in reality these three cases would lead to the same infection or fatality rates. On the one hand, the elderly and those in bad health states are the most vulnerable to this pandemic. Stay home policies specifically geared towards them may help reduce the risks they face. On the other hand, some of the current mitigation measures are directed at reducing the interactions between people and may prove more effective in reducing the spread of the diseases. There certainly is not enough evidence to help pin down the effectiveness of different mitigation measures in reducing the spread of the diseases at the moment. However, it is possible to have a rough idea about how much higher the infection rate would have to be for the economic outcomes in these three cases to be the same. For example, in the case where quarantine applies to the elderly only, the infection rate would have to increase from 6.1% to almost to the entire working age individuals for output to decline 13% as it does under the random lockdown case. Moreover, while the infection rate might be higher under Cases 2 and 3, fatality rate might not be if the elderly and the unhealthy do follow the stay home recommendations.

4.2 Response to Pandemic Assistance

In all our experiments with some mitigation measure in place, we assume that the government provides pandemic assistance to the fraction of the population affected by the lockdown. This aid is set at 25% of average national baseline income for all. As a result, we find interesting heterogeneity in the impact of the lockdown on different sub-groups. First note that flat PA amounts corresponds to an income shock of varying magnitudes for different health, productivity and education type in the model. For instance, for those in the lowest productivity group and without a college degree, PA is 31.7% lower than their baseline earnings. At the same time, for those with a college degree and on top of the productivity distribution, PA is 89.2% lower.

Figure 4 shows macroeconomic aggregates by the idiosyncratic productivity and health levels of the workers relative to the baseline in the random lockdown case. We find that while the decline in hours remains the same for each group, wealth and consumption changes differ significantly. For instance, aggregate consumption drops by roughly 4.8% for the highest productivity group in the best health state and only 0.09% for those in the lowest productivity and worst health group. Analogously, we find that wealth of the former group decreases by 2.1% and of the latter increases by 0.26%. This is mainly due to the fact that PA turns out to be quite generous for the latter group – roughly 200% higher than their baseline earnings. At the same time, for those in the best health and highest productivity level, PA is 87.6% lower.

Covid Economics 13, 4 May 2020: 71-90

CEPR PRESS

Figure 4: Experiments – Aggregates by Labor Productivity and Health

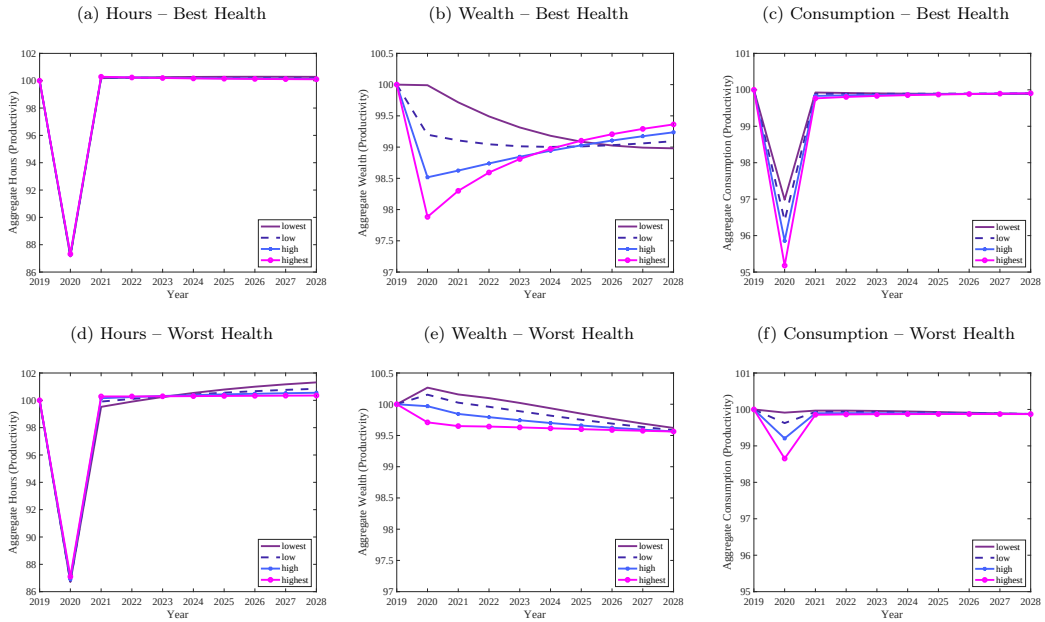

Note: All variables are normalized by their baseline levels to reflect the changes under each experiment relative to baseline transitions.

4.3 Different Infection Rates

Figure 5 shows the time paths of various macroeconomic variables, now under different infection rates. In the first transition period (2020) when the shock hits the economy, there are large economic declines under each scenario. For instance, output drops by roughly 10 and 8 percent in the no mitigation scenarios corresponding to $R_t = 3.1$ and 2.2 respectively as compared to 13% percent in the mitigation scenario discussed above. While the decline in output in the former two cases is driven primarily by loss in worker productivity due to widespread infection levels, decline in the latter scenario is due to the interruption of economic activity due to the lockdown.

Note that while the impact of the shock on output lasts for a single period it persists for roughly twenty periods for consumption and aggregate wealth. This holds true in the model for two reasons. First, in the period of the shock, individuals draw down their wealth due to reduced earnings in all three cases. However, the period after the shock sees a big decline in aggregate wealth/consumption in the no-mitigation cases due

Covid Economics 13, 4 May 2020: 71-90

CEPR PRESS

to large scale deaths. A fraction of infected individuals die in the next period with positive wealth which does not get distributed back into the economy. Second, our assumption of fixed baseline interest rate implies a small open economy where capital moves freely. As a result, reduction in aggregate wealth does not result in further reductions in output.

Figure 5: Experiments – Aggregates

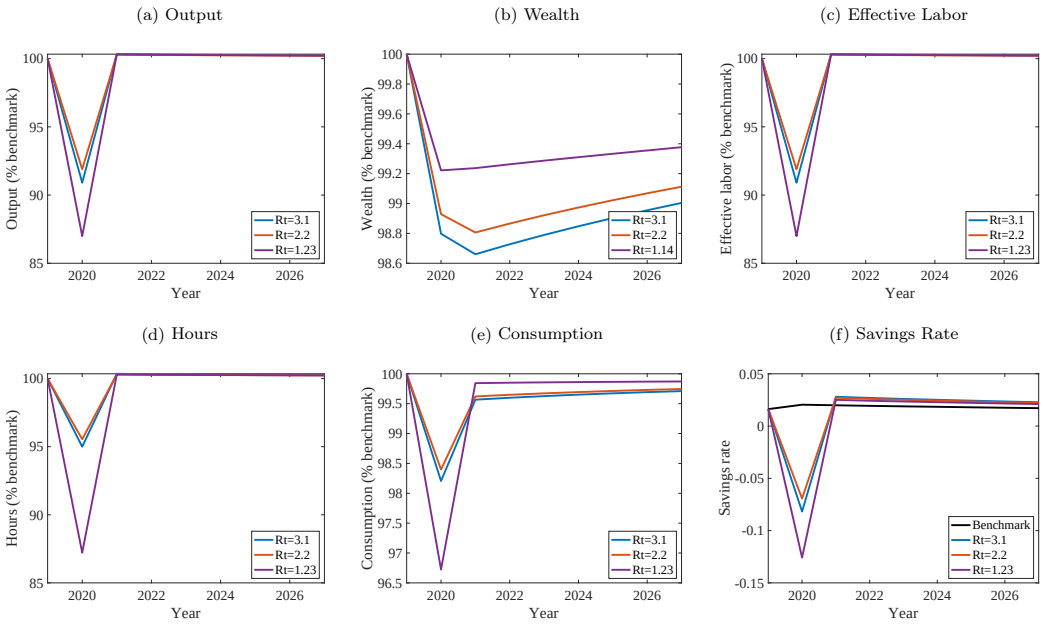

Note: All variables are normalized by their baseline levels to reflect the changes under each experiment relative to baseline transitions.

It should be noted that the reduction in output in figure 5a does not take into account the cost of widespread infection to public health – value of lives lost to the disease. One way to incorporate the impact of the lives lost is to adjust the decline in output for the value of statistical lives (VSL) lost under each case. We use the age-specific estimates of VSL from Aldy and Viscusi 2008 to adjust the decline in output with the value of lives lost in each infection scenario.[14] The dashed lines in Figure 6 show the decline in output after adjusting for the VSL lost due to the disease. It is no surprise that after accounting for the high death rates under the no-mitigation scenario, output declines in the no-mitigation cases supersede that

[14]The authors provide estimates for ages 20 to 62. We assume that VSL of a 62 year old applies to the group 63-65. We further assume that people older than 65 have a VSL of $1 million.

Covid Economics 13, 4 May 2020: 71-90

of the mitigation case.

Figure 6: Adjusting for Value of Statistical Life

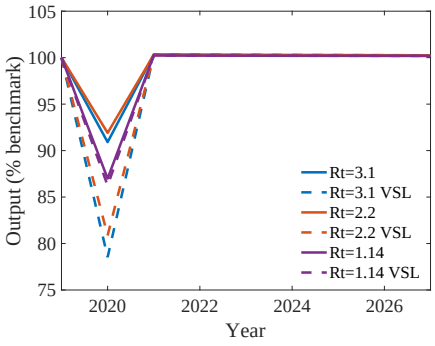

5 Conclusions

Efforts to mitigate the spread of COVID-19 in the U.S. have included closing businesses that are deemed unessential. This has resulted in more than 26 million initial unemployment insurance claims in five weeks. Without large scale testing of the population, it is not clear how the economic activity may resume. In this paper, we show significant differences in the economic consequences of who to quarantine during this pandemic. We find that stay-at-home recommendations that are based on health and age reduce the economic severity of the pandemic by 10% of GDP under very conservative estimates. Going forward, it may be possible to introduce subsides to the elderly or those with underlying health conditions to self-isolate until a vaccine or a cure is available. The fiscal consequences of either of these policies is likely to be much lower that what is currently spent on providing unemployment insurance to a large fraction of the working age population.

Covid Economics 13, 4 May 2020: 71-90

References

Aldy, Joseph E and W. Kip Viscusi (2008). "Adjusting the Value of a Statistical Life for Age and Cohort Effects". In: *The Review of Economics and Statistics* 90.3, pp. 573–581.

Atkeson, Andrew (2020). *What Will Be the Economic Impact of COVID-19 in the US? Rough Estimates of Disease Scenarios*. Tech. rep. National Bureau of Economic Research.

Conesa, Juan Carlos, Daniela Costa, et al. (2018). "Macroeconomic effects of Medicare". In: *The Journal of the Economics of Ageing* 11, pp. 27–40.

Conesa, Juan Carlos, Timothy J Kehoe, et al. (2020). "Implications of increasing college attainment for aging in general equilibrium". In: *European Economic Review* 122, p. 103363.

Fauci, Anthony S, H Clifford Lane, and Robert R Redfield (2020). *Covid-19? Navigating the uncharted*.

Fuster, Luisa, Ayşe İmrohoroğlu, and Selahattin İmrohoroğlu (2007). "Elimination of social security in a dynastic framework". In: *The Review of Economic Studies* 74.1, pp. 113–145.

Riou, Julien et al. (2020). "Adjusted age-specific case fatality ratio during the COVID-19 epidemic in Hubei, China, January and February 2020". In: *medRxiv*.

UN (2019). *World Population Prospects: The 2019 Revision*. New York: United Nations, Department of Economic and Social Affairs, Population Division.

Wang, Huwen et al. (2020). "Phase-adjusted estimation of the number of Coronavirus Disease 2019 cases in Wuhan, China". In: *Cell Discovery* 6.1, pp. 1–8.

Covid Economics 13, 4 May 2020: 71-90

Covid Economics Issue 13, 4 May 2020

Volatility, dark trading and market quality: Evidence from the 2020 COVID-19 pandemic-driven market volatility[1]

Gbenga Ibikunle[2] and Khaladdin Rzayev[3]

Date submitted: 27 April 2020; **Date accepted:** 28 April 2020

We exploit the exogenous shock of the COVID-19 pandemic on financial markets and regulatory restrictions on dark trading to investigate how volatility drives dark market share and trader venue selection. We find that, consistent with theory, excessive volatility on lit exchanges is linked with an economically significant loss of market share by dark pools to lit exchanges. The dynamics of market share loss are driven by the cross-migration of informed and uninformed traders between lit and dark venues. Informed traders migrate from lit venues to dark venues when lit venues' volatility becomes excessive, while uninformed traders, wary of the presence of informed traders in dark pools, shift their trading to lit exchanges rather than delay trading in a volatile market environment. The market quality implications of the cross-migration are mixed: while it improves liquidity on the lit exchange, it results in a loss of informational efficiency.

1 The support of the Economic and Social Research Council (ESRC) in funding the Systemic Risk Centre is gratefully acknowledged [grant numbers ES/K002309/1 and ES/R009724/1]. Rzayev gratefully acknowledges the support of the Trans-Atlantic Platform by the Economic and Social Research Council (ESRC) [grant number ES/R004021/1].

2 Senior Lecturer in Financial Markets and Director, University of Edinburgh Business School.
3 Research Officer, Systemic Risk Centre, LSE.

Covid Economics 13, 4 May 2020: 91-137

Covid Economics 13, 4 May 2020: 91-137

1. Introduction

At the heart of the debate on the effects of trading in non-transparent downstairs-type markets – the so-called dark pools – are the dynamics of venue selection[1] by both informed and uninformed traders. Theory suggests that dark trading dynamics are driven by volatility in the lit market (see Zhu, 2014); however, the endogenous determination of volatility makes it challenging to test this prediction. In this paper, we avoid this empirical issue by exploiting the novel coronavirus (COVID-19) crisis as an excess market volatility-inducing exogenous event to investigate the role of volatility in venue selection by informed and uninformed traders in today's financial markets. Understanding the dynamics of venue selection is critical for the determination of the effects of dark trading on market quality characteristics, especially as the volume of trading activity credited to dark pools continues to reach new levels around the world. For example, the volume of trading executed in dark pools accounted for 9.1% and 9.6% of all on-exchange activity in April and July 2019, respectively. These are the largest shares in the MiFID II era, which already imposes an 8% cap on dark trading in European financial markets over any 12-month period.[2] Furthermore, in the US, dark pools and other off-exchange trading venues executed 38.6% of US equity volume in April 2019.[3]

Indeed, the less than adequate understanding of dark trading dynamics in an empirical sense may be driving the mixed evidence on the impact of dark trading on market quality characteristics. For example, Buti *et al.* (2011) find no supporting evidence that dark trading is harmful to market liquidity. Based on their analyses of FTSE data, Aquilina *et al.* (2017) and Brugler (2015) show that dark trading leads to improved liquidity in the aggregate and the primary exchange respectively. However, Nimalendran and Ray (2014) investigate trading data

[1] Reference to traders' venue selection or choice implies their preference between dark and lit venues.
[2] https://www.thetradenews.com/dark-pool-trading-volumes-surge-pre-mifid-ii-levels/ and https://www.thetradenews.com/dark-trading-volumes-reach-highest-level-mifid-ii/
[3] https://www.wsj.com/articles/dark-pools-draw-more-trading-amid-low-volatility-11556886916

from one of the 32 US dark venues and find that dark trading is associated with increased price impact on quoting exchanges. This is consistent with the findings of Degryse *et al.* (2015); using data from the Dutch market, they show that dark trading has a detrimental effect on market liquidity. Adding complexity to the question is the increasingly popular view that the effects of dark trading on market quality characteristics are non-linear (see Comerton-Forde & Putniņš 2015; Aquilina *et al.* 2017).

Zhu (2014) is increasingly recognised as one of the influential theoretical contributions on dark trading. Zhu's (2014) model predicts a non-linear relationship between volatility and dark market share; specifically, for sufficiently small volatility, dark market share increases with volatility. However, for an excessive level of volatility, dark market share decreases with volatility. In the model, the addition of a dark pool to a market with a lit exchange results in an asymetric self selection involving informed and uninformed traders. Specifically, uninfomed traders gravitate towards the dark pool because they face lower adverse selection risk there, while infomed traders concentrate on the lit exchange due to the higher probability of non-execution they face in the dark pool, since their orders typically bunch on one end of the limit order book. This self selection is linked to an improvement in informational efficiency in the aggregate market, comprising of the lit exchange and the dark pool (see Aquilina *et al.* 2017). If all informed traders hold similar types of information sets (for example, fundamental information about the value of an instrument) as modelled by Zhu (2014), the self-selection induced by dark trading can improve the efficiency of the price discovery process. This is because a reduction in the number of informed trades due to fewer uninformed traders in the lit market (informed orders execute against uninformed orders as in Glosten & Milgrom 1985; Kyle 1985 and many others) results in a lowering of competition on the same private information set held by informed traders.

Covid Economics 13, 4 May 2020: 91-137

Covid Economics 13, 4 May 2020: 91-137

Zhu's (2014) model establishes volatility as a key driver in the overall dynamics of self-selection. As informed trader concentration increases in the lit market, volatility widens the exchange spread and encourages more uninformed (liquidity) traders to migrate to the dark pool – this is the natural state of things when volatility is moderate. Informed traders stay at the lit exchange because when volatility is at a moderate level, the exchange spread is not excessive, and thus the cost of execution risk is greater than the benefit of potential price improvements a dark pool may offer (for example, in Australia and Canada, price improvement is required to trade regular sizes in dark pools).[4] However, when volatility in the exchange exceeds the maximum level needed for informed traders to avoid the dark pool, informed traders start to migrate to the dark pool in search of uninformed counterparties to trade with and in a bid to avoid the widening exchange spread. Thus, liquidity constraints in the lit market can result in informed traders entering into non-transparent/dark venues in order to reduce their transaction costs and increase their profits, as already reported by some empirical studies (see Hendershott & Mendelson 2000; Nimalendran & Ray 2014). The informed traders' migration consequently results in uninformed traders leaving the erstwhile safety of the dark pool for the lit exchange.

Two studies have empirically examined the links between volatility and dark trading.[5] Buti *et al.* (2011) find that dark market share is higher on days with lower volatility, and Ye (2010) finds that stocks with lower volatility have higher dark market shares. Our study differs from Buti *et al.* (2011) and Ye (2010) for at least two reasons. Firstly, our motivation differs from the aforementioned studies. Specifically, Buti *et al.*'s (2011) motivation is investigating the effects of dark trading on market quality, and Ye (2010) aims to study transaction costs in crossing networks and the competition between exchanges and crossing networks. However, we focus on the role of volatility in traders' venue choice in times of stress. As already

[4] See https://www.cfainstitute.org/-/media/documents/issue-brief/policy-brief-trade-at-rules.ashx.
[5] At least one other study examines the effects of dark trading on volatility (see Foley *et al.* 2012) but not vice versa.

Covid Economics 13, 4 May 2020: 91-137

discussed, an important motivation for addressing this question is offered by Zhu (2014). Specifically, Zhu (2014) shows that the relationship between volatility and venue choice is not linear, and while the impact of lit market volatility on dark market share is positive for sufficiently low levels of volatility, it becomes negative during excessive volatility/market stress periods. Secondly, the general endogenous determination of volatility makes it challenging to disentangle whether volatility informs the self-selection dynamics often reported in the finance media.[6] Although Buti *et al.* (2011) and Ye (2010) employ an instrumental variable approach to address endogeneity, further questions regarding the effectiveness of this approach remain.[7] One issue is that the two studies only introduce instruments for dark market activity, since their focus is not the investigation of the effects of volatility on traders' venue choice. Addressing this methodological challenge requires the identification of a truly exogenous volatility-inducing shock event. Hence, by contrast, we employ the onset of the COVID-19 pandemic impact on financial markets, which is clearly exogeneous and is not driven by any market determinants, for this purpose. The exogenous event we use in this study is driven by the spread of a virus that arguably has no comprehension of modern market structures nor directly responds to them.

For clarity, we exploit both the excessive volatility-inducing COVID-19 pandemic, as a shock, and the Markets in Financial Instruments Directive II (MiFID II) double volume cap (DVC) dark trading restrictions in force in the case of 55 European stocks during our sample period, to investigate the role of volatility in the evolution of dark market share and the decision of where to trade in the cases of informed and uninformed traders. We find that, consistent with the theoretical literature (see Zhu 2014), excessive volatility at lit venues is linked with the

[6] See as examples, https://www.wsj.com/articles/dark-pools-draw-more-trading-amid-low-volatility-11556886916 and https://blogs.wsj.com/marketbeat/2011/09/02/investors-flee-dark-pools-as-market-volatility-erupts/

[7] Buti *et al.* (2011) employ the method developed by Hasbrouck and Saar (2013) and use other stocks' dark trading activity during the same time period as an instrument for dark trading activity in a particular stock. Ye (2010) uses the total trading volume as an instrument for total number of shares submitted to a crossing network.

economically significant shift of informed trading activity from lit venues to dark pools. We also show that this move by informed traders drives the migration of uninformed traders, who are wary of being adversely selected, from dark pools to lit venues. The net effect of the cross-migration is a loss of market share by dark pools and an increase in lit venues' market share. We extend our analysis to examine the effects of these dynamics on market quality, and find that lit market liquidity improves (i.e. spreads narrow) during the volatile trading period, while price discovery deteriorates on account of informed traders migrating to the dark pools. Thus, it appears that volatility is a market regulating mechanism driving the share of trading activity in dark pools. Regulators should account for this when designing regulatory mechanisms, such as dark trading caps and waivers.

2. Institutional background

The enactment of the Markets in Financial Instruments Directive (MiFID) in November 2007 introduced alternative high-tech trading venues known as multilateral trading platforms (MTFs). MTFs operate as intermediaries facilitating the exchange of financial instruments between a number of market participants. Concurrently, under MiFID, pre-trade and post-trade transparency requirements are imposed on all trading venues in order to reduce potential adverse selection costs linked to market fragmentation. However, MiFID also offers pre-trade transparency waivers to certain types of orders. These pre-trade transparency waivers include (1) reference price waivers (RPW); (2) negotiated trade waivers (NTW); (3) large in scale (LIS) and (4) order management facilities (OMF). RPW applies to trading systems that match trading at the midpoint current bid and ask price. NTW allows two parties to formalise negotiated transactions. LIS offers block traders the right to hide their trading intention when transaction size is larger than the prevailing normal market size. OMF allows orders to be held by exchanges in an order management facility pending disclosure.

Covid Economics 13, 4 May 2020: 91-137

Covid Economics 13, 4 May 2020: 91-137

Since the commencement of MiFID, trades in dark pools operated by MTFs have benefited mainly from RPW and LIS. Pre-trade opacity and midpoint execution help fund managers to protect their trading intention and reduce transaction costs. However, European regulators, concerned by the potential negative influence of dark liquidity on the price discovery process, enacted a second iteration of MiFID, the so-called MiFID II, and the Market in Financial Instruments Regulation (MiFIR), published in June 2014. An important goal of MiFID II and MiFIR is to secure a high level of market transparency and fairness. As a result, DVC was introduced to curb dark trading and force more trades to be executed on lit venues. DVC dictates that the venue and aggregate market trading limits for each instrument are 4% and 8%, respectively. If the DVC is triggered in an instrument, then dark trading in that instrument will subsequently be suspended for 6 months. The DVC is calculated for each affected instrument on a daily rolling basis and relates to average daily trading volume over the preceding 12-month period. According to the first DVC-related data published in March 2018 by the European Securities and Markets Authority (ESMA), a total of 744 and 643 instruments breached at least one of the caps in January and February 2018 respectively, and were therefore subjected to six-month trading suspensions from 12th March 2018. As of September 2018, six months after the implementation of the DVC, more than 1200 instruments, mainly equities, were under dark trading suspensions. The affected instruments corresponded to about 35% of the most liquid European stocks. For our sample period, spanning 24th January and 24th March 2020, ESMA data shows that 62 instruments'[8] (55 out of which are European stocks) are under DVC dark trading suspensions; their suspensions are from 14th November 2019 until 13th May 2020.

It is worth noting that an enforcement of the DVC in a stock does not fully preclude some form of dark trading in the stock. Large block trades are still allowed to trade in dark

[8] https://www.esma.europa.eu/double-volume-cap-mechanism

pools if the trade size is large enough to qualify for the LIS waiver. The LIS wavier threshold is based on the average daily volume (ADV) for each instrument. For small-cap stocks with ADV of less than €50,000, the LIS waiver threshold is €15,000 and for large-cap stocks with ADVs greater than €100 million, the LIS waiver threshold can be up to €650,000. In any case, market data shows that the dark trading volumes recorded once the DVC is enforced for a stock is zero to negligible.

3. Sample selection and variables

3.1. Sample Selection

Investigating the role of volatility in venue choice is challenging because of the often-endogenous determination of volatility by the venue selection decisions taken by both informed and uninformed traders. For example, uninformed traders deciding to migrate from lit to dark venues will induce volatility on the lit exchange; if the volatility level rises enough, it will force informed traders to move to dark venues in search of liquidity. In addition, it is also very likely that the venue choice process and volatility are determined by common factors, some of which cannot be observed directly. The above issues make identifying a volatility-inducing exogenous shock useful in being able to adequately estimate the impact of volatility on venue choice. Such a shock should satisfy two important criteria: 1) it should have an impact on volatility and 2) it should not be determined by market conditions of dark pool trading. We argue that the market crisis induced by the spreading of COVID-19 is a potential candidate that satisfies these two criteria. Firstly, Baker *et al.* (2020) show that indeed stock market volatility in global markets increases significantly during this period. Secondly, it is obvious that the crisis caused by the pandemic has no direct connection to dark trading, or to any organised trading in financial markets for that matter – the virus is unaware of the existence of market structures. Motivated by this, we investigate the effects of stock price volatility on traders' venue choice by employing

Covid Economics 13, 4 May 2020: 91-137

COVID-19-induced volatility within a natural experimental difference-in-differences (DiD) framework. Our data covers a two-month period from 24th January to 24th March 2020, spanning the period prior to and the period defined by the market crisis occasioned by the rapid spreading of COVID-19. This is because Baker *et al.* (2020) show that the COVID-19-induced excessive volatility in global markets started on 24th February 2020, when the virus started to quickly spread in the US and Europe.

Employing a DiD framework requires the identification of control and treated groups of stocks. Since we study the dynamics of venue choice between dark and lit venues, our treated group includes stocks that trade on both dark and lit venues. By contrast, the control group of stocks are restricted from trading on dark venues during our sample period; this is due to the imposition of a dark trading cap under the MiFID II provisions. This approach allows us to isolate the impact of COVID-19-induced volatility on trading activity in stocks eligible for dark trading from its market-wide effects, and is only possible because of the identification of stocks with dark trading restrictions. The implementation of the DVC creates a very good opportunity to identify our control group of stocks. Specifically, the stocks with suspended dark trading privileges during our sample are ideal candidates for the control group. Thus, we select the 55 European equities serving dark trading suspensions between 14th November 2019 and 13th May 2020, a period inclusive of our sample period (24th January to 24th March 2020).

We use the method described in Shkilko and Sokolov (2020) to create a matched treated sample of stocks; hence, our total sample size equals 110 European stocks. Specifically, we compute the matching error for three metrics commonly used for this purpose: size, price and volume. Then, the 55 stocks with the corresponding lower matching errors for each of the 55 stocks in the control group are included in the treated group. The method works well, because our key metrics do not differ economically and statistically between groups.

Covid Economics 13, 4 May 2020: 91-137

Covid Economics 13, 4 May 2020: 91-137

3.2. Variable construction

For every stock in the treated and control groups, we obtain intraday data from the Thomson Reuters Tick History (TRTH) v2 database. We collect data from the main venues where our selected stocks are traded: 1) the main market where stocks are listed (for example, London Stock Exchange (LSE) for the UK stocks, Xetra for the German stocks, etc.); 2) Cboe Europe, which hosts the most liquid pan-European limit order books and dark pools, including BXE and CXE; and 3) Turquoise, hosting one of the most liquid dark pools in Europe, Turquoise Plato (formerly Turquoise Midpoint Dark). According to market data from Cboe Europe, the venues included in our dataset account for a daily minimum of 93% of the currency trading value for the stocks in our sample; hence, our data is representative in the cases of the stocks in the sample. The dataset contains standard transaction-level variables such as date, exchange time, transaction price, volume, bid price, ask price, bid size and ask size. Using the obtained dataset, we compute daily estimates of trading activity, liquidity, order imbalance, high-frequency trading (HFT) and volatility.

As stated, the main aim of this study is to examine the dynamics of traders' venue selection. We proxy venue choice by using dark market share and trading volume in lit markets, because they embody aggregate trader venue selection. The dark market share, $DMS_{i,d}$, is computed as the dark trading volume divided by the total trading volume for stock i on day d. Trading volume, $Volume_{i,d}$, is the number of shares traded in lit venues for stock i on day d.[9] Within our framework, we aim to control for general market dynamics by including a number of relevant variables. We measure liquidity using relative quoted spread ($Rspread_{i,d}$) and depth ($Depth_{i,d}$). $Rspread_{i,d}$ is the relative quoted spread for stock i on day d and is computed as a time-weighted average of the difference between ask and bid prices divided by the mid-price

[9] Throughout this paper, trading volume refers to trading volume in lit markets. Trading volume in dark markets is stated as dark trading volume.

(mid-price is the average of ask and bid prices) corresponding to each transaction. $Depth_{i,d}$ is the top-of-book depth and computed as the natural logarithm of the sum of the best bid and ask sizes corresponding to each transaction for stock *i* on day *d*.

$Volatility_{i,d}$ is a proxy for volatility and computed as the standard deviation of hourly mid-price returns for stock *i* on day *d* (see Malceniece *et al.* 2019). $OIB_{i,d}$ is the order imbalance metric described in Chordia *et al.* (2008) and is computed as the absolute value of the buyer-initiated volume minus the number of seller-initiated volume divided by total volume stock *i* on day *d*. $HFT_{i,d}$ is the proxy for HFT and computed as the number of messages divided by the number of transactions for stock *i* on day *d* (see Malceniece *et al.* 2019). Table 1 provides an overview of the different variables used in this paper.

Table 1. Variable definitions

This table defines the variables used in this study. *Unit* is the unit of measurement; *Market* is the market for which a variable is computed; and *Definition* provides a short definition and computation method.

Variable	Unit	Market	Definition
$DMS_{i,d}$	%	Dark, Lit	Dark market share; computed as dark trading volume divided by the total trading volume for stock *i* on day *d*
$Volume_{i,d}$	Millions	Lit	Number of shares traded in stock *i* on day *d*
$Rspread_{i,d}$	bps	Lit	Relative quoted spread for stock *i* on day *d*; computed as a time-weighted average of the difference between ask and bid prices divided by the mid-price (mid-price is the average of ask and bid prices) corresponding to each transaction
$Depth_{i,d}$	ln	Lit	The top-of-book depth; computed as the natural logarithm of the sum of the best bid and ask sizes for stock *i* on day *d*.
$Volatility_{i,d}$		Lit	A proxy for volatility; computed as a standard deviation of hourly mid-price returns for stock *i* on day *d*
$OIB_{i,d}$		Lit	Order imbalance defined in Chordia *et al.* (2008); computed as the absolute value of the buyer-initiated volume minus the number of seller-initiated volume divided by total volume stock *i* on day *d*

Covid Economics 13, 4 May 2020: 91-137

$HFT_{i,d}$	Lit	A proxy for HFT and computed as the number of messages divided by the number of transactions for stock *i* on day *d*

3.3. Descriptive Statistics

Table 2 provides descriptive statistics for the 110 stocks, i.e. 55 treated and 55 control stocks, in the sample. Panel A reports summary statistics for the pre-event period (from 24th January 2020 to 23rd February 2020), whereas Panel B presents summary statistics for the post-event period (from 24th February 2020 to 24th March 2020). In both panels, we provide statistics for the treated and control groups of stocks separately and compute the statistical differences in our model variables in order to observe the differences in market dynamics for these groups; standard errors of the mean estimates are used for statistical inferences.

Table 2. Descriptive statistics

This table contains the pre- (Panel A) and event (Panel B) periods stock-day mean and standard deviation estimates for variables using data for 55 European stocks that could be traded at both lit and dark venues, i.e. treated stocks, and for 55 European stocks with dark venue restrictions, i.e. control stocks. The final column presents the t-statistics of two-sample t-tests of differences between the treated group's and the control group's variables. $DMS_{i,d}$ is the dark market share and is computed as the dark trading volume divided by the total trading volume for stock *i* on day *d*, $Volume_{i,d}$ is the number of shares traded for stock *i* on day *d*, $Rspread_{i,d}$ is the relative quoted spread for stock *i* on day *d* and is computed as a time-weighted average of the difference between ask and bid prices divided by the mid-price (mid-price is the average of ask and bid prices) corresponding to each transaction, $Depth_{i,d}$ is the top-of-book depth and is computed as the natural logarithm of the sum of the best bid and ask sizes for stock *i* on day *d*, $Volatility_{i,d}$ is a proxy for volatility and is computed as the standard deviation of hourly mid-price returns for stock *i* on day *d*, $OIB_{i,d}$ is the order imbalance for stock *i* on day *d* and is computed as the absolute value of the buyer-initiated volume minus the number of seller-initiated volume divided by the total volume of stock *i* on day *d*, $HFT_{i,d}$ is a proxy for HFT and is computed as the number of messages divided by the number of transactions for stock *i* on day *d*. The sample period is from 24th January to 24th March 2020. The event start date is 24th February 2020, when the COVID-19-induced excessive volatility is adjudged to have commenced in global financial markets. *, ** and *** correspond to statistical significance at the 0.10, 0.05 and 0.01 levels respectively.

Panel A. Pre-event period

Variable	Treated group		Control group		Difference between means (*t*-statistic)
	Mean	Std. dev	Mean	Std. dev	Treated - control
$DMS_{i,d}$	2.5%	0.023	0.009%	0.001	2.45%*** (37.69)

Covid Economics 13, 4 May 2020: 91-137

$Volume_{i,d}$	1.328	0.261	1.332	0.109	-0.004 (-0.491)
$Rspread_{i,d}$	61.142	7.813	61.386	5.231	-0.244 (-0.902)
$Depth_{i,d}$	13.778	1.305	13.724	0.464	0.054 (1.356)
$Volatility_{i,d}$	0.0151	0.002	0.0152	0.001	-0.0001 (-1.551)
$OIB_{i,d}$	0.321	0.091	0.325	0.013	-0.004 (-1.513)
$HFT_{i,d}$	17.704	6.752	17.931	2.315	-0.227 (-1.106)

Panel B. Event period

Variable	Treated group		Control group		Difference between means (t-statistic)
	Mean	Std. dev	Mean	Std. dev	Treated - Control
$DMS_{i,d}$	2.1%	0.029	0.009%	0.002	2.095%*** (25.071)
$Volume_{i,d}$	3.275	4.115	2.874	2.631	0.401*** (2.855)
$Rspread_{i,d}$	87.952	11.146	94.253	7.705	-6.301*** (-16.176)
$Depth_{i,d}$	14.840	1.331	14.394	0.493	0.446*** (10.930)
$Volatility_{i,d}$	0.0338	0.004	0.0418	0.002	-0.008*** (-62.225)
$OIB_{i,d}$	0.337	0.107	0.394	0.022	-0.057*** (-18.151)
$HFT_{i,d}$	19.979	5.721	18.493	2.317	1.486*** (8.374)

Panel A shows that the stock-day averages of all variables between the two stock groups, with the exception of $DMS_{i,d}$, in the treated group are not statistically different from each other. This underscores the relevance of our matching procedure and evidences that both groups have similar market dynamics prior to the COVID-19-induced market volatility event. There are some important points to note when comparing the evolution of variables during the post-event periods. Firstly, as evident in Panel B, the average values of all variables change substantially during the post-event period, which indicates that market conditions are different after the onset of the COVID-19-induced market volatility event. For example, the average $Volume_{i,d}$ increases by 2.5 (2.2) times for the treated (control) group. Moreover, $Rspread_{i,d}$ widens by

Covid Economics 13, 4 May 2020: 91-137

more than 40% for both groups, indicating liquidity constraints. Secondly, while the average $Volume_{i,d}$ of the control group is marginally higher than the average $Volume_{i,d}$ of the treated group prior to the event, a substantial switch occurs following the onset of the excessive volatility period with the treated group's average $Volume_{i,d}$ suddenly outstripping the control group's by 14%. This is consistent with our argument that excessive volatility contributes to the market dynamics of stocks traded simultaneously on both dark and lit venues. The observed 16% decline in $DMS_{i,d}$ for the treated group of stocks suggests that some traders move to lit venues during excessive volatility periods. However, these traders could have also just exited the market altogether; we formally test this in the next section. Linked to the second point, thirdly, we also observe (in Panel B) statistically and economically significant differences in the estimated variables' values for both groups of stocks during the excessively volatile sample interval, thus evidencing the significance of the impact of the COVID-19-induced excessive volatility/instability on stock characteristics.

The findings presented in Table 2 raise an interesting question about why excessive market-wide volatility affects stocks differently depending on whether they are traded in a relatively unfettered manner in both dark and lit venues. We argue that this phenomenon is linked to dark venue trading availability. This is because when we compare the general market conditions (dark trading, liquidity, volatility, order-book dynamics and HFT activities) of the treated and control groups during the pre-event period, only $DMS_{i,d}$ differs significantly prior to the onset of excessively volatile trading conditions (see Panel A of Table 2). The significant (both economically and statistically) difference in $DMS_{i,d}$ is expected as the control group's stocks have been suspended from dark trading, whereas the treated group's stocks are available for trading in dark pools. This is further confirmed by the number of dark trading transactions in the treated and control groups during the sample period. Specifically, the treated group's stocks have a total of 223,438 transactions in dark pools, while this number is 142 for the control

Covid Economics 13, 4 May 2020: 91-137

group's stocks. Thus, relatively unrestricted trading in dark venues appears as a strong indicator of the post-event differences between the control and treated groups' market determinants. In the next section, we formally test our arguments driven from descriptive statistics analysis.

4. Analyses, results and discussions

4.1. Volatility analysis

The main limitation of the existing empirical papers reporting on the volatility-dark trading relationship (see as an example, Buti *et al.* 2011) is that they ignore the non-linear relationship predicted by Zhu (2014) and, in their frameworks, volatility is endogenously-determined. Excessive volatility and dark market share/venue choice are jointly endogenous as there may be a reverse causality between volatility and dark market share/venue choice. In order to address potential endogeneity concerns, we use the COVID-19-induced excessive volatility as an exogenous shock to investigate the relationship between excessive volatility and traders' venue choice. Baker *et al.* (2020) show that from 24th February to 24th March 2020, US financial markets were dramatically volatile. More explicitly, the authors find that there are 18 market jumps in these 22 trading days and this number is the highest in financial markets history. This finding is strong evidence of the excessive market volatility extensively reported in the media during these periods. Although Baker *et al.*'s (2020) analysis is based on the US financial markets, and we focus on European markets, the volatility trend is consistent as shown in Figure 1.

Covid Economics 13, 4 May 2020: 91-137

Covid Economics 13, 4 May 2020: 91-137

Figure 1. Volatility

The figure plots the day-by-day evolution of the cross-sectional average of $Volatility_{i,d}$ for 110 European stocks employed in the study. $Volatility_{i,d}$ is computed as the standard deviation of hourly mid-price returns for stock i on day d. The sample period covers from 24th January to 24th March 2020. The vertical bar indicates 24th February 2020, when the COVID-19-induced excessive volatility is adjudged to have commenced in global financial markets.

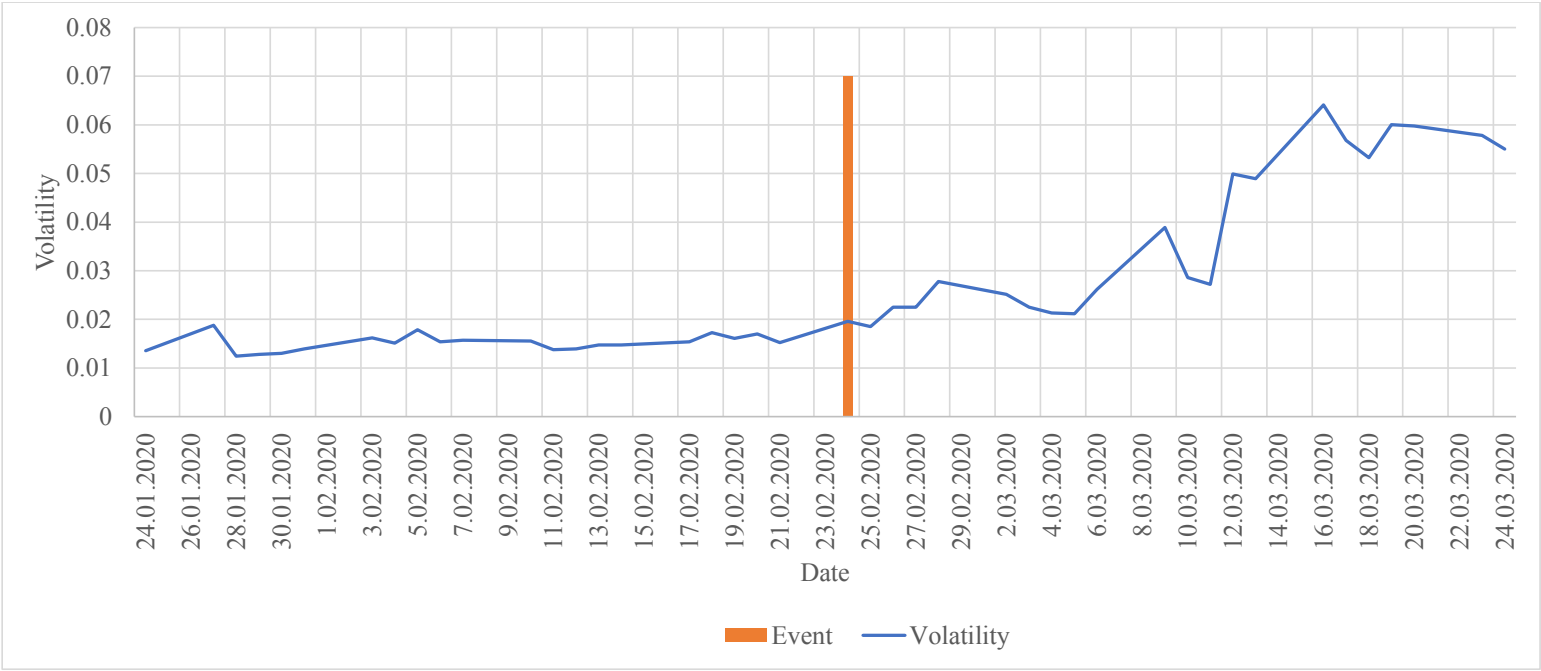

Figure 1 shows the impact of the COVID-19 pandemic on volatility in the 110 stocks in our sample. The volatility proxy is the daily cross-sectional average, $Volatility_{i,d}$, as defined in Section 3.2 and Table 1. Consistent with Baker *et al.* (2020), there is a substantial increase in volatility from 24th February 2020. Specifically, $Volatility_{i,d}$ increases by about 3 times between 24th February and 24th March 2020 in comparison with the month before. This implies that, like US markets, COVID-19 induces excessive volatility in European markets too. The COVID-19-linked excessive volatility observed between 24th February and 24th March 2020 allows us to employ this pandemic as an exogenous shock to investigate the role of volatility in traders' venue choice.

4.2. Venue choice analysis

4.2.1. Dark Market Share analysis

Zhu (2014) shows that excessive volatility increases (reduces) lit (dark) market share. We test this by first conducting a univariate analysis, followed by estimating a multivariate regression model. For the univariate analysis, we compute the evolution of dark market share during our sample period, and then test the null hypothesis that there is no difference between dark pool share during the pre- and excessive volatility periods. It is important to note that this part of the analysis is strictly based on the treated group of stocks, because the control group of stocks are under dark trading suspension during the sample period.

Covid Economics 13, 4 May 2020: 91-137

Figure 2. Dark trading

The figure plots the day-by-day evolution of the dark volume and dark market share for 55 European stocks that could be traded at both lit and dark venues. Dark market share is computed as the dark trading volume for a given day divided by the total trading volume on the same day. The sample period covers from 24th January to 24th March 2020. The vertical bar indicates 24th February 2020, when the COVID-19-induced excessive volatility is adjudged to have commenced in global financial markets.

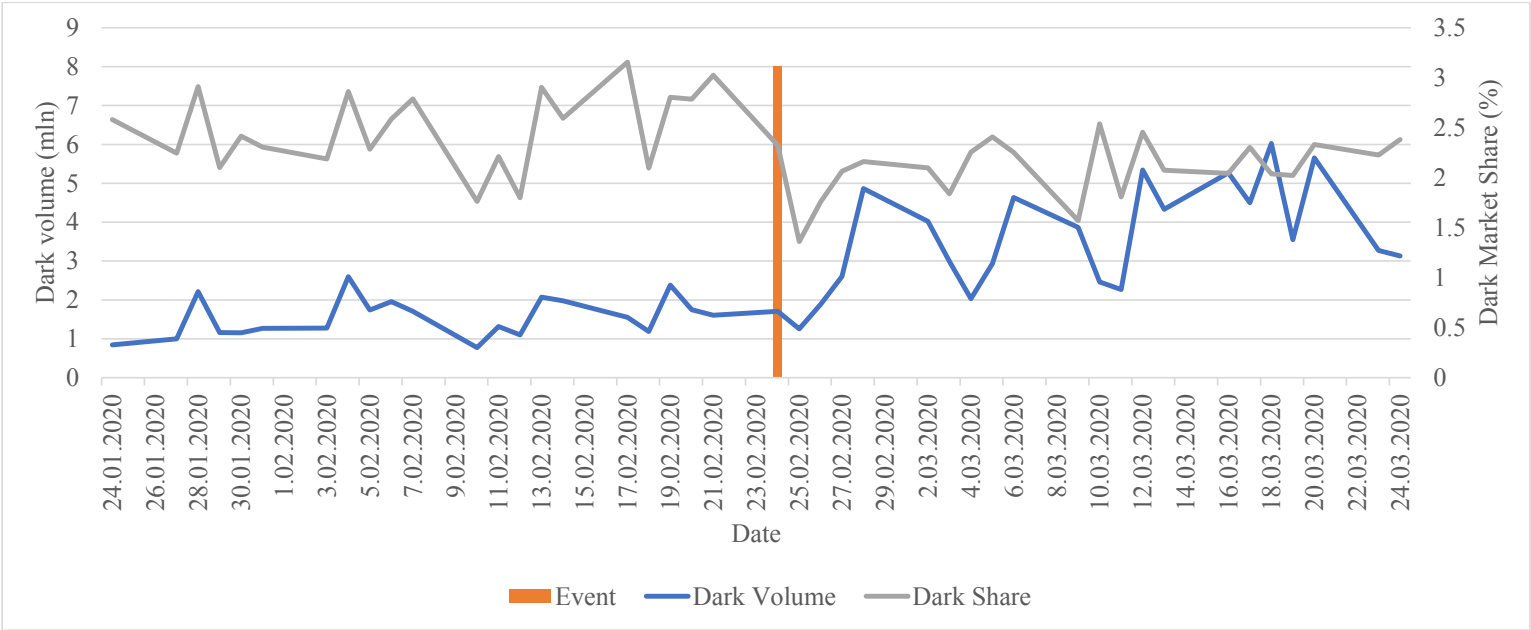

Covid Economics 13, 4 May 2020: 91-137

Table 3. Dark volume

This table presents average daily dark trading volume and dark market share for the treated group during pre- and event periods along with t-statistics of the two-sample t-tests of differences between pre- and event periods' dark volume statistics. The sample period is from 24th January to 24th March 2020. The event start date is 24th February 2020, when the COVID-19-induced excessive volatility is adjudged to have commenced in global financial markets. *, ** and *** correspond to statistical significance at the 0.10, 0.05 and 0.01 levels respectively.

	Dark volume (mln)	Dark market share (%)
Pre-event period	1,77	2.5
Event period	3.57	2.1
Difference (Event – pre)	1.80	-0.4
Percentage change and t-statistic	101%*** (6.42)	-15.6%*** (-3.65)

Covid Economics 13, 4 May 2020: 91-137

Figure 2 and Table 3 present the evolution of dark trading volume and dark market share during pre- and event periods. Although, dark trading volume in the treated stocks doubles during the excessive volatility period, this is only reflective of the overall increase in trading activity driven by the market response to the COVID-19 pandemic (see Figure 3 and Table 4). Indeed, dark market share declines from 2.5% to 2.1% (about 15.6% = (2.5-2.1)/2.5) which implies that the magnitude of the increase in trading activity is higher in the lit venue (the difference between pre-and the excessive market volatility periods is statistically significant at 0.01 level for both dark volume and dark market share). This is consistent with the predictions of Zhu (2014). Nevertheless, the insights are based on univariate analysis and should be backed up by a more robust analysis. Hence, we next conduct a multivariate analysis to further examine the trends described above. Specifically, we estimate the following model:

$$DMS_{i,d} = \alpha_i + \beta_d + \gamma_1 Event_{i,d} + \gamma_2 Volume_{i,d} + \gamma_3 Rspread_{i,d} + \gamma_4 Depth_{i,d} + \gamma_5 Volatility_{i,d} + \gamma_6 OIB_{i,d} + \gamma_7 HFT_{i,d} + \varepsilon_{i,d} \quad (1)$$

where $Event_{i,d}$ is a dummy variable that equals one for the days between 24th February and 24th March 2020 inclusive and zero otherwise. α_i and β_d are stock and time fixed effects.

Standard errors are robust to heteroscedasticity and autocorrelation.[10] All other variables are as defined in Section 3.2 and Table 1.

Table 4. The role of COVID-19 induced excessive volatility in dark market share

This table reports the coefficient estimates from the following regression model:

$$DMS_{i,d} = \alpha_i + \beta_d + \gamma_1 Event_{i,d} + \gamma_2 Volume_{i,d} + \gamma_3 Rspread_{i,d} + \gamma_4 Depth_{i,d} + \gamma_5 Volatility_{i,d} + \gamma_6 OIB_{i,d} + \gamma_7 HFT_{i,d} + \varepsilon_{i,d}$$

where $DMS_{i,d}$ is a dark market share and is computed as the dark trading volume divided by the total trading volume for stock *i* on day *d*, α_i and β_d are stock and time fixed effects respectively, $Event_{i,d}$ is a dummy equalling 1 from 24th February to 24th March 2020 and 0 from 24th January to 23rd February 2020. $Volume_{i,d}$ is the number of shares traded for stock *i* on day *d*, $Rspread_{i,d}$ is the relative quoted spread for stock *i* on day *d* and is computed as a time-weighted average of the difference between ask and bid prices divided by the mid-price (mid-price is the average of ask and bid prices) corresponding to each transaction, $Depth_{i,d}$ is the top-of-book depth and is computed as the natural logarithm of the sum of the best bid and ask sizes for stock *i* on day *d*, $Volatility_{i,d}$ is a proxy for volatility and is computed as the standard deviation of hourly mid-price returns for stock *i* on day *d*, $OIB_{i,d}$ is the order imbalance for stock *i* on day *d* and is computed as the absolute value of the buyer-initiated volume minus the number of seller-initiated volume divided by the total volume of stock *i* on day *d*, $HFT_{i,d}$ is a proxy for HFT and is computed as the number of messages divided by the number of transactions for stock *i* on day *d*. The sample period is from 24th January to 24th March 2020. The sample includes 55 European stocks that could be traded at both lit and dark venues, i.e. treated stocks, and 55 European stocks with dark venue restrictions, i.e. control stocks. Standard errors are robust to heteroscedasticity and autocorrelation. *, ** and *** correspond to statistical significance at the 0.10, 0.05 and 0.01 levels respectively.

Variable	Coefficient	*t*-statistic
$Event_{i,t}$	-1.3**	-2.54
$Rspread_{i,t}$	-0.0008**	-2.21
$Depth_{i,t}$	1.02***	19.14
$Volatility_{i,t}$	-0.0	-0.46
$OIB_{i,t}$	0.07***	3.08
$HFT_{i,t}$	0. 01***	3.14
Stock fixed effects	Yes	
Time fixed effects	Yes	
$\overline{R^2}$	56.2 %	

[10] Standard errors are robust to heteroscedasticity and autocorrelation in all models estimated in the paper.

Covid Economics 13, 4 May 2020: 91-137

Table 4 reports the estimation results for the Equation (1). The estimates suggest a negative and statistically significant relationship (at 0.05 level) between $Event_{i,d}$ and $DMS_{i,d}$. Specifically, $DMS_{i,d}$ declines by 1.3% following the onset of the COVID-19-induced excess volatility in European markets. This implies that, consistent with Zhu (2014), dark market share decreases during periods of excessively high volatility. The result is consistent with the univariate analysis we present in Table 3 and shows that the relationship is still significant after controlling for important market dynamics/variables. The economic significance of the decrease as estimated with the multivariate analysis is even bigger than estimated with the univariate analysis. Explicitly, while in the univariate analysis we find a 15.6% (0.4/2.5) reduction in dark market share, it is about 52% (1.3/2.5) in the multivariate analysis – effectively, more than half of the dark trading share of the market is lost during periods of market stress/volatility. Another important point to note is that, statistically, $Volatility_{i,d}$ is not significantly related to $DMS_{i,d}$. This is expected since $Event_{i,d}$ captures excessive volatility in the stocks examined, and therefore the significance of $Volatility_{i,d}$ disappears after controlling for $Event_{i,d}$ in the model. It implies that, consistent with Zhu (2014), excessive volatility is a more important factor than general volatility when explaining the impact of volatility on traders' venue selection. This further underscores the distinction between this study and the existing literature on volatility and dark trading, which focuses only on endogenous general volatility (see Ye 2010; Buti *et al.* 2011).

The findings presented in Figure 2, Tables 3 and 4 allow us to speculate that, indeed, some fraction of dark market share moves to lit venues. However, this is not the only interpretation. Specifically, one may argue that dark traders delay their trading rather than moving to lit venues, and therefore the reduction in dark market share reported in Table 3 and 4 is the result of this delay. We consider this argument by conducting some volume analysis in the next section.

Covid Economics 13, 4 May 2020: 91-137

Covid Economics 13, 4 May 2020: 91-137

4.2.2. Volume Analysis

The decrease in dark market share reported in Section 4.2.1 could potentially be explained by two mechanisms: 1) traders that use dark pools move to lit venues during periods of excessive volatility; and 2) these traders may delay their trading activity, in which case they are not migrating to lit venues. We employ a DiD framework in order to formally test which of these mechanisms explain our earlier finding.

We demonstrate in Section 3.2 and Table 2 that the two groups of treated and control stocks we employ in this paper have very similar market dynamics prior to the onset of excessive market volatility driven by the COVID-19 pandemic. Specifically, both groups' liquidity, volatility, order-book dynamics and HFT levels do not significantly differ from each before the event (see Table 2). The only identified difference between these groups is the availability of dark trading privileges for the treated group of stocks, with the control group of stocks restricted from dark trading due to their having breached the DVC under MiFID II provisions. Therefore, it is logical to expect that any difference between the impact of COVID-19-induced volatility on treated and control groups' market activities is linked to differences in dark trading privileges for both groups of stocks. In order to test whether this expectation holds, we estimate the following DiD model where the dependent variable is lit volume, $Volume_{i,d}$:

$$Volume_{i,d} = \alpha_i + \beta_d + \gamma_1 Event_{i,d} + \gamma_2 Treated_{i,d} + \gamma_3 Event_{i,d} * Treated_{i,d} + \gamma_4 Rspread_{i,d} + \gamma_5 Depth_{i,d} + \gamma_6 Volatility_{i,d} + \gamma_7 OIB_{i,d} + \gamma_8 HFT_{i,d} + \varepsilon_{i,d} \quad (2)$$

and where $Treated_{i,d}$ is a dummy equalling one for the treated group of stocks and zero for the stocks in the control group. α_i and β_d are stock and time fixed effects, and all other variables are as previously defined. $Event_{i,d} * Treated_{i,d}$ is a key variable, encapsulating the difference between the impact of the COVID-19 crisis on treated and control groups. Specifically, if traders delay their trading in dark pools because of excessive volatility in lit markets, then the impact of COVID-19-sourced excessive volatility should be the same for both treated and

control groups' lit volume. This implies that the coefficient of $Event_{i,d} * Treated_{i,d}$ would not be statistically significant, because dark market availability is the only difference between the control and treated groups' market dynamics during the pre-event period (see Table 2) and that difference should disappear if traders that are using dark pools delay their trading. However, if traders that are active in dark pools before the event move to lit venues, then $Event_{i,d} * Treated_{i,d}$ would be statistically significant because it captures the excess lit venues trading activity impact of traders with access to both lit and dark venues, and it could then be argued that they are shifting some of their trading from dark to lit venues.

Before estimating the Equation (2), it is useful to conduct some univariate analysis aimed at guiding our thinking on what to expect from the multivariate analysis.

Covid Economics 13, 4 May 2020: 91-137

Covid Economics 13, 4 May 2020: 91-137

Figure 3. Trading volume

The figure presents the day-by-day evolution of lit volume for 110 European stocks; Panel A presents the day-by-day evolution of lit volume for the full sample (both the 55 stocks that could be traded at both lit and dark venues, i.e. treated stocks, and the 55 stocks with dark venue restrictions, i.e. control stocks), while Panel B shows the day-by-day evolution of lit volume for the control and treated groups separately. The sample period covers from 24th January to 24th March 2020. The vertical bar indicates 24th February 2020, when the COVID-19-induced excessive volatility is adjudged to have commenced in global financial markets.

Panel A

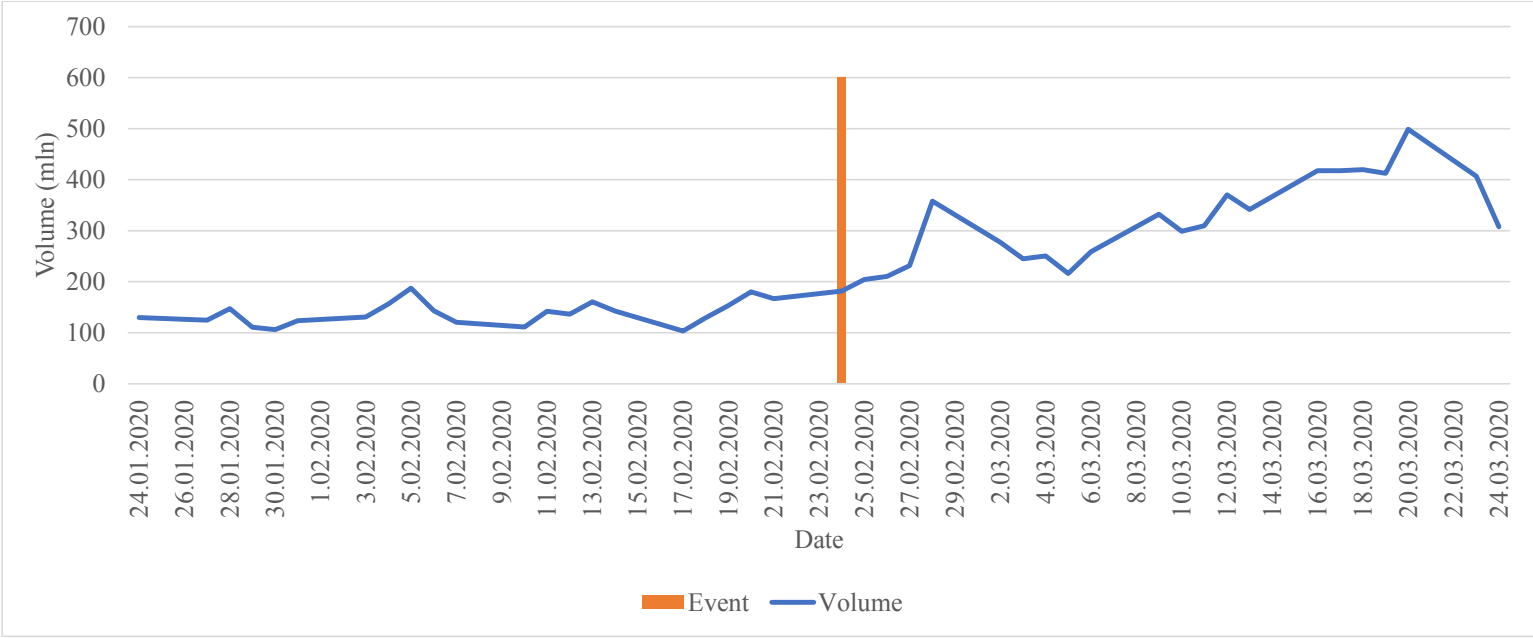

Covid Economics 13, 4 May 2020: 91-137

Panel B

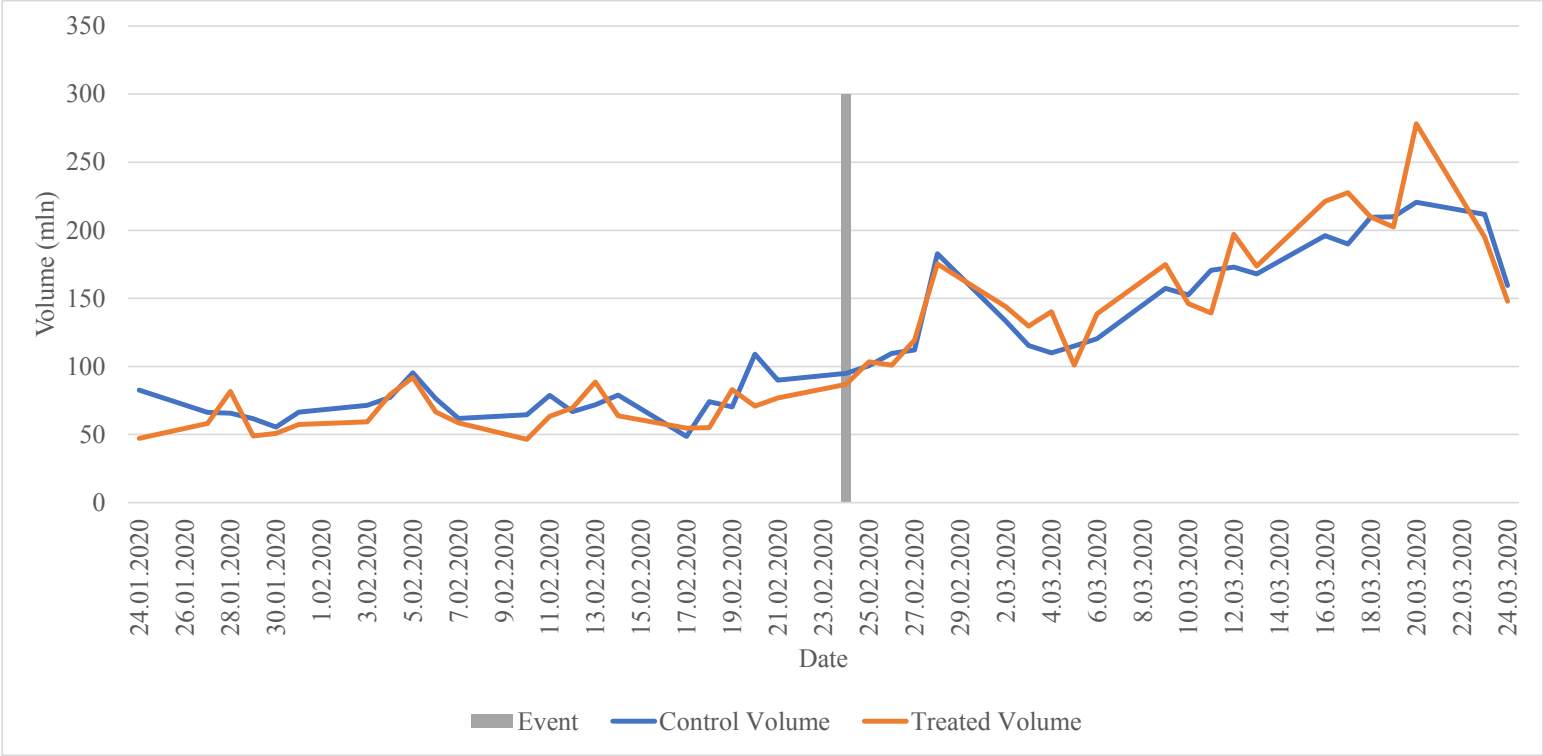

Table 5. Trading volume

This table contains the pre- and event average daily volume estimates for 55 European stocks that could be traded at both lit and dark venues, i.e. treated stocks, and for 55 European stocks with dark venue restrictions, i.e. control stocks. The estimates are reported separately for the treated and control groups along with t-statistics of the two-sample t-tests of differences between pre- and event periods average daily volumes. The sample period is from 24th January to 24th March 2020. The event start date is 24th February 2020, when the COVID-19-induced excessive volatility is adjudged to have commenced in global financial markets. *, ** and *** correspond to statistical significance at the 0.10, 0.05 and 0.01 levels respectively.

	Control group (mln)	Treated group (mln)
Pre-event period	73.04	69.96
Event period	155.15	161.52
Difference (event – pre)	82.11	91.56
Percentage change (*t*-	112.4%*** (6.78)	147.2%*** (7.72)

Panel A of Figure 3 presents the evolution of total trading volume, whereas Panel B presents the evolution of treated and control groups' volume separately. It is important to note that this is the evolution of the day-by-day total volume for all stocks. As evident in Panel A, total daily trading volume increases during the post-event periods. This is not unusual as everyone is trading in an attempt to exploit information or hedge risks during excessive volatility periods. Panel B of Figure 3 offers us a more nuanced view of the impact of the COVID-19 crisis on the trading activity of investors with respect to the treated and control groups of stocks. Specifically, the control groups' volume is slightly higher than the treated group's volume before the event (the difference is not statistically significant). However, the situation changes drastically following the onset of the excessive volatility period and the treated group's volume rises above the control group's (see Table 5 for more details). Another important point to note in Panel B is the correlation between the evolution of the control and treated groups' volume during the pre-event period. It is seen that $Volume_{i,d}$ for both groups have parallel trends in the absence of an event. It implies that the parallel trend assumption – which is vital for the empirical relevance of DiD framework – holds. Indeed, the break in the evolution of volume between the two groups is underscored by the differences in their level of

volume increases after 24th February 2020. Table 5 shows that while the control group's average daily lit volume increases by about 112% between 24th February and 24th March 2020, this increase is about 147% for the treated group, which indicates that the magnitude of increase is about 35% higher for the treated group. This is indeed a huge economic impact and consistent with our main argument regarding the move of traders from dark to lit venues. It is also consistent with estimates in Table 4 indicating significant falls in dark trading market share for our sample of stocks between 24th February and 24th March 2020.

Table 6. The role of COVID-19 induced excessive volatility in lit volume

This table reports the coefficient estimates from the following regression model, estimated using data for 55 European stocks that could be traded at both lit and dark venues, i.e. treated stocks, and for 55 European stocks with dark venue restrictions, i.e. control stocks:

$$Volume_{i,d} = \alpha_i + \beta_d + \gamma_1 Event_{i,d} + \gamma_2 Treated_{i,d} + \gamma_3 Event_{i,d} * Treated_{i,d} + \gamma_4 Rspread_{i,d} + \gamma_5 Depth_{i,d} + \gamma_6 Volatility_{i,d} + \gamma_7 OIB_{i,d} + \gamma_8 HFT_{i,d} + \varepsilon_{i,d}$$

where $Volume_{i,d}$ is the number of shares traded for stock *i* on day *d*, α_i and β_d are stock and time fixed effects respectively, $Event_{i,d}$ is a dummy equalling 1 from 24th February to 24th March 2020 and 0 from 24th January to 23rd February 2020. $Treated_{i,d}$ is a dummy, which equals 1 for the treated group of stocks and 0 for the control group of stocks. $Rspread_{i,d}$ is the relative quoted spread for stock *i* on day *d* and is computed as a time-weighted average of the difference between ask and bid prices divided by the mid-price (mid-price is the average of ask and bid prices) corresponding to each transaction, $Depth_{i,d}$ is the top-of-book depth and is computed as the natural logarithm of the sum of the best bid and ask sizes for stock *i* on day *d*, $Volatility_{i,d}$ is a proxy for volatility and is computed as the standard deviation of hourly mid-price returns for stock *i* on day *d*, $OIB_{i,d}$ is the order imbalance for stock *i* on day *d* and is computed as the absolute value of the buyer-initiated volume minus the number of seller-initiated volume divided by the total volume of stock *i* on day *d*, $HFT_{i,d}$ is a proxy for HFT and is computed as the number of messages divided by the number of transactions for stock *i* on day *d*. The sample period is from 24th January to 24th March 2020. Standard errors are robust to heteroscedasticity and autocorrelation. *, ** and *** correspond to statistical significance at the 0.10, 0.05 and 0.01 levels respectively.

Variable	Coefficient	*t*-statistic
$Event_{i,t}$	1.22***	2.65
$Treated_{i,t}$	-0.15	-1.5
$Event_{i,t} * Treated_{i,t}$	0.460**	2.37
$Rspread_{i,t}$	-0.005***	-4.72
$Depth_{i,t}$	0.93***	10.85
$Volatility_{i,t}$	10.49***	6.34
$OIB_{i,t}$	1.09***	4.33

Covid Economics 13, 4 May 2020: 91-137

$HFT_{i,t}$	0.0004	0.24
Stock fixed effects	YES	
Time fixed effects	YES	
$\overline{R^2}$	67.5%	

We now shift our attention to the outcome of the estimation of Equation (2) as reported in Table 6. There are some important points to note. Firstly, $Event_{i,d}$ is statistically significantly (at 0.01 level) and positively related to $Volume_{i,t}$ implying that indeed there is a substantial increase in lit volume during the COVID-19-driven market volatility period, when compared to the month before. Economically this implies that the number of shares traded daily during the post-event periods increases by about 1.2 million or, on average, 92% (= 1.2/1.3) for the 110 stocks in our sample.[11] This is a significant economic effect and shows that the pandemic crisis has unmistakable impacts on financial markets. Secondly, and most importantly, the interaction coefficient (γ_3) suggests that COVID-19-induced volatility is linked with average daily increases of about 460,000 shares for each of the treated stocks when compared to the control group of stocks; the coefficient is statistically significant at 0.05 level. The economic significance of this relative increase in lit trading activity is obvious. The average $Volume_{i,d}$ for the control group of stocks is about 2 million shares during our sample period. Thus, the magnitude of increases in trading volume is about 23% (=0.46/2) higher for the treated group compared with the control group. This is indeed a substantial change in economic terms. Thus, there is compelling evidence that, although traders increase their lit venue trading activity for all stocks during the COVID-19-induced market volatility period, they do so on a larger scale for stocks with trading privileges in both lit and dark venues. Taken together with the estimates in Table 4 these estimates support the argument that, in times of excessive market volatility and widening lit market spreads, informed traders, who traditionally constitute a small

[11] The stock-day average trading volume during the pre-event period is 1.3 million shares (see Table 2).

Covid Economics 13, 4 May 2020: 91-137

proportion of traders, migrate to dark pools, and thus in turn induce the migration of uninformed traders to lit venues as the latter seek to avoid being adversely selected by the former (see Zhu 2014). Uninformed traders typically constitute the majority share of active market participants; therefore, the net effect of these dynamics is an increase in the lit trading activity of traders in the stocks eligible for trading in both lit and dark venues.

4.3. How volatility drives venue choice by informed traders

Zhu (2014) identifies adverse selection risk as a key driver of the venue selection decisions made by traders, especially in the case of uninformed traders (see also Aquilina *et al.* 2017). Specifically, the study suggests that informed traders stay on the lit exchange under "normal" market conditions, i.e. "normal" conditions means lower volatility and exchange spread. This is because under these conditions exchange spread is not excessive, and thus the cost of execution risk is higher than the price-improvements benefit. However, when there is excessive volatility in financial markets, then informed traders start to move to dark pools to avoid the higher exchange spread. This implies that excessive volatility in lit markets introduces additional adverse selection cost to dark pools. This "new" adverse selection cost forces uninformed\liquidity traders to exit from dark pools. In this scenario, dark pool liquidity traders have two options, either to delay their trading, which can be quite costly when markets are especially volatile as observed in this case, or move to lit exchanges. The results reported in Table 6 show that traders select the second option and move to lit exchanges. In this section, we investigate whether the adverse selection channel proposed by Zhu (2014) explains our finding.

Covid Economics 13, 4 May 2020: 91-137

We proxy adverse selection cost by using the method developed by Lin *et al.* (1995).[12] Specifically, we compute the daily adverse selection component, $ASC_{i,d}$, of the relative spread, $Rspread_{i,d}$, by using intraday high frequency data as obtained from the TRTH database. Then, as in Section 4.2, we compare the adverse selection costs of treated and control groups of stocks. When informed traders move to dark venues during excessive volatility periods, there is a difference between the evolution of $ASC_{i,d}$ (after controlling for the general trend in $Rspread_{i,d}$) in the treated and control groups, as only the treated group's stocks have an unfettered dark pool access option. This is linked to dark pools in Europe executing against the prices displayed by lit venues; they are, hence, essential passive price takers and are less informative than lit venues. As informed traders migrate to the dark pools, their ability to signal information will be curtailed given that midpoint dark pools execute with lit venues' prices as references.

[12] For robustness, we estimate the adverse selection component of the spread by using the approach of Stoll (1989) and obtain qualitatively similar results.

Covid Economics 13, 4 May 2020: 91-137

Covid Economics 13, 4 May 2020: 91-137

Figure 4. Adverse selection component

Panel A presents the day-by-day evolution of the cross-sectional average of $ASC_{i,d}$ for 55 European stocks that could be traded at both lit and dark venues, i.e. treated stocks, and for 55 European stocks with dark venue restrictions, i.e. control stocks. Panel B shows the evolution of the difference between the control group's $ASC_{i,d}$ and the treated group's $ASC_{i,d}$. $ASC_{i,d}$ is the adverse selection component of relative spread $Rspread_{i,d}$ for stock i on day d and is computed by using the method developed by Lin *et al.* (1995). The sample period covers from 24th January to 24th March 2020. The vertical bar indicates 24th February 2020, when the COVID-19-induced excessive volatility is adjudged to have commenced in global financial markets.

Panel A

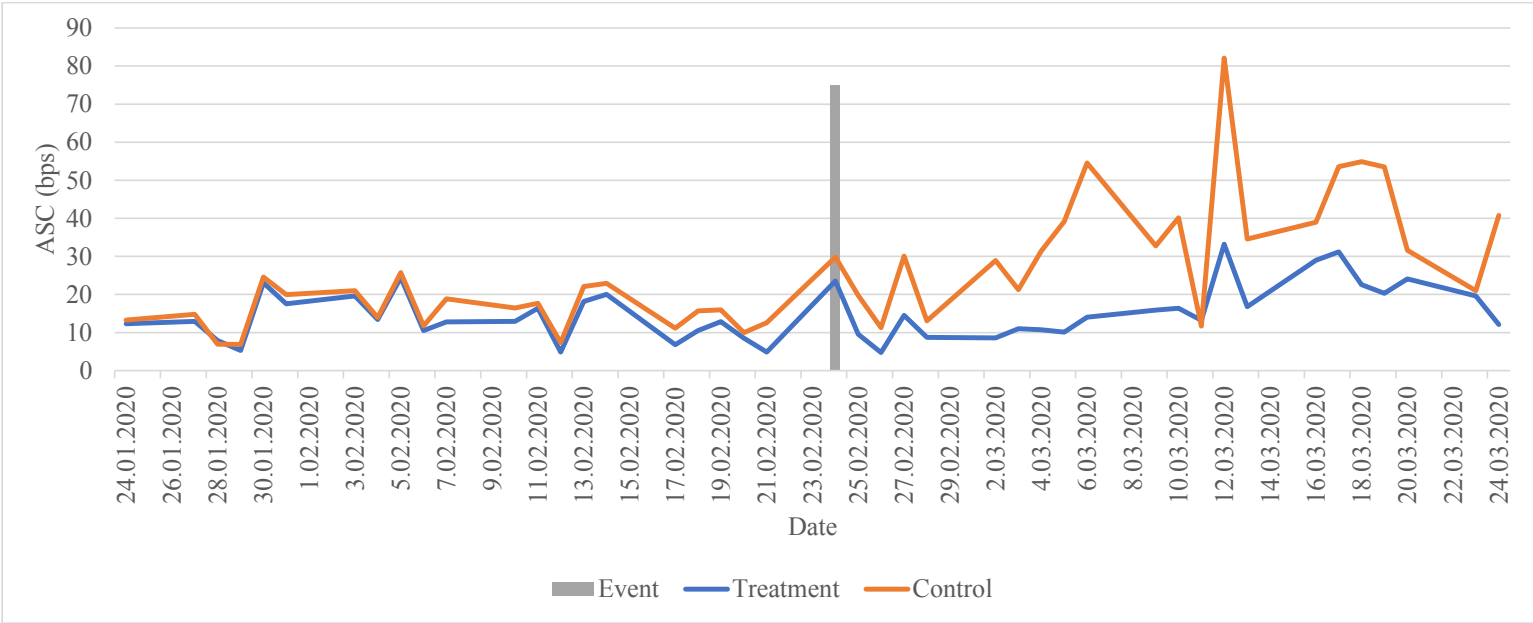

Covid Economics 13, 4 May 2020: 91-137

Panel B

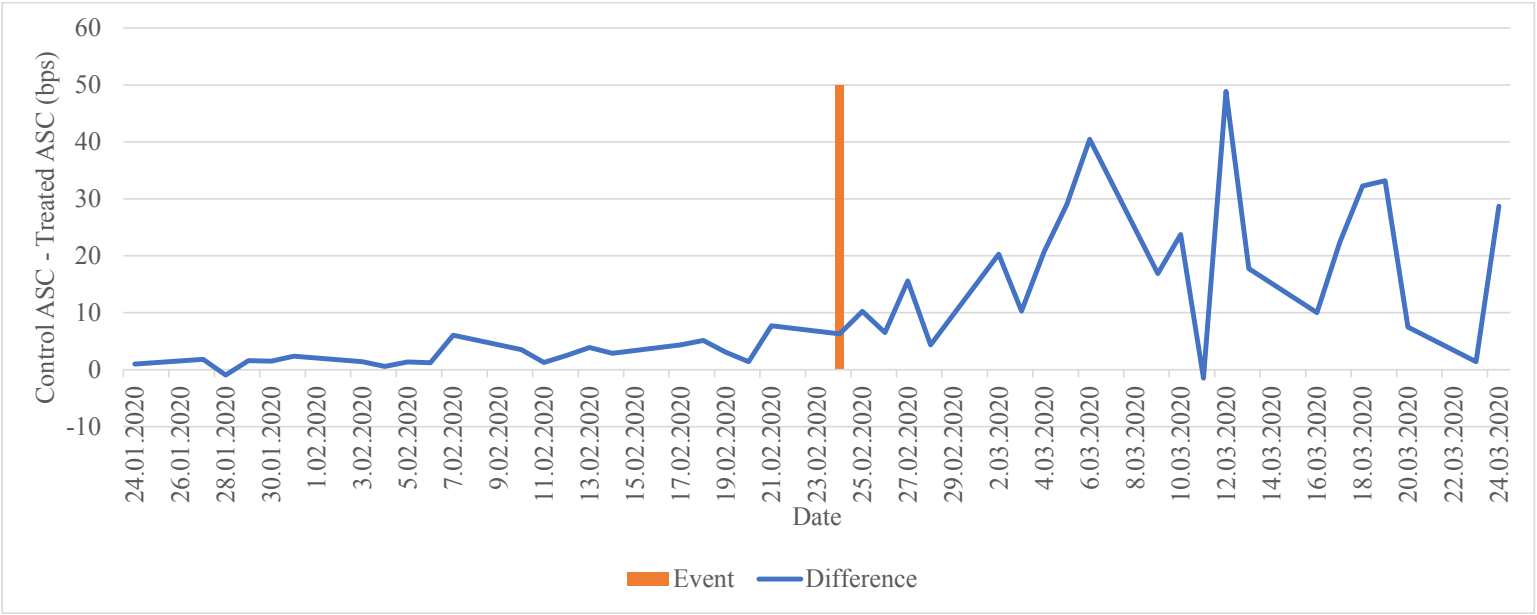

Table 7. Adverse selection component

This table contains the pre- and event stock-day averages of $ASC_{i,d}$ and $ASW_{i,d}$, for 55 European stocks that could be traded at both lit and dark venues, i.e. treated stocks, and for 55 European stocks with dark venue restrictions, i.e. control stocks. The estimates are reported separately for the treated and control groups along with t-statistics of the two-sample t-tests of differences between treated and control groups. $ASC_{i,d}$ is the adverse selection component of $Rspread_{i,d}$ and is computed using the method developed by Lin *et al.* (1995), while $ASW_{i,d}$ is the weight of $ASC_{i,d}$ in $Rspread_{i,d}$, calculated by dividing $ASC_{i,d}$ by $Rspread_{i,d}$ and then multiplying by 100. The sample period is from 24th January to 24th March 2020. The event date is 24th February 2020, when the COVID-19-induced excessive volatility is adjudged to have commenced in global financial markets. *, ** and *** correspond to statistical significance at the 0.10, 0.05 and 0.01 levels respectively.

Panel A

	Pre-event	Event
Treated $ASC_{i,d}$	13.14	16.81
Control $ASC_{i,d}$	15.69	35.22
Difference (control –	2.55 (1.61)	18.41***(3.63)

Panel B

	Pre-event	Event
Treated $ASW_{i,d}$	21%	19%
Control $ASW_{i,d}$	25%	37%
Difference (control – treated)	4% (1.58)	18%***(5.75)

Panel A of Figure 4 presents the evolution of treated and control $ASC_{i,d}$ during the sample period. There are two essential points to note here. Firstly, $ASC_{i,d}$ increases for both groups, indicating that informed traders are more active during the post-event period. This is expected as $Rspread_{i,d}$ increases for both groups too. Thus, an increase in $ASC_{i,d}$ is not very informative by itself. In order to investigate whether adverse selection cost increases or not, we need to compute the percentage of $Rspread_{i,d}$ driven by adverse selection cost and compare its values for before and after the onset of the COVID-19-induced market volatility. For this, we divide $ASC_{i,d}$ by $Rspread_{i,d}$ and then multiply the outcome by 100 to obtain the adverse selection component weighted by $Rspread_{i,d}$, $ASW_{i,d}$. The estimates reported in Panel B of Table 7 show that, for the treated group, the average $ASW_{i,d}$ is 21% (=(13.14/61.14)*100) in

Covid Economics 13, 4 May 2020: 91-137

the pre-event period, reducing to 19% (=(20.19/87.95)*100) during the COVID-19-induced market volatility period. For the control group, the average $ASW_{i,d}$ is 25% (=(15.69/61.39)*100) during the pre-event period, increasing to 37% (=(35.22/94.25)*100) during the COVID-19-induced market volatility period. Thus, while the control group's adverse selection cost increases by 12%, the treated group's adverse selection cost declines by about 2%. This clearly shows that the COVID-19 crisis does not have the same impact on the adverse selection costs of treated and control groups.

The above finding is further strengthened by the evolution of the difference between control and treated groups' $ASC_{i,d}$, shown in Panel B of Figure 5. It is evident that the difference is relatively stable and close to 0 before the event. However, it increases and becomes more unstable after the event, which indicates both the reduction in proportion of information-driven trading activity in the treated stocks and the magnitude of the $ASC_{i,d}$ increases for the control group of stocks during the COVID-19-induced market volatility period. The difference is also found to be statistically significant when we use the standard error of the mean difference for statistical inference as shown in Panel A of Table 7. The estimates presented suggest that the difference between the control and treated groups' $ASC_{i,d}$ prior to the COVID-19 crisis is 2.55 bps and not statistically significant. However, the difference increases to 18.41 bps and becomes statistically significant at the 0.01 level following the onset of the crisis period. The same results hold for $ASW_{i,d}$ (see Panel B). This finding is consistent with Zhu (2014) and our argument that informed traders migrate to dark pools when volatility in lit venues becomes excessive. To formally test the argument in the multivariate framework, we estimate the following model; all variables are as previously defined:

$$ASW_{i,d} = \alpha_i + \beta_d + \gamma_1 Event_{i,d} + \gamma_2 Treated_{i,d} + \gamma_3 Event_{i,d} * Treated_{i,d} + \gamma_4 Depth_{i,d} + \gamma_5 Volatility_{i,d} + \gamma_6 OIB_{i,d} + \gamma_7 HFT_{i,d} + \gamma_8 Volume_{i,d} + \varepsilon_{i,d} \quad (3)$$

Covid Economics 13, 4 May 2020: 91-137

Table 8. The role of COVID-19 induced excessive volatility in adverse selection cost

This table reports the coefficient estimates from the following regression model, estimated using data for 55 European stocks that could be traded at both lit and dark venues, i.e. treated stocks, and for 55 European stocks with dark venue restrictions, i.e. control stocks:

$$ASW_{i,d} = \alpha_i + \beta_d + \gamma_1 Event_{i,d} + \gamma_2 Treated_{i,d} + \gamma_3 Event_{i,d} * Treated_{i,d} + \gamma_4 Depth_{i,d} + \gamma_5 Volatility_{i,d} + \gamma_6 OIB_{i,d} + \gamma_7 HFT_{i,d} + \gamma_8 Volume_{i,d} + \varepsilon_{i,d}$$

where $ASW_{i,d}$ is the weight of $ASC_{i,d}$ in $Rspread_{i,d}$, calculated by dividing $ASC_{i,d}$ by $Rspread_{i,d}$ and then multiplying by 100, $ASC_{i,d}$ is the adverse selection component of $Rspread_{i,d}$ and is computed by using the method developed in Lin *et al.* (1995), $Rspread_{i,d}$ is the relative quoted spread for stock *i* on day *d* and is computed as time-weighted average of the difference between ask and bid prices divided by the mid-price (mid-price is the average of ask and bid prices) corresponding to each transaction. α_i and β_d are stock and time fixed effects respectively, $Event_{i,d}$ is a dummy equal 1 from 24th February to 24th March 2020 and 0 from 24th January to 23rd February 2020, $Treated_{i,d}$ is a dummy equalling 1 for the treated group of stocks and 0 for the control group of stocks. $Depth_{i,d}$ is the top-of-book depth and is computed as the natural logarithm of the sum of the best bid and ask sizes for stock *i* on day *d*, $Volatility_{i,d}$ is a proxy for volatility and is computed as the standard deviation of hourly mid-price returns for stock *i* on day *d*, $OIB_{i,d}$ is the order imbalance for stock *i* on day *d* and is computed as the absolute value of the buyer-initiated volume minus the number of seller-initiated volume divided by the total volume of stock *i* on day *d*, $HFT_{i,d}$ is a proxy for HFT and is computed as the number of messages divided by the number of transactions for stock *i* on day *d*. The sample period is from 24th January to 24th March 2020. Standard errors are robust to heteroscedasticity and autocorrelation. *, ** and *** correspond to statistical significance at the 0.10, 0.05 and 0.01 levels respectively.

Variable	Coefficient	*t*-statistic
$Event_{i,t}$	2.23**	2.17
$Treated_{i,t}$	-1.59	-1.40
$Event_{i,t} * Treated_{i,t}$	-3.08**	-2.03
$Depth_{i,t}$	-0.91***	-3.85
$Volatility_{i,t}$	3.53*	1.71
$OIB_{i,t}$	3.85***	5.53
$HFT_{i,t}$	0.306	0.66
$Volume_{i,t}$	0.54	1.35
Stock fixed effects	YES	
Time fixed effects	YES	
$\overline{R^2}$	33.2%	

Table 8 reports the estimation results for Equation (3). $Event_{i,d}$ is positive and statistically significantly (at 0.05 level), which implies that overall $ASW_{i,d}$ increases during the post-event

Covid Economics 13, 4 May 2020: 91-137

period.[13] However, the interaction coefficient (γ_3) is negative and statistically significant (at 0.05 level) implying that the treated group's $ASW_{i,d}$ reduces over the same period when we compare it with the control group's $ASW_{i,d}$. The magnitude of the association is also economically meaningful. Specifically, $ASW_{i,d}$ of the treated group reduces by 3.08% during the post-event period when we compare it with the control group. The economic significance of this estimate is put into some perspective when we consider that the stock-day average $ASW_{i,d}$ is about 29% for the control group in our sample period. The implication here is that information-based trading activity in stocks with dark trading privileges declines by about 10% (=3.08/29) during the most volatile period of the COVID-19-induced market turmoil in comparison with stocks without this privilege. This is consistent with the predictions of Zhu (2014) and the results presented in Figure 4 and Table 7 and suggests that indeed informed traders move their trading activity to dark pools during periods of excessive volatility. The move in turn drives the exit of uninformed traders from dark pools to lit venues, and this switch causes reductions in dark market share as reported in Table 4 and increases in lit market volume as shown in Table 6. One may argue that informed traders may stop trading, and therefore the reduction in $ASW_{i,d}$ of the treated group is related to this. However, if this is the case, we would expect to see the same effects in the control group; it is implausible that a different factor other than the opportunity to trade in an unfettered manner in dark pools is driving the differential in the evolution of $ASW_{i,d}$ during the COVID-19-induced market volatility period. Thus, our DiD framework allows as to interpret this result as informed traders moving from lit to dark venues.

4.4. Market quality implications

Empirical findings reported in Section 4.2 show that, overall, traders are shifting significant proportions of their trading from dark to lit venues during excessive volatility

[13] As reported in Table 7, this positive relationship is driven by the control group.

Covid Economics 13, 4 May 2020: 91-137

(market stress) periods. More explicitly, we find that in times of excessive market volatility, informed traders migrate to dark pools in order to avoid the higher exchange spread, and this increases adverse selection risk in these markets. Thereafter, increased adverse selection forces uninformed traders to move from lit venues to dark ones (see Section 4.3). While reporting on these dynamics is of academic, and arguably practical, interest, the bottom-line should ultimately be what they mean for market quality. Therefore, in this section, we examine the market quality implications of this cross-migration.

Price discovery and liquidity are generally considered to be two of the most important market quality characteristics (see O'Hara 2003). Hence, we examine the effects of the reported dynamics on both the efficiency of the price discovery process/informational efficiency and liquidity by using a DiD framework similar to those used in Sections 4.2 and 4.3 above. We estimate the following models with market quality metrics on the left-hand side.

$$Rspead_{i,d} = \alpha_i + \beta_d + \gamma_1 Event_{i,d} + \gamma_2 Treated_{i,d} + \gamma_3 Event_{i,d} * Treated_{i,d} + \gamma_4 Depth_{i,d} + \gamma_5 Volatility_{i,d} + \gamma_6 OIB_{i,d} + \gamma_7 HFT_{i,d} + \gamma_8 Volume_{i,d} + \varepsilon_{i,d} \quad (4)$$

$$Corr_{i,d} = \alpha_i + \beta_d + \gamma_1 Event_{i,d} + \gamma_2 Treated_{i,d} + \gamma_3 Event_{i,d} * Treated_{i,d} + \gamma_4 Rspread_{i,d} + \gamma_5 Depth_{i,d} + \gamma_6 Volatility_{i,d} + \gamma_7 OIB_{i,d} + \gamma_8 HFT_{i,d} + \gamma_9 Volume_{i,d} + \varepsilon_{i,d} \quad (5)$$

where the proxy for informational efficiency, $Corr_{i,d}$, is the absolute value of first order return autocorrelation for each stock *i* on day *d,* expressed in basis points (bps). It is computed by first estimating 30 seconds' returns within each stock-day ($ret_{i,t,d}$) and then computing $Corr_{i,d}$ as $Corr_{i,d} = \left|Correlation(ret_{i,t,d}, ret_{i,t-1,d})\right|$. We employ the absolute value of the correlation coefficients as this captures both the under- and over-reaction of returns to information, with smaller values indicating greater efficiency. The empirical relevance of this metric is underscored by its wide use in the literature (see as examples, Hendershott & Jones 2005;

Covid Economics 13, 4 May 2020: 91-137

Comerton-Forde & Putniņš 2015). All other variables are as previously defined. The first model, Equation (4), is used to estimate the impact of the dark trading dynamics in the treated stocks during the volatile period on lit market liquidity, with relative spread as the proxy for liquidity, whereas the second model, Equation (5), examines the role of the dark trading dynamics in the treated stocks during the volatile period in price discovery.

Table 9. The role of COVID-19 induced excessive volatility in liquidity

This table reports the coefficient estimates from the following regression model, estimated using data for 55 European stocks that could be traded at both lit and dark venues, i.e. treated stocks, and for 55 European stocks with dark venue restrictions, i.e. control stocks:

$$Rspread_{i,d} = \alpha_i + \beta_d + \gamma_1 Event_{i,d} + \gamma_2 Treated_{i,d} + \gamma_3 Event_{i,d} * Treated_{i,d} + \gamma_4 Depth_{i,d} + \gamma_5 Volatility_{i,d} + \gamma_6 OIB_{i,d} + \gamma_7 HFT_{i,d} + \gamma_8 Volume_{i,d} + \varepsilon_{i,d}$$

where $Rspread_{i,d}$ is the relative quoted spread for stock *i* on day *d* and computed as time-weighted average of the difference between ask and bid prices divided by the mid-price (mid-price is the average of ask and bid prices) corresponding to each transaction. α_i and β_d are stock and time fixed effects respectively, $Event_{i,d}$ is a dummy equal 1 from 24th February to 24th March 2020 and 0 from 24 January to 23 February 2020, $Treated_{i,d}$ is a dummy equalling 1 for the treated group of stocks and 0 for the control group of stocks. $Depth_{i,d}$ is the top-of-book depth and is computed as the natural logarithm of the sum of the best bid and ask sizes for stock *i* on day *d*, $Volatility_{i,d}$ is a proxy for volatility and is computed as the standard deviation of hourly mid-price returns for stock *i* on day *d*, $OIB_{i,d}$ is the order imbalance for stock *i* on day *d* and is computed as the absolute value of the buyer-initiated volume minus the number of seller-initiated volume divided by the total volume of stock *i* on day *d*, $HFT_{i,d}$ is a proxy for HFT and is computed as the number of messages divided by the number of transactions for stock *i* on day *d*. The sample period is from 24th January to 24th March 2020. Standard errors are robust to heteroscedasticity and autocorrelation. *, ** and *** correspond to statistical significance at the 0.10, 0.05 and 0.01 levels respectively.

Variable	Coefficient	*t*-statistic
$Event_{i,t}$	21.88***	3.21
$Treated_{i,t}$	-1.14	-0.53
$Event_{i,t} * Treated_{i,t}$	-7.25**	-2.54
$Depth_{i,t}$	-6.92***	-5.41
$Volatility_{i,t}$	15.72***	6.46
$OIB_{i,t}$	4.54*	1.72
$HFT_{i,t}$	0.04	1.59
$Volume_{i,t}$	-1.03***	-4.60
Stock fixed effects	YES	
Time fixed effects	YES	

$\overline{R^2}$	75.8%

Table 10. The role of COVID-19 induced excessive volatility in price discovery/informational efficiency

This table reports the coefficient estimates from the following regression model, estimated using data for 55 European stocks that could be traded at both lit and dark venues, i.e. treated stocks, and for 55 European stocks with dark venue restrictions, i.e. control stocks:

$$Corr_{i,d} = \alpha_i + \beta_d + \gamma_1 Event_{i,d} + \gamma_2 Treated_{i,d} + \gamma_3 Event_{i,d} * Treated_{i,d} + \gamma_4 Rspread_{i,d} + \gamma_5 Depth_{i,d} + \gamma_6 Volatility_{i,d} + \gamma_7 OIB_{i,d} + \gamma_8 HFT_{i,d} + \gamma_9 Volume_{i,d} + \varepsilon_{i,d}$$

where $Corr_{i,d}$ is first-order return autocorrelations for each stock *i* on day *d* at 30 seconds frequency. α_i and β_d are stock and time fixed effects respectively, $Event_{i,d}$ is a dummy equalling1 from 24th February to 24th March 2020 and 0 from 24th January to 23rd February 2020, $Treated_{i,d}$ is a dummy equalling 1 for the treated group of stocks and 0 for the control group of stocks. $Rspread_{i,d}$ is the relative quoted spread for stock *i* on day *d* and computed as time-weighted average of the difference between ask and bid prices divided by the mid-price (mid-price is the average of ask and bid prices) corresponding to each transaction. $Depth_{i,d}$ is the top-of-book depth and is computed as the natural logarithm of the sum of the best bid and ask sizes for stock *i* on day *d*, $Volatility_{i,d}$ is a proxy for volatility and is computed as the standard deviation of hourly mid-price returns for stock *i* on day *d*, $OIB_{i,d}$ is the order imbalance for stock *i* on day *d* and is computed as the absolute value of the buyer-initiated volume minus the number of seller-initiated volume divided by the total volume of stock *i* on day *d*, $HFT_{i,d}$ is a proxy for HFT and is computed as the number of messages divided by the number of transactions for stock *i* on day *d*. The sample period is from 24th January to 24th March 2020. Standard errors are robust to heteroscedasticity and autocorrelation. *, ** and *** correspond to statistical significance at the 0.10, 0.05 and 0.01 levels respectively.

Variable	Coefficient	*t*-statistic
$Event_{i,t}$	60.41	0.36
$Treated_{i,t}$	-3.33	-0.47
$Event_{i,t} * Treated_{i,t}$	31.34*	1.71
$Rspread_{i,t}$	-2.06***	-7.19
$Depth_{i,t}$	-5.41***	-13.39
$Volatility_{i,t}$	-26.41***	-3.88
$OIB_{i,t}$	-4.39***	-3.94
$HFT_{i,t}$	-0.26	-0.64
$Volume_{i,t}$	1.98	0.41
Stock fixed effects	YES	
Time fixed effects	YES	
$\overline{R^2}$	24.1%	

Covid Economics 13, 4 May 2020: 91-137

Table 9 reports estimation results for the Equation (4). The interaction variable's coefficient, γ_3, is negative and statistically significant (at 0.05 level) implying that the treated group's $Rspead_{i,d}$ decreases during the excessive volatility periods when compared to the control group's $Rspead_{i,d}$. $Rspead_{i,d}$ is the inverse measure of liquidity, which means that the treated group's liquidity improves over the same period in comparison with the control group's liquidity. This is consistent with earlier reported estimates in this paper, as well as the predictions of Zhu (2014), supporting the notion that the migration of informed traders' to dark pools unleashes an exodus of uninformed (liquidity) traders from dark pools to lit venues. This ultimately results in lit venues increasing their share of liquidity-providing traders and executed orders. The magnitude of the narrowing observed in the treated stocks' $Rspead_{i,d}$ during the COVID-19 impact period is also economically meaningful. Specifically, the spread of stocks with dark trading privileges narrows by about 9% (=7.25/81) during the post-event period when compared with the control group.[14]

Table 10 shows the estimated coefficients for Equation (5). The interaction variable, $Event_{i,d} * Treated_{i,d}$, is positively related to $Corr_{i,d}$; the relationship is statistically significant at the 0.10 level. The first observation here is that the informational efficiency impact of dark trading is not as powerful as its liquidity effects. The asymmetric effects of dark trading dynamics on market quality characteristics is in line with the literature. For example, Zhu (2014) shows that the addition of a dark pool to a lit exchange decreases liquidity on the lit exchange and improves price discovery (see also Buti *et al.*, 2011; Comerton-Forde & Putniņš, 2015). Nevertheless, the significance of the informational efficiency effects is obvious, with the implication that the treated group's informational efficiency deteriorates in response to the volatile trading conditions spurred by the COVID-19 pandemic, when compared to the

[14] The average $Rspead_{i,d}$ for the control group is 81 bps.

Covid Economics 13, 4 May 2020: 91-137

control group's informational efficiency. The change in informational efficiency is also economically meaningful. The average $Corr_{i,d}$ for the control group is 1082 bps, which suggests that the treated group's information efficiency deteriorates by about 2.8% (=31.34/1082) as a result of the COVID-19 pandemic market turmoil, in comparison with that of the control group. This finding is not surprising and is what we would expect to find given the migration of informed traders to dark pools as a result of increased volatility on the lit exchange. Estimates in Table 8 show that, consistent with the theoretical literature (see Zhu, 2014), informed traders migrate from the lit to dark venues during the COVID-19-induced excessive market volatility period. The consequence of this is a delay in the incorporation of information held by the migrating informed traders, since dark pools do now offer pre-trade transparency. Under normal conditions, when trading in a lit venue via the limit order book, information held by informed traders is more likely to be observed earlier than when they trade in dark pools, where they are also more susceptible to non-execution risk. Ultimately, although the (negative) informational efficiency effect of the COVID-19-triggered dark trading dynamics is economically meaningful, it pales in comparison to the liquidity effects.

Covid Economics 13, 4 May 2020: 91-137

5. Conclusion

The most obvious impact of the 2019-20 COVID-19 pandemic on financial markets is the injection of an unprecedented level of price volatility, especially in the cases of developed markets in the US and Europe. In February 2020, the pandemic-driven volatility held European markets in its vice-like grip for weeks, and in the process has induced a series of interesting market dynamics. One of these dynamics is a sharp loss of market share by dark pools as widely reported in the financial media.[15] In this paper, we exploit the exogenous nature of the volatility

[15] See as an example the coverage by Financial Times: https://www.ft.com/content/11c4b4d8-ff8a-49d3-817b-09de8266479a

induced by the pandemic and the existing dark trading caps policy in force in European markets as part of MiFID II provisions to investigate how volatility drives dark market share and the dynamics of venue selection by informed and uninformed traders.

Through a series of univariate and multivariate analyses we show that, in line with the theoretical literature (see Zhu 2014), excessive volatility at lit venues is linked with the migration of informed traders from those venues to dark pools, which in turn drives the migration of adverse selection-wary uninformed traders from dark pools to lit venues. The net effect of the cross-migration is a loss of market share by dark pools and an increase in lit venues' market share. The market quality implications of these dynamics, although mixed, are economically meaningful and statistically significant. While stocks with dark trading privileges experience higher levels of liquidity, i.e. narrower spreads, during the COVID-19-driven market volatility period, the informational efficiency of their prices reduces in comparison to the stocks under dark trading restrictions.

This contribution is timely and has implications for dark trading regulation, given the increasingly intense regulatory constraints being considered for the use of dark pools across the world, and already implemented in Europe. Seemingly appealing and uncomplicated policies aimed at addressing the complex issues in financial markets, such as algorithmic trading, market fragmentation and dark trading, are often inadequate, mainly because they are seldom driven by a full understanding of the factors driving such phenomena. With respect to dark trading, what our results show is the need for regulatory interventions to be flexible and account for changes in market conditions, such as periods of exogenously driven high volatility. This is because provisions designed for normal trading conditions (e.g. dark trading caps and waivers) become irrelevant when markets are impacted by events such as a pandemic.

Covid Economics 13, 4 May 2020: 91-137

Covid Economics 13, 4 May 2020: 91-137

References

Aquilina, M., Diaz-Rainey, I., Ibikunle, G., Sun, Y., 2017. City goes dark: dark trading and adverse selection in aggregate markets. FCA Occasional Paper

Baker, S.R., Bloom, N., Davis, S.J., Kost, K., Sammon, M., Viratyosin, T., 2020. The unprecedented stock market reaction to COVID-19. COVID Economics: Vetted and Real-time Papers, Centre for Economic Policy Research

Brugler, J., 2015. Into the light: dark pool trading and intraday market quality on the primary exchange. Bank of England Staff Working Paper

Buti, S., Rindi, B., Werner, I.M., 2011. Diving into Dark Pools. Charles A. Dice Center Working Paper

Chordia, T., Roll, R., Subrahmanyam, A., 2008. Liquidity and market efficiency. Journal of Financial Economics 87, 249-268

Comerton-Forde, C., Putniņš, T.J., 2015. Dark trading and price discovery. Journal of Financial Economics 118, 70-92

Degryse, H., de Jong, F., Kervel, V.v., 2015. The Impact of Dark Trading and Visible Fragmentation on Market Quality. Review of Finance 19, 1587-1622

Foley, S., Malinova, K., Park, A., 2012. Dark trading on public exchanges. Available at SSRN 2182839

Glosten, L.R., Milgrom, P.R., 1985. Bid, ask and transaction prices in a specialist market with heterogeneously informed traders. Journal of Financial Economics 14, 71-100

Hasbrouck, J., Saar, G., 2013. Low-latency trading. Journal of Financial Markets 16, 646-679

Hendershott, T., Jones, C.M., 2005. Island Goes Dark: Transparency, Fragmentation, and Regulation. The Review of Financial Studies 18, 743-793

Hendershott, T., Mendelson, H., 2000. Crossing Networks and Dealer Markets: Competition and Performance. The Journal of Finance 55, 2071-2115

Kyle, A.S., 1985. Continuous auctions and insider trading. Econometrica, 1315-1335

Lin, J.-C., Sanger, G.C., Booth, G.G., 1995. Trade size and components of the bid-ask spread. The Review of Financial Studies 8, 1153-1183

Malceniece, L., Malcenieks, K., Putniņš, T.J., 2019. High frequency trading and comovement in financial markets. Journal of Financial Economics 134, 381-399

Nimalendran, M., Ray, S., 2014. Informational linkages between dark and lit trading venues. Journal of Financial Markets 17, 230-261

O'Hara, M., 2003. Presidential address: Liquidity and price discovery. The Journal of Finance 58, 1335-1354

Shkilko, A., Sokolov, K., 2020. Every cloud has a silver lining: Fast trading, microwave connectivity and trading costs. Journal of Finance Forthcoming

Stoll, H.R., 1989. Inferring the components of the bid-ask spread: Theory and empirical tests. the Journal of Finance 44, 115-134

Ye, M., 2010. Non-execution and market share of crossing networks. Available at SSRN 1719016

Zhu, H., 2014. Do dark pools harm price discovery? The Review of Financial Studies 27, 747-789

Covid Economics 13, 4 May 2020: 91-137

Covid Economics 13, 4 May 2020: 91-137

Appendix A

This appendix lists the stocks included in the stock sample. The stocks are listed alphabetically using the ISINs.

ISIN	Company Name	Country
AT0000KTMI02	Pierer Mobility Ag	Austria
BE0003755692	Agfa-Gevaert Nv	Belgium
BE0003766806	Ion Beam Applications Sa Iba	Belgium
BMG671801022	Odfjell Drilling Ltd.	Norway
CH0001341608	Hypothekarbank Lenzburg Ag	Switzerland
CH0003390066	Mikron Holding Ag	Switzerland
CH0010754924	Schweiter Technologies Ag	Switzerland
CH0044781141	Gam Precious Metals - Physical Gold	Switzerland
CH0239518779	Hiag Immobilien Holding Ag	Switzerland
CH0386200239	Medartis Holding Ag	Switzerland
CH0406705126	Sensirion Holding Ag	Switzerland
DE0005103006	Adva Optical Networking Se	Germany
DE0006047004	Heidelbergcement AG	Germany
DE0006219934	Jungheinrich Ag	Germany
DE0006569908	Mlp Ag	Germany
DE000A1DAHH0	Brenntag AG	Germany
DK0016188733	Nykredit Invest Balance Defensiv	Denmark
DK0016188816	Nykredit Invest Balance Moderat	Denmark
DK0060010841	Danske Inv Mix Akk Kl	Denmark
DK0060027142	ALK-Abello A/S	Denmark
DK0060580512	Nnit	Denmark
DK0060642726	Maj Invest Value Aktier Akkumulerende	Denmark
DK0060738599	Demant	Denmark
DK0060946788	Ambu	Denmark
ES0171996095	Grifols, S.A.	Spain
ES0177542018	International Airlines Group	Spain
FI0009003727	Wärtsilä Oyj Abp	Finland
FI0009005870	Konecranes Abp	Finland
FI0009009377	Capman	Finland
FI0009010854	Lassila & Tikanoja Oyj	Finland
FI0009800643	Yit Oyj	Finland
FI4000074984	Valmet Oyj	Finland
FI4000312251	Kojamo Oyj	Finland
FR0000050353	Lisi	France
FR0000066672	Gl Events	France
FR0000073298	Ipsos	France
FR0010112524	Nexity	France
FR0010221234	Eutelsat Communications	France
FR0010908533	Edenred	France
FR0011471135	Erytech Pharma	France
GB0000163088	Speedy Hire	United Kingdom
GB0000904986	Bellway	United Kingdom
GB0001110096	Boot (Henry)	United Kingdom

GB0002018363	Clarkson	United Kingdom
GB0002634946	Bae Systems	United Kingdom
GB0004082847	Standard Chartered	United Kingdom
GB0004161021	Hays Plc	United Kingdom
GB0004270301	Hill & Smith Hldgs	United Kingdom
GB0006043169	Morrison(Wm.)Supermarkets	United Kingdom
GB0006640972	4imprint Group Plc	United Kingdom
GB0008085614	Morgan Sindall Group Plc	United Kingdom
GB0009465807	Weir Group	United Kingdom
GB0009633180	Dechra Pharmaceuticals	United Kingdom
GB0033195214	Kingfisher	United Kingdom
GB00B05M6465	Numis Corp	United Kingdom
GB00B0HZPV38	Kaz Minerals Plc	United Kingdom
GB00B0LCW083	Hikma Pharmaceuticals	United Kingdom
GB00B17BBQ50	Investec Plc	United Kingdom
GB00B17WCR61	Connect Group Plc	United Kingdom
GB00B1JQDM80	Marston's Plc	United Kingdom
GB00B1V9NW54	Hilton Food Group Plc	United Kingdom
GB00B1ZBKY84	Moneysupermarket.Com Group Plc	United Kingdom
GB00B4Y7R145	Dixons Carphone Plc	United Kingdom
GB00B63H8491	Rolls-Royce Hldgs Plc	United Kingdom
GB00B7KR2P84	Easyjet	United Kingdom
GB00B8460Z43	Gcp Student Living	United Kingdom
GB00BF4HYT85	Bank Of Georgia Group Plc	United Kingdom
GB00BG0TPX62	Funding Circle Holdings Plc	United Kingdom
GB00BG12Y042	Energean Oil & Gas Plc	United Kingdom
GB00BGLP8L22	Imi	United Kingdom
GB00BJGTLF51	Target Healthcare Reit Plc	United Kingdom
GB00BJTNFH41	Ao World Plc	United Kingdom
GB00BMSKPJ95	Aa	United Kingdom
GB00BYSS4K11	Georgia Healthcare Group Plc	United Kingdom
GB00BYYW3C20	Forterra Plc	United Kingdom
GB00BZ1G4322	Melrose Industries	United Kingdom
GB00BZ3CNK81	Torm Plc	United Kingdom
GB00BZ6STL67	Metro Bank	United Kingdom
GB00BZBX0P70	Gym Group Plc	United Kingdom
GG00B4L84979	Burford Capital Ltd	United Kingdom
IE00BD5B1Y92	Bank Of Cyprus Holdings PLC	Ireland
IE00BDQYWQ65	Ishares	Ireland
IM00B5VQMV65	Gvc Holdings Plc	United Kingdom
IT0000076502	Danieli & C. Officine Meccaniche Spa	Italy
IT0001447348	Mittel	Italy
IT0003007728	Tod S Spa	Italy
IT0004053440	Datalogic	Italy
IT0004056880	Amplifon Spa	Italy
IT0005331019	Carel Industries	Italy
JE00B2419D89	Breedon Group Plc	United Kingdom
JE00BG6L7297	Boohoo.Com Plc	United Kingdom
JE00BJVNSS43	Ferguson Plc	United Kingdom

Covid Economics 13, 4 May 2020: 91-137

LI0315487269	Vpb Vaduz	Liechtenstein
LU0569974404	Aperam S.A	Luxembourg
NL0000339703	Beter Bed Holding Nv	Netherlands
NL0010733960	Lastminute.Com	Netherlands
NL0011832936	Cosmo Pharmaceuticals N.V.	Netherlands
NO0003053605	Storebrand Asa	Norway
NO0010593544	Insr Insurance Group	Norway
NO0010663669	Magseis	Norway
SE0000103699	Hexagon Aktiebolag	Sweden
SE0000105199	Haldex	Sweden
SE0000163628	Elekta Ab (Publ)	Sweden
SE0000379497	Semcon	Sweden
SE0000426546	New Wave	Sweden
SE0005468717	Ferronordic Machines Ab	Sweden
SE0006593919	Klovern	Sweden
SE0009921588	Bilia	Sweden
SE0010468116	Arjo Ab B	Sweden
SE0010948588	Bygghemma Group First Registered	Sweden

Covid Economics 13, 4 May 2020: 91-137

Covid Economics Issue 13, 4 May 2020

Do lockdown and testing help in curbing Covid-19 transmission?

Akbar Ullah[1] and Olubunmi Agift Ajala[2]

Date submitted: 26 April 2020; **Date accepted:** 27 April 2020

This study investigates the effectiveness of lockdown and testing in curbing the transmission of Covid-19 infection. Using a combination of data from the European Centre for Disease Prevention, Roser et al. (2020) and Hale et al. (2020), we carried cross-country analysis covering 69 countries across the 5 continents. To take care of the fact that the number of Covid-19 cases strongly depend on its own lag values, we used two-step system GMM for the estimations. Unlike prior studies that measure lockdown in terms of a fixed intervention date, we relied on the stringency index from Hale et al. (2020) that accommodates for the gradual lockdown measures in different countries. We found that an exogenous lockdown significantly affects the number of confirmed cases after 7 days of its implementation and its lag effects are intact even after 21 days of its implementation. A one unit change in the lockdown index decreases the total number of confirmed cases by 0.19 percent. Testing has no significant effects for at least 14 days after its implementation. However, after 21 days of its implementation, its effects become significant with −0.03 to −0.05 elasticity value.

Covid Economics 13, 4 May 2020: 138-156

1 Research Associate, School of Health Sciences, University of Manchester.
2 Assistant Lecturer, School of Economics, Finance & Accounting, Coventry University.

Covid Economics 13, 4 May 2020: 138-156

1. Introduction

The Coronavirus (Covid-19) crisis has become a universal problem within a time span of three months. To flatten the pandemic curve, many countries around the globe have intervened with measures such as social distancing, school and business closures, restrictions on travel, cancellations of sports and other public events and testing and contact tracing. This has led to immediate economic hardships for both households and businesses and is likely to create severe global economic downturn[1]. While some countries like China and South Korea are on the falling tail of the curve, many countries are experiencing or still waiting for the peak of the pandemic curve. Unfortunately, the problem is not over even for those experiencing a fall in the cumulative Coronavirus cases let alone those who are still on the rising part of the curve. After removal of the so-called lockdown, which cannot be sustained for a long time given its economic costs, the cases may resurge. Moreover, it is not clear entirely that those who are infected develop immunity from the virus. Thus, until a vaccine is developed and is widely available, a clever mix of intervention measures would be needed to balance the health and economic costs of the pandemic.

Therefore, examining the effectiveness of the different intervention measures in curbing transmission of the virus will help not only in controlling the spread of the virus in the future but in reducing the economic costs of future interventions. In this study, we estimate the impacts of the government interventions in slowing down the spread of the virus for a sample of 69 countries. For each country, we consider the time period from the date of its first positive Coronavirus case until 18 April, 2020. Given their different social and economic implications, we divide the intervention measures into two groups: lockdown and testing and contact tracing. Our lockdown measure includes school, workplace and public transport closing, cancellation of public events, restrictions on internal and international travels, and public information campaign. The data on the number of confirmed Coronavirus cases is taken from the European Centre for Disease Prevention and Control, while data on the total tests conducted is taken from Roser et al. (2020). The other intervention measures data is taken from Hale et al. (2020).

[1]Intentional Monetary Fund predicts the 2020 global GDP growth to be −3.0% due to what they call the great lockdown and cumulative output loss of $9 trillion over 2020-21, far greater impacts as compared to the global financial crisis of 2009 (IMF, 2020). For example, in the week ending on April 11, the number of unemployment benefits claims was 5.25 million in the US. The previous week unemployment benefits claims number was 6.6 million: https://oui.doleta.gov/unemploy/DataDashboard.asp.

Covid Economics 13, 4 May 2020: 138-156

The results from fixed and random effects estimations show that both lockdown and testing play a significant role in slowing down the transmission of the virus. Both the policy interventions have affected the total number of confirmed cases after 7 days of its implementation and their effects remain even after 21 days of the initial implementation. However, fixed or random effects estimations may be biased due to the dynamic nature of the virus spread. To overcome this problem, we run system GMM method of estimation. Under the assumption that the policy interventions are exogenous, the results from the GMM show that lockdown still affects the spread of the virus after 7 days of its implementation and its effects are intact even after 21 days, though the latter effects are quite weaker. A one unit change in the lockdown index decreases the total number of confirmed cases by 0.19 percent. Under the GMM estimations, testing has no significant effects for at least 14 days after its implementation. After 21 days, its effects become significant with -0.03 elasticity value. Under the assumption of endogenous policy response, testing still has significant effects after 21 days, but the lockdown variable becomes insignificant. However, it is mainly due to the low variation in the lockdown index.

Existing studies that try to estimate the effects of government intervention on the spread of Covid-19 are Hartl et al. (2020) for Germany and Qiu et al. (2020) for China. In these studies, intervention is measured in terms of a fixed intervention date and the pre and post intervention date growths of the confirmed cases are compared. However, intervention measures are introduced gradually in almost all the countries and deciding a fixed date of intervention is quite arbitrary. Furthermore, the Covid-19 cases follow a strong dynamics; the curve first increases exponentially with time, flattens and then starts falling rapidly. Hartl et al. (2020) fail to include such dynamics in their study. On the other hand, the intervention measures in China are deemed extreme in many European countries and US. The existing study is based on a rich panel dataset of 69 countries and a number of intervention measures, besides extending the study period to 18 April, 2020. Moreover, the panel nature of the study allows us to control for the country fixed effects and problems of endogeneity.

Rest of the study is organised as follow. Section 2 discusses data construction and descriptive statistics. Section 3 presents the estimation strategy. Section 4 presents results and section 5 concludes the study.

Covid Economics 13, 4 May 2020: 138-156

2. Data and Summary Statistics

2.1. **Data Sources and Lockdown Index.** In this subsection, we discuss data sources and the construction of the lockdown index. The data for the study is taken from three different sources. The data on the number of confirmed cases is available from different sources such as Johns Hopkins University, the European Centre for Disease Prevention and Control, etc. We collected this data from the European Centre for Disease Prevention and Control and cross checked against other sources to find it consistent. Data on the number of tests conducted is taken from Our World in Data project, gathered by Roser et al. (2020). They have gathered this data from the national official sources for each country[2]. One limitation of this data is that it is not clear for some countries whether the number of tests show the total number of tests or total number of people tested, as some people may be tested more than once. However, given that the success to find and trace infected people depends on the number of tests conducted, it is important to consider this variable. Moreover, this issue is unlikely to affect our findings in any significant way.

The data on the lockdown measures is taken from the 'Oxford Covid-19 Government Response Tracker' project gathered by Hale et al. (2020). Based on the information Oxford students and staff collected from around the globe, they have constructed ordinal measures on the school, workplace and public transport closing, cancellation of public events, restrictions on internal and international travels, public information campaign, testing, contact tracing, emergency investment in health care and vaccine for all the countries. They have also included data on the monetary and fiscal measures as a response to the Covid-19.

Out of these variables, we have picked the first seven measures, i.e. the school, workplace and public transport closing, cancellation of public events, restrictions on internal and international travels and public information campaign and call it lockdown. It is because these measures involve restricting the movement of all or a large proportion of people and goods. Implementing these measures may involve no or little initial costs for the governments but involve huge socio-economic costs in the form of output and employment losses, loss in government tax revenues and possible health costs for the public due to forced stay at home obligations[3]. On the other hand, testing and contact tracing involve initial costs for the government but has likely far less economic impacts as compared to the lockdown. For

[2]This data and the details of the national resources is available from OurWorldInData.org/covid-testing.
[3]See IMF (2020) for detailed predictions on the output losses.

example, many think that the success of South Korea in curbing the virus relatively better is due to their aggressive testing and contact tracing. Thus, our main focus is to investigate the effectiveness of lockdown versus testing in curbing the transmission of Covid-19.

All the sub-measures of lockdown are constructed with a value of 0 means no measure in place and 2, for some measures 3, means strict measure in place. Additionally, for all the measures except international travel, an additional binary variable is defined with a value of 0 means that the measure is in place in a specific geographic area and 1 means that the measure covers the whole country. Hale et al. (2020) have used the above seven measures to construct what they call government response stringency index, and we call it lockdown. The index is constructed as follow. Suppose that each of the lockdown measure is denoted by X_j and its generality by $G_j \in \{0, 1\}$. Suppose that X_j can take a value ranging from 0 to N_j. Then, the measures other than the international travel can be converted into an index as $Z_j = 100\frac{X_j+G_j}{N_j+1}$ for $j \leq 6$. The international travel index can take a value of $Z_7 = 100\frac{X_7}{N_7}$. The lockdown index is finally constructed as the simple average of the seven measures as $L = \frac{\sum_{j=1}^{7} Z_j}{7}$. To be consistent with other possible studies on this data we use this index as it is in the analysis.

2.2. **Descriptive Statistics.** In this subsection, we present the summary statistics of countries analysed in our study. We also present daily and weekly distributions of the total confirmed cases, lockdown index and the total number of tests conducted. Likewise, we present the geographical visualisation of our key variables.

As stated in the introduction, for each country, we consider the time period from the date of its first positive Coronavirus case until 18 April, 2020. Moreover, we exclude countries that do not have data on testing in our analysis. Our source data has obseravtions for 135 countries. Our data cleaning process resulted in 69 countries across the 5 continents with observations for a maximum time period between February 21, 2020 and April 18, 2020. Table 4 in the appendix, shows the summary of countries for our analysis by continents. Europe makes up about 39% of countries and about 43% of observations in our sample. Countries from the Asian continent make up 22.5%, about 21% from the Americas while Africa and the Oceania make up about 14% of the remaining sample in our data.

Using the number of confirmed cases, we rank countries by calculating the average number of confirmed cases over period of days in our data and present the top 10 affected countries

Covid Economics 13, 4 May 2020: 138-156

and the least 10 affected countries. Table 1, shows that the US has the highest number of confirmed cases, while Nepal has the lowest prevalence ranking. European countries make up 7 out of the 10 top affected countries with no country from Europe in the low 10 countries with prevalence.

Table 1. Ranking of Countries by number of Confirmed Cases

Ranking	Top -10 Countries	Least - 10 Countries
1	United States	Nepal
2	Spain	Ethiopia
3	Italy	Uganda
4	Germany	Paraguay
5	Turkey	Kenya
6	Switzerland	El Salvador
7	United Kingdom	Vietnam
8	Netherlands	Senegal
9	Canada	Bolivia
10	France	Taiwan

*Notes:*Data sourced from the European Centre for Disease Prevention and Control, Roser et al. (2020) and Hale et al. (2020). We exclude countries with no testing and those with no observations for total confirmed cases. Column 2 = Top 10 countries in terms of prevalence ranking. Column 3 = Least 10 countries in terms of prevalence ranking. We computed our ranking using average number of confirmed cased daily over the period of data collected.

Utilising averages of countries across weeks, Table 5 in the appendix, enables us to observe the trends of total cases, stringency of lockdown and testing across the globe. Intervention by countries, measured by lockdown and testing, show increasing trends as number of the total confirmed cases increases. Total cases for the first 6 weeks is 33% of the cases recorded in only the week 7, while total prevalence for the first 7 weeks is about 58% of cases recorded only in the 8th week. The spike continues by the 11th week, average prevalence is about 132% of cumulative cases for previous 10 weeks.

In the below figures we plot the three key variable of our study, namely total confirmed cases, lockdown index and total tests conducted. Figure 1, shows the trend of cases. Figure 1(a), shows the daily trend of cases. The image confirms the upward trend in the number of confirmed cases. Both sub-figures (b) and (c) of Figure 1, show a surge in cases in week 9 of our data. This surge translates to 99% increase against 37% increase the previous week. The trend shows 175% increase in cases between week 9 and 10, in Table 5. Similar review of intervention (measured by lockdown index) in Figure 2, shows that intervention was relatively flat until the seventh week, when lockdown index picked up and moved above 50

Covid Economics 13, 4 May 2020: 138-156

points (71.50) in Table 5 . Figure 2(c), shows that intervention response was not proportional to prevalence rate within the first six weeks.

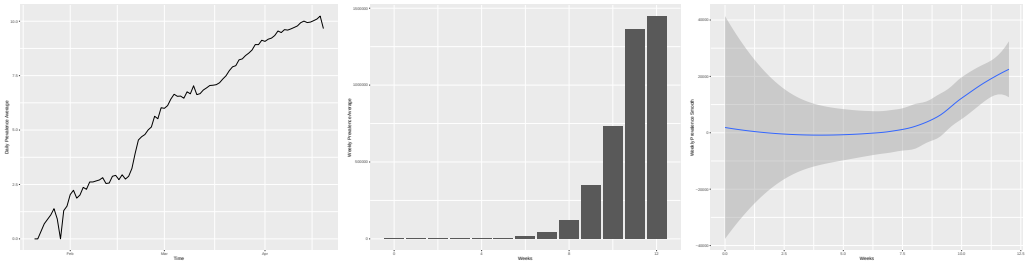

(a) Daily Prevalence **(b)** Weekly Prevalence **(c)** Prevalence Smooth

Figure 1. Plots of Total cases

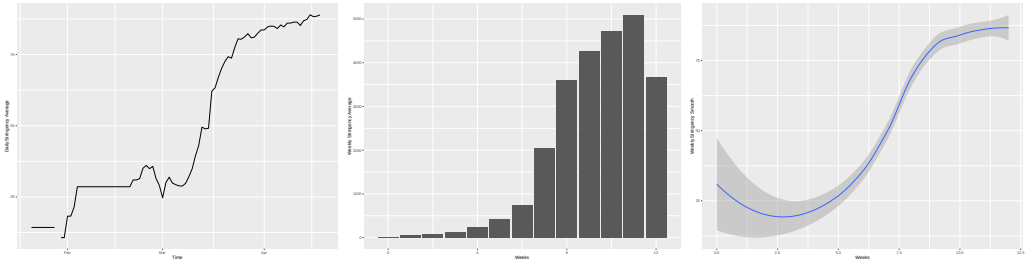

(a) Daily Stringency **(b)** Weekly Stringency **(c)** Stringency Smooth

Figure 2. Plots of lockdown Index

Column 4 of Table 5 and Figures 3(a, b and c), further confirm that testing also did not record upward surge until week 9 of our series when it recorded about 62% increase compared with 11% increase in testing the previous week.

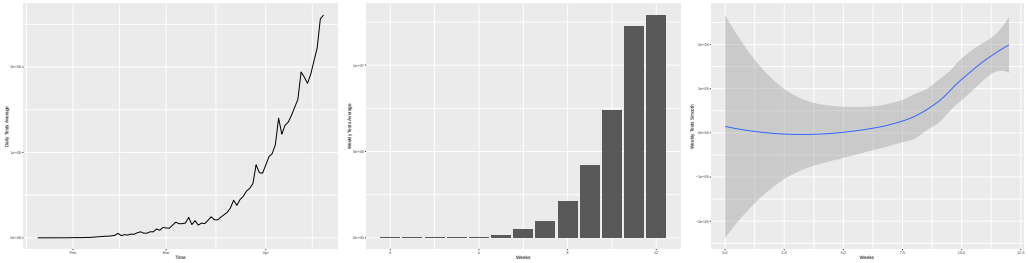

(a) Daily Tests **(b)** Weekly Tests **(c)** Tests Smooth

Figure 3. Plots of Tests

Covid Economics 13, 4 May 2020: 138-156

Covid Economics 13, 4 May 2020: 138-156

The overall scenario is presented in geographical visualisation of prevalence, lockdown and tests for the period under study in Figure 4. The United States has the highest density while Europe has high cluster of countries (judging from the country-name text) in the prevalence map. Africa and Oceania seem under-represented but the map reflects the actual prevalence level across continents. Comparing prevalence and lockdown, the United States and Australia seemed to have lighter density in terms of lockdown when compared with their respective prevalence density. Countries in Africa and Asia seemed to have stronger lockdown density than prevalence density in their respective countries while Canada seemed to have proportionate density in prevalence and in lockdown. In terms of testing, the United States and Canada seemed to be matching the density of prevalence while Russia seemed to have higher density of testing relative to the density of the prevalence.

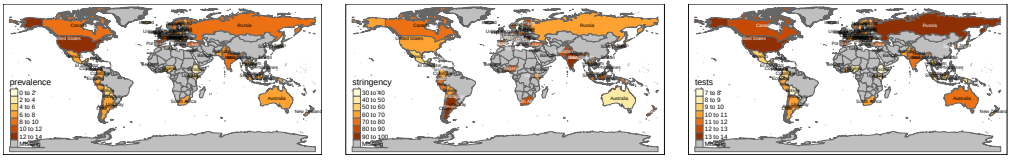

(a) Prevalence Map **(b)** Stringency Map **(c)** Tests Map

Figure 4. Geographical Visualisation of Prevalence, Lockdown and Tests

3. Model and Estimation Strategy

To better understand the rationale behind the econometric specification, we briefly discuss the epidemiological model of a contagious disease. Under the simplifying assumptions of homogenous population and that those who have been previously infected are no longer susceptible, the simple epidemiological SIR model (Kermack and McKendrick, 1927; Allen, 2017) gives the following contagion dynamics

$$\Delta S_t = -\beta I_{t-1} \frac{S_{t-1}}{M_{t-1}}, \tag{1}$$

$$\Delta I_t = [\beta \frac{S_{t-1}}{M_{t-1}} - \gamma] I_{t-1}, \tag{2}$$

$$\Delta R_t = \gamma I_{t-1}, \tag{3}$$

where S_t is the number of susceptible, I_t is the number of infected, R_t is the number of recovered, and M_t is the total population at time t. The coefficient β is the contact or transmission rate and γ is the recovery rate.

This is a simplest possible version of contagion dynamics but convey an important message. That is, an important determinant of the infection rate is its own lag values. According to Equation (2), the infection will increase faster when the susceptible population is high, and the infected population has reached a certain threshold. Thus, in a regression analysis, not including lag(s) of the number of the infections among the explanatory variables can lead to misleading results. Instead of estimating the above structural model as in the epidemiological studies, we estimate a reduced form econometric model to identify the effects of the policy intervention on the number of confirmed cases. This is because we are interested in measuring the total effects of the policy intervention on the number of confirmed cases instead of studying the underlying structural transmission mechanisms. To this end, since total cases are less than 1% or 0.1% of the population in most of the countries and there is no evidence that those recovered are immune to the virus, therefore, the ratio $\frac{S_t}{M_t}$ is stable over time and effectively $\frac{S_t}{M_t} \equiv 1$. Thus, Equation (2) can be written as $\Delta I_t = \Phi I_{t-1}$, where $\Phi = \beta - \gamma$. Now policy intervention can change Equation (2) as $\Delta I_t = \Phi\theta_{t-q} I_{t-1}$, where $\theta_{t-q} \in (0, 1]$ is the policy parameter[4]. We specify $\theta_t = \frac{1}{T_t e^{L_t}}$ to keep it in between zero and one[5]. Thus, taking log in discrete time and including international transmission factor, we can get a simple log linearised model as bellow

$$lnI_{it} = \alpha_0 + lnI_{it-1} - L_{it-q} - lnT_{it-q} + ln\frac{\sum_{j\neq i}^{N_{(t-q)}-1} I_{jt-q}}{N_{(t-q)} - 1} + \mu_{it}, \tag{4}$$

$$\mu_{it} = \alpha_i + \epsilon_{it},$$

Where lnI_{it} denotes natural log of the total number of cases in country i at time t, L_{it-q} denotes the severity of the lockdown in country i at time period $t-q$, T_{it-q} denotes the total number of tests conducted or people tested, $\bar{I}_{jt-q} = \frac{\sum_{j\neq i}^{N_{(t-q)}-1} I_{jt-q}}{N_{(t-q)}-1}$ denotes the mean number of cases in all the countries except country i, a_i denotes time invariant country characteristics and ϵ_{it} is the random error term. According to this specification, the current

[4]Government intervention can affect both the transmission and recovery rates through distancing and investment in health facilities for example.

[5]Where T_t and L_t are testing and lockdown, respectively, as defined in the next paragraph. Since each country data begins with the first reported case in our sample, this implies that $T_t \geq 1$ as the first case can be confirmed only after first test is conducted. This specification implies that severity of intervention decreases θ_t value.

Covid Economics 13, 4 May 2020: 138-156

number of infections depend on the lag infections, status of government policy interventions, the average number of cases in other countries and fixed country characteristics like location, population density, ageing population etc. Since time span of the study is short, we expect a_i to capture many country characteristics. Also this log linear specification is consistent with other studies in this area (Qiu et al., 2020).

The incubation period of Coronavirus varies greatly from person to person but many studies seem to suggest a mean incubation period between 5-6 days. For example, Lauer et al. (2020) show that the median incubation period of Coronavirus is 5.1 days, based on 181 cases. The mean incubation period is 5.2 days in Li et al. (2020) covering 425 cases. Similarly, WHO (2020) suggests a mean incubation period of 5-6 days. Furthermore, the average infectious period is found to be 1.4 days (Wu et al., 2020). Thus, one must wait for at least one week to see the effects of policy interventions. Given this, we take a q value of at least 7. We then check for further lags, particularly the effects of the policy interventions at the end of second and third weeks once it is implemented.

In Equation (4), even if the policy variables are uncorrelated with a_i and ϵ_{it}, lnI_{it-1} is correlated with a_i since lnI_{it-1} contains a_i for all t. This means that lnI_{it-1} is correlated with μ_{it}. This implies that ordinary least square gives biased and inconsistent results. For a fixed time span, the fixed effects estimator is also biased and inconsistent as N increases (Nickell, 1981; Bond, 2002; Phillips and Sul, 2003). To solve this problem the standard approach is the Generalised Method of Moments (GMM) approaches of Arellano and Bond (1991) and Blundell and Bond (1998). The Arellano and Bond (1991) difference GMM uses first difference of Equation (4) to eliminate the fixed effects a_i as

$$\Delta lnI_{it} = \Delta lnI_{it-1} - \Delta L_{it-q} - \Delta lnT_{it-q} + \Delta ln\bar{I}_{jt-q} + \Delta\epsilon_{it}. \tag{5}$$

If ϵ_{it} is serially uncorrelated, then $E(lnI_{it-2}, \Delta\epsilon_{it}) = 0$. This ensures that lnI_{it-2} and earlier values can be used as instruments for ΔlnI_{it-1}. The problem with the difference GMM is that the lagged levels of regressors would be weak instruments for the regressors in first differences if a variable has high degree of persistent, as is the lockdown index in our case. The problem of weak instruments can lead to a bias in finite samples. The system GMM (Blundell and Bond, 1998, 2000) solves this problem by introducing an additional estimation

Covid Economics 13, 4 May 2020: 138-156

equation in the levels of the variables. The variables in the level equation are instrumented with their first differences. This leads to a more efficient estimation than the difference GMM (Baltagi, 2008). On the other hand, the week point of the system GMM is that it uses too many instruments which can reduce the power of the Hansen test, leading to frequent acceptance of the null hypothesis of instruments validity. Keeping this, we rely on as few instruments as possible and collapse the instruments matrix by combining the instruments (Roodman, 2009). Moreover, in all the GMM estimations, we use the two-step estimator to correct for the finite sample standard error (Windmeijer, 2005). The results are presented in the next section.

4. Results and Discussion

For comparison purpose, we present the estimation results from fixed effects, random effects and GMM estimations. The most reliable approach for our econometric specification is the one recommended by Blundell and Bond (2000). Thus, we will mostly rely on the results from the system GMM estimations. Table 2 reports the estimation results of Equation (4) from fixed effects, random effects methods. After controlling for time-invariant country characteristics and time effects common to all countries, and by including only lag of total confirmed cases, one can see from Column 1 that a one percent increase in new infections today leads to 0.94 percentage point more cases the next day. This implies that lag infections are an important predictor of the current cases of Coronavirus as is well known from the epidemiological models. Adding lag 7 of the lockdown index as an additional variable increases the coefficient on the lag total cases even further as is shown in Column 2. As expected, the coefficient on the lag lockdown is negative and highly significant. It implies that a 1 unit increase in the lockdown index will decrease the total infection by 0.14 percent after 7 days.

When the 7^{th} lag of mean number of confirmed cases in the other countries is added into the regression, the other coefficients are not affected by significant amount. The coefficient of the lag mean itself is very high and statistically significant. However, in later specifications it becomes insignificant. When the 7^{th} lag of the total number of tests conducted is added in Column 4, the coefficient of the lag total confirmed cases goes above one and the coefficient of the lag of mean cases in the other countries becomes insignificant at the 5% level of significance. The coefficient of the lag total tests is negative and highly significant. This

Covid Economics 13, 4 May 2020: 138-156

Table 2. Fixed/Random Effects

Variables	(1) FE	(2) FE	(3) FE	(4) FE	(5) RE	(6) FE	(7) FE
lnI_{it-1}	0.9427***	0.9884***	0.9956***	1.0016***	1.0106***	1.0054***	0.9931***
	(0.000)	(0.000)	(0.000)	(0.000)	(0.000)	(0.000)	(0.000)
L_{it-7}		-0.0014***	-0.0015***	-0.0013***	-0.0013***		
		(0.003)	(0.001)	(0.003)	(0.000)		
$ln\bar{I}_{jt-7}$			4.2313**	3.2622*	3.0878*		
			(0.040)	(0.075)	(0.063)		
lnT_{it-7}				-0.0242**	-0.0162**		
				(0.024)	(0.020)		
L_{it-14}						-0.0012**	
						(0.021)	
$ln\bar{I}_{jt-14}$						0.0164	
						(0.395)	
lnT_{it-14}						-0.0247**	
						(0.037)	
L_{it-21}							-0.0008**
							(0.015)
$ln\bar{I}_{jt-21}$							0.0413***
							(0.003)
lnT_{it-21}							-0.0216***
							(0.001)
Constant	-0.0968**	0.0544*	-19.9689**	-15.3983*	-14.5541*	0.2030*	-0.0059
	(0.027)	(0.058)	(0.041)	(0.075)	(0.064)	(0.061)	(0.951)
Observations	2,063	1,523	1,523	1,523	1,523	1,244	927
R-squared	0.996	0.997	0.998	0.998		0.997	0.997
Number of country	64	53	53	53	53	52	48
Time dummies	yes	yes	yes	yes	yes	no	no

Notes: *** Significant at 1%; ** significant at 5%; * significant at 10%. We report heteroskedasticity robust $p-$values in parentheses. Dependent variable is natural log of total cases lnI_{it}, L_{it-q} is lag of lockdown index, lnT_{it-q} is log of total tests at a specific lag and $ln\bar{I}_{jt-q}$ is log of average cases in other countries at a given lag. Data sourced from the European Centre for Disease Prevention and Control, Roser et al. (2020) and Hale et al. (2020). Columns 1, 2, 3, 4, 6 &7 are fixed effects estimates. Column 5 is random effects estimates. The estimated coefficients of the full set of day's effects are not reported for the sake of brevity and are available from the authors upon request.

implies that a 1 percent increase in the number of total tests will decrease the total infection by 0.024 percentage points after 7 days. Estimation with random effects method in Column 5 brings very little difference in the coefficients and its significance as compared to the fixed effects estimations.

Next, when we include 14th lags of the lockdown and total testing into the regression instead of the 7th lags, the coefficient of the lockdown became smaller and insignificant in the presence of time dummies, and the coefficient of the total tests is still significant. However, the time dummies were highly insignificant in that specification[6]. With no time dummies in Column (6), the coefficients of both the lockdown and total testing are exactly the same as under the 7th lags and are significant. Upon including 21st lags, the only difference is that the coefficient of the lockdown becomes smaller and the coefficient of the mean number of confirmed cases smaller but now significant. However, as mentioned earlier, the results in Table 2 carry potential bias due to the presence of the lag dependent variable in the regression. To address this problem, we have carried estimations with system GMM estimator. Our conclusion is

[6]Note that in Columns (4-5) most of the time dummies are significant only at 10% significant level.

Covid Economics 13, 4 May 2020: 138-156

based on the GMM results, as the lag dependent variable is highly significant in all the above estimations.

The results from system GMM estimations are presented in Tables 3 and 6. Table 3 presents results with only lag dependent variable treated as endogenous[7]. First of all, note that the Arellano-Bond test rejects the null of serial correlation in $AR(1)$. This implies that the condition $E(lnI_{it-2}, \Delta\epsilon_{it}) = 0$ is satisfied. Next, both Hansen and Sargan tests cannot reject the null of instruments validity in Column 1. From Column 1, One can see that now a one percent increase in new infections today leads to 1.06 percentage points more cases the next day. Now the coefficient on the lag 7 of the lockdown is negative and significant at 10% level of significance only. It implies that a 1 unit increase in the lockdown index will decrease the total infections by 0.19 percent after 7 days. The coefficient of the lag 7 of total tests is negative, high as compared to earlier but statistically insignificant. Similarly, the the coefficient of the mean number in the other countries at lag 7 is now negative and significant. This last result is unexpected.

Table 3. System GMM with Exogenous Policy Intervention

Variables	(1) 1-Week	(2) 2-Weeks	(3) 3-Weeks
	(1)	(2)	(3)
Variables	1-Week	2-Weeks	3-Weeks
lnI_{it-1}	1.0609***	1.0191***	1.0385***
	(0.000)	(0.000)	(0.000)
L_{it-7}	-0.0019*		
	(0.080)		
$ln\bar{I}_{jt-7}$	-0.0334**		
	(0.011)		
lnT_{it-7}	-0.0563		
	(0.167)		
L_{it-14}		-0.0012***	
		(0.007)	
$ln\bar{I}_{jt-14}$		-0.0098	
		(0.257)	
lnT_{it-14}		-0.0242	
		(0.114)	
L_{it-21}			-0.0005**
			(0.040)
$ln\bar{I}_{jt-21}$			0.0634**
			(0.013)
lnT_{it-21}			-0.0325***
			(0.002)
Constant	0.6599***	0.3349***	104.6265***
	(0.000)	(0.000)	(0.001)
Time trend	no	no	yes
Observations	1,523	1,244	927
Number of country	53	52	48
AR(1) p-value	0.00282	0.00212	0.0529
AR(1) p-value	0.253	0.673	0.621
Hansen test p-value	0.901	0.545	0.771
Sargan test p-value	0.895	0.542	0.378

Notes: *** Significant at 1%; ** significant at 5%; * significant at 10%. We report $p-$values robust to heteroskedasticity in parentheses. Dependent variable is natural log of total cases lnI_{it}, L_{it-q} is lag of lockdown index, lnT_{it-q} is log of total tests at a specific lag and $ln\bar{I}_{jt-q}$ is log of average cases in other countries at a given lag.
GMM-type instruments in Columns 1-3: lag2-lag4 of lnI_{it} collapsed.
Data sourced from the European Centre for Disease Prevention and Control, Roser et al. (2020) and Hale et al. (2020).

[7]For the discussion of whether the policy variables should be treated exogenous, see the discussion at the end of this section

Covid Economics 13, 4 May 2020: 138-156

Column 2 reports results at the 14th lags of the exogenous variables. Once again all the specification tests are satisfied. Now, the coefficient of the lockdown is relatively small but highly significant. The coefficient of the lag total tests is exactly the same as under fixed effects estimation but still statistically insignificant. The coefficient of the mean number in the other countries now becomes insignificant. At the 21st lag in Column 3, all the variables becomes statistically and economically significant and take expected signs. The coefficient on the lag 21 of the lockdown is negative and significant at 5% level of significance. It implies that a 1 unit increase in the lockdown index will decrease the total infections by 0.05 percent after 21 days. The coefficient of the total tests at lag 21 is negative and statistically significant. This implies that a 1 percent increase in the number of total tests will decrease the total infection by 0.03 percentage points after 21 days. Similarly, the coefficient of the mean number in the other countries at lag 21 is now positive and significant.

If the lags of policy interventions are endogenous, then treating it exogenous in the estimation can create biased results (the bias can be upward or downward). We have checked for such an endogeneity and the results are reported in Table 6 in the appendix. Now with lags 7 and 14, only the lag dependent variable is high in magnitude and statistically significant. At the 21st lag, only the coefficient of the lockdown is statistically insignificant. The coefficient of the total tests at lag 21 is negative and statistically significant. It implies that a 1 percent increase in the number of total tests will decrease the total infection by 0.05 percentage points after 21 days. Now the mean number of cases in the other countries have positive and significant effects on the total confirmed cases in the country in question. Though insignificant, the coefficient of lockdown is on average higher under the endogenous treatment.

Thus, with the assumption that the lags policy variables are exogenous, lockdown starts affecting the transmission after 7 days of its implementation and its effects are intact even after 21 lags. The testing variable effects the transmission with quite delay, it cannot affect the transmission significantly for at least after 14 days of its implementation. The main difference under the assumption of endogenous policy changes is in the significance of the lockdown. The lockdown's coefficient is mostly insignificant under the assumption of endogenous policy changes. However, this seems to be due to the fact that the lockdown index has very little variation over time for many countries. With lags and differencing, it losses most of its variation for many countries, and hence its significance. Moreover, the assumption of the endogenous policy change is not common in the literature as it is a political decision

Covid Economics 13, 4 May 2020: 138-156

most of the time. Given this, the other papers that try to estimate the effects of lockdown on the Covid-19 transmission take the policy variable exogenous (Hartl et al., 2020; Qiu et al., 2020). Additionally, we include policy variable with a lag of at least 7 days. This also decreases the possibility of endogeneity. Given that endogenous treatment of testing does not change its significance further strengthens our belief about this, as testing variable has proper variation and instrumentation of it does not create any variation issue in the case of this variable. Finally, though significant, the effects of both the policy variables are small in magnitude.

5. Conclusion

The realisation that the panacea for the COVID-19 epidemic may be remote necessitates the need, to find the optimal blend of policy interventions that could minimise costs of resulting economic disruptions. Though the epidemic remains a worldwide topical issue, analysts and policy makers are constrained by insufficient data to undertake robust analysis as it is a new emergence. Inaction in an anticipation of herds immunity is considered costly, in terms of likely loss of lives and subsequent effects on the labour market and health systems. Likewise, a stringent policy combining closing of schools and workplaces, cancelling of public events, closing public transports, commencing public campaign, restricting internal movement and controlling international travels is also considered economically costly. Thus, the intervention policy must put measures in place that are both effective in curbing the transmission of the virus and create least possible economic damage.

Our analysis confirms that a marginal increase in the stringency index (lockdown) reduces the number of confirmed Coronavirus cases by 0.19 percentage points after one week of its implementation. We do not find any evidence that testing can affect the spread of the virus during the first two weeks. Still, it has significant effects in reducing the virus spread at the end of the third week of its implementation. Though both the policies are effective, their impact is small in magnitude. The main factor behind the number of the confirmed cases of virus is its own past values as predicted by the SIR model of epidemiology. While due caution is required in generalising the conclusion from any analysis, as the total number of confirmed cases depends on the number of tests conducted, our results indicate that for getting immediate results lockdown is relatively more effective in terms of controlling the spread of the virus. On the other hand, in the long terms, testing can play effective role

Covid Economics 13, 4 May 2020: 138-156

curbing the spread of the virus. Thus, testing and contact tracing can prove an effective tool in controlling the re-emergence of the pandemic.

References

Allen, L. J. (2017). A primer on stochastic epidemic models: Formulation, numerical simulation, and analysis. *Infectious Disease Modelling*, 2(2):128–142.

Arellano, M. and Bond, S. (1991). Some tests of specification for panel data: Monte carlo evidence and an application to employment equations. *The review of economic studies*, 58(2):277–297.

Baltagi, B. (2008). *Econometric analysis of panel data*. John Wiley & Sons.

Blundell, R. and Bond, S. (1998). Initial conditions and moment restrictions in dynamic panel data models. *Journal of econometrics*, 87(1):115–143.

Blundell, R. and Bond, S. (2000). Gmm estimation with persistent panel data: an application to production functions. *Econometric reviews*, 19(3):321–340.

Bond, S. R. (2002). Dynamic panel data models: a guide to micro data methods and practice. *Portuguese economic journal*, 1(2):141–162.

Hale, Thomas, Webster, S., Petherick, A., Phillips, T., and Kira, B. (2020). Oxford covid-19 government response tracker. *Blavatnik School of Government*. https://www.bsg.ox.ac.uk/research/research-projects/coronavirus-government-response-tracker.

Hartl, T., Wälde, K., and Weber, E. (2020). Measuring the impact of the german public shutdown on the spread of covid19. *Covid economics, Vetted and real-time papers, CEPR press*, 1:25–32.

IMF (2020). *World Economic Outlook, April 2020: Chapter 1*. International Monetary Fund, Washington, D.C.

Kermack, W. O. and McKendrick, A. G. (1927). A contribution to the mathematical theory of epidemics. *Proceedings of the royal society of london. Series A, Containing papers of a mathematical and physical character*, 115(772):700–721.

Lauer, S. A., Grantz, K. H., Bi, Q., Jones, F. K., Zheng, Q., Meredith, H. R., Azman, A. S., Reich, N. G., and Lessler, J. (2020). The incubation period of coronavirus disease 2019 (covid-19) from publicly reported confirmed cases: estimation and application. *Annals of internal medicine*.

Covid Economics 13, 4 May 2020: 138-156

Li, Q., Guan, X., Wu, P., Wang, X., Zhou, L., Tong, Y., Ren, R., Leung, K. S., Lau, E. H., Wong, J. Y., et al. (2020). Early transmission dynamics in wuhan, china, of novel coronavirus–infected pneumonia. *New England Journal of Medicine*.

Nickell, S. (1981). Biases in dynamic models with fixed effects. *Econometrica: Journal of the Econometric Society*, pages 1417–1426.

Phillips, P. C. and Sul, D. (2003). Dynamic panel estimation and homogeneity testing under cross section dependence. *The Econometrics Journal*, 6(1):217–259.

Qiu, Y., Chen, X., and Shi, W. (2020). Impacts of social and economic factors on the transmission of coronavirus disease 2019 (covid-19) in china. Technical report, GLO Discussion Paper.

Roodman, D. (2009). A note on the theme of too many instruments. *Oxford Bulletin of Economics and statistics*, 71(1):135–158.

Roser, M., Ritchie, H., Ortiz-Ospina, E., and Hasell, J. (2020). Coronavirus disease (covid-19). *Our World in Data*. https://ourworldindata.org/coronavirus.

WHO (2020). Coronavirus disease 2019 (covid-19): situation report, 73.

Windmeijer, F. (2005). A finite sample correction for the variance of linear efficient two-step gmm estimators. *Journal of econometrics*, 126(1):25–51.

Wu, J. T., Leung, K., and Leung, G. M. (2020). Nowcasting and forecasting the potential domestic and international spread of the 2019-ncov outbreak originating in wuhan, china: a modelling study. *The Lancet*, 395(10225):689–697.

Covid Economics 13, 4 May 2020: 138-156

Covid Economics 13, 4 May 2020: 138-156

APPENDIX A

Table 4. Summary of Countries Analysed by Continent

Continents	Number of Countries	Names of Countries	Number of Observations
Africa	8	Ethiopia, Ghana, Kenya, Nigeria Senegal, South Africa, Tunisia, Uganda	175
Americas	15	Argentina, Bolivia, Canada, Chile Colombia, Costa Rica, Cuba, Ecuador El Salvador, Mexico, Panama, Paraguay Peru, United States, Uruguay	430
Asia	16	Bahrain, Bangladesh, India, Indonesia Israel, Japan, Malaysia, Nepal, Pakistan Philippines, Singapore, South Korea Taiwan, Thailand, Turkey, Vietnam	598
Europe	28	Austria, Belgium, Czech Republic Denmark Estonia, Finland, France, Germany, Greece Hungary, Iceland, Ireland, Italy, Latvia Lithuania, Luxembourg, Netherlands, Norway Poland, Portugal, Romania, Russia, Serbia Slovakia, Slovenia, Spain, Sweden, Switzerland United Kingdom	986
Oceania	2	Australia, New Zealand	110

Notes: Data sourced from the European Centre for Disease Prevention and Control, Roser et al. (2020) and Hale et al. (2020). We exclude countries with no testing record and those with no observations for the total confirmed cases. Column 4 = Total number of observations for respective continents measured daily for each country.

Table 5. Summary of Prevalency, Stringency and Tests Across Weeks

Weeks	Total Cases Average	Lockdown Average	Testing Average
1	2.20	14.29	31.40
2	5.63	16.12	167.06
3	11.78	28.57	775.74
4	15.88	28.57	2,793.23
5	68.81	31.11	5,092.64
6	317.50	31.16	9,937.68
7	730.73	30.07	17,712.21
8	1,002.42	48.05	19,675.54
9	1,992.78	71.50	31,809.91
10	5,481.90	81.26	61,947.59
11	10,939.69	84.47	104,207.59
12	17,485.92	85.90	158,621.26
13	22,627.92	88.12	212,712.75

Notes: Data sourced from the European Centre for Disease Prevention and Control, Roser et al. (2020) and Hale et al. (2020). We exclude countries with no testing record and those with no observations for total confirmed cases. Column 2 = Average of total confirmed cases in all countries in our sample on weekly basis. Column 3 = Average of lockdown index (measured in percentage) in all countries in our sample on weekly basis. Column 4 = Average of total tests in all countries in our sample on weekly basis.

Table 6. System GMM with Endogenous Policy Intervention

	(1)	(2)	(3)
Variables	1-Week	2-Weeks	3-Weeks
lnI_{it-1}	0.9993***	1.0552***	0.9499***
	(0.000)	(0.000)	(0.000)
L_{it-7}	-0.0013		
	(0.405)		
$ln\bar{I}_{jt-7}$	-0.0511		
	(0.506)		
lnT_{it-7}	-0.0427		
	(0.495)		
L_{it-14}		-0.0045	
		(0.399)	
$ln\bar{I}_{jt-14}$		0.0213	
		(0.785)	
lnT_{it-14}		-0.0286	
		(0.573)	
L_{it-21}			0.0014
			(0.441)
$ln\bar{I}_{jt-21}$			0.0680**
			(0.037)
lnT_{it-21}			-0.0470**
			(0.015)
Constant	-107.8778	0.0070	0.1858
	(0.528)	(0.979)	(0.137)
Time trend	yes	no	no
Observations	1,523	1,244	927
Number of country	53	52	48
AR(1) p-value	0.00591	0.0107	0.0538
AR(2) p-value	0.249	0.578	0.576
Hansen test p-value	0.626	0.177	0.663
Sargan test p-value	0.374	0.126	0.836

Notes: *** Significant at 1%; ** significant at 5%; * significant at 10%. We report p-values robust to heteroskedasticity in parentheses. Dependent variable is natural log of total cases lnI_{it}, L_{it-q} is lag of lockdown index, lnT_{it-q} is log of total tests at a specific lag and $ln\bar{I}_{jt-q}$ is log of average cases in other countries at a given lag.
GMM-type instruments in Column 1: lag2-lag4 of lnI_{it} collapsed and lag1-lag5 of L_{it-7} & lnT_{it-7} collapsed,
GMM-type instruments in Column 2: lag2-lag4 of lnI_{it} collapsed and lag1-lag2 of L_{it-14} & lnT_{it-14} collapsed,
GMM-type instruments in Column 3: lag2-lag5 of lnI_{it} collapsed and lag1 of L_{it-21} & lnT_{it-21} collapsed.
Data sourced from the European Centre for Disease Prevention and Control, Roser et al. (2020) and Hale et al. (2020).

Covid Economics 13, 4 May 2020: 138-156

CEPR PRESS

Covid Economics **Issue 13, 4 May 2020**

Determinants of social distancing and economic activity during COVID-19: A global view[1]

William Maloney[2] and Temel Taskin[3]

Date submitted: 27 April 2020; **Date accepted:** 28 April 2020

The paper uses Google mobility data to identify the determinants of social distancing during the 2020 COVID-19 outbreak. We find for the U.S. that much of the decrease in mobility is voluntary driven by the number of COVID-19 cases and proxying for greater awareness of risk. Non-Pharmaceutical Interventions (NPI) such as closing non-essential business, sheltering in place, school closings are also effective, although with a total contribution dwarfed by the voluntary. This suggests that much social distancing will happen regardless of the presence of NPIs and that restrictions may often function more like a coordinating device among increasingly predisposed individuals than repressive measures per se. These results are consistent across countries income groups with only the poorest (LICs) showing limited effect of NPIs , and no voluntary component, consistent with resistance to abandon sources of livelihood. We also confirm the direct impact of the voluntary component on economic activity by showing that the majority of the fall in restaurant reservations in the U.S., and movie spending in Sweden occurred before the imposition of any NPIs. Widespread voluntary de-mobilization implies that releasing constraints may not yield a V shaped recovery if the reduction in COVID risk not credible.

1 The opinions are those of the authors and do not represent the official position of the World Bank. Our thanks to Richard Baldwin, Robert Beyer, Nick Bloom, Xavi Cirera, Aart Kraay, Tito Cordella, Pravin Krishna, Norman Loayza, Cedric Okou, Cevdet Cagdas Unal, and Shu Yu for excellent comments.
2 Chief Economist, Equitable Growth, Finance, and Institutions, The World Bank.
3 Economist, Prospects Group, Equitable Growth, Finance, and Institutions, The World Bank.

Covid Economics 13, 4 May 2020: 157-177

Covid Economics 13, 4 May 2020: 157-177

I. Introduction

Understanding the determinants of social distancing is central to addressing both the medical and economic aspects of COVID-19. [4] On the one hand, reducing interactions among people is critical to reducing propagation and a variety of Non-Pharmaceutical Interventions NPIs, such as closure of non-essential businesses, stay at home orders, or school closings have been put in place to this end, with some success.[5] While there is controversy around whether this should be the goal in developing countries as well (Barnett-Howell and Mobarak 2020, Loayza 2020), there is also concern about whether such measures would work: government capabilities to enforce may be weaker, and resistance may be higher since the trade-off with livelihood is harsher. At the other extreme of the cycle - where the debate is when to loosen NPIs as it is in several advance countries – preliminary evidence from Wuhan suggests that when opened, mobility and economic activity may not respond quickly. [6] Similarly, recent polls suggesting that 58% of Americans are concerned that restrictions will be lifted too soon raise the question of how much of an impact opening will have in practice and hence the shape of the recovery, whether V or U.[7]

This paper uses Google mobility data to explore which factors are proving important during the 2020 Covid-19 outbreak in the U.S. and globally. In all but the poorest countries, it confirms that NPIs can be effective, but that voluntary de-mobilization on the part of the population is much more important, driven by fear or perhaps a sense of social responsibility. This suggests that much social distancing will happen regardless of the presence of restrictions and suggests that NPIs may often function more like a coordinating device among increasingly predisposed individuals than repressive measures per se. We also confirm a more direct link of this voluntary effect using data on restaurant reservations in the U.S. and movie releases and revenues in Sweden and show that, these, too, experience most of their fall before any imposition of NPIs. Overall, the evidence suggests that moves to unfreeze the economy will fail unless there is confidence that, in fact, the risk has passed.

[4] There are three margins upon which societies can work to reduce the death toll. 1. Detect and quarantine so the disease never gets a foothold. 2. Once established, reduce social mobility to mitigate the spread (reduce the R factor.) 3. Increase the capability to treat the sick. On the third, Favero (2020) notes that limitations on ICU beds led to the extremely high death rate in Lombardy. In practice, developing countries have far less capability to treat- 10 African countries have no respirators.https://www.nytimes.com/2020/04/18/world/africa/africa-coronavirus-ventilators.html?referringSource=articleShare If northern Italy couldn't ramp up sufficiently enough along this dimension, it is highly unlikely that most poor countries can. On the first, many advanced countries have missed the window to detect and quarantine and again, this may be more challenging in the developing world.

[5] See Chen and Qiu (2020), Gonzalez-Eira and Niepelt (2020) for conceptual treatments of optimal shut down policies. Hartl et al (2020) find for Germany that growth rates of Covid-19 cases fell 50% as a result of German restrictions to shut down schools, stadiums and eventually many restaurants and shops. See Baldwin and Weder de Mauro (2020) for a compilation of recent thinking on Covid Economics.

[6] https://www.bloomberg.com/news/articles/2020-04-15/wuhan-s-life-after-lockdown-isn-t-business-as-usual?

[7] NBC News-Wall Street Journal was conducted between April 13 and April 15 among a sample of 900 registered voters.

Covid Economics 13, 4 May 2020: 157-177

Several recent papers suggest that NPIs have had an impact in the US. Engle at al. (2020) use daily average changes in distance traveled in every U.S. county as a proxy for reduction in exposure to COVID-19 and find that an official stay-at-home restriction order corresponds to reducing mobility by 7.87%. Brzezinski et al (2020), also using cell phone data, find that a lockdown increases the percentage of people who stay at home by 8% across US counties. Painter and Qiu (2020) show that the introduction of shelter-in-place policies is associated with a 5.1 percentage point increase in the probability of staying home (see also Andersen (2020)).

However, voluntary de-mobilizing behavior that intensifies with prevalence of the disease is also an important driver and affects the effectiveness of official measures. Auld (2006), for example finds that during the Aids epidemic, an average respondent decreased risky behavior by about 5% in response to a 10% increase in Aids prevalence. Further, the 1918 Spanish Flu epidemic suggests that the predisposition of the population to demobilize drove both the incidence of official restrictions and their effectiveness. On the one hand, as Crosby(2003) details, that restrictions were binding is revealed by the fact that in San Francisco "The places of amusement opened first, to huge crowds starved for entertainment (p. 99)" and in Philadelphia "The long thirst was over, and arrests on drunken and disorderly charges bounded back up to and beyond normal levels" (p. 85). However, it is also true that while the San Francisco Department of Health could request that people to smother coughs and sneezes, only when enough fatalities were registered were "San Franciscans…scared enough to accept drastic measures to control the epidemic" (p.95)—and ex post, "Fear had been the enforcer of the Board of Health's policies."(p. 108) not the authorities themselves. When schools in San Francisco were opened, many parents kept their children home out of continuing fear. This resonates with the reports from Wuhan today of the anemic rebounding of the small restaurant sector when restrictions were released.

Viewed through this lens, restrictions may often function more like a coordinating device among increasingly predisposed individuals than repressive measure- if we're all working from home, then I won't be viewed badly if I do; whether schools are on line or in person requires a decision that individual concerned parents cannot effect. This, in turn, raises the question of the whether the impact of lock-down measures per se and their subsequent removal is overstated.

II. Data

Mobility and Economic Activity: Using data from the Maps application on smartphones, Google generates COVID-19 Community Mobility Reports[8] that use aggregated, anonymized data to construct an index of how visits and length of stay at different places change compared to a baseline. They can then follow movement trends over time by geography, and across different high-level categories of places such as workplaces, retail and recreation, groceries and pharmacies, parks, transit stations, and residential. These measures are explicitly considered proxies for social distancing and we focus on the first, workplace related

[8] https://www.google.com/covid19/mobility/

Covid Economics 13, 4 May 2020: 157-177

mobility, as most relevant to economic activity and most prominent in the policy debate. The reports consist of per country downloads (with 131 countries covered initially), further broken down into regions/counties in some cases. Because location accuracy and the understanding of categorized places varies from region to region, Google does not recommend using this data to compare changes across countries or regions with different characteristics. To address this, our empirics rely only on within area variation across time and reporting or categorization differences are absorbed in included fixed effects.

This measure is limited by the degree to which coverage of smart phones offers a representative sample of the population. As Annex 1 shows, few developing countries show coverage of smart phones above 50% and Ethiopia, Nigeria, Sudan, Bangladesh, Pakistan hold up the bottom of the top 50 countries with rates under 20% of coverage. This said, several developing countries also have reasonable coverage when we adjust for the share of adults in the population: UK 100%, Sweden: 96%, US 95%, Italy 67%, Japan 63%, Brazil 52%, South Africa 50%. While clearly not representative, the differences between Italy and Japan on the one hand and Brazil and South Africa on the other are not so large as to justifying throwing out the possible information on how developing countries may differ. Further, while we may miss the mobility of for instance, micro firm owners without smartphones, many of their customers will have them and the shutting down of the firm will be partially registered.

Data on restaurant reservations in the US is taken from OpenTable.[9] Movie release and theater revenue data for Sweden from International Movie Database.[10]

Covid-19 Cases: Though there may be several mechanisms through which cases translate into lower mobility, we interpret this as a signal to individuals about the likelihood of a serious negative health outcome. National cases can inform about the overall evolution of the disease, while local numbers fine tune the proximate threat. We standardize by the corresponding population in the figures. In some regressions, we can expand the sample by using log (cases) and the population scaling is absorbed in the corresponding fixed effect. Global data are drawn from the Johns Hopkins Coronavirus Resource Center. Country specific regional data comes from national sources: US: Johns Hopkins Coronavirus Resource Center; Brazil, Italy, Japan, South Africa, Sweden, UK from national sources (see Annex II).

Non-Pharmaceutical Interventions (NPIs): We use mandatory closures of non-essential business as both most relevant to the issue of economic mobility as figuring most prominently in the policy debate. State level data for the US are collected from Raifman et al (2020) and NPIs enter as indicator variables taking a value of 1 if a given NPI is implemented and 0 otherwise. Globally, we employ information on national NPIs available

[9] www.opentable.com
[10] https://www.boxofficemojo.com/

Covid Economics 13, 4 May 2020: 157-177

from the Blavatnik School of Government at Oxford University. For select countries for which we employ subnational mobility data to explore the impact of local case incidence, we use national data on the nationally implemented NPIs as controls. The exception is Brazil for which NPIs are established by states, and we collect data at that level.

III. Results: United States

Figure 1 plots the level of mobility against the log of the number of cases per capita by US state for the US. It further divides the sample by whether the states are covered by restrictions on non-essential businesses (red) or not (blue). Two drivers appear as potentially important. First, the data are consistent with restrictions leading to lower levels of mobility. However, more strikingly, there is a clear downward sloping relationship between reported cases and mobility independent of such restrictions.

Figure 1: Mobility, COVID Cases and Official Restrictions, United States

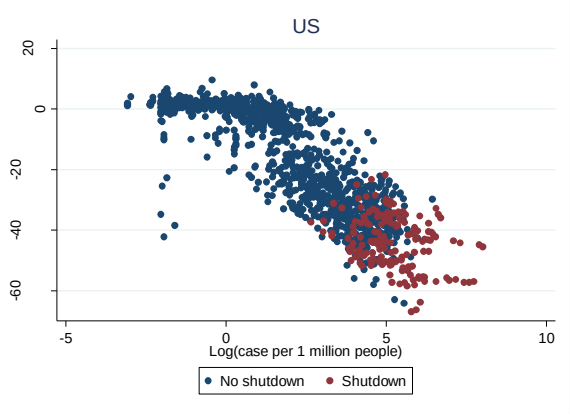

Notes: Workplace mobility is Google measure of work-related mobility index. See text for sources.

Table 1 more formally tests this relationship by estimating

$$Mobility_{it} = \beta_{0+}\beta_1 Cases_{it-1} + \beta_2\ Aggregate\ Cases_{t-1} + \beta_3\ NPI_{it-1} + \mu_i + v_t + \varepsilon_{it} \qquad (1)$$

Where mobility is the Google measure, Cases is the log incidence, Aggregate Cases is the national analogue, NPI are Non-pharmaceutical intervention(s), and u_i are subnational (state) fixed effects that also effectively put cases in per capita terms, and v_t, time fixed effects. There are clear issues of bi-directional causality here. Lower mobility, in theory, lowers the number of cases and may also possibly affect the likelihood of imposing restrictions. This should induce a downward bias to both coefficients on the right-hand side and our results should be taken as a lower bound. As we are working with a larger group of countries, we do not attempt to

instrument which would not be feasible in most, but we lag both explanatory variables 1 period. The results change modestly in magnitude, with even more lags, but the overall patterns remain consistent.

Table 1: Mobility, COVID Cases and NPIs, United States

	(1) Workplace	(2) Workplace	(3) Workplace	(4) Workplace	(5) Residential	(6) Residential
Close N.E. business	-4.373***	-5.281***	-2.071	-3.075***	2.047***	0.830*
	(1.235)	(0.689)	(2.006)	(1.051)	(0.356)	(0.463)
Log cases	-4.502***	-1.291***	-2.904***	-1.284***	0.551***	0.577***
	(1.153)	(0.437)	(0.915)	(0.385)	(0.185)	(0.161)
Log national cases	-2.671**	-3.038***	-2.193**	-2.837***	0.957***	0.875***
	(1.063)	(0.425)	(0.860)	(0.383)	(0.225)	(0.177)
Close K-12			-11.975***	-0.866		-0.092
			(1.704)	(1.169)		(0.407)
Stay home/SIP			-3.289	-3.855***		2.144***
			(2.630)	(1.134)		(0.485)
Constant	24.030***	10.503***	18.981***	9.574***	-4.472***	-3.986***
	(5.191)	(1.756)	(4.526)	(1.509)	(1.250)	(0.968)
Time FE	No	Yes	No	Yes	Yes	Yes
Day of the week FE	Yes	No	Yes	No	No	No
State FE	Yes	Yes	Yes	Yes	Yes	Yes
# of States	51	51	51	51	51	51
Obs.	1189	1189	1189	1189	1189	1189
R-squared	0.836	0.963	0.875	0.964	0.956	0.959

Notes: Regression of Google measure of work/residential related mobility on NPIs, the log of cases, the log of national cases, state, days of the week/time fixed effects. Robust clustered errors are in parenthesis. *** p<0.01, ** p<0.05, *<0.1

Table 1 suggests that both effects are at work although with surprising relative contributions. Columns 1-2 present the impact on mobility of just business closure restrictions, the log of local cases and the log of national cases with and without time fixed effects. Of the roughly 60-point decline in mobility seen in Figure 1, roughly 5 points appear due to official workplace closures. This is of the order of magnitude identified in previous studies on other measures of mobility. However, the component due to case incidence, both national and local appears to be able to account for much of the fall in mobility by itself. For instance, with the 10-log point increase in local cases in Figure 1, roughly 43 points (2/3) of the fall in mobility are accounted for, and more without FE by "voluntary" self-restriction.

Columns 3 and 4 introduce two other NPIs- School closures for K-12 and Stay at Home/Shelter in Place orders. The impact of imposing restrictions on business falls significantly suggesting that, as expected, it was picking up the effects of other correlated measures. The three together can account for almost 8 points of the fall in mobility. This remains dwarfed by the roughly 40% arising from the number of local and national cases whose impact stays roughly the same. Hence, it appears that in the US, the largest effect is due to protective measures taken by individuals as they learn more about the prevalence of the disease. The question then arises, will the effect of removing those restrictions in fact lead to the hoped-for rejuvenating effect on the economy if case numbers remain high?

Covid Economics 13, 4 May 2020: 157-177

As a confirmatory test on the complement to workplace mobility, columns 5 and 6 show that increased NPIs and case incidences lead to a *rise* in residential mobility.

IV. Results: Global Sample

Figures 2 plot the same relationship for six countries of potential interest: Italy, Japan, Sweden and the UK and two upper middle-income countries, Brazil and South Africa, for which we have reasonable smart phone coverage. In every case, the figures show evidence of decreased mobility with the increase in case numbers.

Table 2 formalizes the graphs by running subnational mobility against sub-national and national COVID case incidence, including NPIs appropriate to the country case. The fact that the NPIs are at the country level makes us treat them more as controls than precise estimations of effects for most cases. However, again, alone among the six, Brazil NPIs are set at the state level and the data are therefore subnational. Three findings emerge. First, in Brazil, Italy, South Africa, Sweden, and the UK the semi-elasticities of mobility with respect to case incidence are comparable to those found in the US while Japan has much lower, but still significant effects.

Second, our tentative estimates suggest that NPIs have large effects Italy, South Africa (some with unexpected sign however), and the UK. For Brazil, Italy, South Africa, Sweden, and the UK, however, the "voluntary" component still contributes the largest share.

Third, Sweden and Japan, two countries with limited NPIs show curiously divergence paths. In Sweden, mobility falls 60 points or almost that seen in the U.S. (The extreme 80 point falls are due to the April 10 long holiday weekend). Hence, the sharp contrast often depicted between Sweden and more interventionist countries appears overdrawn- mobility has fallen drastically. It has not, however, in Japan and this presents a puzzle given that it is a country also with both effective governance and high social capital. We argue that this may offer additional evidence for the importance of NPIs as important coordination mechanisms. Although schools were closed and large events were cancelled since early March, business continued as normal until early April 7 when the State of Emergency was declared. But even under the SoE, governors could only request that people stay home and that businesses close. Tokyo's governor asked that people not go out at night but said restaurant and bars could remain open until 8 PM. These tepid measures faced strong headwinds in other social norms. For instance, there is resistance rooted in the country's work culture where employees fear being seen as slackers if they don't appear for work in person.[11] Unless everyone is sent home, everybody goes to work. The lack of

[11] https://www.nytimes.com/2020/04/19/world/asia/tokyo-japan-coronavirus.html?smid=em-share

Covid Economics 13, 4 May 2020: 157-177

a stronger coordination mechanisms through official measures is a plausible explanation for both for the absence of much of an impact of formal measures, as well as limited self-motivated reductions in mobility.

Figures 2a-f: Workplace Mobility vs. Cases and Closure of Non-Essential Businesses

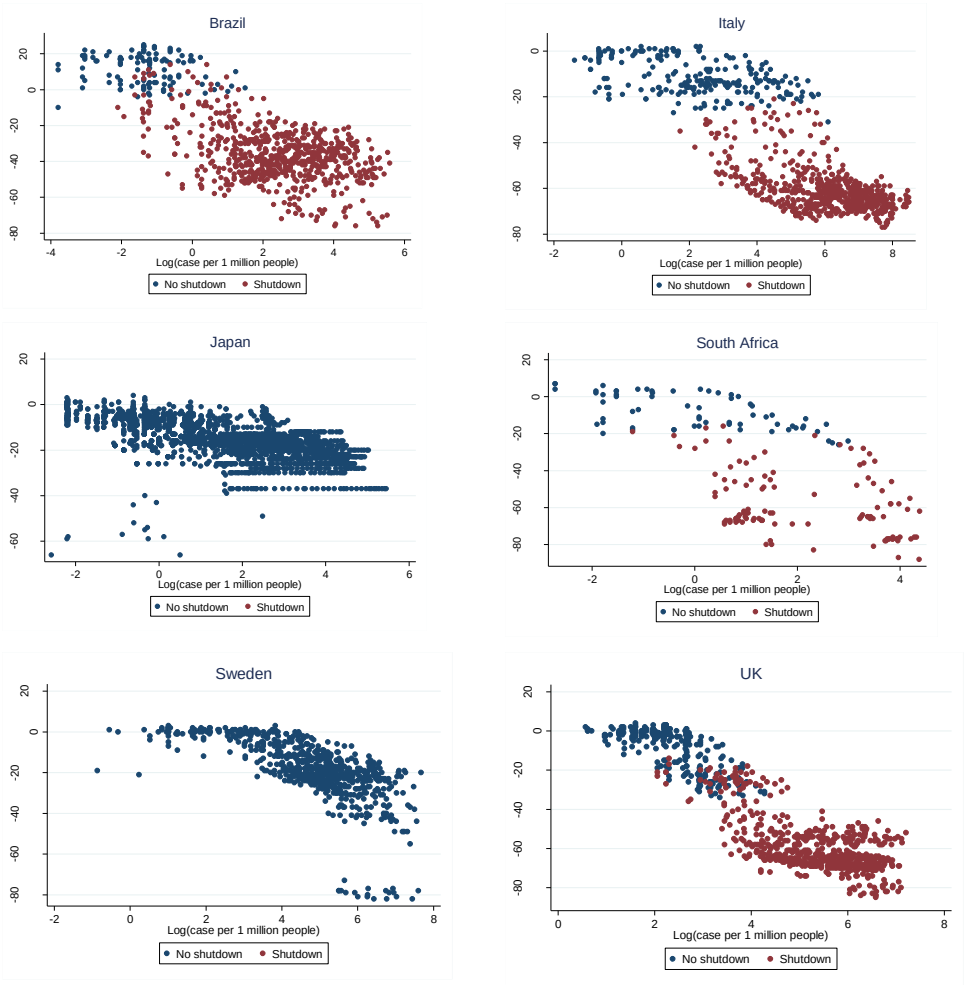

Notes: Workplace mobility is Google measure of work-related mobility index. See Annex II for country-specific sources.

Table 2: Mobility, COVID Cases and NPIs, Select Countries

	(1) Brazil	(2) Italy	(3) Japan	(4) S. Africa	(5) Sweden	(6) UK
Close N.E. business	2.996	-28.781***	3.054	-5.871**		-20.337***
	(2.375)	(0.836)	(2.190)	(2.166)		(0.322)
K-12 closure	-2.135			-13.583***		-12.670***
	(1.680)			(2.275)		(0.462)
Cancel public events	-1.697			10.798***	-7.837***	
	(1.842)			(2.150)	(2.039)	
Close public transport.				4.102*		
				(1.782)		
Public info. camp.				46.285***	12.420***	
				(7.338)	(1.794)	
Restr. on internal mov.				-37.443***		
				(0.924)		
Log cases	-1.413**	-2.775***	0.166	-1.294	-4.499**	0.719
	(0.595)	(0.865)	(0.561)	(1.982)	(1.796)	(0.517)
Log national cases	-3.544***	-3.157**	-3.229***	-4.371**	-2.601	-6.994***
	(0.464)	(1.134)	(0.553)	(1.711)	(2.290)	(0.566)
Constant	9.550***	22.787***	3.909*	25.710***	18.885*	39.349***
	(1.982)	(6.500)	(1.976)	(5.624)	(9.309)	(2.783)
Time FE	Yes	No	No	No	No	No
Day of the week FE	Yes	Yes	Yes	Yes	Yes	Yes
State FE	Yes	Yes	Yes	Yes	Yes	Yes
# of States	27	20	46	7	21	95
Obs.	762	865	2361	169	758	2566
R-squared	0.811	0.945	0.484	0.956	0.637	0.956

Notes: Regression of Google measure of work-related mobility on NPIs, the log of cases, the log of national cases. Mobility, Cases and National Cases at subnational level. NPIs at national level with the exception of Brazil for which all data is at the subnational level. Robust clustered errors are in parenthesis. *** p<0.01, ** p<0.05, *<0.1

Global Sample

Figure 3a-c groups the global sample of countries which have national data on mobility and NPI. Figure 3a divides the sample into those with and without restrictive orders. As in the individual case, there appears to be evidence for both the impact of restrictions and of the relationship with cases incidence. Figure 3b breaks the data apart into 4 income categories, Low Income Countries (LIC), Lower Middle Income (LMIC), Upper Middle Income (UMIC) and High Income (HIC) which include primarily the wealthier OECD countries (see Annex III for categorization). Figure 3c is the same, but only for country/periods when official restrictions on non-essential businesses are in place. In both cases, the downward slope appears across all income categories.

Table 3 largely confirms previous findings. Each specification is presented with and without time fixed effects which, in some categories, consume substantial degrees of freedom. Preliminary explorations suggest that world COVID case incidence does not enter and we drop that term. This makes sense if we think that citizens of a country may pay attention to national trends, as was the case in the US, but maybe less cases across the

Covid Economics 13, 4 May 2020: 157-177

Covid Economics 13, 4 May 2020: 157-177

ocean. The semi-elasticity on home case incidence appears both of larger magnitude than in the US and very similar across LMIC and HICs at around 4.3. Without time fixed effects, UMICs are of similar magnitude, and LICs is a third to a half below that found in the other groups. However, with them, the UMIC falls by more than half and becomes insignificant and the LIC coefficient disappears completely. A monotonic story in income is thus not clean, but it is consistent with the argument that in very poor countries, people cannot afford not to work and hence they will continue to do so.

Figures 3a-c: Mobility, COVID Cases and NPIs, Global Sample

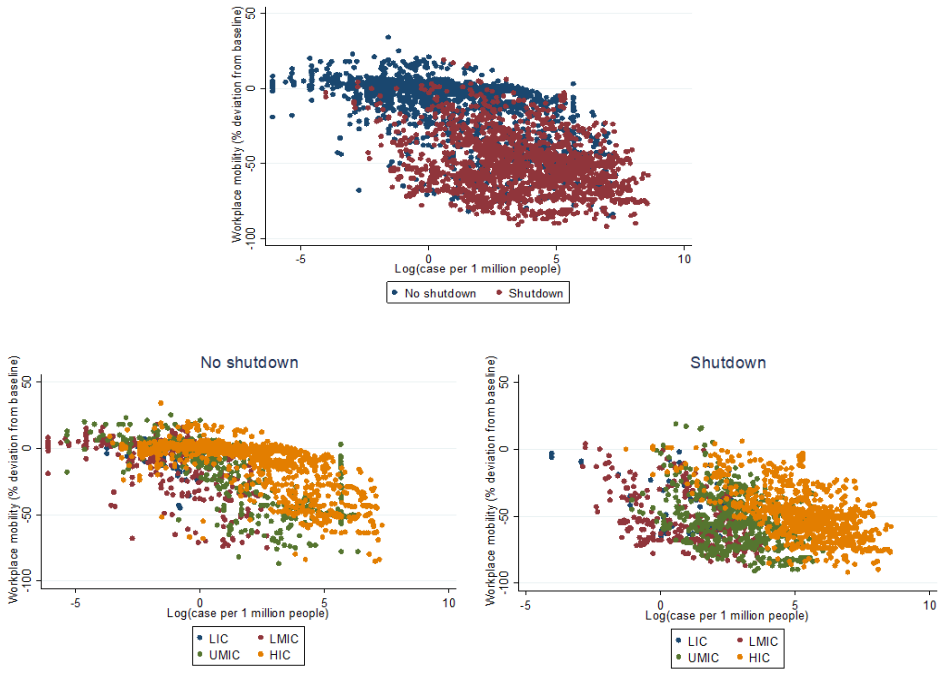

Notes: Workplace mobility is Google measure of work-related mobility index. LIC, LMIC, UMIC, and HIC stand for Low Income Countries, Lower Middle-Income Countries, Upper Middle-Income Countries, and High Income Countries, respectively. See Table AIII for income group classification.

The impact of NPIs themselves is mixed. Workplace closures are most clearly significant in LMICs accounting for almost 9 points of reduced mobility which in UMIC and HIC, the point estimate is roughly half that and becomes insignificant with the inclusion of time fixed effects. School closures are robustly significant and account for 10 points in HIC suggesting that having to school children at home is a limitation on job related mobility. For UMICs, the coefficient is similar without time fixed effects, but falls to 6.6 pts and becomes insignificant with their inclusion. For LICs and LMICs, the point estimates are negative significant, and they

are positive. This monotonic increase with lower incomes is consistent with children playing a different role, perhaps helping in a business with less regard to human capital accumulation foregone.

Again, the sampling for the LIC and LMIC samples for sure are not representative and what we may be finding is simply that people who can afford smart phones behave similarly around the world. Still, either LMIC governments have the capability to, at least, coral the elites, or, again, are simply providing a coordination mechanism.

Cancelling public events never enters significantly with full time fixed effects although the point estimates are often in the -6 to -10 range. The restriction that most robustly reduces mobility among the LICs is closing of public transport, accounting for a massive 16.5 points. In UMICs, and arguably in HICs, the value is a third of that. This would seem the most potent tool of control in the poorest countries.

Public information campaigns curiously enter positively and significantly in LMICs and almost in UMICs with coefficients of roughly 7-10. The intuition is not clear, but it may be the case that guidance on washing hands and wearing masks makes individuals feel more in control and protected and hence, net the impact is to increase mobility.

Restrictions on internal movement have large and significant effects (12, 14.3) in LMICs and UMICs, with much less impact in HIC and virtually none in LICs. In the latter case, this may testify to difficulty in enforcing such shelter in place ordinances relative too, for instance, shutting down public transport.

In sum, in HICs, and LMICs, the voluntary component is still as or more important as NPIs. UMICs look quite similar to HICs with the exception of anomalous lack of impact of case incidence, and the large impact of restrictions on internal movement which it shares with LMICs. It may be that in fact, LMIC and UMIC are more effective in enforcing such measures. Overall, for LICS the voluntary component is absent and the only NPI that appears to have any effect is closing public transportation. Again, with the caveat that cell phone coverage in such countries is around or under 20% of the population, this is consistent, again, with limited state capability and more resistance from the population to stop working.

Again, Annex IV presents the complementary regressions on residential mobility and finds patterns that mirror those presented above.

Covid Economics 13, 4 May 2020: 157-177

Table 3: Workplace Mobility, COVID Cases, and NPIs, Global Sample

	(1) LIC	(2) LIC	(3) LMIC	(4) LMIC	(5) UMIC	(6) UMIC	(7) HIC	(8) HIC
K-12 closure	3.13	0.04	1.24	0.64	-6.62	-10.60**	-10.20***	-13.32***
	(4.83)	(3.03)	(4.61)	(5.11)	(4.80)	(3.90)	(3.16)	(3.85)
Close N.E. business	1.00	-0.80	-8.83*	-9.30	-3.96	-8.59**	-4.73	-8.75***
	(7.40)	(4.45)	(5.01)	(5.61)	(3.37)	(4.09)	(2.84)	(2.90)
Cancel public events	-9.77	-6.37	-5.26	-6.66*	-1.49	-5.66	-2.32	-6.35*
	(5.27)	(4.46)	(3.88)	(3.75)	(5.96)	(4.45)	(3.04)	(3.16)
Close public transp.	-16.51*	-16.17*	-2.20	-5.35	-5.37*	-4.93	-5.06	-6.44**
	(8.37)	(7.18)	(4.93)	(5.02)	(2.86)	(3.64)	(3.03)	(2.71)
Public info. camp.	0.77	-0.40	9.90***	10.47***	7.32	8.99**	4.71*	5.59**
	(3.23)	(3.35)	(2.89)	(2.31)	(4.91)	(4.07)	(2.62)	(2.70)
Restr. on internal mov.	-1.21	-1.85	-12.03***	-10.52**	-14.32***	-16.81***	-2.72	-5.53**
	(3.57)	(3.13)	(2.98)	(3.81)	(3.78)	(4.46)	(2.04)	(2.18)
Log cases	-0.03	-2.43*	-4.30***	-5.57***	-1.50	-3.85***	-4.61***	-3.42***
	(1.89)	(1.17)	(1.13)	(0.56)	(1.63)	(0.80)	(0.97)	(0.75)
Constant	3.76	14.08**	-5.82	6.46	-0.50	8.68*	-1.73	10.41***
	(3.41)	(5.84)	(4.46)	(4.02)	(5.05)	(4.75)	(2.58)	(2.49)
Time FE	Yes	No	Yes	No	Yes	No	Yes	No
Day of the week FE	No	Yes	No	Yes	No	Yes	No	Yes
Country FE	Yes	Yes	Yes	Yes	Yes	Yes	Yes	Yes
# of Countries	8	8	24	24	29	29	40	40
Obs.	193	193	720	720	945	945	1777	1777
R-squared	0.69	0.62	0.77	0.73	0.85	0.80	0.86	0.80

Notes: Regression of Google measure of work-related mobility on NPIs, the log of national cases, country, and days of the week/time fixed effects. Robust clustered errors are in parenthesis. *** p<0.01, ** p<0.05, *<0.1. LIC, LMIC, UMIC, and HIC stand for Low Income Countries, Lower Middle Income Countries, Upper Middle Income Countries, and High Income Countries, respectively. See Table AIII for income group classification.

V. Mapping to Economic Activity

Do these voluntary declines in Google mobility in fact map to economic activity? Preliminary evidence from the U.S. and Sweden suggests they do. Figure 4 presents restaurant reservations by state against COVID incidence for the U.S. What is immediately clear is that the fall in reservations predated the closing of non-essential businesses. This is confirmed by Table 4 which suggests a combined elasticity of over 10 and virtually no impact of business closing measures. That is, the entire fall can be accounted for with the increase in cases. The results suggest that what slowed economic activity was not the NPIs, but rather voluntary de-mobliization as evidence of the magnitude of the threat accumulated.

In the same vein, Figure 5 presents preliminary national data from movie theater releases and revenues in Sweden, again, a country with no restrictions on non-essential businesses. Consistent with this, releases continue more or less unchanged while revenues drop off entirely. Supply remains unaffected, but, consistent with the declines in overall mobility, demand evaporates. Since the data are at the national level, we cannot pursue these trends more formally.

Covid Economics 13, 4 May 2020: 157-177

Covid Economics 13, 4 May 2020: 157-177

Figure 4: Decline in Restaurant Reservations vs. COVID Cases

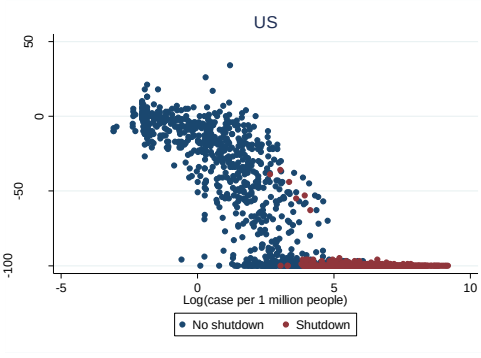

Figure 5: Decline in Movie Theater Revenues and Releases vs. COVID Cases

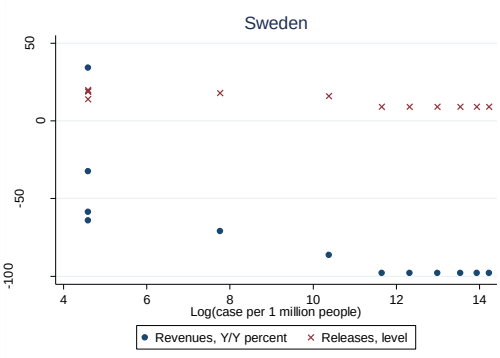

Notes: U.S. Restaurant reservations against COVID incidence. Sweden: Movie releases and theater revenues against COVID incidence. See text for sources.

In both the cases of restaurant reservations in the U.S. and theater demand in Sweden, demand has fallen sharply and independent of NPIs. This suggests that, as in Wuhan, it is likely that release of NPIs will have little effect unless individuals are confident that the risk has diminished.

VI. Conclusion

Several key findings thus emerge. First, clearly, the pattern of demobilization varies across countries with the political choices made. The US and Japan have radically different degrees of demobilization.

Second, decreased mobility seems more driven by "voluntary" individual response to increased local and national COVID-19 case incidence, proxying for awareness or fear or social responsibility, rather than formal measures. For all except the poorest countries (LICs) the response of mobility with respect to cases is of similar orders of magnitude and can explain most of the reduction in mobility, dwarfing the effect of NPIs.

Third, that said, there is evidence that less affluent countries were also able to implement NPIs. LMICs and UMICs appear to have been able to engineer as much or more of a fall in mobility through NPIs as some High-Income Countries.

Fourth, our global data suggest that other measures beyond closing non-essential workplaces have important impacts-school closures, restrictions on internal mobility/shut-down of public transportation. Counterintuitively, public information campaigns appear to raise mobility- information on protective measures may make individuals feel more confident moving about.

Covid Economics 13, 4 May 2020: 157-177

Table 4: Restaurant Reservations, COVID Cases, and NPIs, United States

	(1) Restaurant reservations
Close N.E. business	0.818
	(1.381)
Close K-12	2.349
	(1.720)
Stay home/SIP	0.952
	(1.139)
Log cases	-0.678
	(1.125)
Log national cases	-9.775***
	(0.884)
Constant	31.251***
	(6.388)
Time FE	Yes
State FE	Yes
# of States	49
Obs.	1877
R-squared	0.958

Notes: Regression of restaurant reservations (Y/Y percent change) from OpenTable, on NPIs, the log of cases, the log of national cases, state, time fixed effects. Robust clustered errors are in parenthesis. *** p<0.01, ** p<0.05, *<0.1

Fifth, the dominant contribution of voluntary self-restraint along with historical and anecdotal evidence suggests that formal NPIs may be as much coordination mechanisms as repressive measures. For instance, no parent may want to send his/her child to school, but only when schools force all students on line can continued safe learning at a distance be realized. As in Japan, no one may want to be seen as the slacker by not showing up at work, but if the government signals that this is the safe thing to do, then all can work from home without stigma.

Sixth, these findings offer both good and bad news. First, they imply that for many countries in the world, self-enforcing dynamics and NPIs can reduce mobility and business activity substantially. That mobility fell almost as much in Sweden, with no NPIs, as the U.S. dramatically illustrates this point and suggests that the focus on government NPI policy in explaining Sweden's mortality rate may not be justified. The finding that only shutting down public transport has any effect in LICs is consistent with arguments that government capacity may be generally low, and resistance to demobilizing is high where it implies lost livelihoods.

Seventh, the potentially bad news is that releasing constraints may not, as appears to be the case in Wuhan have the economically rejuvenating effect that was expected if people are not convinced that, in fact, the coast is

clear. Given this, we are more likely to be facing a U-shaped recovery rather than a V propelled by the release of constraints.

Covid Economics 13, 4 May 2020: 157-177

Covid Economics 13, 4 May 2020: 157-177

VII. References

Anderson, R., H. Heesterbeek, D. Klinkenberg, and D. Hollingsworth (2020). "How will country-based mitigation measures influence the course of the COVID-19 epidemic?" *The Lancet* 395 (10228), 931–934.

Auld, M. C. (2006). "Estimating behavioral response to the AIDS epidemic." *The BE Journal of Economic Analysis & Policy* 5(1).

Baldwin, R. and B. Weder de Mauro (2020). *Economics in the Time of COVID-19*, https://voxeu.org/content/economics-time-covid-19.

Barnett-Howell, Z. and A.M. Mobarak (2020). "Should Low-Income Countries Impose the Same Social Distancing Guidelines as Europe and North America to Halt the Spread of COVID-19?" Yale School of Management and Y-RISE.

Brzezinski, A., G. Deiana, V. Kecht and D. Van Dijcke (2020). "The COVID-19 pandemic: Government versus community action across the United States," *Covid Economics*, Issue 7.

Chen, X. and Z. Qiu (2020). "Issue Scenario analysis of non-pharmaceutical interventions on global COVID-19 transmissions," *Covid Economics*, Volume 7.

Crosby, A. W. (2003). *America's Forgotten Pandemic: The Influenza of 1918*. Cambridge University Press.

Engle, S J. Stromme and Z. Anson (2020). "Staying at home: Mobility effects of Covid-19" *Covid Economics*, Issue 4.

Favero, C. (2020). "Why is Covid-19 mortality in Lombardy so high? Evidence from the simulation of a SEIHCR model," *Covid Economics*, Issue 4.

Gonzalez-Eiras, M. and D. Niepelt (2020). "On the optimal 'lockdown' during an epidemic," *Covid Economics*, Issue 7.

Hale, T., A. Petherick, T. Phillips, S. Webster (2020a). "Variation in government responses to COVID-19" BSG Working Paper Series BSG-WP-2020/031 Version 4.0 April 2020.

Hale, T., S. Webster, A. Petherick, T. Phillips, and B. Kira (2020b). Oxford COVID-19 Government Response Tracker, Blavatnik School of Government: https://www.bsg.ox.ac.uk/research/research-projects/coronavirus-government-response-tracker

Hartl, T., K. Wälde and E. Weber (2020). "Measuring the impact of the German public shutdown on the spread of COVID-19," *Covid Economics,* Issue 1.

Loayza, N. (2020). "Costs and Trade-Offs in the Fight against COVID-19," World Bank, Washington, DC.

Painter, M. O. and T. Qiu (2020). "Political belief affect compliance with COVID-19 social distancing orders," *Covid Economics*, Issue 4.

Raifman J., Nocka K., Jones D., Bor J., Lipson S., Jay J., and P. Chan (2020). "COVID-19 US state policy database," available at: www.tinyurl.com/statepolicies

Covid Economics 13, 4 May 2020: 158-200

Annex I. Smartphone Coverage

Country	Smartphone penetration	
United Kingdom	82.20%	1
Netherlands	79.30%	2
Sweden	78.80%	3
Germany	78.80%	4
United States	77.00%	5
Belgium	76.60%	6
France	76.00%	7
Spain	72.50%	8
Canada	72.10%	9
Australia	68.60%	10
South Korea	68.00%	11
Kazakhstan	64.90%	12
Poland	64.00%	13
Russian Federation	63.80%	14
Taiwan	60.00%	15
Italy	58.00%	16
Malaysia	57.50%	17
Japan	55.30%	18
China	55.30%	19
Romania	53.80%	20
Ukraine	48.30%	21
Argentina	46.90%	22
Saudi Arabia	46.00%	23
Mexico	45.60%	24
Philippines	44.90%	25
Chile	44.20%	26
Thailand	43.70%	27
Brazil	41.30%	28
Venezuela	40.80%	29
Colombia	39.80%	30
Morocco	37.90%	31
Turkey	37.90%	32
Vietnam	37.70%	33
South Africa	35.50%	34
Iran (Islamic Republic of)	64.60%	35
Peru	32.10%	36
Uzbekistan	31.30%	37
Algeria	29.10%	38
Egypt	28.00%	39
India	27.70%	40

Indonesia	27.40%	41
Ghana	24.00%	42
Myanmar	21.80%	43
Kenya	20.90%	44
Sudan	19.70%	45
Bangladesh	16.10%	46
Uganda	15.60%	47
Pakistan	13.80%	48
Nigeria	13.00%	49
Ethiopia	11.20%	50

Source: *Newzoo's Global Mobile Market Report* (2018) as cited at https://en.wikipedia.org/wiki/List_of_countries_by_smartphone_penetration

Covid Economics 13, 4 May 2020: 158-200

CEPR PRESS

Annex II. Subnational Data Sources

Brazil: Official state websites, Platforma COVID Brazil by the Government of Brazil: https://covid19br.wcota.me/

Italy: Dipartimento della Protezione Civile: https://github.com/pcm-dpc/COVID-19

Japan: Japan COVID-19 Data Repository: https://github.com/sanpei3/covid19jp

South Africa: Department of Health: https://github.com/dsfsi/covid19za

Sweden: https://www.boxofficemojo.com/weekend/by-year/2020/?area=SE

UK: Department of Health and Social Care: https://github.com/tomwhite/covid-19-uk-data

Covid Economics 13, 4 May 2020: 158-200

Covid Economics 13, 4 May 2020: 158-200

Annex III. Income Groups

LIC	LMIC	UMIC	HIC
Afghanistan	Angola	Argentina	Australia
Burk. Faso	Bangladesh	Belize	Austria
Mali	Bolivia	Bos. and Herz.	Belgium
Mozambique	Cameroon	Botswana	Canada
Niger	Cape Verde	Brazil	Chile
Rwanda	Egypt	Bulgaria	Croatia
Tanzania	El Salvador	Colombia	Czechia
Uganda	Ghana	Costa Rica	Denmark
	Honduras	Dominican Republic	Estonia
	India	Ecuador	Finland
	Indonesia	Guatemala	France
	Kenya	Iraq	Germany
	Kyrgyzstan	Jamaica	Greece
	Laos	Jordan	Hong Kong
	Mongolia	Kazakhstan	Hungary
	Myanmar (Burma)	Lebanon	Ireland
	Nicaragua	Libya	Israel
	Nigeria	Malaysia	Italy
	Pakistan	Mauritius	Japan
	Papua New Guinea	Mexico	Luxembourg
	Philippines	Namibia	Netherlands
	Vietnam	Paraguay	New Zealand
	Zambia	Peru	Norway
	Zimbabwe	Romania	Panama
		South Africa	Poland
		Sri Lanka	Portugal
		Thailand	Puerto Rico
		Turkey	Saudi Arabia
		Venezuela	Singapore
			Slovakia
			Slovenia
			South Korea
			Spain
			Sweden
			Switzerland
			Trinidad and Tobago
			United Arab Emirates
			United Kingdom
			United States
			Uruguay

CEPR PRESS

Covid Economics 13, 4 May 2020: 158-200

Annex IV.

Table A4: Residential mobility, global sample

	(1) LIC	(2) LIC	(3) LMIC	(4) LMIC	(5) UMIC	(6) UMIC	(7) HIC	(8) HIC
K-12 closure	-1.59	-1.81	1.78	1.86	4.34**	5.67***	3.71**	5.18***
	(3.57)	(2.00)	(2.33)	(2.57)	(2.04)	(1.74)	(1.39)	(1.57)
Close N.E. business	0.84	0.49	4.37**	4.63*	2.69*	4.68***	1.65	3.10**
	(1.75)	(2.16)	(2.06)	(2.35)	(1.31)	(1.46)	(1.39)	(1.34)
Cancel public events	7.34***	4.03	0.67	1.39	1.39	2.71	0.87	2.83**
	(1.61)	(2.58)	(1.71)	(1.82)	(2.54)	(1.98)	(1.38)	(1.31)
Close public transp.	2.74	4.78	-0.07	1.25	0.42	0.30	3.25**	3.19**
	(2.26)	(2.93)	(2.07)	(2.07)	(1.61)	(1.77)	(1.38)	(1.21)
Public info. camp.	-2.71**	-2.34	-5.94***	-6.16***	-5.27**	-5.22***	-2.32	-2.41*
	(0.96)	(2.37)	(1.89)	(1.45)	(2.28)	(1.72)	(1.43)	(1.34)
Restr. on internal mov.	2.46	3.06	6.35***	5.83***	7.90***	9.26***	0.69	1.34
	(1.68)	(1.63)	(1.23)	(1.67)	(1.74)	(1.77)	(1.01)	(0.98)
Log cases	0.84	1.37*	1.68***	2.20***	0.12	1.25***	1.99***	1.55***
	(0.83)	(0.60)	(0.42)	(0.27)	(0.74)	(0.38)	(0.55)	(0.36)
Constant	7.28***	1.43	5.60**	2.52	1.35	-1.25	1.01	-4.48***
	(1.22)	(3.99)	(2.28)	(2.18)	(2.52)	(1.88)	(1.35)	(1.18)
Time FE	Yes	No	Yes	No	Yes	No	Yes	No
Day of the week FE	No	Yes	No	Yes	No	Yes	No	Yes
Country FE	Yes	Yes	Yes	Yes	Yes	Yes	Yes	Yes
# of Countries	8	8	24	24	29	29	40	40
Obs.	193	193	711	711	942	942	1775	1775
R-squared	0.78	0.71	0.80	0.77	0.83	0.80	0.85	0.79

Notes: Regression of Google measure of residential mobility on NPIs, the log of national cases, country, and days of the week/time fixed effects. Robust clustered errors are in parenthesis. *** p<0.01, ** p<0.05, *<0.1. LIC, LMIC, UMIC, and HIC stand for Low Income Countries, Lower Middle Income Countries, Upper Middle Income Countries, and High Income Countries, respectively. See Table AIII for income group classification

CEPR PRESS

Covid Economics **Issue 13, 4 May 2020**

Startups and employment following the COVID-19 pandemic: A calculator

Petr Sedlácek[1] and Vincent Sterk[2]

Date submitted: 28 April 2020; **Date accepted:** 30 April 2020

Early indicators suggest that startup activity is heavily disrupted by the COVID-19 pandemic and the associated lockdown. At the same time, empirical evidence has shown that such disturbances may have long-lasting effects on aggregate employment. This paper presents a calculator which can be used to compute these effects under dierent scenarios regarding (i) the number of startups, (ii) the growth potential of startups, and (iii) the survival rate of young firms. We find that employment losses can be substantial and last for more than a decade, even when the assumed slump in startup activity is only short-lived.

Covid Economics 13, 4 May 2020: 178-200

1 Professor of Economics at the University of Oxford and CEPR Research Affiliate.
2 Associate Professor. Department of Economics. University College London and CEPR Research Affiliate.

Covid Economics 13, 4 May 2020: 178-200

1 Introduction

Due to the global coronavirus (COVID-19) pandemic, 2020 is set to be a tragic year for many businesses. Startups are likely to be affected particularly strongly, as they find themselves in a fragile stage of the lifecycle, being sensitive to disruptions in demand, supply, or credit conditions. This is already showing in the statistics. In the last week of March 2020, new business applications were down forty percent compared to the same week one year earlier, a contraction that is even sharper than during the Great Recession, see Haltiwanger (2020).

These developments are likely to have important macroeconomic implications, which may last well beyond the pandemic itself. The reason is that seemingly small changes to startups can create persistent and increasingly strong ripple effects on the macroeconomy as cohorts of new firms age and grow into larger businesses. Therefore, startups deserve special attention in this situation.

This paper provides an empirical perspective on what the disruption of startup activity might imply for the U.S. economy, in terms of the severity and persistence of employment losses. To this end, we developed a Startup Calculator, available on our websites, which allows anyone to easily compute employment losses under various scenarios of choice.[1]

The calculator allows one to vary three key margins, which pertain entry and exit of young businesses. As such, these effects are not easily reversed and may have important effects on the macroeconomy in the medium- and long run. The first margin is the number of startups. A fall in this number directly reduces the number of new jobs created by startups. Importantly, however, this "lost generation" of firms then creates a persistent dent in aggregate employment as subsequent years are characterized by a lower number of young firms, see e.g. Gourio, Messer, and Siemer (2016) and Sedláček (forthcoming).

The second margin is the growth potential of startups. Sedláček and Sterk (2017) show that firms born during recessions not only start smaller but also tend to stay smaller in future years even when the aggregate economy recovers. These movements in growth potential are attributed to changes in the composition of the type of startups. In the current situation, it seems particularly challenging to start a highly

[1] The calculator and an excel document with the underlying computations can be found at http://users.ox.ac.uk/~econ0506/Main/StartupCalculator.html.

scalable businesses, since supply chains are heavily distorted, credit conditions are poor, and customer may be demand difficult to acquire during a lockdown.

The third and final margin included in the calculator is the survival rate of young businesses. Startups and young firms in general have much higher exit rates than older firms, see e.g. Haltiwanger, Jarmin, and Miranda (2013), and during downturns these exit rates tend to increase.

Given a scenario for each of these three margins, the calculator computes the implied change in time path for aggregate US employment, from 2020 onwards. The Startup Calculator uses publicly available data from the U.S. Business Dynamics Statistics (BDS). We take a conservative stance and only consider changes to firms younger than 10 years of age. In other words, we leave 40 percent of all businesses unaffected in our calculations and as such the results may be taken as lower bounds.

Our baseline scenario is one in which all three margins fall to their minimum levels observed since 1977 (the starting point of the BDS). Assuming that this decline lasts for one year, after which all three margins revert back to normal, we find that the effect on aggregate employment in 2020 is a 1.1 percent reduction. Importantly, however, the effect of aggregate employment is very persistent. Cumulated over the first 10 years, we find an employment loss of 10.6 million.

The calculator is an accounting tool, simulating employment of cohorts and then aggregating. As such, it abstracts from potential equilibrium feedback effects. To adjust for such effects, we integrate the calculator into a "shell" of a basic equilibrium heterogeneous-firms model. Based on this model (and assumptions on the wage elasticity of labour demand and supply) we provide an adjustment for equilibrium effects. We find that this adjustment dampens the aggregate employment effect by about 20 percent.

The remainder of this paper is organized as follows. Section 2 reviews existing evidence on the importance of startups for aggregate job creation and discusses some early evidence on the effects of the COVID-19 pandemic on business formation. Section 3 presents the calculator, as well as the equilibrium heterogeneous-firms model. Section 4 presents results under several scenarios and discusses the importance of the three margins mentioned above. We emphasize, however, that using the calculator on our website it is easy for anyone to compute results under different scenarios. Finally, Section 5 concludes.

Covid Economics 13, 4 May 2020: 178-200

2 The Importance of Startups

There are four main reasons why we focus on startups, and in turn young firms. First, new and young businesses are the dominant creators of new jobs. In the U.S. an average of 16.3 million jobs are created and about 14.9 million jobs are destroyed every year. Put together, this means that annually about a third of all jobs in the U.S. are either new or get destroyed. Strikingly, startups create a net amount of 2.9 million jobs per year. These values suggest that startups are the only business category which is characterized by positive net job creation and existing firms only shed jobs on average.

It is true, however, that young firms also exhibit a higher rate of exit, suggesting that not all jobs created by startups are long-lasting. Nevertheless, the data shows that surviving young firms tend to grow faster than the average incumbent, see e.g. Haltiwanger, Jarmin, and Miranda (2013). These patterns of high rates of exit and growth among young firms have been dubbed "up-or-out dynamics".

The second reason to focus on startups relates precisely to the up-or-out dynamics described above. This high rate of labor market churn associated with startups has been linked to measures of productivity and profitability growth (see e.g. Bartelsman and Doms (2000) or Foster, Haltiwanger, and Krizan (2001). Therefore, the data suggest that surviving young businesses are the ones that are crucial for aggregate productivity growth.

Third, these findings are exacerbated by new evidence on young high-growth firms, so called "gazelles". Haltiwanger, Jarmin, Kulick, and Miranda (2017) document that this small share of startups with exceptional growth potential accounts for about 40 percent of aggregate TFP growth, 50 percent of aggregate output growth and 60 percent of aggregate employment growth.

Finally, changes startup activity may have very persistent effects at the macroeconomic level, either via the number of firms (Gourio, Messer, and Siemer (2016), Sedláček (forthcoming)) or via changes in the type of entrants (Sedláček and Sterk (2017)). In addition Pugsley, Sedláček, and Sterk (2017) show that most of the cross-sectional heterogeneity in firm-level employment can be attributed to ex-ante factors, already present at or before birth of the firm. Together, this body of evidence suggests that disruptions of startup activity, like the one experienced currently, may have long-lasting implications.

Covid Economics 13, 4 May 2020: 178-200

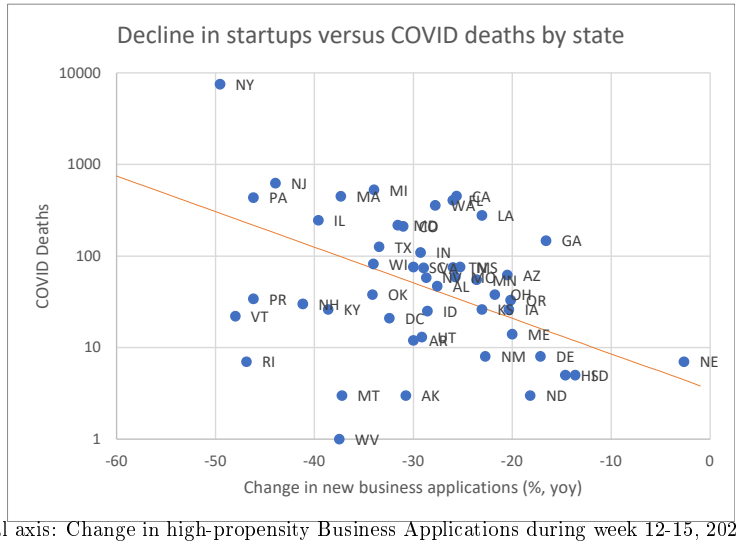

Horizontal axis: Change in high-propensity Business Applications during week 12-15, 2020, relative to the same weeks in 2019, by US State. Source: Business Formation Statistics. Vertical axis: total number of COVID related deaths in the US. Source: Centers for Disease Control and Prevention. Data were downloaded on April 17, 2020.

2.1 Startups during the COVID-19 pandemic

It is still too early to tell exactly how hard startups will be hit by the COVID crisis. The available data, however, suggest that the situation is severe. Figure 1 plots state-level data on COVID deaths versus the number of (high-propensity) business applications, a strong early indicator of startup activity, see Bayard, Dinlersoz, Dunne, Haltiwanger, J. Miranda, and Stevens (2017). Haltiwanger (2020) shows that in late March 2020, business applications in the US declined strongly, about as much as during the Great Recession (although it is unclear how long the decline will last this time).

Figure 1 shows that, not only have business applications declined strongly in many states, there is also a clear relation with the severity of the pandemic. Particularly striking is New York state (NY), which suffered both the largest number of deaths and the strongest declines in business applications.

Covid Economics 13, 4 May 2020: 178-200

3 The Startup Calculator

In this section, we provide details on the data and its treatment, used in our analysis. The next section presents the results.

3.1 Data

Throughout this paper, we use publicly available information from the Business Dynamcis Statistics (BDS) of the U.S. Census Bureau spanning the period of 1977 to 2016. This dataset includes (among other things) information on the number of firms and employment by firm age. For our purposes, we use information on the number of firms, their employment and their exit rates by age, where the latter is considered in the following age categories: 0 (startups), 1, 2, 3, 4, 5, 6 to 10 and all. From this information, we can also construct aggregate employment.

The **number of firms** of age a in year t, $n_{a,t}$, is directly observable in the BDS data, as is employment by age, $e_{a,t}$. We use employment and the number of firms by age to compute **average firm size** as $s_{a,t} = e_{a,t}/n_{a,t}$.[2] Finally, we are also interested in survival rates of firms by age. We compute these by using the information on firm deaths, $d_{a,t}$, which give the number of firms of a given age in which all establishments shut down. We define the **survival rate** by age as $1 - x_{a,t} = 1 - d_{a,t}/n_{a,t}$.

3.2 Accounting for startups: methodology

Because firms aged 6 to 10 are grouped together in the BDS, it is necessary to interpolate information for each of the individual age categories.[3] In addition, because the sample period ends in 2016, it is necessary to extrapolate the information up until 2019, just before we perform our scenario analysis. In what follows, we describe the interpolation and extrapolation methods employed in the Startup Calculator.

3.2.1 Interpolation of age-specific information

Number of firms and exit rates. To interpolate information on the number of firms aged 6 to 10 years we assume that exit rates between the ages of 5 and 10 are

[2] This is the so-called "current-year" definition of size.

[3] Not interpolating gives similar results but overstates the impact of changes in startups. This is because when new firms reach the age of 6, they are assigned the average size of 6 to 10 year old firms. This exacerbates the impact of changes in startups on aggregate employment.

Covid Economics 13, 4 May 2020: 178-200

linearly related such that

$$x_{a,t} = x_{a-1,t-1}(1 - \Delta_x) \quad \text{for } a = 5, ..., 10,$$

where $\Delta_{x,t}$ is a year-specific growth rate, but which is the same for firms between the ages of 5 and 10. Given the exit rates by age, we can compute the number of firms between the ages 6 and 10 as

$$n_{a,t} = n_{6-10,t} \frac{\Pi_{j=1}^{a-5}(1 - x_{a-j+1,t-j+1})}{\sum_{a=6}^{10} \Pi_{j=1}^{a-5}(1 - x_{a-j+1,t-j+1})} \quad \text{for } a = 6, ..., 10.$$

The above therefore takes the observed number of firms aged 6 to 10 years and decomposes it into the shares of 6, 7, 8, 9 and 10 year old firms where the shares are computed using the age-specific survival rates.

Finally, we compute $\Delta_{x,t}$ by minimizing

$$\left| x_{6-10,t} - \sum_{a=6}^{10} \left(\frac{n_{a,t}}{\sum_{a=6}^{10} n_{a,t}} x_{a,t} \right) \right|.$$

Firm size. We interpolate firm size for businesses aged 6 to 10 in the same way as above. We assume that firm size is linearly increasing between the ages of 5 and 10 such that

$$s_{a,t} = s_{a-1,t-1}(1 + \Delta_{s,t}) \quad \text{for } a = 5, ..., 10,$$

where Δ_s is a year-specific growth rate, but which is the same for firms between the ages of 5 and 10. Given the age-specific exit rates described above, we then compute $\Delta_{s,t}$ by minimizing

$$\left| s_{6-10,t} - \sum_{a=6}^{10} \left(\frac{n_{a,t}}{\sum_{a=6}^{10} n_{a,t}} s_{a,t} \right) \right|.$$

The results of this interpolation are shown in Figure 2, which depicts the actual and the interpolated data for firm size and exit rates by age.

3.2.2 Extrapolation of information until 2019

Information on startups and young firms. In order to extrapolate the necessary data between 2017 and 2019, we assume that firm size by age and exit rates by age (up to age 10), and the number of startups, all linearly converge to their 1977-2016

Covid Economics 13, 4 May 2020: 178-200

Figure 2: Actual and interpolated data

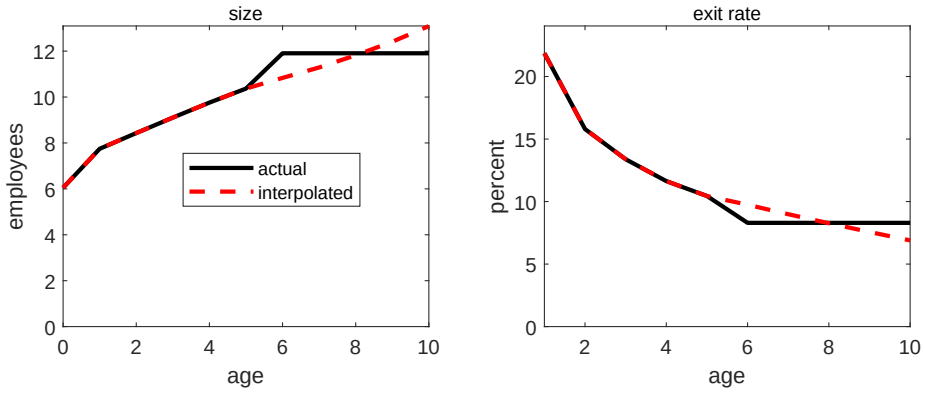

Note: Actual and interpolated data for firm size and exit rates by age.

averages:

$$x_{a,2016+\tau} = x_{a,2016} + \frac{\tau}{3}(\overline{x}_a - x_{a,2016}),$$
$$s_{a,2016+\tau} = s_{a,2016} + \frac{\tau}{3}(\overline{s}_a - s_{a,2016}),$$
$$n_{0,2016+\tau} = n_{0,2016} + \frac{\tau}{3}(\overline{n}_0 - n_{0,2016}),$$

for $\tau = 1, 2, 3$ and $a = 1, 2, ..., 10$, and where $\overline{x}_a$, $\overline{s}_a$ and $\overline{n}_0$ denote the 1977 to 2016 averages of age-specific exit rates, firm sizes and the number of startups, respectively.[4] Using the above, we can then recover the number of firms for the ages of 1 to 10 as $n_{a,t} = n_{a-1,t-1}(1 - x_{a,t})$, for $a = 1, 2, ..., 10$ and $t = 2017, 2018, 2019$.

The result of this extrapolation are shown in Figure 3, which depicts the actual and extrapolated number of startups, average startup size and exit rates of 1 to 10 year old firms.

Number of older firms. The number of all businesses in the US economy has been steadily increasing over the sample period. This is, however, essentially entirely because of an increasing number of older firms. This can be seen from Figure 3 which

[4] Only startups are observed from 1977. Therefore, averages of older businesses of age a are taken over the period 1977+a to 2016. For instance, the averages for two-year-old firms is based on 1979 to 2016.

Covid Economics 13, 4 May 2020: 178-200

Figure 3: Actual and extrapolated data

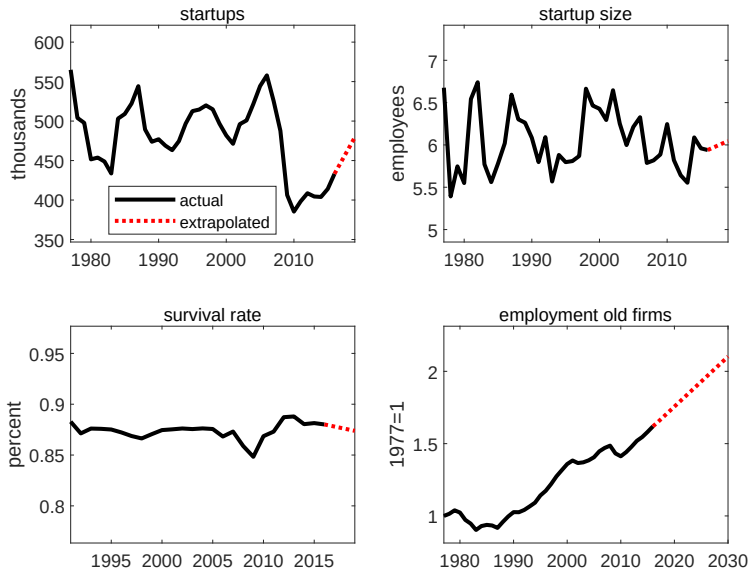

Note: Actual and extrapolated data for the number of startups, startup size, survival rates (of young, i.e. <10 years) firms and employment in old (11+ years) firms.

shows that the *number* of startups has fluctuated cyclical around a relatively stable mean.

The increasing number of firms is then reflected in rising aggregate employment. Given that our analysis focuses on the impact changes in young firms' performance have on aggregate employment, we need to account for the trend growth of older firms. We do so by estimating a linear trend for employment in firms aged 11 years and more, using the period between 2010 and 2016. Using this estimated trend we then extrapolate employment in this group of firms for the years 2017 to 2030.

The bottom right panel of Figure 3 shows the actual and extrapolated employment in firms aged 11 and more, where we scale both time-series by their values in 1977.

3.2.3 Constructing alternative scenarios

Having the above information, we are ready to conduct scenarios starting in 2020 and running through to 2030. We consider three types of margins: (i) changes in

the number of startups, (ii) changes in growth potential and (iii) changes in survival rates.

Scenarios involving (i) and (iii) are straightforward. Upon impact, we lower the number of startups and/or the survival rates of young firms by a certain value and keep this value for a certain period. Growth potential works on the same principle, but applies to the *cohort* of startups which enters in 2020. Therefore, lowering the growth potential by a certain percentage value results in the entire *growth profile* of firms born in 2020 shifting downwards. Importantly, the size of firms which in 2020 are older than 0 years is unaffected.

To be concrete, for a given scenario, let us denote the initial percentage decreases in the number of startups, the growth potential of startups and the survival rate of young firms by $\zeta_j \in (0,1)$, where $j = \{n, s, x\}$, respectively. Let us further denote the duration of these effects by $\tau_j > 0$, where $j = \{n, s, x\}$, respectively. The given scenarios are then given by

$$\begin{aligned} n_{0,2019+t} &= n_{0,2019}(1-\zeta_n), \quad \text{for } t = 1, ..., \tau_n, \\ s_{a,2019+t+a} &= s_{a,2019}(1-\zeta_s), \quad \text{for } t = 1, ..., \tau_s, \text{ and } a = 0, 1, 2, ..., 10, \\ x_{a,2019+t} &= x_{a,2019}(1-\zeta_x), \quad \text{for } t = 1, ..., \tau_n, \text{ and } a = 1, 2, ..., 10. \end{aligned}$$

Notice that in the above, the changes in growth potential apply to *cohorts* of startups. For instance, if the effect of the pandemic lasts only for one year ($\tau_s = 1$), then only startups in 2020 are affected. In 2021, it is one year old firms which have lower growth potential, i.e. the cohort born in 2020, while firms of all other ages (including new startups), are unaffected. In contrast, the pandemic affects the survival rates of all young firms simultaneously and therefore businesses aged 0 to 10 years experience a drop in survival rates in 2020. Also note that the number of businesses older than (i.e. $a > 0$) years is given by $n_{a,t} = (1 - x_{a,t})n_{a-1,t-1}$.

Our calculator can also accommodate bounce-back scenarios. These are always defined as certain values above the 1977-2016 averages of the number of startups, average sizes and survival rates of young firms. Recall that all these margins converge precisely to the respective 1977-2016 averages by 2019.

Specifically, let us denote the percentage increase (above the respective long-run average) in the bounce-back scenario related to the number of startups, the growth potential of young firms and their survival rates by χ_j, where $j = \{n, s, x\}$, respec-

Covid Economics 13, 4 May 2020: 178-200

tively. Furthermore, let us denote the length of the bounce-back period by σ_j, where $j = \{n, s, x\}$, respectively. The given bounce-back scenarios are then given by

$$\begin{aligned} n_{0,2019+\tau_n+t} &= n_{0,2019}(1+\chi_n), \quad \text{for } t = 1, ..., \tau_n, \\ s_{a,2019+\tau_s+t+a} &= s_{a,2019}(1+\chi_s), \quad \text{for } t = 1, ..., \tau_s, \text{ and } a = 0, 1, 2, ..., 10, \\ x_{a,2019+\tau_x+t} &= x_{a,2019}(1+\chi_x), \quad \text{for } t = 1, ..., \tau_n, \text{ and } a = 1, 2, ..., 10. \end{aligned}$$

Finally, in all scenarios aggregate employment in a given year is computed simply as the sum of employment in firms aged 0 to 10 and the (extrapolated) employment of firms older than 11 years. Therefore, we are being conservative in the sense that we are not allowing businesses aged 11 and more years to be affected by the crisis. Our results should, therefore, be considered as a lower bound on the given scenarios.[5] While the margins of startups and growth potential would only "kick in" after 2030 for these older firms, their survival rates may very well be affected in 2020 already.

3.3 Adjusting for equilibrium effects

The calculations above abstract from potential equilibrium effects. In this subsection, we describe how to adjust for this, by placing the calculator within a "shell" formed by a basic but standard heterogeneous-firm model. This model also clarifies how the calculator connects to canonical equilibrium models of firm dynamics.

In the model, there is a measure M of heterogeneous firms.[6] Let the production function of firm i be given by

$$y_i = z_i n_i^{\alpha},$$

where y_i is the firm's output, n_i its employment level, z_i is the firm's productivity level, and $\alpha \in (0, 1)$ is the elasticity of production with respect to labor input.[7] The wage per employee is taken as given by firms, and denoted by w. The firm chooses its level of employment in order to maximize profits, given by $y_i - wn_i$. This implies

[5] Old firms (11+ years) account for 40 percent of all businesses, but almost 80 percent of employment.

[6] Although the model is dynamic, it can be described entirely in static terms, hence we omit time subscripts.

[7] We abstract from capital for simplicity. Augmenting the model with capital would not change any of our results.

Covid Economics 13, 4 May 2020: 178-200

the following familiar solution for labor demand by firm i:

$$n_i = (z_i)^{\frac{1}{1-\alpha}} \left(\frac{w}{\alpha}\right)^{\frac{1}{\alpha-1}}$$

Aggregating over all firms, aggregate labor demand is given by:

$$N = M \left(\frac{w}{\alpha}\right)^{\frac{1}{\alpha-1}} \chi$$

where $\chi \equiv \int z^{\frac{1}{1-\alpha}} dF(z)$, where F is the CDF of the productivity distribution. Taking logs and differentiating (keeping idiosyncratic productivities constant), we can decompose changes in aggregate labor demand as:

$$d\ln N = \underbrace{d\ln M}_{\text{\#firms}} + \underbrace{d\ln \chi}_{\text{growth potential}} + \underbrace{\frac{1}{\alpha-1} d\ln w}_{\text{wages}} \tag{1}$$

The first two terms reflect changes in, respectively, the number of firms and their growth potential (productivity), whereas the third term captures equilibrium effects due to wage conditions.[8] Equation (1) can be understood as an aggregate labor demand curve, which is shifted by the number of firms and their growth potential.

To close the model, we need to specify how labor supply is determined. We assume there is a representative household with Greenwood-Hercowitz-Huffmann preferences. Specifically, the household's level of utility is given by: $U(C,N) = \frac{1}{1-\sigma}\left(C - \mu\frac{N^{1+\kappa}}{1+\kappa}\right)^{1-\sigma}$, where C denotes consumption and μ, κ, $\sigma > 0$ are preference parameters. The household chooses C and N to maximize utility, subject to a budget constraint given by $C = wN + \Pi$, where Π are aggregate firm profits. Utility maximization implies the following labor supply curve: $\mu N^{\kappa} = w$. Taking logs and differentiating gives the labor supply schedule:

$$d\ln N = \frac{1}{\kappa} d\ln w \tag{2}$$

Combining the labor demand and supply schedules, Equations (1) and (2), we can

[8] Other sources of equilibrium dampening could derive from endogenous entry and exit, which we abstract from here.

Covid Economics 13, 4 May 2020: 178-200

solve for the equilibrium level of aggregate employment:

$$d\ln N = \underbrace{\Psi}_{\text{equilibrium dampening}} \underbrace{(d\ln M + d\ln \chi)}_{\text{calculator output}} \tag{3}$$

where $\Psi \equiv \frac{1}{1-\kappa\epsilon_{nw}} \in (0,1)$, where $\epsilon_{nw} = \frac{1}{\alpha-1}$ is the wage elasticity of labor demand. Equation (3) expresses aggregate employment (in deviation from some baseline trend) as a function of the number of firms and their growth potential. The latter two we obtain as outputs from the calculator.[9] The parameter Ψ is an equilibrium dampening coefficient, which depends on the elasticity of labor demand (ϵ_{nw}) and the Frisch elasticity of labor supply ($\frac{1}{\kappa}$). Based on these two parameters and the output from the calculator, we can thus compute the equilibrium change in aggregate employment from Equation (3).

To gauge how large such equilibrium dampening effects could be we consider standard values for the model parameters. Specifically, we assume a unit Frisch elasticity of labor supply ($\kappa = 1$) which is in the ballpark of the estimates in the micro and macro literature. The parameter α could be set in accordance with the labor share of aggregate income, which is around sixty percent in the US, implying $\alpha = 0.6$. Given these numbers, we obtain $\Psi = 0.29$, i.e. equilibrium effects dampen just over seventy percent of the decline in aggregate employment.

Note however, that the above model does not contain any labor market frictions. In the presence of such frictions, labor demand is likely to be less sensitive to wages. We therefore prefer to use a direct empirical estimate of the labor demand elasticity. Lichter, Peichl, and Siegloch (2015) conduct a meta study of empirical estimates and recommend an elasticity of -0.246. Setting $\epsilon_{nw} = -0.246$ (and again $\kappa = 1$) we obtain a coefficient of $\Psi = 0.80$, i.e. 20% dampening. We will use this value as our baseline for the dampening coefficient. This value also conforms with other evidence that equilibrium dampening effects may not be that strong. For instance, Sedláček (forthcoming) shows that a search and matching model with heterogeneous firms displays relatively weak equilibrium dampening effects. In a recession, the slack labor market (increasing the chances of hiring and reducing wages) is not a strong enough force to overturn the impact of a missing generation of startups.

Finally, we note that if a scenario is based on empirical observations for average size

[9] Alternatively, one could model an explicit entry and exit block of the model.

Covid Economics 13, 4 May 2020: 178-200

of young firms (for the startup growth potential margin), then it may be important to account for the fact that this number itself is subject to equilibrium dampening. Therefore, the true change in growth potential might be larger than what the data suggest. To do so, we use Equation (1), but this time aggregated over only startups, as opposed to all firms.[10] Using Equation (2) to substitute out the wage and rearranging, we obtain the following expression for startup growth potential:

$$d\ln\chi^{startup} = \underbrace{d\ln N^{startup} - d\ln M^{startup}}_{\text{avg startup size}} - \underbrace{\kappa\epsilon_{nw} d\ln N}_{\text{equil. adjustment}} .$$

On the right hand side, the first two terms jointly are the change in average startup size. From this one subtracts the $\kappa\epsilon_{nw}$ times the change in *aggregate* employment in order to obtain the change in the growth potential of startups.[11]

4 Results

4.1 Baseline scenario

At this point, we do not know whether the current contraction will be short-lived or develop into a full-blown recession. Therefore, we take a scenario-based approach. Based on the early indicator discussed earlier, we select as a baseline scenario a strong but short-lived contraction. Specifically, we assume that the startup rate, the growth potential and the survival rate all drop to their lowest levels since 1977 (the beginning of our data sample). These values are in fact closely linked to the Great Recession, which was the worst period for startup activity since the start of the sample.[12] However, we let the contraction last for just one year, based on the observation that several countries seem to have moved past the peak of the pandemic within a several months, and assuming a relatively swift recovery of overall macroeconomic conditions.

Figure 4 plots the effects on aggregate employment. Two key observations stand out. First, the decline in startup activity has sizeable aggregate effects. In the first

[10] This gives $d\ln N^{startup} = d\ln M^{startup} + d\ln\chi^{startup} + \epsilon_{nw}\ln w$.

[11] Note that the adjustment only matters when aggregate employment is away from its trend level. It turns out that in our application here, this adjustment has only negligible effects, and hence we omit it in our calculations.

[12] That said, the nature of the current contraction is clearly very different from the Great Recession. An important motivation for our calculator is to give the possibility of computing different alternative scenarios.

Covid Economics 13, 4 May 2020: 178-200

Figure 4: Baseline scenario in the calculator

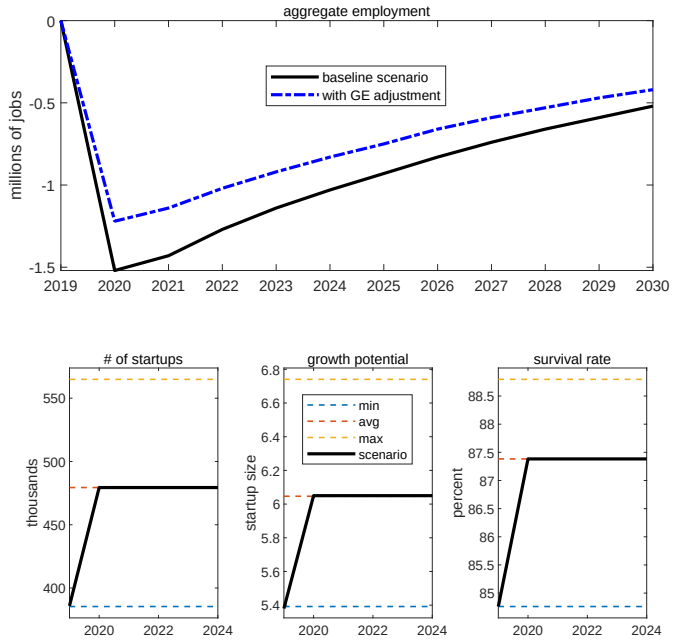

Note: General Equilibrium (GE) adjustment is obtained based on Equation (3) $\Psi = 0.8$.

year, about 1.5 million jobs are lost, relative to a scenario without the pandemic. This loss is about six percent of the employment of firms aged below ten, and 1.1 percent of aggregate employment.

Second, the macroeconomic effects are very persistent, even though the shock itself lasts for only one year. Cumulated from 2020 until 2030, the job losses are about 10.6 million. Moreover, each of the three margins plays a substantial role. The decline in the number of startups accounts for about 4.6 million of the cumulated job losses, the decline in growth potential for about 2 million, and the decline in survival for about 3.5 million. The remaining 0.5 loss is due to interactions between the three margins.

4.2 Bounce-back scenario

Quite possibly, however, the shock will last longer than 1 year. Based on the calculator, we find that the cumulative employment loss is roughly proportional to the

Covid Economics 13, 4 May 2020: 178-200

Figure 5: Bounceback scenario in the calculator

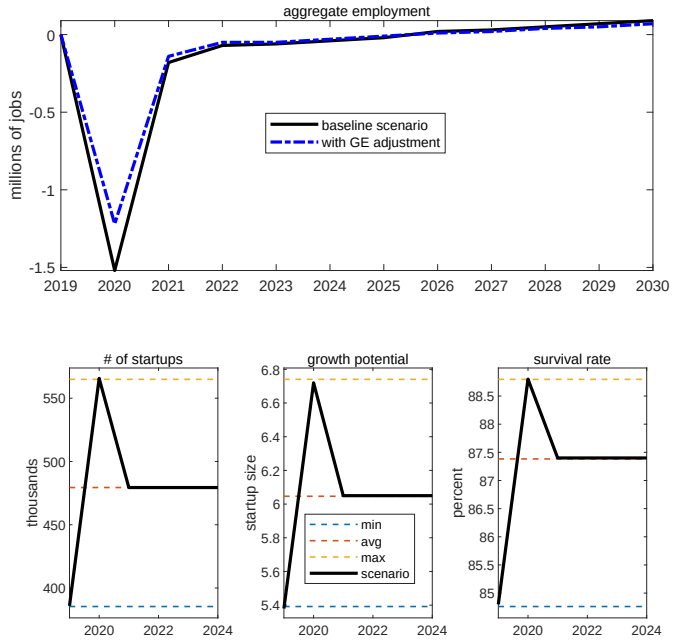

Note: General Equilibrium (GE) adjustment is obtained based on Equation (3) with $\Psi = 0.8$.

duration of the shock. If the crisis lasts for two years, it will result in roughly 20 million jobs lost between 2020 and 2030. Alternatively, it is possible that the shock will be followed by a "bounceback", which is also allowed for in the calculator. Figure 5 shows a scenario in which one year after the pandemic, all three margins reach the highest levels observed in our data sample. In this case, aggregate employment losses are much shorter-lived, but nonetheless some effects persist. Not only is the cumulative job loss up to 2030 about 2 million, but it is only around 2028 when aggregate employment finally catches up to its initial trajectory. In other words, even a short-lived crisis with a strong bounce-back will have a sizeable negative impact on the aggregate economy for the next decade.

How likely is such a reversal scenario? This question is difficult to answer. Historically, however, strong bouncebacks have been uncommon, as in the data all three margins show strong and positive autocorrelations over time. Another possibility is

Covid Economics 13, 4 May 2020: 178-200

that older firms will hire more, compensating for the employment losses due to startups. To fully offset the startup job losses in the baseline scenario, this would mean that older firms would need to create an additional 1.5 million jobs in 2020. For comparison, net job creation by firms older than 10 was only about 0.6 million. From this perspective, creating the 1.5 million extra jobs needed appears to be a large challenge. In fact, our equilibrium dampening effect suggests that only about 0.3 million jobs may be created by older firms in reaction to the slump in young firms' activity.

5 Conclusion

In this paper, we provide an empirical analysis of the medium-run impact of the coronavirus-induced slump in startup activity on aggregate U.S. employment. The analysis specifically recognizes three margins through which young firms may impact the aggregate economy: (i) decline in the number of startups, (ii) decline in the growth potential of startups and (iii) a decline in survival rates of young firms.

The key contribution of this paper is to develop a simple tool - the Startup Calculator - which is accessible to anyone on our websites.[13] Analysing a few possible scenarios, the results suggest that even a short-lived disruption in startup activity may have large and very persistent effects on the aggregate economy in the next decade.

While the outlook for startups may look gloomy, there are also some glimmers of hope. First, the high sensitivity of startups to economic conditions likely implies that they may also respond positively to policies which aim to support them. Given that startups can be relatively easily identified, such policies might be relatively cost effective. Second, the change in our daily lives might inspire entrepreneurs, and create new opportunities, to come up with new ideas and new ways of running businesses, which could foster growth in the long run.

References

Bartelsman, E. J., and M. Doms (2000): "Understanding Productivity: Lessons from Longi-tudinal Microdata," *Journal of Economic Literature*, 38(3), 569–594.

[13] To access the Calculator, please visit http://users.ox.ac.uk/~econ0506/Main/StartupCalculator.html

Covid Economics 13, 4 May 2020: 178-200

Bayard, K., E. Dinlersoz, T. Dunne, J. Haltiwanger, J. J. Miranda, and J. Stevens (2017): "Early-Stage Business Formation: An Analysis of Applications for Employer Identification Numbers," *CES Working paper*, 18-52.

Foster, L., J. Haltiwanger, and C. J. Krizan (2001): "Aggregate Productivity Growth: Lessons from Microeconomic Evidence," in *New Developments in Productivity AnalysisLabor Markets, Employment Policy and Job Creation*, ed. by C. Hulten, E. Dean, and M. Harper, pp. 303–372. National Bureau of Economic Research, University of Chicago Press.

Gourio, F., T. Messer, and M. Siemer (2016): "Firm Entry and Macroeconomic Dynamics: A State-level Analysis," *American Economic Review, Papers and Proceedings*, 106(5), 214–218.

Haltiwanger, J. (2020): "Applications for New Businesses Contract Sharply in Recent Weeks: A First Look at the Weekly Business Formation Statistics," mimeo, April.

Haltiwanger, J., R. Jarmin, R. Kulick, and J. Miranda (2017): "High Growth Firms: Contribution to Job, Output and Productivity Growth," in *Labor Markets, Employment Policy and Job Creation*, ed. by J. Haltiwanger, E. Hurst, J. Miranda, and A. Schoar, pp. 11–62. National Bureau of Economic Research, University of Chicago Press.

Haltiwanger, J., R. Jarmin, and J. Miranda (2013): "Who Creates Jobs? Small vs. Large vs. Young," *The Review of Economics and Statistics*, 45(2), 347–361.

Lichter, A., A. Peichl, and S. Siegloch (2015): "The Own-Wage Elasticity of Labor Demand: A Meta-Regression Analysis," *European Economic Review*, 80(C), 94–119.

Pugsley, B., P. Sedláček, and V. Sterk (2017): "The Nature of Firm Growth," *CEPR Discussion Papers*, 12670.

Sedláček, P. (forthcoming): "Lost Generations of Firms and Aggregate Labor Market Dynamics," *Journal of Monetary Economics*.

Sedláček, P., and V. Sterk (2017): "The Growth Potential of Startups Over the Business Cycle," *American Economic Review*, 107(10), 3182–3210.

Covid Economics 13, 4 May 2020: 178-200